Finite Horizon Model Order Reduction of Linear Systems

A Thesis

Submitted in Partial Fulfilment of the Requirements

for the Dual Degree of

MS (Engineering)

&

DOCTOR OF PHILOSOPHY

By

Kasturi Das

Department of Electronics and Electrical Engineering
Indian Institute of Technology Guwahati
Guwahati, India.

July, 2024

Dedicated to

Deuta, Ma and Putu
for their encouragement, love and support

Certificate

This is to certify that the thesis entitled "**Finite Horizon Model Order Reduction of Linear Systems**", submitted by **Kasturi Das** (166302002), a dual degree (MS(Engg.)+ PhD) student in the *Department of Electronics and Electrical Engineering, Indian Institute of Technology Guwahati*, for the award of the dual degree **MS(Engineering)** and **Doctor of Philosophy**, has been carried out by her under our supervision and guidance. The thesis has fulfilled all requirements as per the regulations of the Institute and, in our opinion, has reached the standard needed for submission. The results embodied in this thesis have not been submitted to any other university or institute for the award of any degree or diploma.

Date :
Place : Guwahati

Dr. Srinivasan Krishnaswamy
Associate Professor,
Dept. of Electronics and Electrical Engineering,
Indian Institute of Technology Guwahati,
Assam - 781039.

Date :
Place : Guwahati

Prof. Somanath Majhi
Professor,
Dept. of Electronics and Electrical Engineering,
Indian Institute of Technology Guwahati,
Assam - 781039.

Declaration

I declare that this written submission represents my ideas in my own words. Where others' ideas or comments have been included, I have adequately cited and referenced the sources. I also declare that I have adhered to all principles of academic honesty and integrity and have not misrepresented, fabricated, or falsified any idea/data/fact/source in my submission. I understand that any violation of the above will cause disciplinary action by the Institute and can also evoke penal action from the sources which have thus not been appropriately cited or from whom proper permission has not been taken when needed.

Date:
Place: Guwahati

Kasturi Das
Roll No: 166302002

Acknowledgements

First and foremost, I sincerely thank my thesis supervisors, Dr. Srinivasan Krishnaswamy and Prof. Somanath Majhi, for their guidance, patience and support during this work. Dr Srinivasan Krishnaswamy Sir encouraged me to take up challenging subjects during my coursework, inspired me to work with mathematical rigour and provided valuable insights into my work. This helped me acquire new skills and improved my reading, writing and thinking capacity. Prof. Somanath Majhi Sir, on the other hand, motivated me to work diligently and finish the work in a timely manner. The expertise and experiences he shared with me were invaluable in completing this thesis.

I express my gratitude to the members of my doctoral committee, Prof. Chitralekha Mahanta, Dr Indrani Kar and Dr Hanumant Singh Sekhawat, for reviewing the progress of my work. Their advice and suggestions have been of great help to me. I am thankful to the Head, the technical and office staff members of the EEE department, IIT Guwahati, for their support and help in laboratory and official works.

I want to express my deep gratitude to Prof. K.N.Shubhanga (NITK, Surathkal, EEE Department) for his guidance and encouragement during my BTech minor and major projects. His dedication to research work motivated me to pursue a PhD programme after BTech. I am greatly indebted to my BTech friends Manasa, Srishti, Deepa and Meghna for their advice, support and help during various stages of my academic life.

I would like to convey my sincere gratitude to my labmates in Control and Instrumentation Lab-I (CIL-I): Mandar da, Susanta da, Suman da, Arghya da, Trusna di, Kamakshi di, Sumi ba, Gautam bhaiyya, Mriganka da, Manmohan, Sami, and Raju for their help and joyful company. I am grateful to my juniors in CIL-1: Tamen, Anindya, Shiv Santosh, Saikat, Paraj, Pooja, Sanjeev, Gangadari, Biswanath, Athoibi and Nitisha for their cooperation. I wish to thank Uddipana ba and Abhijit da for their help, advice, and research discussions.

I am grateful to my IITG seniors and friends, Nupur di, Mohit bhaiyya, Madhurima ba, and Popy, for their help, unconditional support and consistent encouragement throughout my PhD journey. I thank my hostel neighbours, Saswati ba, Bhuvana, Anjali, Vandana, and Gloria, for their help and joyful company.

Last but definitely not least, I would like to express my gratitude to my parents and my sister for their sacrifices and hard work. This journey would not be possible without their unconditional love and support.

Date: **Kasturi Das**

Abstract

The study of model order reduction involves approximating the dynamics of an original large-scale model by a reduced-order model to a high degree of accuracy. This thesis focuses on model order reduction of continuous-time Linear Time-Invariant (LTI) and Linear Time-Varying (LTV) systems over a finite time interval. The reduced-order models obtained are based on minimising an appropriate error criterion.

To begin with, the finite horizon H_2 error norm for the LTI system is expressed in terms of the pole-residue representation of the reduced-order system. This helps in deriving interpolation-based time-limited H_2 optimality conditions. A projection framework for rational interpolation-based model reduction over a finite time interval is introduced based on the optimality conditions. An iterative algorithm for time-limited H_2 optimal model reduction is proposed using the interpolatory framework. The reduced-order models obtained by the algorithm satisfy the optimality conditions approximately. The distance to optimality of the reduced-order models is also quantified.

Secondly, the finite horizon H_2 error norm for LTI systems is expressed using a gramian framework. Based on this, analytical expressions of the gradients of the time-limited H_2 error norm are derived. The gradients are used with a standard quasi-Newton procedure to obtain reduced-order models, which satisfy the time-limited H_2 optimality conditions more accurately than projection-based algorithms. Equating the gradients to zero gives Lyapunov-based conditions for time-limited H_2 optimality. Further, it is proved that these optimality conditions are equivalent to the interpolation-based optimality conditions discussed in the previous work.

Next, the focus is on LTV systems. Two methods for computing the reachability gramian of a continuous-time LTV system are proposed using output trajectory information obtained by simulating the system with various inputs. The concept of the modified adjoint of an LTV system is discussed, and the relation between the gramians of the original and the modified adjoint LTV system is obtained. This result is used to propose another method for numerically computing the reachability gramian of an LTV system. Then, a finite horizon H_2 norm for continuous-time LTV systems is discussed. This norm can be expressed using system gramians similar to the time-limited H_2 norm for LTI systems.

Finally, the finite horizon H_2 norm, introduced in the previous work, is used to define a finite horizon H_2 error norm. The error norm is used as a performance measure for model reduction of continuous-time LTV systems. The functional derivatives of the finite horizon H_2 error norm are obtained using a gramian framework. When equated to zero, the gradients give conditions for the optimality of the error norm. These conditions are used to propose a projection-based iterative

scheme for the model order reduction of LTV systems.

Contents

List of Figures

List of Tables

List of Algorithms

List of Abbreviations

LTI	linear time-invariant
LTV	linear time-varying
LTP	linear time periodic
MOR	model order reduction
ROM	reduced-order model
BT	balanced truncation
TL-BT	time-limited balanced truncation
SVD	singular value decomposition
TSIA	two-sided iterative algorithm
TL-TSIA	time-limited two-sided iterative algorithm
IRKA	iterative rational Krylov algorithm
TL-IRKA	time-limited iterative rational Krylov algorithm
SISO	single-input single-output
MIMO	multiple-input multiple-output
ALE	algebraic Lyapunov equation
DLE	differential Lyapunov equation

List of Symbols

$\mathbb{R}$, $\mathbb{C}$	real and complex number fields
$\mathbb{R}_+$	positive real numbers
$\mathbb{R}^n$, $\mathbb{C}^n$	vector spaces of n real or complex-valued tuples
$\mathbb{R}^{m\times n}$, $\mathbb{C}^{m\times n}$	vector spaces of real or complex valued matrices with size $m \times n$
i	imaginary number ($i^2 = -1$)
$\|s\|$	absolute value of real or complex scalar
s^* or $\overline{s}$	complex conjugate of complex scalar
$\arg(s)$	argument of complex scalar
$\mathrm{Re}(s)$, $\mathrm{Im}(s)$	real and imaginary components of complex scalar
e_k	k^{th} column of the identity matrix of appropriate size
I_n	the $n \times n$ identity matrix
$\mathrm{diag}(a_1, \ldots, a_n)$	diagonal matrix of size n with entries $a_1, \ldots, a_n$
$g(t) * u(t)$	$:= \int_0^t g(t-\tau)u(\tau)d\tau$, convolution operator
$G'(s)$	$:=\frac{dG(s)}{ds}$, first-order derivative of $G(s)$
$G^{(k)}(s)$	$:=\frac{d^kG(s)}{ds^k}$, k^{th} order derivative of $G(s)$
A^T	transpose of matrix A if A is real, conjugate transpose if A is complex
A^{-1}	the inverse of matrix A if A is square matrix
A^{-T}	the inverse of A^T if A is square matrix
$\det(A)$	determinant of square matrix A
$\lambda_i(A)$	i^{th} eigenvalue of square matrix A
$\rho(A)$	spectral radius of A
$\mathrm{tr}(A)$	the trace of A
$\mathrm{Orth}(A)$	Gram-Schmidt orthogonalization of the columns of A

$\mathrm{Ran}(A)$	subspace generated by the columns of the matrix A or the columnspace of A
$\mathrm{Ker}(A)$	kernel of the matrix A
$\dim(\mathcal{V})$	dimension of the subspace $\mathcal{V}$
$\|\cdot\|_2$	ℓ^2 vector or induced matrix norm
$\|\cdot\|_\infty$	ℓ^∞ vector or induced matrix norm
$\|A\|_F$	$:=\sqrt{\mathrm{Tr}(A^TA)}$, Frobenius matrix norm
$\|u\|_{L_2([0,\infty))}$	$:=\left(\int_0^\infty \|u(t)\|_2^2\, dt\right)^{\frac{1}{2}}$, Infinite horizon L_2 norm
$\|u\|_{L_\infty([0,\infty))}$	$:=\sup_{t>0} \|u(t)\|_\infty$, Infinite horizon L_∞ norm
$\|u\|_{L_2([t_0,t_f])}$	$:=\left(\int_{t_0}^{t_f} \|u(t)\|_2^2\, dt\right)^{\frac{1}{2}}$, Finite horizon L_2 norm
$\|u\|_{L_\infty([t_0,t_f])}$	$:=\sup_{t\in[t_0,t_f]} \|u(t)\|_\infty$, Infinite horizon L_∞ norm
$\kappa(A)$	$:=\|A\|_2\ \|A\|_2^{-1}$, condition number of A
$\delta(t-\tau)$	the unit impulse input at $t=\tau$
$\frac{\partial}{\partial x}f(x,y)$	partial derivative of f with respect to x

List of Publications

Journal publications

1. K. Das, S. Krishnaswamy and S. Majhi, "Near-optimal interpolation-based time-limited model order reduction", *International Journal of Control, Taylor & Francis, pp 1-11, 2023,* https://doi.org/10.1080/00207179.2023.2174408.

2. K. Das, S. Krishnaswamy and S. Majhi, "H_2 optimal model order reduction over a finite time interval", *IEEE Control Systems Letters, Vol. 6, pp 2467-2472, 2022,* https://doi.org/10.1109/LCSYS.2022.3164036.

3. K. Das, S. Krishnaswamy and S. Majhi, "Finite horizon model order reduction of continuous-time LTV systems", *Under review.*

Conference publications

1. K. Das, S. Krishnaswamy and S. Majhi, "Empirical Computation of Reachability Gramian for Linear Time-Varying Systems",*IFAC PapersOnline, Vol.54, Issue 9, pp 119-124, 2021,* https://doi.org/10.1016/j.ifacol.2021.06.183.

2. K. Das, B. S. Rangnath, S. Krishnaswamy and S. Majhi, "An Empirical Method for Approximate H_2 Optimal Model Order Reduction ",*IFAC PapersOnline, Vol.55, Issue 1, pp 838-842, 2022,* https://doi.org/10.1016/j.ifacol.2022.04.137.

Chapter 1

Introduction and literature survey

Dynamical models are used for simulating the behaviour of physical systems. These models are obtained using different modelling techniques such as lumped parameter modelling, which leads to models with ordinary differential equation (ODE) [41]; distributed parameters modelling, which produces models with partial differential equation (PDE) [25]; data-driven modelling [96], etc. Among these techniques, the PDE models obtained by distributed parameter modelling are approximated as a connection of many small lumped-parameter ODE submodels using spatial discretisation methods such as the finite element or finite volume method [42]. This process of obtaining linear models from physical systems is described in Figure 1.1. The final linear models obtained usually consist of high-order differential equations. Such models can accurately capture the behaviour of complex physical systems.

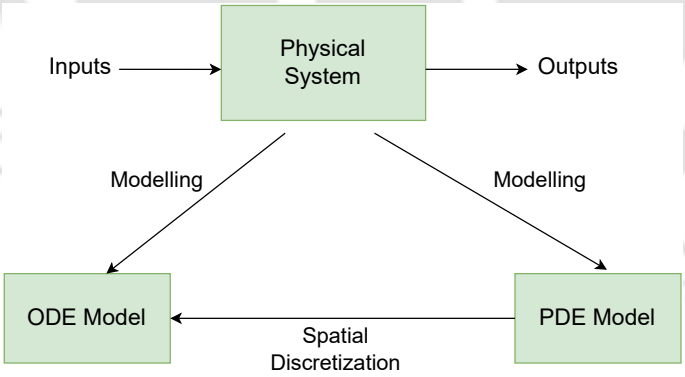

Figure 1.1: Modelling of dynamical systems by differential equations.

Consider the example of a cantilever beam. They are widely seen in physical structures, such as bridges (Figure 1.2), the wings of fixed-winged aircraft, microelectromechanical systems (MEMS), chemical sensor applications, etc. The dynamics of the beam are modelled as a partial differential equation (PDE). Spatial discretization of the PDE leads to a high-order ODE model. Such a high-order SISO model of a cantilever beam with a state-space representation of order 348 is available in the collection *SLICOT Benchmark Examples for Model Reduction* [16], [66].

Another example of a system that gives rise to a high-order model is the Zvezda Service Module

Figure 1.2: Cantilever bridge.

(ISS-1R) of the International Space Station (ISS) (shown in Figure 1.3a and Figure 1.3b). This module was launched on 12th December 2000 and installed on 25th December 2000. It provides electrical power distribution, life support systems, data processing systems, flight control systems, station living quarters and propulsion systems. It also provides a communication system and a docking port. A linear model of the Zvezda Service Module (ISS-1R) is also available in the collection *SLICOT Benchmark Examples for Model Reduction* [16], [66]. This model captures the vibration dynamics caused by the docking of an incoming spaceship. It has 270 states with 3 inputs and 3 outputs and is obtained by using finite element modelling techniques.

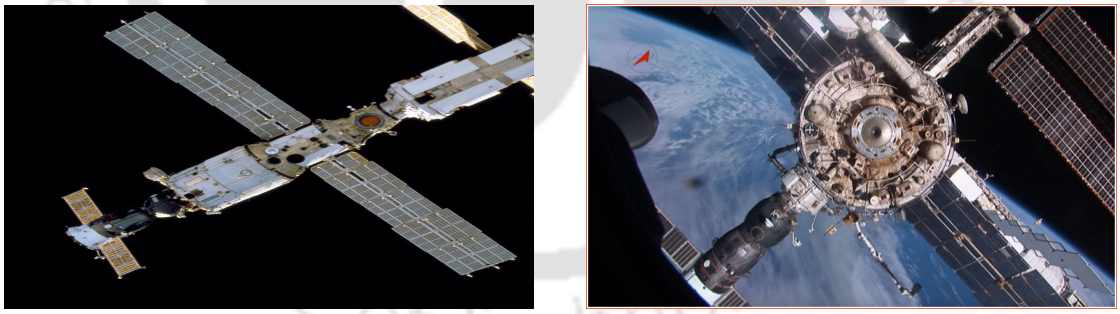

(a) (b)

Figure 1.3: (a) View of the nadir side of the Zvezda Service Module (ISS-1R). (b) Section of Zvezda Service Module (ISS-1R) as seen from an approaching transport vehicle.

Simulations of high-dimensional models such as the ones described above take considerable time and computational resources. Hence, reduced-order modelling techniques are used to obtain smaller-order approximations of high-order models based on specific performance measures. The reduction process of linear models with a high dimensional state-space representation, such as the two models stated above, can be demonstrated using Figure 1.4. In the figure, x, u, and y are the full-order model's state, input and output variables. For the same input, x_r and y_r are the state and output of the reduced-order model. The reduced-order model is a good approximation of the

original model if $y \approx y_r$.

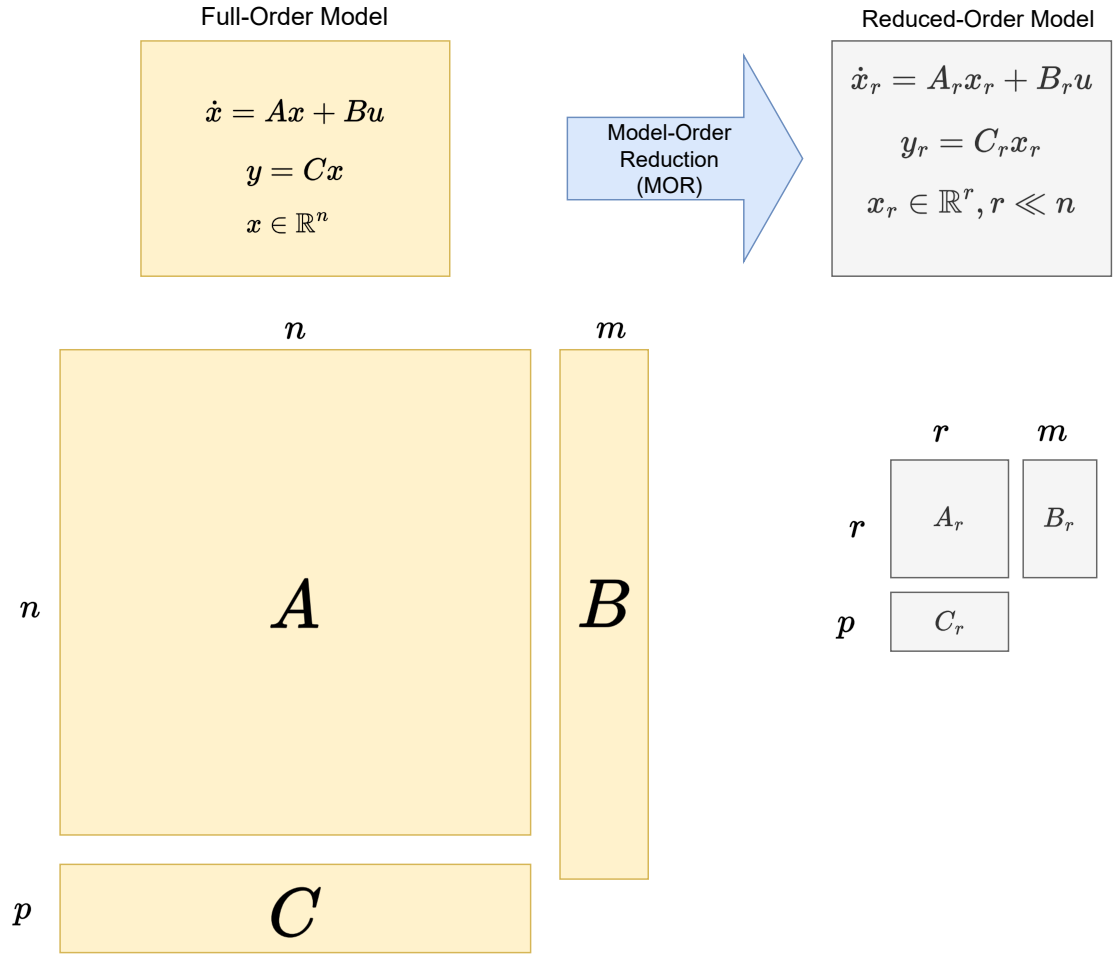

Figure 1.4: Objective of model order reduction (MOR).

The reduced-order models can be used for running real-time simulations of complex physical systems for hardware testing, creating or simplifying digital twin models, designing controllers, etc. Many areas, such as computational aerodynamics, large-scale network systems, microelectronics, electromagnetic systems, chemical processes, etc., use model order reduction techniques [12]. A comprehensive discussion on many of these techniques is available in [13] and [11].

For LTI systems, the model order reduction problem over infinite-time intervals has received considerable attention. The infinite horizon model reduction algorithms obtain reduced-order models whose output approximates the original model output over an infinite time interval $[0, \infty)$. However, in certain situations, it may be desirable to obtain reduced-order models which capture the original model's dynamics only for a finite time interval—for instance, obtaining reduced-order approximations which capture the transient response of a system (response for a fixed time interval, $[0, \tau]$ where τ is less than the system's settling time). This has led to the finite interval model order reduction problem.

Using infinite horizon model reduction algorithms for solving finite horizon model reduction problems results in substantially sub-optimal reduced-order models. The algorithms specifically designed for finite horizon model reduction perform much better for such problems. This is seen in the following examples.

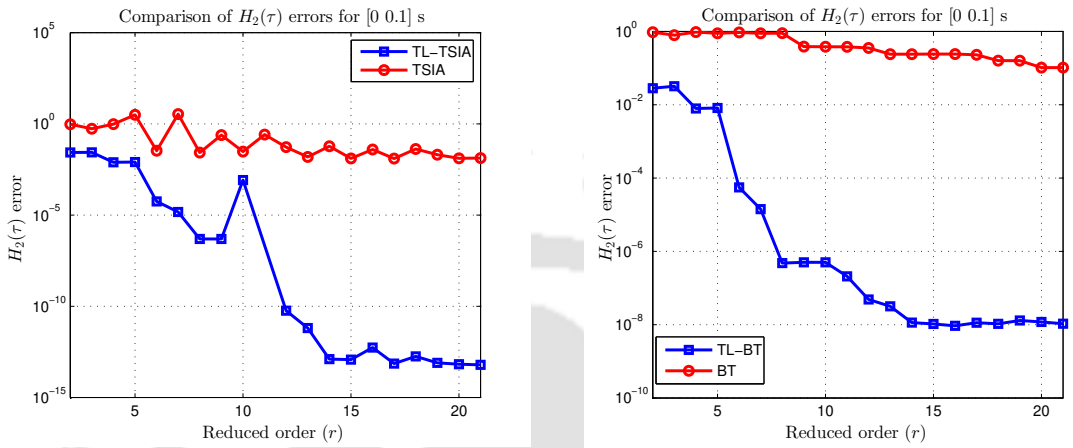

(a) (b)

Figure 1.5: (a) Approximation errors for TSIA vs TL-TSIA for the beam model. (b) Approximation errors for BT vs TL-BT for the beam model .

Consider the problem of model order reduction (MOR) of the cantilever beam model for the time interval $[0, 0.1]$ s. The beam model is asymptotically stable, and the time 0.1 s is smaller than the system's settling time. Using the popular MOR methods, BT (Balanced Truncation) and TSIA (Two-Sided Iterative Algorithm), and the finite horizon counterparts TL-BT (Time-Limited Balanced Truncation) and TL-TSIA (Time-Limited Two-Sided Iterative Algorithm), reduced-order models of orders ranging from 2 to 21 with increments of 1 are obtained. These algorithms have been explained in detail in Section 2.4, Chapter 2. The errors are measured using the $H_2(\tau)$ norm, described in Section 2.3, Chapter 2. The comparison of the $H_2(\tau)$ errors of the infinite horizon algorithms and their finite horizon counterparts are displayed in Figure 1.5a and Figure 1.5b.

Consider the MOR problem of the above ISS model for the time interval $[0, 0.5]$ s. The model is asymptotically stable, and the time interval is much smaller than the system's settling time. Reduced-order models for orders ranging from 2 to 42, with increments of 2, are obtained using BT, TSIA, TL-BT, and TL-TSIA. Figure 1.6a compares the $H_2(\tau)$ errors of TSIA and TL-TSIA whereas Figure 1.6b compares the $H_2(\tau)$ errors of BT and TL-BT.

In the above examples, it is observed that the reduced-order models obtained by finite horizon model reduction methods have $H_2(\tau)$ error norms, which are several orders of magnitude lesser than those obtained by the infinite horizon model reduction methods. Thus, the above examples justify the development of finite horizon model reduction algorithms for capturing the transient response of LTI systems.

The dynamics of systems that don't change with time or change very slowly with time can be modelled by LTI systems. However, many systems in the real world have intrinsic time-varying behaviour over a finite time interval with fixed start and end points. Such systems are modelled

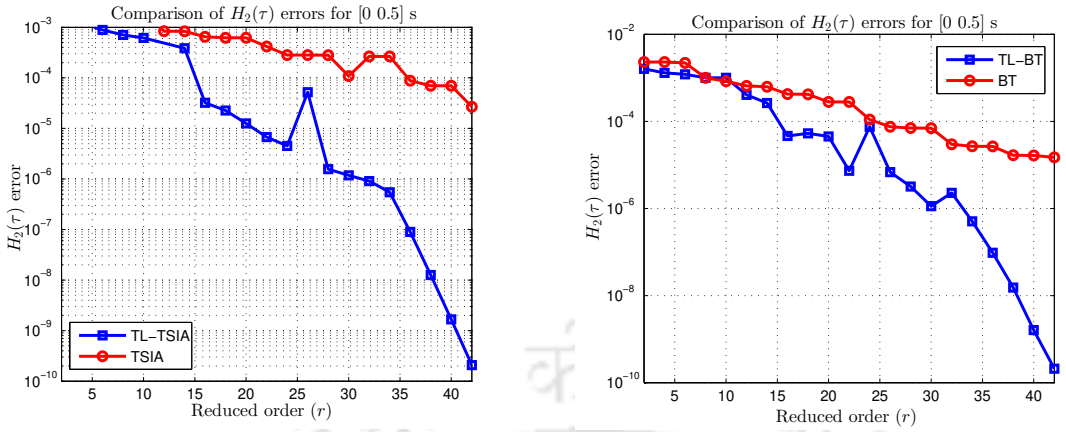

(a) (b)

Figure 1.6: (a) Approximation errors for TSIA vs TL-TSIA for the ISS model (b) Approximation errors for BT vs TL-BT for the ISS model.

by finite horizon LTV models. A typical example of such a process is a missile system (shown in Figure 1.7). The load of a missile system varies along its path. Consequently, it has time-varying system dynamics. Other examples of finite horizon time-varying systems besides missile systems are controlled swarm robots, robotic manipulators with deployable joints and flexible links, deployable space structures, bridges with crossing vehicles and many more.

Figure 1.7: The Prithvi (P-II) Missile.

Like large-scale LTI models, considerable time and computational resources are required to simulate and perform model-based control design tasks of high-order finite horizon LTV systems. Also, the time-varying nature of the parameters of LTV models further adds to the degree of complexity of the problem.

The above-mentioned reasons motivate the development of finite horizon model order reduction

techniques for obtaining accurate low-order LTI and LTV approximations of higher-order LTI and LTV models, respectively.

1.1 Literature survey

This thesis focuses on finite horizon model reduction of linear systems - both LTI and LTV systems. Before addressing research gaps in finite horizon model reduction, a brief literature survey of model reduction techniques for both finite and infinite horizons is given. Among the methods mentioned below, a few popular ones which are relevant to the work in this thesis are described in detail in Chapter 2.

1.1.1 Model order reduction of LTI systems

LTI models are characterized by two properties: linearity and time invariance. Though such models are simpler to analyze than other classes of dynamical models, they are used for describing many essential systems. An extensive amount of model order reduction literature exists for LTI systems. This includes SVD-based, interpolation-based, and H_2 optimal model order reduction methods, which are discussed below.

SVD-based methods include algorithms like Balanced Truncation (BT) [64, 65], Balanced Singular Perturbation Approximation (BSPA) [57] and Optimal Hankel Norm Approximation (OHNA) [29]. Among these algorithms, BT has been extensively studied. It involves computing the system gramians, namely, the controllability and the observability gramians, for obtaining projection matrices used for model reduction. The gramians are computed by solving a pair of algebraic Lyapunov equations (ALEs), which is computationally expensive for large-scale systems. To solve this issue, low-rank approximations of the solutions of the ALEs are computed. There are various methods for doing this, such as Krylov subspace methods (the Lanczos and the Arnoldi process) [44, 83], explicit integral representation of the gramians [33, 54], alternating direction implicit iteration (ADI) method and Smith method [56, 70].

The second category of interpolation-based MOR methods involves rational interpolation by projection and was first proposed in [100, 106]. Employing Ruhe's rational Krylov subspace method [81], Grimme proposed a robust projection framework for interpolation-based model reduction [32]. Gallivan et al. developed a tangential interpolation framework in [27]. The Krylov-based model reduction methods require matrix-vector multiplications and some sparse linear solvers, which can be implemented iteratively. Additionally, these model reduction techniques can match moments without computing them explicitly. This is crucial as the computation of moments is generally ill-conditioned. This motivates the use of Krylov-based methods. Because of this, interpolatory model reduction methods are also called moment-matching methods. Other works on model reduction by interpolation include [3, 6, 20, 21].

The H_2 optimal model reduction problem involves finding locally optimal lower order models by minimizing a H_2 error norm [35]. Finding global minimizers is difficult as the H_2 optimization problem is non-convex. Thus, the existing methods in the literature focus on finding reduced-order models that satisfy the first-order necessary conditions for H_2 optimality. The optimality

conditions are divided into two categories: Lyapunov-based and interpolation-based. Depending on the techniques employed to construct the reduced-order models, the H_2 optimal model reduction methods can be further classified into projection-based and gradient-based methods.

The Iterative Rational Krylov Algorithm (IRKA) [35] is a projection-based iterative algorithm for H_2 approximation. It is based on interpolation-based H_2 optimality conditions and uses Krylov-based interpolation methods to obtain the reduced-order model at every iteration. Another projection-based iterative algorithm for H_2 optimal model reduction is the Two-Sided Iterative Algorithm (TSIA) [104]. It employs Lyapunov-based optimality conditions. The primary challenge for gradient-based H_2 approximation methods is obtaining analytical expressions for the gradients. These expressions are substituted in gradient flow, quasi-Newton or trust-region-based algorithms to obtain reduced order models [103, 105, 88, 89]. Reference [74] obtains analytical expressions of the gradients of a frequency-limited H_2 cost function, which are used with standard optimization software to get reduced-order models which are H_2 optimal over a finite frequency interval.

1.1.2 Finite horizon model reduction of LTI systems

The above reduction methods are applicable for model order reduction over an infinite time horizon. However, one may have access to simulation data over a finite time horizon, or one might be interested in approximating the output trajectory of the original system over a finite time interval. This has inspired the model order reduction problem over a finite time horizon. Accuracy outside this time interval is not essential. SVD-based finite-time model reduction schemes include Proper Orthogonal Decomposition (POD) [40] and Time-Limited Balanced Truncation (TL-BT) [28, 34, 90]. As its name suggests, the TL-BT algorithm is a finite-time version of the infinite-time model reduction algorithm BT. Error bounds for TL-BT are derived in [78, 77]. An extensive comparison between TL-BT and modified variations of TL-BT can be found in [101]. For asymptotically stable systems, as the final time tends to infinity, the error bound in [77] converges to the H_∞ error bound for BT. The modified time-limited BT algorithm proposed in [34] preserves stability and has an apriori error bound. TL-BT is adapted for model reduction of large-scale continuous-time LTI systems in [50] and large-scale discrete-time LTI systems in [23]. In [30], a time-limited H_2 error norm - defined for a fixed time interval $[0, \tau]$ - is used as an error measure for time-limited model reduction and a model reduction algorithm minimizing this error norm is proposed. Using the same error norm, [94] proposes a descent-based iterative algorithm for model reduction, valid only for SISO systems. Further, [109] proposes an iteration-free, time-limited pseudo-optimal rational Krylov algorithm (TL-PORK).

1.1.3 Model order reduction of LTV systems

Most existing results in control theory are for LTI systems as they are simpler to analyze than time-varying models. If the time scale of the model is small compared to the life span of the modelled process, time-invariance is a reasonable assumption. This is not the case if the time scale and the life span are comparable. In such cases, LTV systems can be used for modelling physical processes as they offer a trade-off between model simplicity and the ability to describe the process's

behaviour accurately. Further, the operation of time-invariant nonlinear systems around nominal trajectories can be well approximated by LTV systems. Many theoretical results for LTI systems have been generalized to LTV systems. This section focuses on various model reduction methods for LTV systems available in the literature.

The concept of balanced realization for an LTI system has been extended to continuous-time LTV systems by [91, 93, 99]. This concept has been applied for an infinite time interval for a class of systems known as uniform LTV systems in [91]. This is similar to balanced realization in the LTI case and is used for model order reduction by truncation. The preservation of stability, controllability and observability in the reduced-order models obtained is investigated in [93]. These ideas are then extended to discrete-time LTV systems in [92]. They also propose a Hankel matrix-based model reduction approach and discuss its equivalence with uniform balanced truncation for discrete-time LTV systems. Model reduction of discrete-time LTV systems based on Hankel norm approximation is discussed in [18]. In [99], it is shown that for analytic continuous-time finite horizon LTV systems, there exists a coordinate transformation which converts the LTV system to a balanced realization at every instant of the finite horizon. This is known as finite horizon balanced realization, which is used for finite horizon balanced truncation of LTV systems.

In [51], balanced realizations are obtained using generalized gramians, which are solutions of linear matrix inequalities instead of the usual linear matrix equations. Error bounds are derived, and a model reduction procedure satisfying the error bounds is proposed. Like the previous work, [87] also uses finite-time generalized gramians - obtained by solving a pair of differential and difference Lyapunov matrix inequalities for continuous- and discrete-time LTV systems. The gramians are used to obtain a time-varying balanced realization. The realization is utilized for model order reduction, and generalized error bounds are derived, which include the error bounds derived in [51]. It is further shown that the proposed model reduction procedure preserves the input-output stability of the full-order model. Due to the use of Lyapunov inequalities instead of equations, the balanced realizations and, hence, the singular values are non-unique. This has several advantages, like the existence of balanced truncated realisations and the possibility of tighter error bounds. Error bounds for balanced truncation of LTV systems are also obtained in [39].

In [17], two recursive algorithms for model order reduction of discrete-time LTV systems are presented. These algorithms are the Recursive Low-Rank Gramian (RLRG) and the Recursive Low-Rank Hankel (RLRH) algorithms. RLRG and RLRH recursively compute projection matrices that capture the dominant behaviour of the gramians and the Hankel map, respectively. RLRH is preferred over RLRG as it is not sensitive to the coordinate system used to represent the original system. In [60, 61], a finite horizon H_2 error norm is introduced for discrete-time LTV systems. A projection-based iterative algorithm is proposed to obtain reduced-order models that minimize the error norm.

1.2 Research motivation

As evident from the literature survey, the field of time-limited model reduction for continuous-time LTI systems is less explored compared to the infinite time case. Additionally, for the case of continuous-time LTV systems, only the finite interval balanced truncation algorithm has been

extensively studied. Therefore, there is a scope for developing finite horizon model order reduction techniques for both LTI and LTV systems. This is the main focus of this thesis. Several aspects of finite horizon model order reduction where further work is possible are mentioned below.

- Although many projection-based model reduction techniques using a Krylov framework are available for infinite horizon model reduction of LTI systems, such techniques have not been explored for the finite horizon case. This research gap is addressed in the thesis.
- For time-limited H_2 optimal model reduction, the projection-based methods do not yield reduced-order models satisfying the time-limited optimality conditions exactly. This opens the possibility of using gradient-based methods to reduce the distance to optimality of the reduced models obtained by the projection-based methods. Such a method is available in [94], though it is valid only for SISO LTI systems. This motivates the development of gradient-based methods for time-limited model order reduction that are valid for both SISO and MIMO LTI systems.
- The H_2 optimal model reduction problem for LTI systems can be extended to continuous-time and discrete-time LTV systems. In [61], a H_2 error norm is proposed for discrete-time LTV systems, and a model reduction algorithm for minimizing the error norm is proposed. This leads to the possibility of developing a similar error-based model reduction technique for continuous-time LTV systems.

1.3 Contributions

Based on the above motivations, the following are the main contributions of this thesis:

- An interpolation-based Krylov framework is proposed for finite horizon model reduction. A projection-based algorithm for finite horizon H_2 optimal model reduction of continuous-time LTI systems is proposed based on it.
- Closed-form expressions of the gradients of the finite horizon H_2 error norm of LTI systems are obtained. Using them, a gradient-based method employing a standard quasi-Newton algorithm is proposed for finite horizon H_2 optimal model order reduction of continuous-time LTI systems.
- Conditions for optimality of a finite horizon H_2 error norm of continuous-time LTV systems are obtained. Based on the conditions, a projection-based iterative algorithm is proposed for finite horizon H_2 optimal model order reduction of LTV systems.

The proposed numerical methods for time-limited model order reduction of LTI and LTV systems are simulated in MATLAB. To evaluate their efficacy, the methods are compared with standard model reduction algorithms available in the literature.

1.4 Organisation of the thesis

The rest of this thesis is organised as follows.

In Chapter 2, some concepts about LTI systems theory are stated, and several algorithms for infinite horizon model order reduction of such systems are discussed. Several finite horizon model reduction algorithms for LTI systems are discussed. Concepts related to LTV systems are introduced, and a model reduction algorithm for such systems is discussed.

In Chapter 3, a projection-based model reduction method for time-limited H_2 optimal model reduction is proposed. The reduced-order models obtained by the method don't satisfy the time-limited H_2 optimality conditions exactly. The distance to optimality of the reduced-order models is also quantified.

Chapter 4 obtains closed-form expressions of the gradients of the time-limited H_2 error norm using a gramian framework. The gradients are used to propose a gradient-based optimization method, which obtains reduced-order models closer to optimality than the previous chapter's projection-based method.

Chapter 5 proposes numerical methods for computing the finite horizon reachability gramian of LTV systems, studies a finite horizon H_2 norm for LTV systems and expresses it using the system gramians.

Chapter 6 defines a finite horizon H_2 error norm between the original and the reduced-order system based on the finite horizon H_2 norm studied in Chapter 5. Conditions for minimization of the error norm are derived, and a projection-based iterative algorithm for finite horizon model order reduction of LTV systems is proposed.

Chapter 7 presents the conclusion of the research work and provides some possible future directions.

Chapter 2

Preliminaries

This chapter briefly discusses a few model order reduction (MOR) algorithms for LTI and LTV systems available in the literature. Before proceeding to the MOR techniques, some standard concepts in LTI and LTV systems are briefly introduced. Then, a few infinite and finite horizon MOR techniques are discussed. The MOR techniques described in this chapter are those against which the algorithms proposed in this thesis are benchmarked. The concepts reviewed in this chapter will provide the framework for the work on finite horizon model order reduction, which will be presented in the subsequent chapters.

2.1 Description of LTI systems

Consider an LTI system Σ of order n, with m inputs, p outputs and the following state-space realization:

$$\begin{aligned} \dot{x}(t) &= Ax(t) + Bu(t), \\ y(t) &= Cx(t), \end{aligned} \tag{2.1}$$

where $A \in \mathbb{R}^{n\times n}$, $B \in \mathbb{R}^{n\times m}$ and $C \in \mathbb{R}^{p\times n}$. The initial condition is $x(0) = x_0$ where $x_0 \in \mathbb{R}^n$.

The state transition matrix of the LTI system, given by (2.1), is the matrix exponential denoted by e^{At}. It appears in the solution of the LTI system as follows,

$$x(t) = e^{At}x(0) + \int_0^t e^{A(t-\tau)}Bu(\tau)d\tau.$$

In the above expression, the first term is the zero-input response, representing the system's state trajectory in the absence of input. The second term is called the zero-state response and it shows how the system inputs affect the state trajectory. The matrix exponential e^{At} is an $n \times n$ matrix, and it can also be expressed via the power series,

$$e^{At} = \sum_{k=0}^{\infty} \frac{1}{k!} A^k t^k,$$

where $A^0 = I_n$. The state transition matrix can also be expressed as the unique solution of the following matrix differential equation:

$$\frac{d}{dt}e^{At} = Ae^{At}$$

with initial condition $e^{At}\big|_{t=0} = I_n$. The matrix exponential is non-singular i.e. $\det(e^{At}) \neq 0$. Some of the important properties of the matrix exponential are as follows:

$$\begin{aligned} &1) \quad e^{At}e^{As} = e^{A(t+s)}, \\ &2) \quad (e^{At})^{-1} = e^{-At}, \\ &3) \quad e^{PAP^{-1}} = Pe^{A}P^{-1}, \end{aligned}$$

where P is a non-singular square matrix of appropriate size.

For $s \in \mathbb{C}$, the Laplace transform of the matrix exponential is as follows

$$\begin{aligned} &\mathcal{L}(e^{At}) \\ &= \mathcal{L}\left(I_n + tA + \frac{1}{2!}t^2A^2 + \frac{1}{3!}t^3A^3 + \cdots\right) \\ &= \mathcal{L}(1)I_n + \mathcal{L}(t)A + \frac{1}{2!}\mathcal{L}(t^2)A^2 + \frac{1}{3!}\mathcal{L}(t^3)A^3 + \cdots \end{aligned}$$

Using $\mathcal{L}(1) = \frac{1}{s}$ and $\mathcal{L}(tf(t)) = -\frac{dF}{ds}$, the above equation can be simplified as follows

$$\begin{aligned} \mathcal{L}(e^{At}) &= \frac{1}{s}I_n + \frac{1}{s^2}A + \frac{1}{2!}\frac{2!}{s^3}A^2 + \frac{1}{3!}\frac{3!}{s^4}A^3 + \cdots \\ &= \frac{1}{s}\left(I_n + \frac{1}{s}A + \frac{1}{s^2}A^2 + \frac{1}{s^3}A^3 + \cdots\right) \\ &= \frac{1}{s}\left(I_n - \frac{1}{s}A\right)^{-1} \\ &= (sI_n - A)^{-1}. \end{aligned} \tag{2.2}$$

The impulse response of the LTI system Σ is a characterization of its input-output behaviour in the time domain. It is given by the mapping $g : \mathbb{R}_+ \to \mathbb{R}^{p\times m}, t \mapsto g(t)$ where $g(t) = Ce^{At}B$ for $t \geq 0$. For zero initial condition and an admissible input $u : \mathbb{R}_+ \to \mathbb{R}^m$, the output of the system is given by $y(t) = g(t) * u(t)$.

The transfer function $G(s)$ of the LTI system Σ is the Laplace transform of the impulse response $g(t)$. It characterizes the input-output behaviour of the system in the frequency domain and is given by the mapping $G : \mathbb{C} \to \mathbb{C}^{p\times m}$, $s \mapsto G(s)$ where

$$\begin{aligned} G(s) &= \mathcal{L}(g(t)) \\ &= C\mathcal{L}(e^{At})B \quad \text{(using equation (2.2))} \\ &= C(sI_n - A)^{-1}B. \end{aligned} \tag{2.3}$$

Here, $G(s)$ is a complex-valued $p \times m$ matrix-valued rational function of degree n.

If $U(s) = \mathcal{L}(u(t))$ and $Y(s) = \mathcal{L}(y(t))$ are the Laplace transforms of the input $u(t)$ and output $y(t)$, respectively, then $Y(s) = \mathcal{L}(g(t))U(s) = G(s)U(s)$.

The results in this section are taken from [45].

2.2 System norms and gramians of LTI systems

System norms are important to measure the accuracy of lower-order approximation of high-order models. The norms considered in this thesis are the infinite and finite time versions of the H_2

norm. This section briefly describes these norms. Further, the infinite and the finite horizon system gramians, which are also essential for MOR, are also described in this section.

2.2.1 System norms

The dynamical system Σ, given by the state-space representation (2.1), can be viewed as a linear operator. System norms are used to measure the magnitude of the system operator. This section briefly describes the H_2 and the $H_2(\tau)$ system norms. In the later sections, they are used for quantifying the error between the full-order model and the reduced-order approximations in MOR problems.

H_2 norm [35, 108]: The H_2 norm of an asymptotically stable system Σ is defined as

$$\|\Sigma\|_{H_2} = \left(\frac{1}{2\pi}\int_{-\infty}^{\infty} \|G(i\omega)\|_F^2 \, d\omega\right)^{\frac{1}{2}}. \tag{2.4}$$

It is related to the $L_\infty([0,\infty))$ norm of $y(t)$ and $L_2([0,\infty))$ norm of $u(t)$ as follows:

$$\|y\|_{L_\infty([0,\infty)])} \leq \|\Sigma\|_{H_2} \, \|u\|_{L_2([0,\infty))}. \tag{2.5}$$

Thus, the H_2 norm is the $L_2([0.\infty))-L_\infty([0,\infty))$-induced norm of the underlying convolution operator ($y(t) = g(t) * u(t)$) for MISO ($p = 1$), SIMO ($m = 1$) and SISO (m=p=1) systems.

By Parseval's theorem, the H_2 norm of an asymptotically stable system Σ can also be expressed in the time domain as follows:

$$\|\Sigma\|_{H_2} = \|g\|_{L_2([0,\infty))} = \left(\int_0^{\infty} \|g(t)\|_F^2 \, dt\right)^{\frac{1}{2}}. \tag{2.6}$$

$H_2(\tau)$ norm [30, 94]: The $H_2(\tau)$ norm of the system Σ, given by (2.1), is defined as follows:

$$\|\Sigma\|_{H_2(\tau)} = \left(\int_0^{\tau} \|g(t)\|_F^2 \, dt\right)^{\frac{1}{2}}. \tag{2.7}$$

The $H_2(\tau)$ norm is related to the $L_2([0,\tau])$ norm of $u(t)$ and the $L_\infty([0,\tau])$ norm of $y(t)$ as follows:

$$\|y\|_{L_\infty([0,\tau])} \leq \|\Sigma\|_{H_2(\tau)} \, \|u\|_{L_2([0,\tau])}. \tag{2.8}$$

2.2.2 Infinite horizon system gramians

The infinite time system gramians of the system Σ are defined over the infinite time-interval $[0,\infty)$. They are obtained from the controllability and observability maps of the system. The non-singularity of the gramians is an indicator of the controllability and observability of the system.

Definition 2.2.1 (Section 9.2, [45])**.** The infinite horizon controllability and observability gramians associated with the system Σ, denoted by P and Q, respectively, are as follows:

$$P = \int_0^{\infty} e^{At} B B^T e^{A^T t} dt \,, \tag{2.9}$$

$$Q = \int_0^{\infty} e^{A^T t} C^T C e^{At} dt. \tag{2.10}$$

It is obvious from the above definition that the infinite horizon gramians are defined only if the system Σ is asymptotically stable. These gramians are computed by solving a pair of Lyapunov equations. The controllability gramian P is computed by solving the ALE,

$$AP + PA^T + BB^T = 0. \tag{2.11}$$

The observability gramian Q is computed by solving the ALE,

$$A^TQ + QA + C^TC = 0. \tag{2.12}$$

If $\text{spec}(A) \cap \text{spec}(-A) = \phi$, then P and Q are the unique solutions of the ALE's (2.11) and (2.12), respectively.

2.2.3 Finite horizon system gramians

The finite horizon system gramians of the system Σ are defined over a finite time interval. Here, a time interval of the form $[0, \tau]$ where $\tau < \infty$, is considered. Unlike the infinite horizon gramians, the finite horizon gramians may be defined even if the system Σ is not asymptotically stable.

Definition 2.2.2 ([28]). For the LTI system Σ, the time-limited controllability and observability gramians associated with the system over the finite time interval $[0, \tau]$, denoted by P_τ and Q_τ, respectively, are defined as,

$$P_\tau = \int_0^\tau e^{At}BB^Te^{A^Tt}dt\ , \tag{2.13}$$

$$Q_\tau = \int_0^\tau e^{A^Tt}C^TCe^{At}dt. \tag{2.14}$$

The time-limited gramians are computed by solving a pair of time-limited ALEs. The time-limited controllability gramian P_τ is obtained by solving the time-limited ALE

$$AP_\tau + P_\tau A^T + BB^T - e^{A\tau}BB^Te^{A^T\tau} = 0. \tag{2.15}$$

The time-limited observability gramian Q_τ is obtained by solving the time-limited ALE

$$A^TQ_\tau + Q_\tau A + C^TC - e^{A^T\tau}C^TCe^{A\tau} = 0. \tag{2.16}$$

2.3 The model order reduction problem and error norms

This section first discusses the MOR problem for finite and infinite horizon cases. An essential component of the MOR problem is choosing an appropriate error measure for obtaining a high-fidelity reduced-order approximation of the original large-scale model. The distance between the original and the reduced-order model is measured using error norms. This section describes the H_2 and the $H_2(\tau)$ error norm that is used subsequently in this thesis.

Consider a reduced-order LTI system Σ_r with the following state-space representation:

$$\begin{aligned} \dot{x}_r(t) &= A_rx_r(t) + B_ru(t), \\ y_r(t) &= C_rx_r(t), \end{aligned} \tag{2.17}$$

where $A_r \in \mathbb{R}^{r\times r}$, $B_r \in \mathbb{R}^{r\times m}$ and $C_r \in \mathbb{R}^{p\times r}$ with $r \ll n$ such that the output $y_r(t)$ is a good approximation of the original output $y(t)$ over the time-interval $[0,\infty)$ with respect to a suitable norm. Let $g_r(t) = C_r e^{A_r t} B_r$ be the impulse response of the system. The output of the system for any admissible input $u(t)$ is $y_r(t) = g_r(t) * u(t)$.

Similar to (2.2), the Laplace transform of $e^{A_r t}$ is $\mathcal{L}(e^{A_r t}) = (sI_r - A_r)^{-1}$. Let $G_r(s)$ be the Laplace transform of the impulse response $g_r(t)$. It is known as the transfer function of the system and is given by

$$\begin{aligned} G_r(s) &= \mathcal{L}(g_r(t)) \\ &= C_r \mathcal{L}(e^{A_r t}) B_r \\ &= C_r \left(sI_r - A_r\right)^{-1} B_r. \end{aligned} \tag{2.18}$$

Let $Y_r(s)$ be the Laplace transform of the system output. It is given by $Y_r(s) = G_r(s)U(s)$.

The objective of infinite horizon MOR is to obtain a reduced-order model Σ_r, which approximates the full-order model Σ over the infinite time interval $[0,\infty)$. This is true if the original system output $y(t)$ is close to the reduced-order system output $y_r(t)$ over the infinite time interval $[0,\infty)$ for an appropriate norm. For finite horizon MOR, the objective is to obtain a reduced-order model Σ_r, which approximates the full-order model Σ over the finite time interval $[0,\tau]$ with $\tau < \infty$. Thus, in this case, the original system output $y(t)$ has to be close to the reduced system output for an appropriate norm over the finite time interval $[0,\tau]$. The closeness of the system outputs outside this time interval is not essential.

The error norms that are used to measure the closeness of the system outputs are discussed now. In the time domain, the error between the system outputs is given by $y(t) - y_r(t) = (g(t) - g_r(t)) * u(t)$, whereas the error between the system outputs in the frequency domain can be expressed as $Y(s) - Y_r(s) = (G(s) - G_r(s))U(s)$. Thus, in the time domain, the closeness of $y(t)$ and $y_r(t)$ is directly related to the closeness of $g(t)$ and $g_r(t)$. In the frequency domain, the closeness of $Y(s)$ and $Y_r(s)$ is directly related to the closeness of $G(s)$ and $G_r(s)$. For infinite horizon MOR, the closeness is measured using the H_2 error norm. Further, for the finite horizon case, the $H_2(\tau)$ error norm is used for measuring the quality of the reduced-order approximation.

- **H_2 error norm [35, 108] :** The H_2 error norm between the systems Σ and Σ_r, given by (2.1) and (2.17), respectively, is defined as follows:

$$\|\Sigma - \Sigma_r\|_{H_2} = \left(\int_0^\infty \|g(t) - g_r(t)\|_F^2 \, dt \right)^{\frac{1}{2}}. \tag{2.19}$$

  This error norm satisfies the following relation,

$$\|y - y_r\|_{L_\infty([0,\infty))} \leq \|\Sigma - \Sigma_r\|_{H_2} \|u\|_{L_2([0,\infty))}. \tag{2.20}$$

  Due to the above relation, if a model reduction method produces a small H_2 error norm, then (2.20) ensures that the reduced model output $y_r(t)$ is close to the original output $y(t)$ for all admissible inputs $u(t)$ with finite $L_2([0,\infty))$ norm.

- **$H_2(\tau)$ error norm [30, 94]:** The $H_2(\tau)$ error norm between systems Σ and Σ_r, given by

(2.1) and (2.17), respectively, is defined as follows:

$$\|\Sigma - \Sigma_r\|_{H_2(\tau)} = \left(\int_0^\tau \|g(t) - g_r(t)\|_F^2 \, dt \right)^{\frac{1}{2}}. \tag{2.21}$$

The error norm satisfies the following relation:

$$\|y - y_r\|_{L_\infty([0,\tau])} \leq \|\Sigma - \Sigma_r\|_{H_2(\tau)} \|u\|_{L_2([0,\tau])}. \tag{2.22}$$

Due to the above relation, the $H_2(\tau)$ error norm is an upper bound of the norm induced by the operator $(\Sigma - \Sigma_r)$ from the $L_2([0,\tau])$ space to the $L_2([0,\tau])$ space. If a time-limited model reduction method produces a small $H_2(\tau)$ error norm, then the inequality (2.22) ensures that the reduced model output $y_r(t)$ is close to the original output $y(t)$ for all admissible inputs $u(t)$ with a finite $L_2([0,\tau])$ norm.

2.4 Finite and infinite horizon MOR methods

Following the definition of the finite and infinite horizon MOR problems in the previous section, several methods for MOR available in the literature are introduced in this section. These methods are broadly divided into two categories: projection-based and descent-based methods. Both categories and MOR methods associated with them are discussed below.

2.4.1 Projection-based model reduction methods

In methods based on projection-based model reduction [9], an n^{th} order system is projected onto a lower r dimensional subspace to obtain a reduced-order approximation of order r. While projecting onto a lower dimensional subspace, it must be ensured that the projected system has an r-dimensional state-space representation. This is done by choosing a pair of r-dimensional subspaces of $\mathbb{R}^n$, namely, $\mathcal{V}$ and $\mathcal{W}$. Let $V, W \in \mathbb{R}^{n\times r}$ be matrices such that $\mathcal{V} = \text{Ran}(V)$ and $\mathcal{W} = \text{Ran}(W)$. The n-dimensional state trajectory $x(t)$ is approximated by another n-dimensional trajectory $\tilde{x}(t)$ which satisfies the following two conditions:

1. $\tilde{x}(t)$ is contained in $\mathcal{V}$, and
2. $\frac{d\tilde{x}}{dt} - A\tilde{x} - Bu$ is contained in $\mathcal{W}^\perp$.

The first condition implies that there exists $x_r(t) \in \mathbb{R}^r$ such that $\tilde{x}(t) = Vx_r(t)$. The second condition implies that

$$W^T\left(\frac{d\tilde{x}}{dt} - A\tilde{x} - Bu\right) = 0. \tag{2.23}$$

Substituting $\tilde{x}(t) = Vx_r(t)$ in the above equation gives

$$W^TV\frac{d}{dt}x_r(t) = W^TAVx_r(t) + W^TBu(t).$$

If W^TV is non-singular, then

$$\frac{d}{dt}x_r(t) = (W^TV)^{-1}W^TAVx_r(t) + (W^TV)^{-1}W^TBu(t).$$

The output of the approximation is given by

$$y_r(t) = C\tilde{x}(t) = CVx_r(t) \tag{2.24}$$

A state-space representation of the projected system is obtained above. Setting $Z^T = (W^TV)^{-1}W^T$, the state-space matrices of the reduced-order model are obtained as

$$A_r = Z^TAV, \quad B_r = Z^TB \quad \text{and} \quad C_r = CV. \tag{2.25}$$

If $W = V$, then the projection method is called a Galerkin projection and the reduced-order model obtained is called a Galerkin projection-based reduced-order model. If $W \neq V$, the above projection method is called a Petrov-Galerkin projection and the reduced-order model is called a Petrov-Galerkin projection-based reduced-order model.

The subspaces $\mathcal{W}$ and $\mathcal{V}$ are chosen such that the input-output behaviour of the reduced-order system is close to that of the original system. The norm under which this closeness is measured and the specific techniques used for constructing matrices W and V spanning $\mathcal{W}$ and $\mathcal{V}$, respectively, give rise to a variety of projection-based infinite and finite horizon model reduction techniques. The infinite horizon methods include Balanced Truncation (BT) and the H_2 optimal model reduction techniques, namely, the Iterative Rational Krylov Algorithm (IRKA) and the Two-Sided Iterative Algorithm (TSIA). The finite horizon methods include Time-Limited Balanced Truncation (TL-BT) and the $H_2(\tau)$ optimal model reduction method called Time-Limited Two-Sided Iterative Algorithm (TL-TSIA). These methods are described below in detail.

2.4.1.1 Balanced Truncation (BT)

The Balanced Truncation (BT) algorithm, proposed in [64], is an SVD-based model reduction algorithm for LTI systems. It involves obtaining a balanced realization of an LTI system by simultaneously diagonalizing the system's controllability and observability gramians, denoted by P and Q, respectively, using a similarity transformation known as the balancing transformation, T_{BAL}. In the balanced realization, the controllability and the observability gramians are in diagonal form and are identical. The diagonal elements of the gramians of the balanced system are known as Hankel singular values (σ_i). They are the positive square roots of the eigenvalues of PQ, i.e. $\sigma_i = (\lambda_i(PQ))^{\frac{1}{2}}$. These singular values are invariant under basis transformations, and in the case of many LTI systems, they decay rapidly. The states corresponding to smaller Hankel singular values are difficult to control and observe. These states can be truncated to obtain reduced-order models without significantly affecting the input-output behaviour of the original system. If the original model is asymptotically stable, then the reduced-order model obtained by BT is also asymptotically stable [73]. Further, an error bound between the original and the reduced-order model is obtained in [24, 29]. BT involves truncating the balanced realization of the full-order system to obtain a reduced-order approximation. In [85], it is shown that when some modes of the full-order system are nearly uncontrollable or unobservable, the product PQ has a high condition number. In such a case, calculating the balancing transformation T_{BAL} may be poorly conditioned. Two algorithms for obtaining reduced-order approximations without balancing the original model are proposed to overcome this drawback in [85]. One of them is the square root method. An outline of this method is given below.

Algorithm 1: Square-root Balanced Truncation without balancing [85]

Input: The system matrices (A, B, C) belonging to an asymptotically stable system of order n;
reduced order r;

Output: The matrices (A_r, B_r, C_r) of the reduced-order system;

1. Compute the controllability and the observability gramians P and Q by solving the ALEs (2.11) and (2.12), respectively ;
2. Obtain the matrices L_P and L_Q by the Cholesky decomposition of P and Q, respectively, as follows:

$$P = L_P L_P^T, \quad Q = L_Q L_Q^T \quad ;$$

3. Compute the singular value decomposition:

$$L_Q^T L_P = \begin{bmatrix} U_1 & U_2 \end{bmatrix} \begin{bmatrix} \Sigma_1 & \mathbf{0}_{k\times(n-k)} \\ \mathbf{0}_{(n-k)\times k} & \Sigma_2 \end{bmatrix} \begin{bmatrix} V_1^T \\ V_2^T \end{bmatrix},$$

where $\Sigma_1 = \text{diag}\{\sigma_1, \ldots, \sigma_k\}$ contains the k-largest Hankel singular values. ;

4. Construct the following projection matrices,

$$Z_r = L_Q U_1 \Sigma_1^{-\frac{1}{2}} \quad \in \mathbb{R}^{n\times k},$$
$$V_r = L_P V_1 \Sigma_1^{-\frac{1}{2}} \quad \in \mathbb{R}^{n\times k}.$$

5. Obtain the reduced-order model using the Petrov-Galerkin projection method (2.25), as follows:

$$A_r = {Z_r}^T A V_r, \; B_r = {Z_r}^T B, \text{ and } C_r = C V_r.$$

The BT algorithm outlined above produces good reduced-order models. However, as it involves solving two Lyapunov equations to obtain the system gramians, it is computationally expensive for large-scale systems.

2.4.1.2 Projection-based H_2 optimal MOR

The H_2 optimal model reduction problem involves obtaining Σ_r, an r^{th} order approximation of the system Σ, which is the solution of the following minimization problem:

$$\Sigma_r = \underset{\text{s.t. } \text{ord}(\hat{\Sigma})=r}{\text{argmin}} \left\| \Sigma - \hat{\Sigma} \right\|_{H_2}, \tag{2.26}$$

where $\left\| \Sigma - \hat{\Sigma} \right\|_{H_2}$ is the H_2 error norm between Σ and $\hat{\Sigma}$, as defined in (2.19).

The H_2 optimization problem, given by (2.26), is non-convex and finding a global minimizer is difficult. Usually, the problem is solved by finding a locally optimal reduced-order model satisfying first-order necessary conditions for H_2 optimality. The optimality conditions can be formulated as Lyapunov-based [103] and interpolation-based [59] conditions. Based on these conditions, algorithms are proposed for obtaining reduced-order models satisfying these conditions. The Lyapunov-

based and interpolation-based optimality conditions, model reduction algorithms based on them and the connection between them are discussed below.

Interpolation-based method [35]: For LTI systems, the MOR problem can be formulated as a rational approximation problem of finding a degree r rational function $G_r(s)$ which approximates the degree n rational function $G(s)$ accurately with respect to an appropriate error norm. Interpolation is commonly used for function approximation as polynomial interpolants are easy to calculate. For SISO systems, the interpolation-based MOR problem involves obtaining the interpolating rational function $G_r(s)$ such that $G(\sigma_i) = G_r(\sigma_i)$ for a set of r interpolation points $\{\sigma_1, \ldots, \sigma_r\}$.

For MIMO systems, apart from interpolation points, the interpolation-based MOR problem involves interpolation directions called tangential directions. The points and directions can be divided into left and right categories. The interpolation problem, in this case, is as follows: Given a set of r right interpolation points $\{\sigma_1, \ldots, \sigma_r\} \in \mathbb{C}$, r right tangential directions $\{b_1, \ldots, b_r\} \in \mathbb{C}^m$, r left interpolation points $\{\mu_1, \ldots, \mu_r\} \in \mathbb{C}$ and r left tangential directions $\{c_1, \ldots, c_r\} \in \mathbb{C}^p$, obtain a degree-$r$ reduced transfer function $G_r(s)$ so that

$$G(\sigma_i)b_i = G_r(\sigma_i)b_i, \tag{2.27}$$

$$c_i^T G(\mu_i) = c_i^T G_r(\mu_i) \tag{2.28}$$

for $i = 1, \ldots, r$. If $\sigma_i = \mu_i$, then

$$c_i^T G^{'}(\sigma_i)b_i = c_i^T G_r^{'}(\sigma_i)b_i. \tag{2.29}$$

where $G^{'}(s) = \frac{dG}{ds}(s)$ and $G_r^{'}(s) = \frac{dG_r}{ds}(s)$. The following theorem (based on the Petrov-Galerkin projection method) proposes a technique for deciding the model reduction basis V and W so that the reduced-order model satisfies the tangential interpolation conditions stated above.

Theorem 2.4.1 ([35], Lemma 2.1)**.** *Consider the transfer functions $G(s)$ of Σ and $G_r(s)$ of Σ_r, given by (2.1) and (2.17), respectively. Let the state-space matrices of Σ_r be as follows: $A_r = (W^TV)^{-1}W^TAV$, $B_r = (W^TV)^{-1}W^TB$ and $C_r = CV$. Assume that $\sigma, \mu \in \mathbb{C}$ and $(sI_n - A)$ and $(sI_r - A_r)$ are invertible for $s = \sigma, \mu$. If $b \in \mathbb{C}^m$ and $c \in \mathbb{C}^p$ are fixed non-trivial vectors, then*

1. *If $(\sigma I_n - A)^{-1}Bb \in \mathrm{Ran}(V)$, then*

$$G(\sigma)b = G_r(\sigma). \tag{2.30}$$

2. *If $(\mu I_n - A)^{-T}C^Tc \in \mathrm{Ran}(W)$, then*

$$c^TG(\mu) = c^TG_r(\mu). \tag{2.31}$$

3. *If both (2.30) and (2.31) hold and $\sigma = \mu$, then*

$$c^TG^{'}(\sigma)b = c^TG_r^{'}(\sigma)b.$$

The above theorem suggests a method for constructing the projection matrices V and W in order to obtain reduced-order models satisfying the tangential interpolation conditions (2.28) and (2.27). A pair of such projection matrices V and W are given by

$$\text{Ran}(V) = \text{Ran}([(\sigma_1 I_n - A)^{-1}Bb_1 \ \dots \ (\sigma_r I_n - A)^{-1}Bb_r]), \quad \text{and} \tag{2.32}$$

$$\text{Ran}(W) = \text{Ran}([(\mu_1 - A)^{-T}C^T c_1 \ \dots\dots \ (\mu_r - A)^{-T}C^T c_r]). \tag{2.33}$$

In the case of SISO systems, the columnspaces of the projection matrices V and W resemble rational Krylov subspaces (described in Remark 1). Hence, interpolation-based model reduction for SISO systems is also referred to as rational Krylov method. For MIMO systems, the columnspaces of V and W are not rational Krylov subspaces unless all tangent directions are the same. Therefore, in this case, the term interpolation-based method is more appropriate.

Remark 1. Krylov subspaces are used in iterative methods for computing eigenvalues of structured/sparse matrices [84]. Given a matrix A (whose eigenvalue is to be computed), an initial vector v and $j \in \mathbb{N}$, the Krylov subspace $\mathcal{K}^j(A, v)$ is defined as $\text{Ran}\{v, Av, \dots, A^{j-1}v\}$. In [81], [82], rational functions in A are used for eigenvalue computation instead of the standard powers of A. Here, the central idea is to use the Krylov subspace $\mathcal{F}^j(A, v) = \{\phi_1(A)v, \phi_2(A)v, \dots, \phi_j(A)v\}$, where $\phi_i(\lambda)$ are rational functions in λ. These modified Krylov subspaces are known as rational Krylov subspaces. The motivation of the rational Krylov methods is to choose the rational functions in a manner which speeds up the convergence of the iterative methods.

The Petrov-Galerkin projection method for interpolation-based MOR discussed above obtains a reduced-order model, which is a tangential interpolation of the full-order model for a given set of interpolation points and tangential directions. However, to obtain H_2 optimal reduced-order models, a proper strategy for choosing the interpolation points and directions is required. Such a strategy can be obtained from the interpolation-based first-order necessary conditions for H_2 optimality, stated in the following theorem.

Theorem 2.4.2 ([98, 35]). *Let the reduced-order system Σ_r with transfer function $G_r(s)$ be the best r^{th} order rational approximation of the full-order system Σ with transfer function $G(s)$, with respect to the H_2 norm. The pole-residue representation of $G_r(s)$ is given by,*

$$G_r(s) = \sum_{k=1}^{r} \frac{c_k b_k^T}{s - \lambda_k}, \tag{2.34}$$

where $\lambda_k \in \mathbb{C}$, $c_k \in \mathbb{C}^p$ and $b_k \in \mathbb{C}^m$ for $k = 1, \ldots, r$. Then,

$$\begin{aligned} G(-\lambda_k)b_k &= G_r(-\lambda_k)b_k, \\ c_k^T G(-\lambda_k) &= c_k^T G_r(-\lambda_k), \quad \textit{and} \\ c_k^T G'(-\lambda_k)b_k &= c_k^T G_r{}'(-\lambda_k)b_k, \end{aligned}$$

for $k = 1, \ldots, r$.

The above theorem connects H_2 optimal model reduction problem and tangential interpolation. The optimal interpolation points and tangent directions are obtained from the pole-residue representation of the transfer function $G_r(s)$ of the optimal reduced-order model. The optimal interpolation points are the mirror images of the poles of the transfer function $G_r(s)$, and the residues associated with the poles are the optimal tangential directions. If the optimal interpolation points and tangential directions are known a priori, right and left projectors V and W, respectively, can be constructed. These projectors can then obtain a reduced-order model via Petrov-Galerkin projection. From Theorem 2.4.2, it is seen that the reduced-order model should satisfy the interpolation-based H_2 optimality conditions. However, the optimal interpolation points and tangential directions are not known beforehand. An iterative correction framework called Iterative Rational Krylov Algorithm (IRKA) for constructing the projectors V and W is proposed in [35]. An outline of IRKA is stated below.

Algorithm 2: Iterative Rational Krylov Algorithm (IRKA)[35]

Input: The system matrices: A, B, C;

Initial interpolation points: $\{\sigma_1, \ldots, \sigma_r\}$;

Initial tangential directions: $\tilde{B} = [b_1, \ldots, b_r]$ and $\tilde{C} = [c_1, \ldots, c_r]$;

Output: The reduced matrices A_r, B_r, C_r;

1. Compute the projection matrices, V_r and W_r, such that

$$\text{Ran}(V_r) = \text{Ran}([(\sigma_1 I_n - A)^{-1} B b_1 \ldots (\sigma_r I_n - A)^{-1} B b_r]), \quad \text{and} \tag{2.35}$$

$$\text{Ran}(W_r) = \text{Ran}([(\sigma_1 I_n - A)^{-T} C^T c_1 \ldots\ldots (\sigma_r I_n - A)^{-T} C^T c_r]), \tag{2.36}$$

respectively, and let ${Z_r}^T = ({W_r}^T V_r)^{-1} {W_r}^T$;

2. **while** *(not converged)* **do**

   a. $A_r = {Z_r}^T A V_r$, $B_r = {Z_r}^T B$, $C_r = C V_r$;

   b. Compute $A_r = R \Lambda R^{-1}$ where R^{-1} and R are the left and right eigenvectors of A_r ;

   c. Update interpolation points and tangential directions as follows:

      i. $\sigma_i \leftarrow -\lambda_i(\Lambda)$ for $i = 1, 2, \ldots, r$,

      ii. $\tilde{B} = {B_r}^T R^{-T}$ and

      iii. $\tilde{C} = C_r R$;

   d. Update V_r and W_r using (2.35) and (2.36), respectively, and let ${Z_r}^T = ({W_r}^T V_r)^{-1} {W_r}^T$;

end

3. $A_r = {Z_r}^T A V_r$, $B_r = {Z_r}^T B$, $C_r = C V_r$;

A convergence proof of IRKA for LTI systems with a symmetric state-space representation is given in [26]. Numerical experiments have shown that for a fixed reduced-order, IRKA, upon convergence, yields high-fidelity reduced-order models for general LTI systems. These reduced-order models satisfy the H_2 optimality conditions.

Lyapunov-based method: Based on the Lyapunov-based H_2 optimality conditions stated in Corollary 2.4.4, a projection-based MOR algorithm called TSIA is proposed in [104]. The optimality conditions are obtained from the gradients of the H_2 error norm using a gramian-based framework. They are stated in the following theorem.

Theorem 2.4.3 ([98], Theorem 3.3). *For $J := \|\Sigma - \Sigma_r\|_{H_2}$, the gradients $\nabla_{A_r} J$, $\nabla_{B_r} J$ and $\nabla_{C_r} J$ are given by*

$$\begin{aligned} \nabla_{A_r} J &= 2(Q_r P_r + Y^T X), \\ \nabla_{B_r} J &= 2(Q_r B_r + Y^T B), \quad \textit{and} \\ \nabla_{C_r} J &= 2(C_r P_r - C X), \end{aligned}$$

where

$$A^TY + YA - C^TC_r = 0, \qquad AX + XA_r{}^T + BB_r{}^T = 0, \tag{2.37}$$

$$A_r{}^TQ_r + Q_rA_r + C_r{}^TC_r = 0, \qquad A_rP_r + P_rA_r{}^T + B_rB_r{}^T = 0. \tag{2.38}$$

The two Sylvester equations in (2.37) have unique solutions if $\text{spec}(A) \cap \text{spec}(-A_r) = \phi$. Similarly, the two Lyapunov equations in (2.38) have unique solutions if $\text{spec}(A_r) \cap \text{spec}(-A_r) = \phi$.

The above theorem leads to Lyapunov-based first-order necessary conditions for H_2 optimality, given by the following corollary.

Corollary 2.4.4. *Let the reduced-order system Σ_r, with state-space representation (2.17), be the best r^{th} order approximation of the full-order system Σ, with state-space representation (2.1), then*

$$\nabla_{A_r} J = Q_rP_r + Y^TX = 0, \tag{2.39}$$

$$\nabla_{B_r} J = Q_rB_r + Y^TB = 0, \quad \textit{and} \tag{2.40}$$

$$\nabla_{C_r} J = C_rP_r - CX = 0, \tag{2.41}$$

where the matrices P_r and Q_r are solutions of the ALEs given by (2.38). The matrices X and Y are solutions of the Sylvester equations given by (2.37).

The above corollary results in the following theorem.

Theorem 2.4.5 ([98], Theorem 3.4)**.** *The following identities are obtained for every stationary point of J (as defined in Theorem 2.4.3) where P_r and Q_r are invertible.*

$$A_r = W^TAV, \quad B_r = W^TB, \quad C_r = CV, \quad W^TV = I_n, \tag{2.42}$$

with $W \coloneqq -YP_r^{-1}$, $V \coloneqq XP_r^{-1}$, where X, Y, P_r and Q_r satisfy the equations (2.38) and (2.37).

The above theorem can be rewritten as the following projection problem: a projector $\pi \coloneqq VW^T$ is constructed where V and W are obtained by solving the following Sylvester equations:

$$(Q_rW^T)A + A_r^T(Q_rW^T) + C_r^TC = 0,$$
$$A(VP_r) + (VP_r) + BB_r^T = 0.$$

P_r and Q_r are normalization which ensure that $W^TV = I_n$. Equations (2.37), (2.38) and (2.42) can be considered as the coupled equations:

$$(X, Y, P_r, Q_r) = f(A_r, B_r, C_r) \quad \text{and} \quad (A_r, B_r, C_r) = g(X, Y, P_r, Q_r*),$$

which leads to a fixed-point $(A_r, B_r, C_r) = g(f(A_r, B_r, C_r))$ at every stationary point of $J(A_r, B_r, C_r)$. This indicates that an iterative procedure $(X, Y, P_r, Q_r) = f(A_r, B_r, C_r)_{i+1}$, $(A_r, B_r, C_r) = g(X, Y, P_r, Q_r)$ converges to a nearby fixed point.

The above explanation is the idea behind the iterative correction framework TSIA, where each iteration involves obtaining two projection matrices by solving Sylvester equations. A reduced-order model is obtained by Petrov-Galerkin projection. An outline of TSIA is given below.

Algorithm 3: Two-Sided Iterative Algorithm (TSIA) [104]

Input: The full-order system matrices: A, B, C;

The initial reduced-order system matrices: A_r, B_r, C_r;

Output: The reduced matrices A_r, B_r, C_r satisfying (2.39), (2.40) and (2.41);

while *(not converged)* **do**

1. Solve the following pair of Sylvester equations:

$$AX + XA_r{}^T + BB_r{}^T = 0, \tag{2.43}$$

$$A^Y Y + YA_r - C^T C_r = 0; \tag{2.44}$$

2. Obtain $V_r, W_r \in \mathbb{R}^{n\times r}$ such that $\text{Ran}(V_r) = \text{Ran}(X)$ and $\text{Ran}(W_r) = \text{Ran}(Y)$ with W_r and V_r having orthonormal columns. Also compute $Z_r^T = (W_r^T V_r)^{-1} W_r^T$;
3. Obtain the reduced model

$$A_r = Z_r^T A V_r, \quad B_r = Z_r^T B, \quad \text{and} \quad C_r = CV_r \tag{2.45}$$

end

For a fixed r, the reduced model obtained upon convergence of TSIA satisfies the Lyapunov-based H_2 optimality conditions. The derivations of the theorems stated above and discussion regarding the motivation for TSIA are given in [98].

Comparison of the interpolation-based and Lyapunov-based H_2 optimality conditions: The statements of the interpolation-based and the Lyapunov-based conditions for H_2 optimality lead to the following query: whether the optimality conditions are equivalent. The following theorem establishes the equivalence between them.

For $i = 1, \ldots, r$, let λ_i be an eigenvalue of A_r and let r_i and l_i be the corresponding right and left eigenvectors. Then

$$A_r r_i = \lambda_i r_i, \quad l_i^T A_r = \lambda_i l_i^T, \quad C_r r_i = \hat{c}_i, \quad \text{and} \quad l_i^T B_r = \hat{b}_i^T. \tag{2.46}$$

Theorem 2.4.6 ([98], Theorem 4.1)**.** *Let the transfer function of the system Σ_r with state-space representation (2.17) have the pole-residue formulation: $G_r(s) = \sum_{k=1}^{r} \frac{c_k b_k^T}{s-\lambda_k}$ with distinct first-order poles. Consider the left and right eigenvectors of the state-space matrix A_r and the other notations as given by (2.46). Then for $i, j = 1, \ldots, r$ and $i \neq j$*

$$\begin{aligned}
\frac{1}{2}(\nabla_{B_r} J)^T r_i &= \left[G^T(-\hat{\lambda}_i) - G_r{}^T(-\hat{\lambda}_i)\right] \hat{c}_i, \\
\frac{1}{2} l_i^T (\nabla_{C_r} J)^T &= b_i^T \left[G^T(-\hat{\lambda}_i) - G_r{}^T(-\hat{\lambda}_i)\right], \\
\frac{1}{2} l_i^T (\nabla_{A_r} J)^T r_i &= b_i^T \left.\frac{d}{ds}\left[G^T(s) - G_r{}^T(s)\right]\right|_{s=-\hat{\lambda}_i} \hat{c}_i, \\
\frac{1}{2} l_i^T (\nabla_{A_r} J)^T r_j &= \frac{1}{2(\hat{\lambda}_i - \hat{\lambda}_j)} \left[\hat{b}_i^T (\nabla_{B_r} J)^T r_j - l_i^T (\nabla_{C_r} J)^T \hat{c}_j\right].
\end{aligned}$$

Let $R = [r_i \ldots r_r]$, then from the above theorem, it is seen that the off-diagonal elements of $R^{-1}(\nabla_{A_r} J)^T R$ disappear when $(\nabla_{B_r} J)^T$ and $(\nabla_{C_r} J)^T$ disappear. Thus, to characterize the Lyapunov-based optimality conditions, only the terms $\text{diag}(R^{-1}(\nabla_{A_r} J)^T R)$, $(\nabla_{B_r} J)^T$ and $(\nabla_{C_r} J)^T$ are necessary.

Using the above theorem, it is easily verified that the interpolation-based and the Lyapunov-based H_2 optimality conditions are equivalent.

Comparison of IRKA and TSIA: The equivalence between the interpolation-based and the Lyapunov-based H_2 optimality conditions is established above. This naturally leads to exploring the equivalence between the projection-based iterative corrections frameworks based on them, namely IRKA and TSIA, respectively. This has been done in the following theorem for SISO systems.

Theorem 2.4.7 ([14], Theorem 1)**.** *Let Σ, given by (2.1) be a full-order model and Σ_r, given by (2.17) be its reduced-order approximation. Let the transfer function of the reduced-order system $G_r(s)$ have the pole-residue representation given by (2.34). Assume that (A_r, B_r) is controllable and $({A_r}^T, {C_r}^T)$ is observable. Also, assume that $\sigma_i = -\lambda_i(A_r)$ for $i = 1, \ldots, r$ and construct V and W using (2.32) and (2.33), respectively. Further, let X and Y be obtained by solving (2.43) and (2.44), respectively. Then,* $\mathrm{Ran}(X) = \mathrm{Ran}(V)$ *and* $\mathrm{Ran}(Y) = \mathrm{Ran}(W)$.

The above theorem shows that IRKA and TSIA produce comparable projection subspaces; thus, the two algorithms are alternative formulations of each other. As TSIA uses the interpolation idea implicitly, the same interpolation point convergence criteria can be used for both algorithms.

The model reduction algorithms discussed above are for the infinite horizon case. In the following subsections, finite horizon counterparts of these methods are discussed.

2.4.1.3 Time-Limited Balanced Truncation (TL-BT)

The first finite horizon MOR algorithm discussed is a time-limited version of BT, proposed in [28], called TL-BT. Similar to BT, a balanced realization of the full-order system is first obtained where the time-limited controllability(P_τ) and observability gramians(Q_τ), respectively, are diagonal and equal. The diagonal entries are the square roots of the eigenvalues of $P_\tau Q_\tau$, known as time-limited Hankel singular values. The states corresponding to small time-limited Hankel singular values are truncated to obtain reduced-order models. Unlike BT, TL-BT does not preserve the asymptotic stability of the full-order model. Various error bounds exist for TL-BT. An H_2 type error bound is derived in [78]. Another error bound for TL-BT is derived in [77], which converges to the H_∞ error bound for asymptotically stable systems.

Computing a balancing transformation and truncating a balanced system to obtain a reduced-order model may not be well-conditioned if the full-order system is nearly uncontrollable or unobservable. A modified time-limited version of Algorithm 1 obtains a reduced-order model without balancing the full-order model [50]. An outline of the algorithm is given below.

Algorithm 4: Square-root Time-Limited Balanced Truncation without balancing [50]

Input: The system matrices (A, B, C) belonging to an asymptotically stable system of order n; reduced order r; the finite time-interval $[0, \tau]$ with $\tau < \infty$;

Output: The system matrices (A_r, B_r, C_r) of the reduced-order system;

1. Compute the time-limited controllability and the time-limited observability gramians P_τ and Q_τ by solving the time-limited ALEs given by (2.13) and (2.14), respectively ;
2. Obtain the matrices L_{P_τ} and L_{Q_τ} by the Cholesky decompositions of P_τ and Q_τ, respectively ;
3. Compute the SVD:

$$L_{Q_\tau}^T L_{P_\tau} = \begin{bmatrix} U_{\tau,1} & U_{\tau,2} \end{bmatrix} \begin{bmatrix} \Sigma_{\tau,1} & \mathbf{0}_{k\times(n-k)} \\ \mathbf{0}_{(n-k)\times k} & \Sigma_{\tau,2} \end{bmatrix} \begin{bmatrix} V_{\tau,1}^T \\ V_{\tau,2}^T \end{bmatrix},$$

where $\Sigma_{\tau,1} = \text{diag}\{\sigma_{\tau,1}, \ldots, \sigma_{\tau,k}\}$ contains the k-largest Hankel singular values. ;

4. Construct the following matrices,

$$\begin{aligned} Z_{r,\tau} &= L_{Q_\tau} U_{\tau,1} \Sigma_{\tau,1}^{-\frac{1}{2}} \quad \in \mathbb{R}^{n\times k}, \\ V_{r,\tau} &= L_{P_\tau} V_{\tau,1} \Sigma_{\tau,1}^{-\frac{1}{2}} \quad \in \mathbb{R}^{n\times k}; \end{aligned}$$

5. Obtain the reduced-order model by Petrov-Galerkin projection,

$$A_r = {Z_{r,\tau}}^T A V_{r,\tau},\ B_r = {Z_{r,\tau}}^T B, \text{ and } C_r = C V_{r,\tau};$$

Another modified version of TL-BT is proposed in [34], and an error bound for the algorithm is also derived. The TL-BT algorithm involves the computation of two time-limited gramians, P_τ and Q_τ, by solving two time-limited ALEs. This makes it computationally intractable to reduce large-scale systems. Alternatively, low-rank approximations of P_τ and Q_τ are obtained by using rational Krylov subspace methods in [50]. This has expanded the applicability of TL-BT to large-scale systems.

2.4.1.4 Projection-based $H_2(\tau)$ optimal MOR

The $H_2(\tau)$ optimal MOR problem is the restriction of the H_2 optimal MOR problem, given by (2.26), to a finite time interval $[0, \tau]$. It involves obtaining the reduced-order approximation Σ_r of the full-order model Σ, which minimizes the time-limited cost function,

$$\Sigma_r = \underset{\text{s.t. } \text{ord}(\hat{\Sigma})=r}{\text{argmin}} \left\| \Sigma - \hat{\Sigma} \right\|_{H_2(\tau)}, \tag{2.47}$$

where $H_2(\tau)$ is the time-limited H_2 error norm, given by (2.21). From the expression (2.22), it is evident that minimizing this norm minimizes the maximum value of $\|y(t) - y_r(t)\|$ over the finite time interval $[0, \tau]$ for all admissible inputs $u(t)$.

The $H_2(\tau)$ optimization problem, given by (2.47), similar to the H_2 optimization problem given by (2.26), is non-convex and obtaining global minimizers is not easy. The preferred approach is obtaining the first-order necessary conditions for $H_2(\tau)$ optimality. Lyapunov-based conditions for $H_2(\tau)$ optimality are obtained in [30], while interpolation-based conditions for $H_2(\tau)$ optimality are

obtained in [94]. These conditions are used to propose model reduction algorithms. The Lyapunov-based $H_2(\tau)$ optimality conditions and a corresponding projection-based model reduction algorithm are stated below.

Lyapunov-based method: The $H_2(\tau)$ error norm, given by (2.21), can be expressed in terms of the finite horizon gramians, P_τ and Q_τ. This is evident from Proposition 2.4.8 given below. Further, this expression of the error norm is used to obtain the Lyapunov-based first-order necessary conditions for $H_2(\tau)$ optimality, stated in Theorem 2.4.9.

Proposition 2.4.8 ([30], Proposition 2.2,2.3)**.** *Consider the full-order system Σ and the reduced-order system Σ_r, given by the state-space representations (2.1) and (2.17), respectively. The square of the $H_2(\tau)$ error norm, given by (2.21), can be expressed as*

$$\|\Sigma - \Sigma_r\|^2_{H_2(\tau)} = \mathrm{Tr}(CP_\tau {C_r}^T) + \mathrm{Tr}(C_r P_{r,\tau} {C_r}^T) - 2\mathrm{Tr}(CX_\tau {C_r}^T), \tag{2.48}$$

$$= \mathrm{Tr}(B^T Q_\tau B) + \mathrm{Tr}({B_r}^T Q_{r,\tau} B_r) - 2\mathrm{Tr}(B_r^T Y_\tau B). \tag{2.49}$$

The gramian matrices P_τ and Q_τ are obtained by solving the time-limited ALEs given by (2.15) and (2.16), respectively. The matrices $P_{r,\tau}$ and $Q_{r,\tau}$ are the finite horizon controllability and observability gramians obtained by solving the following time-limited ALEs,

$$A_r P_{r,\tau} + P_{r,\tau} {A_r}^T + B_r {B_r}^T - e^{A_r \tau} B_r {B_r}^T e^{{A_r}^T \tau} = 0, \tag{2.50}$$

$${A_r}^T Q_{r,\tau} + Q_{r,\tau} A_r + {C_r}^T C_r - e^{{A_r}^T \tau} {C_r}^T C_r e^{A_r \tau} = 0. \tag{2.51}$$

The matrices X_τ and Y_τ are obtained by solving the following time-limited Sylvester equations,

$$AX_\tau + X_\tau {A_r}^T + B B_r - e^{A\tau} B B_r e^{{A_r}^T \tau} B = 0, \tag{2.52}$$

$$A^T Y_\tau + Y_\tau A_r + C^T C_r - e^{A^T \tau} C^T C_r e^{A_r \tau} = 0. \tag{2.53}$$

Assuming that A_r is diagonalizable, let $A_r = S^{-1} D S$ be its spectral decomposition where $D = \mathrm{diag}\{\lambda_1, \ldots, \lambda_r\}$. Let $\tilde{B} = SB_r$, $\tilde{C} = C_r S^{-1}$, $\tilde{P}_\tau = S P_{r,\tau} S^T$, $\tilde{X}_\tau = X_\tau S^T$, $\tilde{Q}_\tau = S^{-T} Q_{r,\tau} S^{-1}$ and $\tilde{Y}_\tau = S^{-T} Y_\tau$. Then, equations (2.52), (2.50), (2.53) and (2.51) yield

$$A\tilde{X}_\tau + \tilde{X}_\tau D + B\tilde{B}^T - e^{A\tau} B \tilde{B}^T e^{D\tau} = 0, \tag{2.54}$$

$$D\tilde{P}_\tau + \tilde{P}_\tau D + \tilde{B}\tilde{B}^T - e^{D\tau} \tilde{B}\tilde{B}^T e^{D\tau} = 0, \tag{2.55}$$

$$D\tilde{Y}_\tau + \tilde{Y}_\tau A + \tilde{C}^T C - e^{D\tau} \tilde{C}^T C e^{D\tau} = 0, \quad \text{and} \tag{2.56}$$

$$D\tilde{Q}_\tau + \tilde{Q}_\tau D + \tilde{C}^T \tilde{C} - e^{D\tau} \tilde{C}^T \tilde{C} e^{D\tau} = 0. \tag{2.57}$$

Consider the new quantities $\tilde{Q}_\infty$ and $\tilde{Y}_\infty$ which are the solutions of the following matrix equations

$$D\tilde{Q}_\infty + \tilde{Q}_\infty D + \tilde{C}^T \tilde{C} = 0, \tag{2.58}$$

$$D\tilde{Y}_\infty + \tilde{Y}_\infty A^T + \tilde{C}^T C = 0. \tag{2.59}$$

Theorem 2.4.9 ([30], Theorem 3.2)**.** *Let the reduced system Σ_r, given by state-space representation (2.17), be an optimal approximation of the full-order system Σ, given by the state-space*

representation (2.1), with respect to the $H_2(\tau)$ error norm. Then

$$\tilde{C}\tilde{P}_\tau = C\tilde{X}_\tau, \tag{2.60}$$

$$\tilde{Q}_\tau\tilde{B} = \tilde{Y}_\tau B, \quad \textit{and} \tag{2.61}$$

$$e_i^T\tilde{Y}_\infty\left[\tilde{X}_\tau - \tau e^{A\tau}B\tilde{B}^T e^{D\tau}\right]e_i = e_i^T\tilde{Q}_\infty\left[\tilde{P}_\tau - \tau e^{D\tau}B\tilde{B}^T e^{D\tau}\right]e_i, \tag{2.62}$$

$\forall \quad i = 1, 2, \ldots, r$ *where e_i is the i^{th} unit vector and matrices $\tilde{P}_\tau$, $\tilde{X}_\tau$, $\tilde{Q}_\tau$, $\tilde{Y}_\tau$, $\tilde{Q}_\infty$ and $\tilde{Y}_\infty$ are solutions to the matrix equations (2.55), (2.54), (2.57), (2.56), (2.58) and (2.59), respectively.*

An iterative corrective scheme is proposed in [30] based on the $H_2(\tau)$ optimality conditions. At every iteration, a pair of finite horizon Sylvester equations are solved to obtain a pair of projection matrices. An outline of the scheme is given below.

Algorithm 5: Time-Limited Two-Sided Iterative Algorithm (TL-TSIA) [30]

Input: The full-order system matrices: A, B, C;
The reduced-order system matrices: A_r, B_r, C_r, which are the initial conditions;
The finite-time interval $[0, \tau]$;

Output: The reduced matrices A_r, B_r, C_r;

while *(not converged)* **do**

1. Obtain the spectral decomposition of A_r and let,

$$D = SA_rS^{-1}, \quad \tilde{B} = SB_r, \quad \tilde{C} = C_rS^{-1}; \tag{2.63}$$

2. Solve the following pair of Sylvester equations:

$$AV_r + V_rD + B\tilde{B}^T - e^{AT}B\tilde{B}^Te^{DT} = 0, \tag{2.64}$$

$$A^TW_r + W_rD + C^T\tilde{C} - e^{A^TT}C^T\tilde{C}e^{DT} = 0; \tag{2.65}$$

3. Orthogonalize V_r and W_r as $V_r = \text{Orth}(V_r)$ and $W_r = \text{Orth}(W_r)$;
4. Compute $Z_r^T = (W_r^TV_r)^{-1}W_r^T$ and obtain the reduced model as follows

$$A_r = Z_r^TAV_r, \quad B_r = Z_r^TB, \quad \text{and} \quad C_r = CV_r; \tag{2.66}$$

end

The above scheme, upon convergence, produces a reduced-order model which satisfies the time-limited $H_2(\tau)$ optimality conditions approximately. Error expressions quantifying the distance to optimality of the reduced-order model, including their derivation, are available in Theorem 3.3 of [30].

2.4.2 Gradient-based model order reduction methods

As the H_2 and $H_2(\tau)$ optimization problems are non-convex, finding global minimizers is difficult. Hence, the existing methods focus on finding local minimizers. Apart from the projection-based methods discussed above, gradient-based methods can also be used to find local minimizers. For such methods, the primary challenge is obtaining an analytical expression of the gradients of the error norm. These gradient expressions are substituted in gradient flow, quasi-Newton or trust-region-based algorithms to obtain reduced-order models.

2.4.2.1 Descent-based H_2 optimal MOR

The convergence of IRKA is guaranteed only for LTI systems with symmetric state-space realizations. Numerous numerical experiments have shown that IRKA performs well for general systems, but convergence is not guaranteed. A descent-based H_2 optimal model reduction technique, proposed in [7], produces a sequence of reduced-order models with decreasing H_2 error norms. This ensures global convergence to a reduced-order model satisfying the interpolation-based H_2 optimality conditions. At the heart of the descent-based approach is an expression of the H_2 error norm for MIMO dynamical systems, given by the following theorem.

Theorem 2.4.10 ([7],Theorem 2.1)**.** *Given a full-order system Σ with transfer function $G(s)$, consider a reduced-order system Σ_r with transfer function $G_r(s)$, which has the pole-residue representation given by (2.34). The H_2 error norm, as defined by (2.19), can be expressed as:*

$$\|\Sigma - \Sigma_r\|_{H_2}^2 = \|\Sigma\|_{H_2}^2 - 2\sum_{k=1}^{r} c_k^T G(-\lambda_k) b_k + \sum_{k,l=1}^{r} \frac{c_k^T c_l b_l^T b_k}{-\lambda_k - \lambda_l}.$$

The parameters for the descent-based approach are the poles and residues of the reduced-order model Σ_r given by $\{\lambda_i, c_i, b_i\}$ for $i = 1, \ldots, r$. In the above expression, the H_2 error norm is formulated in terms of these parameters. Using the above expression, the gradient and Hessian of the H_2 error norm with respect to the pole-residue parameters are conveniently obtained. The gradient and Hessian are used with a trust-region-based descent method that globally converges to a reduced-order model, satisfying the interpolation-based H_2 optimality conditions.

2.4.2.2 Descent-based $H_2(\tau)$ optimal MOR

The reduced-order models obtained by projection-based time-limited model reduction methods (such as TL-BT and TL-TSIA) do not satisfy the $H_2(\tau)$ optimality conditions exactly. This distance from optimality can be reduced by using gradient-based methods.

Given a pole-residue representation of the impulse response $g_r(t)$ of the reduced-order system Σ_r, the $H_2(\tau)$ error norm can be characterized in terms of the poles and residues of the impulse response. The following proposition gives this.

Proposition 2.4.11 ([94], Lemma 3.2)**.** *Considering $g(t) = \sum_{j=1}^{n} l_j r_j^T e^{\mu_j t}$ and $g_r(t) = \sum_{i=1}^{r} c_i b_i^T e^{\lambda_i t}$ as the pole-residue representation of the impulse responses of the full-order system Σ and the reduced-order system Σ_r, respectively, the square of the $H_2(\tau)$ error norm between them is given by,*

$$\begin{aligned}\|\Sigma - \Sigma_r\|_{H_2(\tau)}^2 &= \|g - g_r\|_{H_2(\tau)}^2 \\ &= \|g\|_{H_2(\tau)}^2 - 2\langle g, g_r\rangle_{H_2(\tau)} + \|g_r\|_{H_2(\tau)}^2,\end{aligned}$$

where $\langle g, g_r\rangle_{H_2(\tau)} = \sum_{j=1}^{n}\sum_{i=1}^{r} c_i^T l_j r_j^T b_i \frac{e^{(\lambda_i+\mu_j)\tau}-1}{\lambda_i+\mu_j}$ and $\|g_r\|_{H_2(\tau)}^2 = \sum_{i=1}^{r}\sum_{j=1}^{r} c_i^T c_j b_j^T b_i \frac{e^{(\lambda_i+\lambda_j)\tau}-1}{\lambda_i+\lambda_j}$.

The above characterization is essential for obtaining the interpolation-based first-order necessary conditions of the $H_2(\tau)$ optimal model reduction problem, expressed in the theorem below. The optimality conditions require computation of the gradients of the $H_2(\tau)$ error norm with respect to the poles and residue directions, given by $\{\lambda_k\}$, $\{c_k\}$ and $\{b_k\}$.

Theorem 2.4.12 ([94], Theorem 3.1). *Let the reduced-order system Σ_r be the best r^{th} order approximation of the full-order system Σ with respect to the $H_2(\tau)$ norm defined over the finite time-interval $[0, \tau]$. Let $G_r(s) = \sum_{k=1}^{r} \frac{c_k b_k^T}{s-\lambda_k}$ be the pole-residue representation of the transfer function of the reduced-order system Σ_r. Let $G_\tau(s)$ and $G_{r,\tau}(s)$ be the time-limited transfer functions of the systems Σ and Σ_r, respectively. Then for $k = 1, \ldots, r$*

$$c_k^T G_\tau(-\lambda_k) = c_k^T G_{r,\tau}(-\lambda_k), \tag{2.67}$$

$$G_\tau(-\lambda_k) b_k = G_{r,\tau}(-\lambda_k) b_k, \quad \text{and} \tag{2.68}$$

$$c_k^T G_\tau(-\lambda_k) b_k = c_k^T G_{r,\tau}(-\lambda_k) b_k, \tag{2.69}$$

where $G_\tau(s)$ and $G_{r,\tau}(s)$ are given by

$$G_\tau(s) = -e^{-s\tau} C (sI_n - A)^{-1} e^{A\tau} B + G(s) \tag{2.70}$$

$$G_{r,\tau}(s) = -e^{-s\tau} C_r (sI_r - A_r)^{-1} e^{A_r\tau} B_r + G_r(s). \tag{2.71}$$

In the above-stated optimality conditions, $G_{r,\tau}(s)$ tangentially interpolates $G_\tau(s)$ at the mirror images of the poles and along the residue directions of the transfer function $G(s)$ of the optimal reduced-order model. These optimality conditions look similar to the interpolation-based optimality conditions of the H_2 optimal model reduction problem, given by [35]. However, the quantity being interpolated and the interpolant are different in both cases.

The following corollary, valid for SISO systems, is obtained based on the above-mentioned optimality conditions.

Corollary 2.4.13 ([94], Corollary 4.2). *Assume that the full-order system Σ and the reduced-order system Σ_r are SISO systems. Let $G(s)$ and $G_r(s)$ be the respective transfer functions and $G_\tau(s)$ and $G_{r,\tau}(s)$ be as defined in (2.70) and (2.71). Let the poles of the transfer function of the reduced-order system $G_r(s)$, i.e. $\{\lambda_i, i = 1, \ldots, r\}$ be fixed. Then $G_r(s)$ is the best r^{th} order approximation of $G(s)$ with respect to the $H_2(\tau)$ norm if and only if $E\phi = \delta$ where $\phi = [\phi_1\ \phi_2\ \ldots\ \phi_r]^T \in \mathbb{C}^r$ is the vector of residues, $\delta \in \mathbb{C}^r$ is the vector with entries*

$$\delta_i = e^{\lambda_i \tau} C \left(-\lambda_i I_n - A\right)^{-1} e^{A\tau} B - G(-\lambda_i), \quad i = 1, 2, \ldots, r;$$

and $E \in \mathbb{C}^{r \times r}$ is the matrix with entries $E_{i,j} = \frac{e^{(\lambda_i + \lambda_j)\tau} - 1}{\lambda_i + \lambda_j}$ for $i, j = 1, 2, \ldots, r$.

Based on the above corollary, a numerical algorithm called FHIRKA is proposed in [94] for model order reduction of SISO systems over a finite time interval. The $H_2(\tau)$ error norm is a function of the poles and residues of the transfer function $G_r(s)$ of the reduced-order system. Assuming λ's as optimization parameters, the error norm can be optimized using a quasi-Newton-type optimization technique. The initial conditions of the optimization are obtained from reduced models acquired by projection-based methods such as TL-BT, TL-TSIA, etc. After the completion of every optimization step involving the λ's, the residues ϕ's are updated by solving the $r \times r$ linear system $E\phi = \delta$, as given by Corollary 2.4.13. The reduced model obtained upon convergence satisfies the interpolation-based $H_2(\tau)$ optimality conditions.

Remark 2. The primary focus of this thesis is finite horizon MOR and, more specifically, $H_2(\tau)$ optimal MOR. This is the motivation for introducing the H_2 and the $H_2(\tau)$ optimal model reduction

problems for LTI systems in this section. In Chapter 3 and Chapter 4, model reduction methods for $H_2(\tau)$ optimal model reduction of LTI systems are proposed. These methods are benchmarked against the MOR techniques discussed in this section.

Apart from LTI systems, the model order reduction of LTV systems is also considered in this thesis. Therefore, the representation and some important properties of LTV systems are considered in the next section. The concept of time-varying gramians for such systems is also discussed.

2.5 Description of LTV systems

Consider an LTV system Σ defined on $[t_0, t_f]$ with $-\infty < t_0 < t_f < \infty$,

$$\begin{aligned} \dot{x}(t) &= A(t)x(t) + B(t)u(t), \\ y(t) &= C(t)x(t), \end{aligned} \tag{2.72}$$

where $x(t)$ is the state variable at time t. It is also assumed that the functions $A(\cdot) : [t_0, t_f] \to \mathbb{R}^{n\times n}$, $t \mapsto A(t)$, $B(\cdot) : [t_0, t_f] \to \mathbb{R}^{n\times m}$, $t \mapsto B(t)$ and $C(\cdot) : [t_0, t_f] \to \mathbb{R}^{p\times n}$, $t \mapsto C(t)$ are continuous and bounded. This guarantees the existence and uniqueness of the solutions over the time interval $[t_0, t_f]$.

For $u \equiv 0$, the differential equation for the system Σ is given by

$$\dot{x}(t) = A(t)x(t) \tag{2.73}$$

The state transition matrix represents the solution of the above linear differential equation. It is useful in representing the impulse response of the LTV system Σ.

Let $\phi_i(\cdot, \tau)$ be solution of (2.73) with value at τ equal to e_i, the i^{th} column of the identity matrix I_n. Consider the matrix

$$\phi(\cdot, \tau) = [\phi_1(\cdot, \tau) \dots \phi_n(\cdot, \tau)]. \tag{2.74}$$

For the linear differential equation (2.73), let $x(t_0) = x_0$ and $x_{i0} \in \mathbb{R}$ be the i^{th} component of x_0. Due to linearity,

$$\sum_{i}^{n} \phi_i(\cdot, t_0)x_{i0} = \phi(\cdot, t_0)x_0, \tag{2.75}$$

is the unique solution of (2.73). Thus, the solution $x(t)$ of the same differential equation can be expressed as

$$x(t) = \phi(t, t_0)x_0. \tag{2.76}$$

Based on its definition, the state transition matrix satisfies the following matrix differential equation

$$\frac{d}{dt}\phi(t, t_0) = A(t)\phi(t, t_0), \quad \phi(t_0, t_0) = I_n. \tag{2.77}$$

The following are some important properties of the state transition matrix:

$$1) \quad \phi(t, t) = I_n \quad \text{for} \quad t \in [t_0, t_f], \tag{2.78}$$

$$2) \quad \phi(t_1, t_2) = \phi(t_1, t_3)\phi(t_3, t_2), \text{ for } \{t_1, t_2, t_3\} \in [t_0, t_f] \quad \text{and} \tag{2.79}$$

$$3) \quad \phi^{-1}(t_1, t_2) = \phi(t_2, t_1). \tag{2.80}$$

The properties mentioned above are derived as follows. The first property (2.78) follows from the assumptions (2.74) and (2.75).

The second property is known as the semi-group property and is obtained in the following way:

Let $J(t) = \phi(t, t_3)\phi(t_3, t_2)$ and $K(t) = \phi(t, t_2)$. Then

$$\frac{dJ(t)}{dt} = A(t)\phi(t, t_3)\phi(t_3, t_2) = A(t)J(t). \quad \text{and}$$
$$\frac{dK(t)}{dt} = A(t)\phi(t, t_2) = A(t)K(t).$$

Therefore, $J(t)$ and $K(t)$ obey the same differential equation. At $t = t_3$,

$$J(t_3) = \phi(t_3, t_3)\phi(t_3, t_2) = \phi(t_3, t_2) = K(t_3).$$

The linear differential equation has a unique solution, and therefore, $J(t) \equiv K(t)$.

The third property is obtained from the second property in the following way:

$$\phi(t_1, t_2)\phi(t_2, t_1) = \phi(t_1, t_1) = I_n,$$
$$\phi(t_2, t_1)\phi(t_1, t_2) = \phi(t_2, t_2) = I_n.$$

Thus, by definition, $\phi^{-1}(t_1, t_2) = \phi(t_2, t_1)$.

Remark 3. The above definition of the state transition matrix of LTV systems, its properties and their derivation are taken from [45].

The impulse response of a continuous-time LTV system is a characterization of the system's input-output behaviour. For an input $u(t) = \delta(t - \tau)$, the impulse response is given by

$$h(t, \tau) = \begin{cases} 0, & t_0 \leq t < \tau, \\ C(t)\phi(t, \tau)B(\tau), & \tau \leq t \leq t_f. \end{cases} \tag{2.81}$$

The impulse response remains invariant under state-space transformations of the LTV system. Lyapunov transformations preserve the input-output properties, boundedness and internal stability of state-space realizations. They are defined as follows.

Definition 2.5.1 ([91], Definition 1, 2)**.** Consider a time-varying matrix $T(t)$, non-singular at every instant of the time interval $[t_0, t_f]$, which transforms a state-space realization $(A(t), B(t), C(t))$ to the realization $(\hat{A}(t), \hat{B}(t), \hat{C}(t))$, where $\hat{A}(t) = T^{-1}(t)(A(t)T(t) - \dot{T}(t))$, $\hat{B}(t) = T^{-1}(t)B(t)$ and $\hat{C}(t) = C(t)T(t)$. If $T(t)$, $\dot{T}(t)$ and $T^{-1}(t)$ are continuous and bounded, then $T(t)$ is known as a Lyapunov transformation.

State-space realizations, related by such transformations, are said to be topologically equivalent. That is, $(\hat{A}(t), \hat{B}(t), \hat{C}(t))$ is topologically equivalent to $(A(t), B(t), C(t))$.

2.5.1 System gramians of LTV systems

The reachability and observability properties of an LTV state-space realization can be analyzed with the help of system gramians. The reachability gramian of a linear system is related to the reachability map of the system. Similarly, the observability gramian is linked to the observability

map. The non-singularity of the gramians is an indicator of system reachability and observability. This has been extensively discussed in [45]. The structure of the reachability and the observability gramians for LTV systems is discussed now. For $t \in [t_0, t_f]$, the reachability gramian of the LTV system, given by (2.72), is as follows,

$$P(t, t_0) = \int_{t_0}^{t} \phi(t, \tau) B(\tau) (B(\tau))^T (\phi(t, \tau))^T d\tau. \tag{2.82}$$

The above gramian can be computed by solving the following DLE:

$$\frac{dP(t, t_0)}{dt} = A(t)P(t, t_0) + P(t, t_0)(A(t))^T + B(t)(B(t))^T, \tag{2.83}$$

which is solved for t varying from $t = t_0$ to $t = t_f$ with initial condition $P(t_0, t_0) = 0$.

The observability gramian for $t \in [t_0, t_f]$ is given by

$$Q(t_f, t) = \int_{t}^{t_f} (\phi(\tau, t))^T (C(\tau))^T C(\tau) \phi(\tau, t) d\tau. \tag{2.84}$$

This above gramian can also be obtained by solving the following DLE:

$$\frac{dQ(t_f, t)}{dt} = -(A(t))^T Q(t_f, t) - Q(t_f, t)A(t) - (C(t))^T C(t), \tag{2.85}$$

which is solved for t varying from $t = t_f$ to $t = t_0$ with final condition $Q(t_f, t_f) = 0$.

The two gramians stated above play a pivotal role in the finite horizon balanced truncation algorithm for continuous-time LTV systems, discussed in the next section. Further, they also play an essential role in Chapter 6 where a gramian-based framework is used to propose an iterative scheme for model reduction of continuous-time LTV systems.

2.6 MOR algorithms for LTV systems

Consider the continuous-time LTV system Σ_r of order r, where $r < n$, with the following state-space representation:

$$\begin{aligned} \dot{x}_r(t) &= A_r(t)x_r(t) + B_r(t)u(t), \\ y_r(t) &= C_r(t)x_r(t). \end{aligned} \tag{2.86}$$

Let the above system be a reduced-order approximation of the full-order system Σ, given by (2.72). Here, $x_r(t)$ is the reduced-order state variable at time t. It is assumed that the time-varying state-space parameters $A_r(\cdot) : [t_0, t_f] \to \mathbb{R}^{n \times n}$, $t \mapsto A_r(t)$, $B_r(\cdot) : [t_0, t_f] \to \mathbb{R}^{n \times m}$, $t \mapsto B_r(t)$ and $C_r(\cdot) : [t_0, t_f] \to \mathbb{R}^{p \times n}$, $t \mapsto C_r(t)$ are continuous and bounded. The reduced-order output $y_r(t)$ should be a good approximation of the system output $y(t)$ of the LTV system Σ over the time-interval $[t_0, t_f]$ with respect to a suitable norm.

The following sections discuss a few model reduction methods for LTV systems.

2.6.1 Finite horizon balanced truncation

If the matrices $A(t)$, $B(t)$ and $C(t)$ are real analytic (matrix) functions in the interval $[t_0, t_f]$, the elements of the singular value decomposition of $P(t, t_0)$ and $Q(t_f, t)$ are continuous and differentiable

in $[t_0, t_f]$. This ensures the existence of a time-varying Lyapunov transformation $T(t)$ in the interval $[t_0, t_f]$, which transforms the state-space representation of the system to a balanced realization. Let $(\hat{A}(t), \hat{B}(t), \hat{C}(t))$ be the balanced realization for which the reachability and observability gramians are diagonal and identical, i.e. $\hat{P}(t, t_0) = \Lambda(t) = \hat{Q}(t_f, t)$. Here, $\Lambda(t) = \text{diag}(\lambda_1(t), \lambda_2(t), \ldots, \lambda_n(t))$ is known as the canonical gramian.

The canonical gramian measures the relative importance of each dimension with respect to reachability and observability. This makes the balanced realization useful for model reduction. A reduced model is obtained by partitioning the full-order balanced realization $(\hat{A}(t), \hat{B}(t), \hat{C}(t))$ as

$$\hat{A}(t) = \begin{bmatrix} \hat{A}_{11}(t) & \hat{A}_{12}(t) \\ \hat{A}_{21}(t) & \hat{A}_{22}(t) \end{bmatrix}, \quad \hat{B}(t) = \begin{bmatrix} \hat{B}_1(t) \\ \hat{B}_2(t) \end{bmatrix}, \quad \hat{C}(t) = \begin{bmatrix} \hat{C}_1(t) & \hat{C}_2(t) \end{bmatrix}, \tag{2.87}$$

corresponding to the following partition of the canonical gramian,

$$\Lambda(t) = \begin{bmatrix} \Lambda_1(t) & \\ & \Lambda_2(t) \end{bmatrix}, \quad \Lambda_1 > \Lambda_2. \tag{2.88}$$

The realization $(\hat{A}_{11}(t), \hat{B}_1(t), \hat{C}_1(t))$, obtained by truncation of (2.87), corresponds to the reduced-order subsystem. This system is bounded input bounded state stable in $[t_0, t_f]$.

The results stated in this subsection are from [99].

2.6.2 An improved finite horizon balanced truncation

The point-wise balancing coordinate transformation $T(t)$ defined over the finite time horizon $[t_0, t_f]$ may have unfavourable numerical properties. This has been explored in detail for the LTI case in [85], which introduces the idea of non-balancing projections for balanced truncation. The conversion of the original system to a balanced realization is thus avoided. Similar projections have been extended to discrete-time LTV systems in [17]. Such projections have also been extended to continuous-time LTV systems in [55, 86]. They are naturally time-varying projections defined at every point of a finite time interval. An outline of the modified finite horizon balanced truncation method is given in Algorithm 6.

2.6.3 Few additional algorithms for MOR of LTV systems

This subsection states some model reduction methods for continuous and discrete-time LTV systems in the literature. The methods are briefly mentioned and not discussed in detail.

The balanced truncation methods discussed in the previous subsections involve solving a pair of DLEs to obtain the system gramians. They are subsequently used to construct projection matrices for model reduction of continuous-time LTV systems. In [87], generalized gramians are obtained for continuous-time LTV systems by solving linear matrix inequalities (LMIs). These gramians are used to construct projection matrices for generalized balanced truncation, and error bounds are derived. It is also proved that the reduced-order model obtained by generalized balanced truncation preserves the input-output stability of the original model.

In [92], the authors define a uniformly balanced realization for discrete-time LTV systems and study its properties. The uniform realizations are helpful as reduced-order models are obtained

Algorithm 6: Finite Horizon Balanced Truncation for LTV systems [55]

Input: System matrices $(A(t), B(t), C(t))$ belonging to a system of order n; reduced order r;

Output: Reduced-order matrices $(A_r(t), B_r(t), C_r(t))$ of order r;

1. Compute the reachability and the observability gramians $P(t, t_0)$ and $Q(t_f, t)$ for all $t \in [t_0, t_f]$ by solving the DLEs (2.83) and (2.85), respectively ;
2. Obtain the matrices $S_R(t)$ and $S_L(t)$ by the Cholesky decompositions of $P(t, t_0)$ and $Q(t_f, t)$, respectively, as follows,

$$P(t, t_0) = S_R(t)(S_R(t))^T, \quad Q(t_f, t) = S_L(t)(S_L(t))^T \quad ;$$

3. Compute the following SVD:

$$(S_R(t))^T S_L(t) = \begin{bmatrix} U_1(t) & U_2(t) \end{bmatrix} \begin{bmatrix} \Sigma_1(t) & \mathbf{0}_{r\times(n-r)} \\ \mathbf{0}_{(n-r)\times r} & \Sigma_2(t) \end{bmatrix} \begin{bmatrix} (V_1(t))^T \\ (V_2(t))^T \end{bmatrix},$$

where $\Sigma_1(t) = \text{diag}\{\sigma_1(t), \ldots, \sigma_r(t)\}$ contains the r-largest time-varying Hankel singular values;

4. Construct the following projection matrices,

$$W(t) = S_L(t)V_1(t)(\Sigma_1(t))^{-\frac{1}{2}} \quad \in \mathbb{R}^{n\times r},$$
$$Z(t) = S_R(t)U_1(t)(\Sigma_1(t))^{-\frac{1}{2}} \quad \in \mathbb{R}^{n\times r};$$

5. Obtain the reduced-order model,

$$A_r(t) = (W(t))^T \left(A(t)Z(t) - \frac{dZ(t)}{dt} \right), \; B_r(t) = W(t)^T B(t), \text{ and } C_r(t) = C(t)Z(t);$$

by truncating these realizations. The stability of the reduced models is also guaranteed. The authors propose another model reduction algorithm by decomposing a generalized Hankel matrix for discrete-time LTV systems. They further prove that the reduced models obtained by the two methods are identical. A model reduction method is proposed based on optimising the Hankel norm of the error between the full-order and reduced-order LTV systems in [18].

In [51], a model order reduction method for discrete-time LTV systems is proposed. A pair of linear matrix inequalities are solved, and generalized gramians are obtained, which are then used to obtain generalized balanced realizations. The balanced realizations are truncated to obtain reduced-order models. Upper bounds are given on the induced-two norm of the error between the full-order and the reduced-order system. A model reduction method for discrete-time LTV systems is also proposed in [87]. They also obtain generalized error bounds in the induced-2 norm, which include the error bounds of [51]. Further, they show that the input-output stability of the full-order system is preserved in the reduced-order model.

A finite horizon H_2 error norm for discrete-time LTV systems is presented in [60, 61]. The gradients of the error norm are derived. The stationary points corresponding to the minimum of the error norm are characterized using quantities computed with Stein-like recurrences. Based on

this characterisation, a fixed-point iterative algorithm for model order reduction is proposed. This method is different from the various balanced truncation algorithms discussed till now. Here, the construction of the reduced-order model is based on the minimization of a well-defined error norm.

2.7 Summary

In this chapter, preliminary results for model order reduction of LTI and LTV systems have been discussed. Firstly, the state-space representations of LTI systems, including properties like impulse response, gramians, and system norms, have been stated. Further, the infinite horizon and the finite horizon model reduction problem for LTI systems have been reviewed. Then, several algorithms for infinite and finite horizon model order reduction of LTI systems have been stated. Similarly, state-space representation and associated properties like impulse response, gramians and norms of continuous-time LTV systems have been stated. Finally, the model order reduction problem for LTV systems and several algorithms for model order reduction of LTV systems have been discussed.

Chapter 3

Near-optimal time-limited interpolation-based model order reduction

The H_2 optimal model order reduction (MOR) problem considers a H_2 error norm, whereas the $H_2(\tau)$ optimal MOR problem deals with a finite horizon $H_2(\tau)$ error norm. Chapter 2 discusses two H_2 optimal model reduction algorithms, namely, IRKA and TSIA. While IRKA is based on interpolation-based H_2 optimality conditions, TSIA is based on Lyapunov-based H_2 optimality conditions. TSIA has been extended to propose a finite horizon H_2 optimal model reduction algorithm in [30], referred to as TL-TSIA in this thesis. This motivates a similar finite horizon extension for IRKA and is the focus of this chapter.

The main objective of this chapter is to propose a $H_2(\tau)$ optimal model reduction algorithm, which is a finite horizon extension of the IRKA algorithm. To begin with, a different proof for deriving the interpolation-based $H_2(\tau)$ optimality conditions (Theorem 3.1, [94]) is provided. Secondly, a modified rational Krylov framework is proposed for finite-time rational interpolation. Unlike infinite-time rational interpolation, the reduced models do not precisely satisfy the time-limited rational interpolation conditions. The deviations from these conditions are quantified, and the factors affecting their magnitude are discussed. Then, an iterative algorithm called TL-IRKA, which uses the modified rational Krylov framework to construct the projection matrices at every iteration, is proposed. Further, if TL-IRKA and TL-TSIA converge theoretically, it is shown that they converge to the same reduced-order model. Finally, the validity of the proposed algorithm is tested with the help of a few numerical examples.

This chapter is organised as follows. Section 3.1 states the $H_2(\tau)$ optimal model reduction problem. Section 3.2 presents a new proof for deriving interpolation-based $H_2(\tau)$ optimality conditions. A time-limited rational Krylov framework for time-limited rational interpolation is introduced, and the interpolation errors are quantified in Section 3.3. In Section 3.4, a projection-based iterative algorithm is proposed and its computational complexity is discussed. Section 3.5 compares the proposed algorithm with TL-TSIA. Three numerical examples are presented in Section 3.6. The

chapter is concluded in Section 3.7.

3.1 H_2 optimal model reduction over a finite-time interval

In this section, the time-limited impulse response and the time-limited transfer function of an LTI system are defined. The $H_2(\tau)$ error norm is defined in terms of the time-limited impulse response of the system. This error norm is used to formulate the $H_2(\tau)$ optimal model reduction problem.

3.1.1 Time-limited impulse response and transfer function

Given an interval $I \subset \mathbb{R}$, the Hilbert space $L_2(I)$ consists of square-integrable and Lebesgue measurable matrix-valued functions defined on the interval I.

Definition 3.1.1 ([108]). For $f, g \in L_2(I)$, the inner product is defined as

$$\langle f, g\rangle_{L_2(I)} = \int_I \mathrm{Tr}((f(t))^T g(t))dt = \int_I \mathrm{Tr}(f(t)(g(t))^T)dt. \tag{3.1}$$

Based on this inner product, the induced inner product norm is defined as

$$\|f\|_{L_2(I)} = \sqrt{\langle f, f\rangle_{L_2(I)}}. \tag{3.2}$$

Consider the LTI system Σ given by the state space representation (2.1). The time-limited impulse response matrix of the system Σ, given by the mapping $g_\tau : [0, \infty) \to \mathbb{R}^{p\times m}$, is defined as

$$g_\tau(t) = \begin{cases} g(t), & t \in [0, \tau], \\ 0, & t \in (\tau, \infty). \end{cases} \tag{3.3}$$

The Laplace transform of the time-limited impulse response is given by

$$\begin{aligned} G_\tau(s) &= \int_0^\infty g_\tau(t)e^{-st}dt \\ &= \int_0^\tau Ce^{At}Be^{-st}dt \\ &= C\left(\int_0^\infty e^{At}e^{-st}dt\right)B - C\left(\int_\tau^\infty e^{At}e^{-st}dt\right)B \\ &= C(sI_n - A)^{-1}B - C\left(\int_0^\infty e^{A(t+\tau)}e^{-s(t+\tau)}dt\right)B \qquad (3.4) \\ &= C(sI_n - A)^{-1}B - C\left(\int_0^\infty e^{At}e^{-st}dt\right)e^{A\tau}e^{-s\tau}B \\ &= C(sI_n - A)^{-1}\left(I_n - e^{-(sI_n - A)\tau}\right)B. \qquad (3.5) \end{aligned}$$

The above expression is known as the time-limited transfer function [94]. Expanding the term $e^{A(t+\tau)}$ in step (3.4) as $e^{A(t+\tau)} = e^{At}e^{A\tau}$ leads to (3.5). Alternatively, writing $e^{A(t+\tau)}$ as $e^{A(t+\tau)} = e^{A\tau}e^{At}$ leads to $G_\tau(s) = C\left(I_n - e^{-(sI_n - A)\tau}\right)(sI_n - A)^{-1}B$.

Consider the reduced-order LTI system Σ_r given by the state space representation (2.17). The time-limited impulse response matrix for the system Σ_r is obtained from the impulse response matrix as follows:

$$g_{r,\tau}(t) = \begin{cases} g_r(t), & t \in [0, \tau], \\ 0, & t \in (\tau, \infty). \end{cases} \tag{3.6}$$

The corresponding time-limited transfer function matrix is

$$\begin{aligned} G_{r,\tau}(s) &= C_r(sI_r - A_r)^{-1}\left(I_r - e^{-(sI_r - A_r)\tau}\right)B_r \quad \text{or} \\ &= C_r\left(I_r - e^{-(sI_r - A_r)\tau}\right)(sI_r - A_r)^{-1}B_r \end{aligned}$$

As $g_\tau(t)$ is non-zero over a finite-time interval, it follows that $g_\tau \in L_2([0,\infty))$. Using $g_\tau(t)$, the $H_2(\tau)$ norm, introduced in equation (2.7), is reframed.

Definition 3.1.2. The time-limited H_2 norm or the $H_2(\tau)$ norm of the system Σ can be defined as $\|\Sigma\|_{H_2(\tau)} = \|g_\tau\|_{L_2([0,\infty))}$.

Using the above definition of $H_2(\tau)$ norm, the $H_2(\tau)$ optimal model reduction problem is reformulated in the next subsection.

3.1.2 Problem Statement

The $H_2(\tau)$ optimal model reduction problem involves obtaining Σ_r, an r^{th} order approximation of the full-order model Σ, which solves the minimization problem given by (2.47), where $\left\|\Sigma - \hat{\Sigma}\right\|^2_{H_2(\tau)} = \|g_\tau - \hat{g}_\tau\|^2_{L_2([0,\infty))}$. Let $g_{r,\tau}(t)$ be the time-limited impulse response of the system Σ_r. Since $g_{r,\tau}(t) \in L_2([0,\infty))$, the reduced-order approximation Σ_r need not be asymptotically stable even if the original system Σ is asymptotically stable. The next section derives interpolation-based optimality conditions for the $H_2(\tau)$ optimal model reduction problem. The optimality conditions are then used to propose a time-limited version of the algorithm IRKA in Section 3.3.

3.2 Interpolation-based $H_2(\tau)$ optimality conditions

The interpolation-based optimality conditions for the time-limited H_2 optimal model reduction problem have been derived in [94]. In Theorem 3.2.2, these conditions are derived using a different method. The following lemma is critical for proving Theorem 3.2.2.

Lemma 3.2.1. *Consider the impulse response matrix, $g_1(t) \in \mathbb{R}^{p\times m}$ for $t \in [0,\infty)$, and the transfer function, $G_1(s) \in \mathbb{C}^{p\times m}$, of an LTI system. Let $c \in \mathbb{C}^p$, $b \in \mathbb{C}^m$ and $\mu \in \mathbb{C}$. Let $g_2(t) = cb^T e^{\mu t}$ and $g_3(t) = cb^T te^{\mu t}$ for $t > 0$. Let $g_{1,\tau}(t)$, $g_{2,\tau}(t)$ and $g_{3,\tau}(t)$ be defined as*

$$g_{i,\tau}(t) = \begin{cases} g_i(t), & t \in [0,\tau], \\ 0, & t \in (\tau,\infty), \end{cases}$$

for $i = 1, 2$ and 3. Further, let $G_{1,\tau}(s)$ be the Laplace transform of $g_{1,\tau}(t)$. Then,

$$\langle g_{1,\tau}, g_{2,\tau}\rangle_{L_2([0,\infty))} = \overline{c^T G_{1,\tau}(-\mu)b}, \tag{3.7}$$

$$\|g_{2,\tau}\|_{L_2([0,\infty))} = \frac{\|b\|\,\|c\|}{\sqrt{2|Re(\mu)|}}\sqrt{|1 - e^{2\tau Re(\mu)}|}\ , \ \textit{and} \tag{3.8}$$

$$\langle g_{1,\tau}, g_{3,\tau}\rangle_{L_2([0,\infty))} = -\overline{c^T G'_{1,\tau}(-\mu)b}. \tag{3.9}$$

Proof. As $g_{1,\tau}(t),\ g_{2,\tau}(t) \in L_2([0,\infty))$, their inner product is given as follows,

$$\begin{aligned}\langle g_{1,\tau}, g_{2,\tau}\rangle_{L_2([0,\infty))} &= \int_0^\infty Tr(g_{1,\tau}(t)\overline{bc^T}e^{\mu^* t})dt \\ &= \overline{c^T}\left(\int_0^\infty g_{1,\tau}(t)e^{\mu^* t}dt\right)\overline{b} \\ &= \overline{c^T}\left(\overline{\int_0^\infty g_{1,\tau}(t)e^{\mu t}dt}\right)\overline{b}.\end{aligned}$$

As $G(s) = \int_0^\infty g(t)e^{-st}dt$,

$$\langle g_{1,\tau}, g_{2,\tau}\rangle_{L_2([0,\infty))} = \overline{c^T G_{1,\tau}(-\mu)b}.$$

Using (3.2) and (3.3), the $L_2([0,\infty])$ norm of $g_{2,\tau}(t)$ is obtained as follows,

$$\begin{aligned}\|g_{2,\tau}\|^2_{L_2([0,\infty))} &= \int_0^\tau Tr(cb^T e^{\mu t}bc^T e^{\mu^* t})dt \\ &= \int_0^\tau c^T \|b\|^2 ce^{(\mu+\mu^*)t}dt \\ &= \int_0^\tau \|b\|^2 \|c\|^2 e^{2(Re(\mu))t}dt \\ &= \frac{\|b\|^2\|c\|^2}{2|Re(\mu)|}|e^{2(Re(\mu))\tau} - 1|.\end{aligned}$$

Taking the positive square root of the above expression gives (3.8).

Finally, it is obvious that $g_{3,\tau}(t) \in L_2([0,\infty))$, and thus, its inner product with $g_{1,\tau}(t)$ is given by

$$\begin{aligned}\langle g_1, g_3\rangle_{L_2([0,\infty))} &= \int_0^\infty Tr(g_{1,\tau}(t)\overline{bc^T}te^{\mu^* t})dt \\ &= \int_0^\tau \overline{c^T}g_1(t)te^{\mu^* t}\overline{b}dt \\ &= \overline{c^T}\left(\overline{\int_0^\tau g_1(t)te^{\mu t}dt}\right)\overline{b} \\ &= \overline{c^T}\left(\overline{\int_0^\infty g_{1,\tau}(t)te^{\mu t}dt}\right)\overline{b}\end{aligned}$$

As $-G'(s) = \int_0^\infty g(t)te^{-st}dt$,

$$\langle g_1, g_3\rangle_{L_2([0,\infty))} = -\overline{c^T G'_{1,\tau}(-\mu)b}.$$

□

Theorem 3.2.2. *Let Σ_r, given by (2.17), be the $H_2(\tau)$ optimal r^{th} order approximation of the system Σ, given by (2.1). It is assumed that Σ_r have no poles on the imaginary axis. The pole-residue representation of the impulse response matrix of Σ_r is given by*

$$g_r(t) = \sum_{k=1}^{r} c_{r,k}b_{r,k}^T e^{\lambda_k t}, \tag{3.10}$$

with $\lambda_k \in \mathbb{C}$, $c_{r,k} \in \mathbb{C}^p$ and $b_{r,k} \in \mathbb{C}^m$ for $k = 1, \cdots, r$. Let $g_\tau(t)$ and $g_{r,\tau}(t)$ be the time-limited impulse response matrices of Σ and Σ_r, respectively. Then, for $k = 1, 2, \cdots, r$,

$$G_\tau(-\lambda_k)b_{r,k} = G_{r,\tau}(-\lambda_k)b_{r,k}, \tag{3.11}$$

$$c_{r,k}^T G_\tau(-\lambda_k) = c_{r,k}^T G_{r,\tau}(-\lambda_k), \text{ and} \tag{3.12}$$

$$c_{r,k}^T G_\tau'(-\lambda_k)b_{r,k} = c_{r,k}^T G_{r,\tau}'(-\lambda_k)b_{r,k}, \tag{3.13}$$

where $G_\tau(s)$ and $G_{r,\tau}(s)$ are the time-limited transfer functions of Σ and Σ_r, respectively.

Proof. Let $a \in \mathbb{C}^p$ be an arbitrary vector with $\|a\|_2 = 1$ and k be an index with $1 \le k \le r$. It is claimed that $\langle g_\tau - g_{r,\tau}, ab_{r,k}^T e^{\lambda_k t}\rangle_{L_2([0,\infty))} = 0$. This claim is proved using contradiction. Assume to the contrary that

$$\langle g_\tau - g_{r,\tau}, ab_{r,k}^T e^{\lambda_k t}\rangle_{L_2([0,\infty))} = \alpha (\neq 0). \tag{3.14}$$

Let $\arg(\alpha) = \theta_0$. For some arbitrary $\epsilon > 0$, let $g_r^\epsilon(t)$ be given by the following expression

$$g_r^\epsilon(t) = (c_{r,k} + \epsilon e^{i\theta_0} a) b_{r,k}^T e^{\lambda_k t} + \sum_{i \neq k} c_{r,i} b_{r,i}^T e^{\lambda_i t}. \tag{3.15}$$

Observe that $g_r^\epsilon(t)$ is obtained by perturbing $g_r(t)$. Subtracting (3.15) from (3.10) and taking the $L_2([0,\infty)])$ norm,

$$\begin{aligned} \left\| g_{r,\tau} - g_{r,\tau}^\epsilon \right\|_{L_2([0,\infty))} &= \left\| -\epsilon e^{i\theta_0} a b_{r,k}^T e^{\lambda_k t} \right\|_{L_2([0,\tau])} \\ &= |\epsilon| |e^{i\theta_0}| \left\| a b_{r,k}^T e^{\lambda_k t} \right\|_{L_2([0,\tau])}. \end{aligned}$$

Using (3.8), the above expression simplifies as

$$\begin{aligned} \left\| g_{r,\tau} - g_{r,\tau}^\epsilon \right\|_{L_2([0,\infty))} &= \epsilon \frac{\|a\|_2 \left\| b_{r,k}^T \right\|_2}{\sqrt{2|Re(\lambda_k)|}} \sqrt{|1 - e^{2\tau Re(\lambda_k)}|} \\ &= \epsilon \frac{\|b_{r,k}\|_2}{\sqrt{2|Re(\lambda_k)|}} \sqrt{|1 - e^{2\tau Re(\lambda_k)}|}. \end{aligned} \tag{3.16}$$

Let $\left\| g_{r,\tau} - g_{r,\tau}^\epsilon \right\|_{L_2([0,\infty))} = \epsilon S_k$ where $S_k = \frac{\|b_{r,k}\|_2}{\sqrt{2|Re(\lambda_k)|}} \sqrt{|1 - e^{2\tau Re(\lambda_k)}|}$. Since $g_{r,\tau}(t)$ solves the $H_2(\tau)$ optimization problem given by (2.47), the following holds,

$$\begin{aligned} \|g_\tau - g_{r,\tau}\|_{L_2([0,\infty))}^2 &\le \left\| g_\tau - g_{r,\tau}^\epsilon \right\|_{L_2([0,\infty))}^2 \\ &\le \left\| (g_\tau - g_{r,\tau}) + (g_{r,\tau} - g_{r,\tau}^\epsilon) \right\|_{L_2([0,\infty))}^2 \\ &\le \|g_\tau - g_{r,\tau}\|_{L_2([0,\infty))}^2 + 2\mathrm{Re}\langle g_\tau - g_{r,\tau}, g_{r,\tau} - g_{r,\tau}^\epsilon \rangle_{L_2([0,\infty))} + \left\| g_{r,\tau} - g_{r,\tau}^\epsilon \right\|_{L_2([0,\infty))}^2. \end{aligned}$$

Substituting the value of $(g_{r,\tau} - g_{r,\tau}^\epsilon)$ in the above inequality and using (3.14) and (3.16),

$$\begin{aligned} 0 &\le 2\mathrm{Re}\langle g_\tau - g_{r,\tau}, -\epsilon e^{i\theta_0} a b_{r,k}^T e^{\lambda_k t}\rangle_{L_2([0,\infty))} + \left\| g_{r,\tau} - g_{r,\tau}^\epsilon \right\|_{L_2([0,\infty))}^2 \\ &\le 2\mathrm{Re}\left(\overline{-\epsilon e^{i\theta_0}} \langle g_\tau - g_{r,\tau}, ab_{r,k}^T e^{\lambda_k t}\rangle_{L_2([0,\infty))} \right) + \left(\epsilon \frac{\|b_{r,k}\|_2}{\sqrt{2|Re(\lambda_k)|}} \sqrt{|1 - e^{2\tau Re(\lambda_k)}|} \right)^2 \\ &\le 2\mathrm{Re}\left(-\epsilon e^{-i\theta_0} |\alpha| e^{i\theta_0} \right) + \epsilon^2 \frac{\|b_{r,k}\|_2^2}{2|Re(\lambda_k)|} |1 - e^{2\tau Re(\lambda_k)}|. \end{aligned}$$

The above discussion implies that $0 \leq -2\epsilon|\alpha| + \epsilon^2 S_k^2$ for arbitrary value of $\epsilon > 0$. This is possible only if $\alpha = 0$. From (3.14), it follows that

$$\langle g_\tau - g_{r,\tau}, a b_{r,k}^T e^{\lambda_k t} \rangle_{L_2([0,\infty))} = 0.$$

Due to (3.7), the above equation can be written as,

$$\overline{a^T (G_\tau - G_{r,\tau})(-\lambda_k) b_{r,k}} = 0.$$

As a was chosen arbitrarily,

$$(G_\tau - G_{r,\tau})(-\lambda_k) b_{r,k} = 0,$$

which results in (3.11). Similarly, (3.12) can be proved by repeating the above analysis with $c_{r,k} d^T e^{\lambda_k t}$ instead of $a b_{r,k}^T e^{\lambda_k t}$ for some arbitrary $d \in \mathbb{C}^m$ and $\|d\|_2 = 1$.

In order to prove (3.13), it is claimed that $\langle g_\tau - g_{r,\tau}, c_{r,k} b_{r,k}^T t e^{\lambda_k t} \rangle_{L_2([0,\infty))} = 0$. This claim is proved using contradiction. Assume to the contrary that

$$\langle g_\tau - g_{r,\tau}, c_{r,k} b_{r,k}^T t e^{\lambda_k t} \rangle_{L_2([0,\infty))} = \beta (\neq 0). \tag{3.17}$$

Let $\theta_1 = \arg(\beta)$. For sufficiently small $\epsilon > 0$,

$$g_r^\epsilon(t) = c_{r,k} b_{r,k}^T e^{(\lambda_k + \epsilon e^{i\theta_1})t} + \sum_{i \neq k} c_{r,i} b_{r,i}^T e^{\lambda_i t}. \tag{3.18}$$

For the above expression of $g_r^\epsilon(t)$,

$$\begin{aligned}
&\left\| g_{r,\tau} - g_{r,\tau}^\epsilon \right\|_{L_2([0,\infty))} \\
&= \left\| c_{r,k} b_{r,k}^T e^{\lambda_k t} (1 - e^{\epsilon e^{i\theta_1} t}) \right\|_{L_2([0,\tau])} \\
&= \left\| c_{r,k} b_{r,k}^T e^{\lambda_k t} (-\epsilon e^{i\theta_1} t - \epsilon^2 e^{2i\theta_1} t^2 - \cdots) \right\|_{L_2([0,\tau])}
\end{aligned}$$

As $g_{r,\tau}(t)$ solves the $H_2(\tau)$ optimization problem (2.47),

$$0 \leq 2\mathrm{Re}\langle g_\tau - g_{r,\tau}, g_{r,\tau} - g_{r,\tau}^\epsilon \rangle_{L_2([0,\infty))} + \left\| g_{r,\tau} - g_{r,\tau}^\epsilon \right\|_{L_2([0,\infty))}^2. \tag{3.19}$$

The first term of the right-hand side of the above inequality can be written as

$$\begin{aligned}
&2\mathrm{Re}\langle g_\tau - g_{r,\tau}, g_{r,\tau} - g_{r,\tau}^\epsilon \rangle_{L_2([0,\infty))} \\
&= 2\mathrm{Re}\langle g_\tau - g_{r,\tau}, c_{r,k} b_{r,k}^T e^{\lambda_k t} (-\epsilon e^{i\theta_1} t - \epsilon^2 e^{2i\theta_1} t^2 - \cdots) \rangle_{L_2([0,\infty))} \\
&= 2\mathrm{Re}\langle g_\tau - g_{r,\tau}, c_{r,k} b_{r,k}^T e^{\lambda_k t} (-\epsilon e^{i\theta_1} t) \rangle_{L_2([0,\infty))} + 2\mathrm{Re}\langle g_\tau - g_{r,\tau}, c_{r,k} b_{r,k}^T e^{\lambda_k t} (-\epsilon^2 e^{2i\theta_1} t^2 - \cdots) \rangle_{L_2([0,\infty))}.
\end{aligned} \tag{3.20}$$

By applying the Cauchy-Schwarz inequality,

$$\begin{aligned}
&2\mathrm{Re}\langle g_\tau - g_{r,\tau}, c_{r,k} b_{r,k}^T e^{\lambda_k t} (-\epsilon^2 e^{2i\theta_1} t^2 - \cdots) \rangle_{L_2([0,\infty))} \\
&\leq 2 \left\| g_\tau - g_{r,\tau} \right\|_{L_2([0,\infty))} \left\| c_{r,k} b_{r,k}^T e^{\lambda_k t} (-\epsilon^2 e^{-2i\theta_1} t^2 - \cdots) \right\|_{L_2([0,\tau])} \\
&\leq \epsilon^2 T_k.
\end{aligned}$$

Using the above inequality in (3.20) and the definition of β, it follows that

$$\begin{aligned} 2\mathrm{Re}\langle g_\tau - g_{r,\tau}, g_{r,\tau} - g^\epsilon_{r,\tau}\rangle_{L_2([0,\infty))} &\leq 2\mathrm{Re}(-\epsilon e^{i\theta_1}\langle g_\tau - g_{r,\tau}, c_{r,k} b_{r,k}^T t e^{\lambda_k t}\rangle_{L_2([0,\infty))}) + \epsilon^2 T_k \\ &\leq 2\mathrm{Re}(-\epsilon e^{i\theta_1}|\beta| e^{-i\theta_1}) + \epsilon^2 T_k. \end{aligned}$$

The above discussion implies that (3.19) can be simplified to $0 \leq -2\epsilon|\beta| + \epsilon^2 T_k$. This is true for arbitrary small values of ϵ only if $\beta = 0$. If $\beta = 0$, then

$$\langle g_\tau - g_{r,\tau}, c_{r,k} b_{r,k}^T t e^{\lambda_k t}\rangle_{L_2([0,\infty))} = 0.$$

Using (3.9) in the above expression yields

$$-\overline{c_{r,k}^T (G_\tau - G_{r,\tau})'(-\lambda_k) b_{r,k}} = 0.$$

Thus, (3.13) is obtained. □

3.3 Rational interpolation over a restricted time interval

This section introduces an interpolation-based projection framework for time-limited model reduction. A pair of modified rational Krylov subspaces is computed, and a reduced model is obtained by projecting the full-order model onto them. The subspaces are calculated such that the reduced system's time-limited transfer function approximates the full-order system's time-limited transfer function at a given set of interpolation points along given tangential directions. For a set of r distinct interpolation points $\{\sigma_1, \cdots, \sigma_r\}$ and corresponding tangential directions $\{b_1, \cdots, b_r\}$ and $\{c_1, \cdots, c_r\}$, the modified Krylov subspaces are obtained as follows,

$$\mathcal{V}_r = \underset{i=1,2,\ldots,r}{\text{span}} \{(\sigma_i I_n - A)^{-1}(I_n - e^{-\sigma_i \tau} e^{A\tau}) B b_i\}, \text{ and} \tag{3.21}$$

$$\mathcal{W}_r = \underset{i=1,2,\ldots,r}{\text{span}} \{(\sigma_i{}^* I_n - A^T)^{-1}(I_n - e^{-\sigma_i{}^* \tau} e^{A^T \tau}) C^T c_i\}. \tag{3.22}$$

The complex-valued interpolation points and tangential directions are closed under conjugation. Let $V_r \in \mathbb{R}^{n\times r}$ and $W_r \in \mathbb{R}^{n\times r}$ be the basis matrices for the subspaces $\mathcal{V}_r$ and $\mathcal{W}_r$, respectively. Let $Z_r^T = (W_r^T V_r)^{-1} W_r^T$ such that $Z_r^T V_r = I_{r\times r}$. The state-space matrices of the reduced-order system are obtained by Petrov-Galerkin projection as follows:

$$A_r = Z_r^T A V_r,\ B_r = Z_r^T B, \text{ and } C_r = C V_r. \tag{3.23}$$

The reduced model obtained above does not result in the exact interpolation of the time-limited transfer functions. The following theorem quantifies the interpolation errors.

Theorem 3.3.1. *Consider the subspaces $\mathcal{V}_r$ and $\mathcal{W}_r$ and the matrices V_r and W_r, as defined above. Let $\Pi = V_r Z_r^T$. Let $\sigma \in \{\sigma_1, \cdots, \sigma_r\}$ be an interpolation point and b and c be the corresponding right and left tangential directions such that σ is not an eigenvalue of A or A_r. Let A and A_r be diagonalizable matrices with eigenvalue decompositions, $A_r = Q_{A_r} \Lambda Q_{A_r}^{-1}$ and $A = Q_A \Gamma Q_A^{-1}$,*

respectively, where $\Lambda = diag(\lambda_1, \ldots, \lambda_r)$ *and* $\Gamma = diag(\gamma_1, \ldots, \gamma_n)$. *Then,*

$$G_\tau(\sigma)b - G_{r,\tau}(\sigma)b = e^{-\sigma\tau}CV_r(\sigma I_r - A_r)^{-1}Z_r^T(e^{A\Pi\tau} - e^{A\tau})Bb, \tag{3.24}$$

$$c^TG_\tau(\sigma) - c^TG_{r,\tau}(\sigma) = e^{-\sigma\tau}c^TC(e^{\Pi A\tau} - e^{A\tau})V_r(\sigma I_r - A_r)^{-1}Z_r^TB, \tag{3.25}$$

$$c^TG_\tau{}'(\sigma)b - c^TG_{r,\tau}{}'(\sigma)b = R_{P_1}(\sigma) + R_{P_2}(\sigma), \text{ and} \tag{3.26}$$

$$c^TG_\tau{}'(\sigma)b - c^TG_{r,\tau}{}'(\sigma)b = R_{Q_1}(\sigma) + R_{Q_2}(\sigma), \tag{3.27}$$

where $R_{P_1}(\sigma)$, $R_{P_2}(\sigma)$, $R_{Q_1}(\sigma)$ *and* $R_{Q_2}(\sigma)$ *are given by*

$$R_{P_1}(\sigma) = -e^{-\sigma\tau}c^TCV_r(\sigma I_r - A_r)^{-2}((\sigma I_r - A_r)\tau + I_r)Z_r^T(e^{A\Pi\tau} - e^{A\tau})Bb, \tag{3.28}$$

$$R_{P_2}(\sigma) = e^{-\sigma\tau}c^TC(I_n - P(\sigma))(\sigma I_n - A)^{-2}\left((\tau(\sigma I_n - A) + I_n) - e^{\tau(\sigma I_n - A)}\right)e^{A\tau}Bb, \tag{3.29}$$

$$R_{Q_1}(\sigma) = -e^{-\sigma\tau}c^TC(e^{\Pi A\tau} - e^{A\tau})V_r(\sigma I_r - A_r)^{-2}(I_r + \tau(\sigma I_r - A_r))Z_r^TBb, \text{ and} \tag{3.30}$$

$$R_{Q_2}(\sigma) = e^{-\sigma\tau}c^TCe^{A\tau}\left((\tau(\sigma I_n - A) + I_n) - e^{\tau(\sigma I_n - A)}\right)(\sigma I_n - A)^{-2}(I_n - Q(\sigma))Bb. \tag{3.31}$$

Here, $P(s)$ *and* $Q(s)$ *are matrix-valued functions defined as*

$$P(s) = V_r(sI_r - A_r)^{-1}Z_r^T(sI_n - A), \text{ and} \tag{3.32}$$

$$Q(s) = (sI_n - A)V_r(sI_r - A_r)^{-1}Z_r^T. \tag{3.33}$$

These functions are projectors for any $s \in \mathbb{C}$ *that is not an eigenvalue of* A *or* A_r.

Proof. As σ is not an eigenvalue of A and A_r, a neighbourhood of $s = \sigma$ exists where the matrix-valued functions $P(s)$ and $Q(s)$ are analytic. For $P(s)$, the following result is obtained.

$$\begin{aligned}(P(s))^2 &= P(s)P(s)\\ &= V_r(sI_r - A_r)^{-1}Z_r^T(sI_n - A)V_r(sI_r - A_r)^{-1}Z_r^T(sI_n - A)\\ &= V_r(sI_r - A_r)^{-1}(sI_r - A_r)(sI_r - A_r)^{-1}Z_r^T(sI_n - A)\\ &= V_r(sI_r - A_r)^{-1}Z_r^T(sI_n - A)\\ &= P(s).\end{aligned}$$

As a consequence of the above relation, the following result holds.

$$\mathcal{V}_r = \text{Ran } P(s) = \text{Ker } (I_n - P(s)). \tag{3.34}$$

Similarly, the following relation is obtained for the matrix $Q(s)$.

$$\begin{aligned}(Q(s))^2 &= Q(s)Q(s)\\ &= (sI_n - A)V_r(sI_r - A_r)^{-1}Z_r^T(sI_n - A)V_r(sI_r - A_r)^{-1}Z_r^T\\ &= (sI_n - A)V_r(sI_r - A_r)^{-1}(sI_r - A_r)(sI_r - A_r)^{-1}Z_r^T\\ &= Q(s).\end{aligned}$$

The following is obtained based on the above result.

$$\mathcal{W}_r{}^\perp = \text{Ker } Q(s) = \text{Ran } (I_n - Q(s)). \tag{3.35}$$

The error in the right tangential interpolation condition is given by

$$G_\tau(s)b - G_{r,\tau}(s)b = C(sI_n - A)^{-1}(I_n - e^{-s\tau}e^{A\tau})Bb - C_r(sI_r - A_r)^{-1}(I_r - e^{-s\tau}e^{A_r\tau})B_r b.$$

Substituting A_r, B_r and C_r from (3.23) in the above expression and using the identity $e^{A_r\tau}B_r = Z_r^T e^{A\Pi\tau}B$ gives

$$\begin{aligned}
&G_\tau(s)b - G_{r,\tau}(s)b \\
&= C(I_n - P(s))(sI - A)^{-1}(I_n - e^{-s\tau}e^{A\tau})Bb + \\
&CV_r(sI_r - A_r)^{-1}Z_r^T(sI_n - A)(sI_n - A)^{-1}(I_n - e^{-s\tau}e^{A\tau})Bb - \\
&CV_r(sI_r - A_r)^{-1}(B_r - e^{-s\tau}e^{A_r\tau}B_r)b \\
&= C(I_n - P(s))(sI - A)^{-1}(I_n - e^{-s\tau}e^{A\tau})Bb + CV_r(sI_r - A_r)^{-1}(Z_r^T B - e^{-s\tau}Z_r^T e^{A\tau}B)b \\
&- CV_r(sI_r - A_r)^{-1}(B_r - e^{-s\tau}Z_r^T e^{A\Pi\tau}B)b \\
&= C(I_n - P(s))(sI - A)^{-1}(I_n - e^{-s\tau}e^{A\tau})Bb + e^{-s\tau}CV_r(sI_r - A_r)^{-1}Z_r^T(e^{A\Pi\tau} - e^{A\tau})Bb. \quad (3.36)
\end{aligned}$$

For $s = \sigma$, by definition, the vector $(\sigma I_n - A)^{-1}\left(I_n - e^{-\sigma\tau}e^{A\tau}\right)Bb \in \mathcal{V}_r$. Further, due to (3.34), this vector also lies in the nullspace of $(I_n - P(\sigma))$. Hence, evaluating the above expression at $s = \sigma$ results in (3.24).

Similar to the right tangential interpolation error, for the left tangential interpolation error, using the identity $C_r e^{A_r\tau} = Ce^{\Pi A\tau}V_r$ and substituting A_r, B_r and C_r from (3.23) yields

$$\begin{aligned}
&c^T G_\tau(s) - c^T G_{r,\tau}(s) \\
&= c^T C(I_n - e^{-s\tau}e^{A\tau})(sI_n - A)^{-1}B - c^T C_r(I_r - e^{-s\tau}e^{A_r\tau})(sI_r - A_r)^{-1}B_r \\
&= c^T C(I_n - e^{-s\tau})(sI_n - A)^{-1}(I_n - Q(s))B + \\
&c^T C(I_n - e^{-s\tau}e^{A\tau})(sI_n - A)^{-1}(sI_n - A)V_r(sI_r - A_r)^{-1}B_r - \\
&c^T(C_r - e^{-s\tau}C_r e^{A_r\tau})(sI_r - A_r)^{-1}B_r \\
&= c^T C(I_n - e^{-s\tau}e^{A\tau})(sI_n - A)^{-1}B + c^T(C_r - e^{-s\tau}e^{A\tau}V_r)(sI_r - A_r)^{-1}B_r \\
&- c^T(C_r - e^{-s\tau}Ce^{\Pi A\tau}V_r)(sI_r - A_r)^{-1}B_r \\
&= ((sI_n - A^T)^{-1}(I_n - e^{-s\tau}e^{A^T\tau})C^T c)^T(I - Q(s))B \\
&+ e^{-s\tau}c^T C(e^{\Pi A\tau} - e^{A\tau})V_r(sI_r - A_r)^{-1}B_r. \quad (3.37)
\end{aligned}$$

As $(\sigma I_n - A^T)^{-1}(I_n - e^{-\sigma\tau}e^{A^T\tau})C^T c \in \mathcal{W}_r$ and by (3.35), evaluating the above expression at $s = \sigma$ gives (3.25).

Pre multiplying the left-hand side of (3.36) by c^T, denoting $(I_n - e^{-s\tau}e^{A\tau})$ by $E(s)$ and differentiating the expression obtained in a neighbourhood of $s = \sigma$ where $P(s)$ is analytic gives

$$\begin{aligned}
&c^T G_\tau'(s)b - c^T G_{r,\tau}'(s)b \\
&= c^T \frac{d}{ds}\left(G_\tau(s)b - G_{r,\tau}(s)b\right) \\
&= c^T C\left(-\frac{d}{ds}P(s)\right)(sI_n - A)^{-1}E(s)Bb + c^T C(I_n - P(s))\frac{d}{ds}\left((sI_n - A)^{-1}E(s)Bb\right) + \\
&\frac{d}{ds}\left(e^{-s\tau}c^T CV_r(sI_r - A_r)^{-1}\right)Z_r{}^T(e^{A\Pi\tau}B - e^{A\tau}B)b. \quad (3.38)
\end{aligned}$$

The first term of the expression given by (3.38) can be simplified as

$$\begin{aligned}
&c^T C\left(-\frac{d}{ds}P(s)\right)(sI_n - A)^{-1}E(s)Bb \\
&= c^T C\left(V_r(sI_r - A_r)^{-2}Z_r(sI_n - A) - V_r(sI_r - A_r)^{-1}Z_r^T(sI_n - A)\right)(sI_n - A)^{-1}E(s)Bb. \quad (3.39)
\end{aligned}$$

The second term of the expression given by (3.38) can be simplified as

$$\begin{aligned}
&c^T C(I_n - P(s))\frac{d}{ds}\left((sI_n - A)^{-1}E(s)\right)Bb \\
&= c^T C(I_n - P(s))\left(-(sI_n - A)^{-2}\left(I_n - e^{-(sI_n - A)\tau}\right) + (sI_n - A)^{-1}\tau e^{-(sI_n - A)\tau}\right)Bb \\
&= c^T C(I_n - P(s))(sI - A)^{-2}\left(-(I_n - e^{-(sI_n - A)\tau}) + \tau(sI_n - A)e^{-(sI_n - A)\tau}\right)Bb \\
&= c^T C(I_n - P(s))(sI - A)^{-2}e^{-s\tau}\left(-e^{(sI_n - A)\tau} + I_n + \tau(sI_n - A)\right)e^{A\tau}Bb \\
&= e^{-s\tau}c^T C(I_n - P(s))(sI - A)^{-2}\left((sI_n - A)\tau + I_n - e^{(sI_n - A)\tau}\right)e^{A\tau}Bb. \quad (3.40)
\end{aligned}$$

The third term of the expression given by (3.38) can be simplified as

$$\begin{aligned}
&\frac{d}{ds}\left(e^{-s\tau}c^T CV_r(sI_r - A_r)^{-1}\right){Z_r}^T(e^{A\Pi\tau}B - e^{A\tau}B)b \\
&= c^T CV_r\left(-\tau e^{-s\tau}(sI_r - A_r)^{-1} - e^{-s\tau}(sI_r - A_r)^{-2}\right)Z_r^T(e^{A\Pi\tau} - e^{A\tau})Bb \\
&= e^{-s\tau}c^T CV_r(sI_r - A_r)^{-2}\left(-\tau(sI_r - A_r) - I_r\right)Z_r^T(e^{A\Pi\tau} - e^{A\tau})Bb. \quad (3.41)
\end{aligned}$$

Substituting the expressions (3.39), (3.40) and (3.41) in (3.38) yields

$$\begin{aligned}
&c^T G_\tau'(s)b - c^T G_{r,\tau}'(s)b \\
&= c^T C\{V_r(sI_r - A_r)^{-2}Z_r^T(sI_n - A) - V_r(sI_r - A_r)^{-1}Z_r^T\}(sI_n - A)^{-1}E(s)Bb + \\
&e^{-s\tau}c^T C(I_n - P(s))(sI_n - A)^{-2}\left((\tau(sI_n - A) + I_n) - e^{(sI_n - A)\tau}\right)e^{A\tau}Bb - \\
&e^{-s\tau}c^T CV_r(sI_r - A_r)^{-2}((sI_r - A_r)\tau + I_r)Z_r^T(e^{A\Pi\tau} - e^{A\tau})Bb.
\end{aligned}$$

Substituting $s = \sigma$ in the last term above, the last two terms are non-zero, and the remaining term vanishes as $(\sigma I_n - A)^{-1}E(s)Bb \in \mathcal{V}_r$. Thus, (3.26) is obtained.

Finally, right multiplying (3.37) by b and differentiating the expression with respect to s in a neighbourhood of $s = \sigma$ gives

$$\begin{aligned}
&c^T G_\tau'(s)b - c^T G_{r,\tau}'(s)b \\
&= \frac{d}{ds}\left(\left((sI_n - A^T)^{-1}(I_n - e^{-s\tau}e^{A^T\tau}C^T c)\right)^T\right)(I_n - Q(s))Bb + \\
&\left((sI_n - A^T)^{-1}(I_n - e^{-s\tau}e^{A^T\tau}C^T c)\right)^T\left(-\frac{dQ(s)}{ds}\right)Bb + \\
&\frac{d}{ds}\left(e^{-s\tau}c^T C(e^{\Pi A\tau} - e^{A\tau})V_r(sI_r - A_r)^{-1}B_r b\right) \\
&= c^T CE(s)(sI_n - A)^{-1}\left((sI_n - A)V_r(sI_r - A_r)^{-2}Z_r^T - V_r(sI_r - A_r)^{-1}Z_r^T\right)Bb + \\
&e^{-s\tau}c^T Ce^{A\tau}\left((\tau(sI_n - A) + I_n) - e^{\tau(sI_n - A)}\right)(sI_n - A)^{-2}(I_n - Q(s))Bb + \\
&-e^{-s\tau}c^T C(e^{\Pi A\tau} - e^{A\tau})V_r(sI_r - A_r)^{-2}(I_r + \tau(sI_r - A_r)){Z_r}^T Bb. \quad (3.42)
\end{aligned}$$

For $s = \sigma$ in the last term above, the vector $(\sigma^* I_n - A^T)^{-1}(E(s))^T C^T c$ lies in $\mathcal{W}_r$. Hence, only the last two terms remain while the remaining term vanishes, (3.27) is obtained. □

When the interpolation errors are small, the projection-based interpolation framework introduced at the beginning of this section works well. The following results are utilized to quantify the interpolation errors.

1. For a given $x \in \mathbb{R}^n$, the vector $\hat{x} \in \mathbb{R}^n$ that satisfies the constraint $Z^T\hat{x} = 0$, where $Z \in \mathbb{R}^{n\times r}$ with $r \leq n$ such that $Z^TZ = I_r$ and minimizes $\|x - \hat{x}\|^2$ is given by $\hat{x} = (I_n - ZZ^T)x$. This is, by definition, the distance of the vector x from the Kernel of Z^T. It is an application of the projection theorem of linear algebra (Theorem 2, Section 3.3, [58]).

2. Assuming K to be diagonalizable matrix with eigendecomposition $K = Q_K\Lambda_K Q_K^{-1}$, $\|K\|_2 \leq \kappa(Q_K)\rho(K)$, $\left\|K^{-1}\right\|_2 \leq \kappa(Q_K)/\rho(K)$, $\left\|K^{-2}\right\|_2 \leq \kappa(Q_K)/\rho(K^2)$ and $\left\|e^K\right\|_2 \leq \kappa(Q_K)\rho(e^K)$.

The upper bounds of the interpolation errors are now examined. From (3.24),

$$\|G_\tau(\sigma)b - G_{r,\tau}(\sigma)b\|_2 \leq |e^{-\sigma\tau}|\|CV_r\|_2 \left\|(\sigma I_r - A_r)^{-1}\right\|_2 \left\|Z_r^T(e^{A\Pi\tau} - e^{A\tau})Bb\right\|_2. \tag{3.43}$$

The first term of the upper bound equals $|e^{-\sigma\tau}| = |e^{-(\mathrm{Re}(\sigma)\tau)}e^{-j(\mathrm{Im}(\sigma)\tau)}| = |e^{-(\mathrm{Re}(\sigma)\tau)}|$ because $e^{-j(\mathrm{Im}(\sigma)\tau)} = 1$. A bound for the third term by applying the second result stated above is obtained as follows: $\left\|(\sigma I_r - A_r)^{-1}\right\|_2 \leq \kappa(Q_{A_r})/\rho(\sigma I_r - A_r)$. Considering the first result stated above, it can be shown that the vector $(I_n - Z_rZ_r^T)(e^{A\Pi\tau} - e^{A\tau})Bb$ minimizes $\left\|Z_r^T(e^{A\Pi\tau} - e^{A\tau})Bb\right\|_2^2$. Hence, the fourth term is, by definition, the distance of the vector $(e^{A\Pi\tau} - e^{A\tau})Bb$ from the kernel of Z_r^T.

Similarly, (3.25) yields

$$\left\|c^TG_\tau(\sigma) - c^TG_{r,\tau}(\sigma)\right\|_2 \leq |e^{-\sigma\tau}|\left\|c^TC(e^{\Pi A\tau} - e^{A\tau})V_r\right\|_2\left\|(\sigma I_r - A_r)^{-1}\right\|_2\left\|Z_r^TB\right\|_2, \tag{3.44}$$

The first and third terms of the above error bound are the same as those of the error bound of (3.43). Hence, they can be analyzed similarly. Further, using the first result stated above, it can be shown that the second term of the upper bound in (3.44) is the distance of $(e^{A^T\Pi^T\tau} - e^{A^T\tau})C^Tc$ from the kernel of V_r^T.

Finally, from (3.26) gives

$$\begin{aligned}
\left\|c^TG_\tau'(\sigma)b - c^TG_{r,\tau}'(\sigma)b\right\|_2 &\leq \|R_{P_1}(\sigma)\|_2 + \|R_{P_2}(\sigma)\|_2 \text{ where} \\
\|R_{P_1}(\sigma)\|_2 &\leq |e^{-\sigma\tau}|\left\|c^TCV_r\right\|_2\left\|(\sigma I_r - A_r)^{-2}\right\|_2 \times \\
&\quad \|((\sigma I_r - A_r)\tau + I_r)\|_2\left\|Z_r{}^T(e^{A\Pi\tau} - e^{A\tau})Bb\right\|_2, \text{ and} \qquad (3.45)\\
\|R_{P_2}(\sigma)\|_2 &\leq |e^{-\sigma\tau}|\left\|c^TC(I_n - P(\sigma))\right\|_2\left\|(\sigma I_n - A)^{-2}\right\|_2 \times \\
&\quad \left\|\left((\tau(\sigma I_n - A) + I_n) - e^{\tau(\sigma I_n - A)}\right)\right\|_2\left\|e^{A\tau}\right\|_2\|Bb\|_2. \qquad (3.46)
\end{aligned}$$

There are several terms in the above upper bounds which are similar to those in (3.44) and (3.43). They can be analyzed similarly. Based on the first result, it is seen that the third term of the bound in (3.45) is bounded above by $\kappa(Q_{A_r})/\rho((\sigma I_r - A_r)^2)$. Similarly, the third term in (3.46) is bounded above by $\kappa(Q_A)/\rho((\sigma I_n - A)^2)$, and the fourth term is bounded above by $\kappa(Q_A)\rho(e^{A\tau})$. The upper bounds of the two components R_{Q_1} and R_{Q_2} of (3.27) can be analysed similarly.

If $\mathrm{Re}(-\sigma)\tau \gg 1$, the term $e^{-Re(\sigma)\tau}$ has a notable impact on the upper bounds of all the errors. If $\rho(\sigma I_r - A_r) \ll 1$, it will contribute significantly to the upper bounds of (3.43), (3.44) and

(3.45). Further, if $\rho((\sigma I_n - A)^2) \ll 1$, it will have a notable contribution to the error bound of the bitangential interpolation error. If the matrix A has unstable eigenvalues ($\gamma_i \gg 0$) such that $\rho(e^{A\tau}) \gg 1$, it will contribute significantly to the upper bound of (3.46). Also, as $\tau \to 0$, the second term of the upper bound of (3.44) and fourth terms of the upper bound of (3.43), (3.45) and (3.46) vanish. This ensures that all the error bounds are negligible for sufficiently small values of τ.

3.4 An interpolation-based algorithm for $H_2(\tau)$ optimal model reduction

In this section, a numerical algorithm for $H_2(\tau)$ optimal model reduction is proposed, which utilizes the interpolation-based projection framework introduced in the previous section and its computational complexity is also discussed.

3.4.1 TL-IRKA model reduction algorithm

As the interpolation data is not known apriori, constructing a reduced-order model satisfying the time-limited H_2 optimality conditions is difficult. Therefore, the time-limited rational interpolation framework proposed above is used to develop an iterative correction method given by Algorithm 7.

Algorithm 7: Time-Limited Iterative Rational Krylov Algorithm (TL-IRKA)

Input: The system matrices: A, B, C;
Initial interpolation points: $\{\sigma_1, \ldots, \sigma_r\}$;
Initial tangential directions: $\tilde{B} = [b_1, \ldots, b_r]$ and $\tilde{C} = [c_1, \ldots, c_r]$;
A finite-time interval $[0, \tau]$ s;

Output: The reduced matrices A_r, B_r, C_r;

1. Compute V_r and W_r using (3.21) and (3.22) respectively and let ${Z_r}^T = ({W_r}^T V_r)^{-1} {W_r}^T$;
2. **while** *(not converged)* **do**
   a. $A_r = {Z_r}^T A V_r,\ B_r = {Z_r}^T B,\ C_r = C V_r$;
   b. Compute $A_r = R \Lambda R^{-1}$ where R^{-1} and R are the left and right eigenvectors of A_r ;
   c. Update interpolation points and tangential directions as follows:
      i. $\sigma_i \leftarrow -\lambda_i(\Lambda)$ for $i = 1, 2, \ldots, r$,
      ii. $\tilde{B} = {B_r}^T R^{-T}$ and
      iii. $\tilde{C} = C_r R$;
   d. Update V_r and W_r using (3.21) and (3.22), respectively, and let ${Z_r}^T = ({W_r}^T V_r)^{-1} {W_r}^T$;

end

3. $A_r = {Z_r}^T A V_r,\ B_r = {Z_r}^T B,\ C_r = C V_r$;

The algorithm is stopped when the change in eigenvalues of the reduced state matrix A_r for two consecutive iterations becomes less than a preset tolerance. A formal proof of the convergence of TL-IRKA is not provided. However, the algorithm has been tested on a number of examples. For a proper set of initial interpolation points and tangential directions, it is observed that the algorithm converges after a finite number of iterations. The reduced model obtained using TL-IRKA will not satisfy the first-order necessary conditions for time-limited H_2 optimality exactly. The closeness to optimality of the reduced model is estimated using the error expressions derived in Theorem 3.3.1.

Remark 4. The interpolation points and tangential directions of TL-IRKA can be initialized using various techniques. The initial interpolation points and tangential directions can be randomly chosen. A second possible technique is randomly initializing conventional IRKA and using the reduced-order system to obtain the initial interpolation points and tangential directions of TL-IRKA. A third possible method of initializing TL-IRKA is using the dominant pole algorithm [79] to compute eigenvalues and corresponding left and right eigenvectors corresponding to the dominant residues.

Remark 5. The proposed method aims to find a reduced model whose impulse response approximates the impulse response of the original system with zero initial conditions. However, the reduced-order model can behave differently from the original model for non-zero initial conditions. For example, suppose the original system is stable, and the reduced-order model is unstable. In that case, if the initial conditions are chosen in the region spanned by the eigenvectors corresponding to the unstable eigenvalues of the reduced-order system, the system responses can significantly diverge.

3.4.2 Computational cost of TL-IRKA

Similar to other Krylov-based model reduction strategies, the implementation of TL-IRKA involves the use of matrix-vector multiplications and linear solvers. The implementation of TL-IRKA also includes the computation of terms like $e^{A\tau}b$. The matrix exponential term $e^{A\tau}$ is computed with the MATLAB function 'expm'. This term is computed only once at the start of the iteration process and has a cost of $\mathcal{O}(n^3)$. Then, two sets of r linear equations are solved for every iteration. The equations are given by $\{(\sigma_i I_n - A)x_i = (I_n - e^{-\sigma_i \tau}e^{A\tau})Bb_i, i = 1, \ldots, r\}$ and $\{(\sigma_i^* I_n - A^T)y_i = (I_n - e^{-\sigma_i^* \tau}e^{A^T\tau})C^T c_i, i = 1, \ldots, r\}$. The cost of computing the right-hand side of the equations is $\mathcal{O}(2n^2 r)$. The direct LU solver in MATLAB is used for solving the linear equations, which costs $\mathcal{O}(2n^3 r)$. If N is the number of iterations required for convergence of TL-IRKA, its computational complexity is given by $\mathcal{O}(n^3 + N(2n^2 r + 2n^3 r))$.

3.5 Comparison of TL-IRKA with TL-TSIA

This section will compare the time-limited H_2 optimal model reduction algorithms TL-TSIA and TL-IRKA. This is inspired by the comparison of the algorithms IRKA and TSIA in [14], discussed in Section 2.4 of the thesis. TL-TSIA is a projection-based iterative algorithm. A reduced model of order r, obtained using IRKA, is used for initializing TL-TSIA. At every iteration, the right and

left projection matrices are obtained by solving the following time-limited Sylvester equations,

$$AX + XA_r{}^T + BB_r{}^T - e^{A\tau}BB_r{}^T e^{A_r{}^T\tau} = 0, \text{ and} \tag{3.47}$$

$$A^TY + YA_r + C^TC_r - e^{A^T\tau}C^TC_r e^{A_r\tau} = 0, \tag{3.48}$$

where X is the right projection matrix. To ensure that $((Y^TX)^{-1}Y^T)X = I_r$, the left projection matrix is chosen as $(Y^TX)^{-1}Y^T$. The projection matrices are used to obtain new reduced-order matrices. They are used in the subsequent iteration to construct a new set of projection matrices. The iterations are stopped when the relative change in the eigenvalues of the state matrix A_r of the reduced-order system becomes less than a fixed tolerance value. A similar convergence criterion has been used for the algorithm TL-IRKA proposed in Algorithm 7.

Theorem 3.5.1. *Let, the state matrix A of the system Σ, given by (2.1), and the state matrix A_r of Σ_r, given by (2.17) and obtained using IRKA, are diagonalizable. It is assumed that TL-IRKA is initialized with the poles and residues of Σ_r, and TL-TSIA is initialized with the state-space matrices of Σ_r. If TL-IRKA and TL-TSIA converge, they converge to equivalent reduced-order models.*

Proof. The projection subspaces $\mathcal{V}_r$ and $\mathcal{W}_r$ are computed using the formulas (3.21) and (3.22), respectively, for the first iteration of the algorithm TL-IRKA. Similarly, for the first iteration of the algorithm TL-TSIA, the projection matrices, X and Y, are obtained using (3.47) and (3.48), respectively. It is claimed that $\mathcal{V}_r = \text{Ran}(X)$, i.e., the right projection subspace $\mathcal{V}_r$ and the right projection subspace spanned by the columns of the matrix X are equivalent. This claim is proved as follows.

For the reduced-order model Σ_r, let A_r, B_r and C_r be the state-space matrices, and $\{(\lambda_i, b_i, c_i), i = 1, \ldots, r\}$ be the poles and residues. Let $A_r = SDS^{-1}$ be the eigen-decomposition of A_r. Similarly, let $e^{A_r\tau} = Se^{D\tau}S^{-1}$ be the eigen-decomposition of $e^{A_r\tau}$. The eigen-decompositions of A_r and $e^{A_r\tau}$ are substituted in (3.47) and this yields

$$\begin{aligned}
&AX + X(SDS^{-1})^T + B\hat{B}^T - e^{A\tau}B\hat{B}^T(Se^{D\tau}S^{-1})^T = 0\\
&\Rightarrow AX + XS^{-T}D^TS^T + B\hat{B}^T - e^{A\tau}B\hat{B}^TS^{-T}e^{D^T\tau}S^T = 0\\
&\Rightarrow AXS^{-T} + XS^{-T}D^T + BB_r{}^TS^{-T} - e^{A\tau}BB_r{}^TS^{-t}e^{D^T\tau} = 0\\
&\Rightarrow A\hat{X} + \hat{X}D^T + B\tilde{B}^T - e^{A\tau}B\tilde{B}^Te^{D^T\tau} = 0,
\end{aligned} \tag{3.49}$$

where $\hat{X} = XS^{-T}$ and $\tilde{B}^T = (B_r)^TS^{-T}$. Let $\{\hat{X}_1, \cdots, \hat{X}_r\}$ be the columns of the matrix $\hat{X}$. The columns of X and $\hat{X}$ span the same subspace since S is a nonsingular matrix, i.e. $\text{Ran}(X) = \text{Ran}(\hat{X})$. Let $\{b_1, \cdots, b_r\}$ be the columns of $\tilde{B}$ and let $D = \text{diag}\{\lambda_1, \cdots, \lambda_r\}$, where λ_i's are the eigenvalues of A_r. Equation (3.49) gives $\hat{X}_i = (-\lambda_i^*I_n - A)^{-1}(I_n - e^{\lambda_i^*\tau}e^{A\tau})Bb_i$ for $i = 1, \ldots, r$. Thus, $\text{Ran}(\hat{X}) = \text{span}\{(-\lambda_i^*I_n - A)^{-1}(I_n - e^{\lambda_i^*\tau}e^{A\tau})Bb_i, i = 1, \ldots, r\}$. This subspace is also the right projection subspace $\mathcal{V}_r$ of TL-IRKA, where $-\lambda_i$'s are the interpolation points and b_i's are the right tangential directions. Thus, $\mathcal{V}_r = \text{Ran}(X) = \text{Ran}(\hat{X})$ is obtained. Similarly, substituting the eigendecompositions of A_r and $e^{A_r\tau}$ in the equation (3.48), it can shown that $\mathcal{W}_r = \text{Ran}(Y)$. If the projection matrices obtained in the first iteration of TL-IRKA and TL-TSIA are equivalent, the corresponding reduced-order models obtained using (3.23) are also equivalent. This will also

be valid for the subsequent iterations. Hence, if the algorithms converge, they should converge to equivalent reduced-order models. □

3.6 Numerical examples

A proof of convergence of the proposed TL-IRKA algorithm, given by Algorithm 7, is not available. Hence, in this section, a comparative study based on simulations is done on three benchmark examples to uphold the practicality of the algorithm. The first two examples are SISO models, and for them, the performance of TL-IRKA is compared with TL-TSIA, TL-BT, IRKA and TL-PORK. The third example is a MIMO model, and for this case, TL-IRKA is compared with TL-TSIA, TL-BT and IRKA. TL-PORK-1 is initialized with a reduced-order model obtained from TL-IRKA. Also, TL-PORK-2 is initialized with a reduced-order model obtained from IRKA. Among these algorithms, TL-TSIA, TL-BT and IRKA are discussed in Section 2.4, whereas TL-PORK is from [109]. The simulations are done in MATLAB version 8.3.0.532(R2014a) on an Intel(R) Core(TM) i5-6500 CPU running at 3.20GHz with 16 GB RAM and Windows 10, Version 20H2 Operating System.

For simulating the impulse responses in all three examples, the MATLAB command "impulse" is used. The error norm used for comparing the performance of the various model reduction algorithms is defined as $\text{AbsErr}(t) = \|\text{vec}((g(t) - g_r(t))\|_2$. The relative $H_2(\tau)$ error is given by $\text{Rel}\,\|\text{Err}\|_{H_2(\tau)} = \frac{\|g-g_r\|_{L_2([0,\tau])}}{\|g\|_{L_2([0,\tau])}}$ where $g(t)$ and $g_r(t)$ are the impulse responses of the full-order and the reduced-order system, respectively. Additionally, the following errors for measuring the distance to optimality of the reduced-order models are obtained using TL-IRKA and IRKA.

1. Right tangential interpolation errors, $\text{RTerr}(i) = \|G_\tau(\sigma_i)b_i - G_{r,\tau}(\sigma_i)b_i\|_2$ and relative right tangential interpolation error, $\|\text{RTerr}\|_{\text{rel}} = \sum_1^r \frac{\text{RTerr}(i)}{\|G_\tau(\sigma_i)b_i\|_2}$ for $i = 1, \ldots, r$.
2. Left tangential interpolation errors, $\text{LTerr}(i) = \left\|c_i^T G_\tau(\sigma_i) - c_i^T G_{r,\tau}(\sigma_i)\right\|_2$ and relative left tangential interpolation error, $\|\text{LTerr}\|_{\text{rel}} = \sum_1^r \frac{\text{LTerr}(i)}{\left\|c_i^T G_\tau(\sigma_i)\right\|_2}$.
3. Bitangential interpolation errors, $\text{derr}(i) = \left\|{c_i}^T {G_\tau}'(\sigma_i)b_i - {c_i}^T {G_{r,\tau}}'(\sigma_i)b_i\right\|_2$ and relative bitangential interpolation error, $\|\text{derr}\|_{\text{rel}} = \sum_1^r \frac{\text{derr}(i)}{\left\|c_i^T G_\tau'(\sigma_i)b_i\right\|_2}$.

Here, $G_\tau(s)$ and $G_{r,\tau}(s)$ are the time-limited transfer functions of the full-order and the reduced-order system, respectively. The σ_i's are the interpolation points, b_i's are the right tangential directions, and c_i's are the left tangential directions. The tangential directions are scalars, and the left and right tangential errors are equal in the case of SISO systems.

3.6.1 Example 1

The first example considered is the cantilever beam model discussed in Chapter 1. For the time intervals $[0, 0.1]$ s and $[0, 2]$ s, reduced models of order $r = 12$ are obtained. The iterative algorithms are stopped when the change in the eigenvalues of the reduced state matrix, A_r, is less than 10^{-5}. TL-IRKA and TL-TSIA are initialized randomly. They converge for both the time intervals considered. The number of iterations required for convergence depends on the initial conditions.

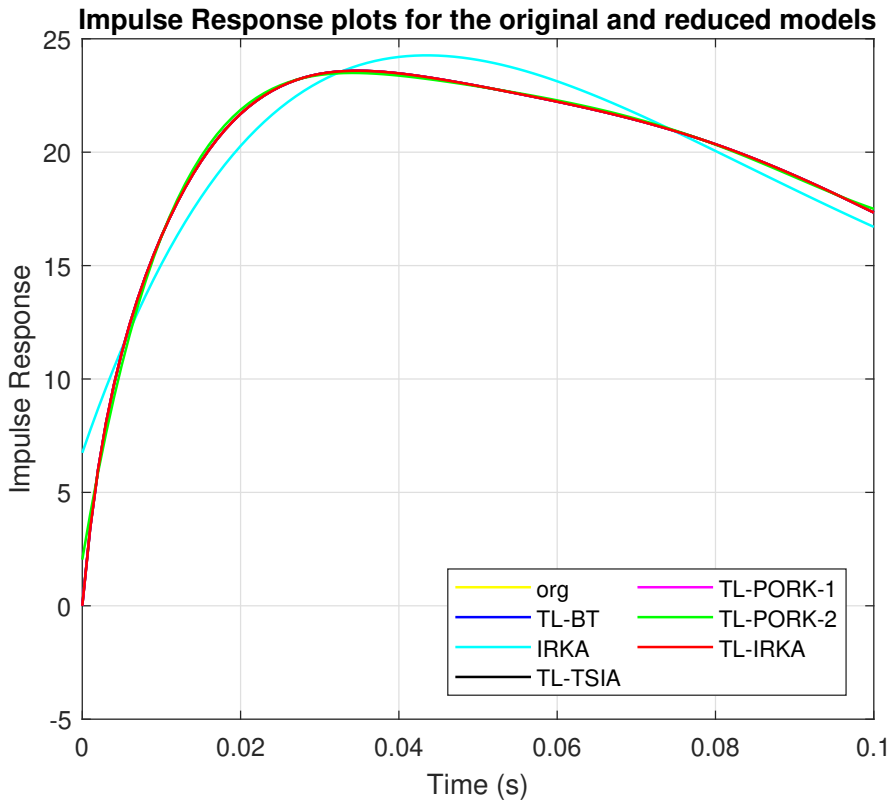

Figure 3.1: Beam example: Impulse response plots for final time $\tau = 0.1$ s

Figure 3.1 compares the impulse responses of the original and the reduced-order models for $[0, 0.1]$ s. For the same time interval, Figure 3.2 compares the errors $\mathrm{AbsErr}(t)$. Similarly, Figure 3.3 compares the impulse responses, and Figure 3.4 compares the errors $\mathrm{AbsErr}(t)$ of the reduced-order models obtained by various model reduction algorithms for the time interval $[0, 2]$ s.

The relative $H_2(\tau)$ errors for the different algorithms are compared in Table 3.1 for both time intervals. The relative $H_2(\tau)$ errors of the reduced-order models obtained from TL-IRKA and TL-TSIA are several orders of magnitude less than that of the reduced-order models obtained by the other algorithms for the smaller time interval. Table 3.1 shows that TL-IRKA and TL-PORK-1 have smaller $H_2(\tau)$ errors than the other algorithms for $\tau = 2$ s. Also, TL-IRKA and TL-TSIA converge to different local optima for the same time interval. Theorem 3.5.1 shows that if both TL-IRKA and TL-TSIA converge, then theoretically, they should converge to the same local minimum. However, both algorithms may converge to different local minima due to floating point arithmetic, leading to different $H_2(\tau)$ errors.

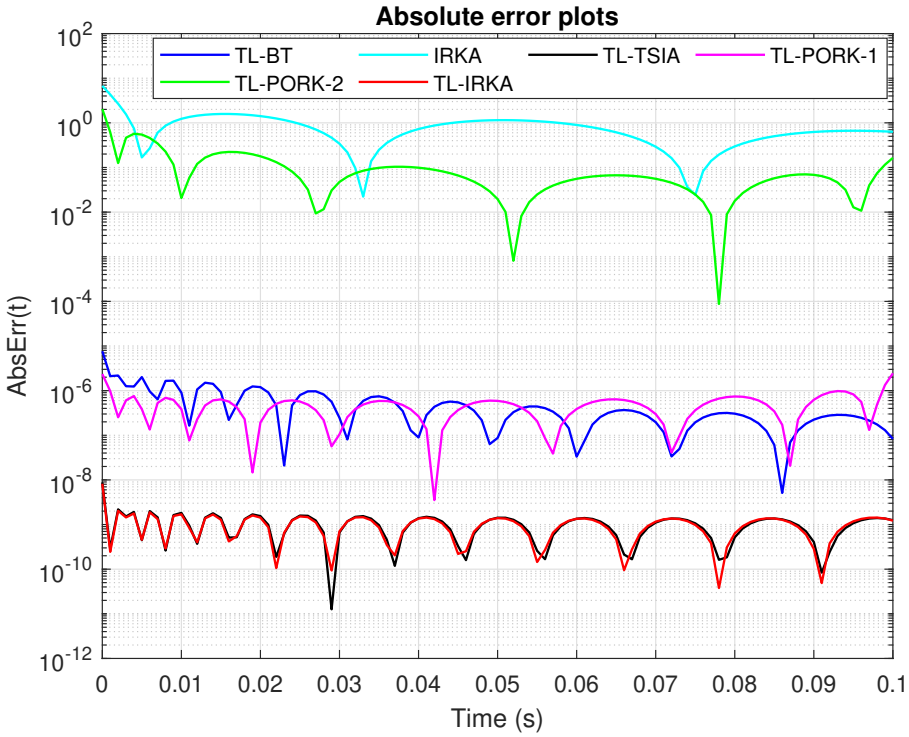

Figure 3.2: Beam example: Error plots for final time $\tau = 0.1$ s

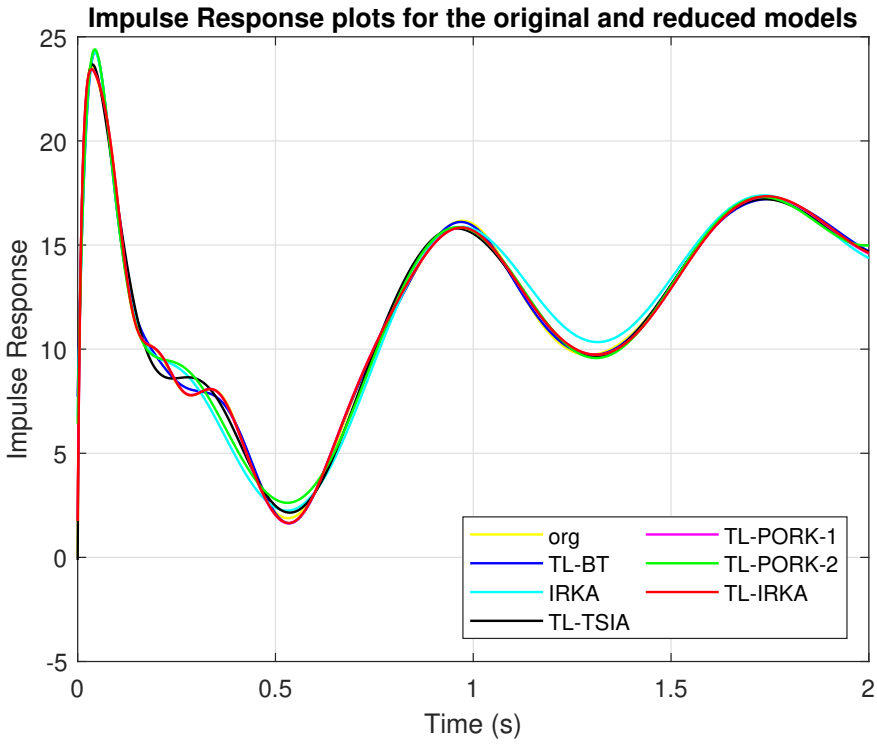

Figure 3.3: Beam example: Impulse response plots for final time $\tau = 2$ s

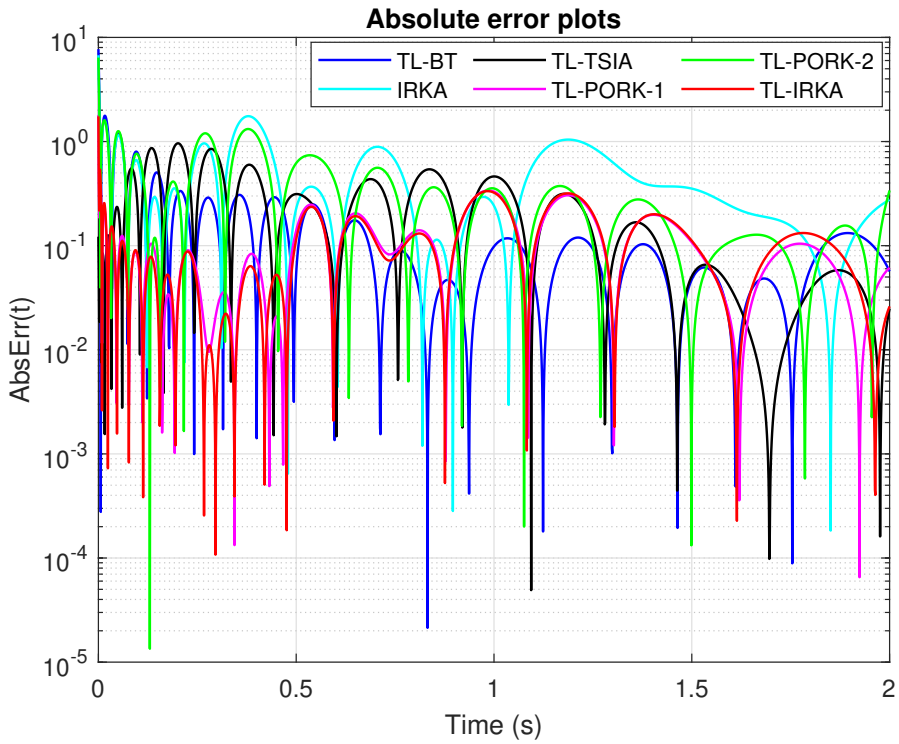

Figure 3.4: Beam example: Error plots for final time $\tau = 2$ s

Algorithm	TL-BT	TL-IRKA	IRKA	TL-TSIA	TL-PORK-1	TL-PORK-2
$\text{Rel}\|\text{Err}\|_{H_2(\tau)}$ $\tau = 0.1$ s	6.79×10^{-8}	6.55×10^{-11}	0.0580	6.85×10^{11}	9.25×10^{-9}	0.0123
$\text{Rel}\|\text{Err}\|_{H_2(\tau)}$ $\tau = 2$ s	0.0262	0.0115	0.0476	0.0243	0.0114	0.0375

Table 3.1: Relative $H_2(\tau)$ Errors for Beam example

Final-Time	i	$\mathrm{Re}(\lambda_i)\tau$	$\rho(\lambda_i I_r + A_r)$	RTerr(i)	LTerr(i)	derr(i)
$\tau = 0.1$ s	1	-52.7	1054	4.2×10^{-17}	4.2×10^{-17}	9.5×10^{-20}
	2	-45.5	981.7	4.7×10^{-17}	4.7×10^{-17}	1.5×10^{-19}
	3	-13.8	671.9	1.8×10^{-16}	1.8×10^{-16}	7.5×10^{-18}
	5	-7.3	604.4	1.9×10^{-15}	1.9×10^{-15}	1.9×10^{-16}
	7	-2.8	559.7	2.2×10^{-13}	2.2×10^{-13}	2.4×10^{-14}
	9	-1.3	541.9	9.6×10^{-13}	9.6×10^{-13}	1.0×10^{-13}
	11	-0.6	532.9	1.9×10^{-12}	1.9×10^{-12}	1.9×10^{-13}
	12	1.2	515.0	1.2×10^{-11}	1.2×10^{-11}	1.4×10^{-12}
$\tau = 2$ s	1	-91.2	101.5	3.1×10^{-15}	3.1×10^{-15}	6.1×10^{-14}
	3	-22.2	89.6	1.7×10^{-13}	1.7×10^{-13}	3.6×10^{-12}
	5	-7.1	65.3	3.1×10^{-6}	3.1×10^{-6}	6.5×10^{-6}
	7	-1.2	55.3	0.0077	0.0077	0.0221
	9	0.2	50.7	0.0136	0.0136	0.0289
	10	-1.3	51.4	0.0026	0.0026	0.0066
	11	-1.9	53.8	0.0026	0.0026	0.0066

Table 3.2: Interpolation errors for various time intervals for Beam Example

The interpolation errors quantify the distance to optimality of the reduced-order system obtained by TL-IRKA. The errors for both the time intervals are listed in Table 3.2. The index i refers to the i^{th} interpolation point. From the table, it is observed that the errors corresponding to the interpolation points (-λ_i's) with $\mathrm{Re}(\lambda_i)\tau \ll -1$ and with higher values of the spectral radius of the matrix $(\lambda_i I_r + A_r)$ have negligible interpolation errors. As $\mathrm{Re}(\lambda_i)\tau$ increases and the spectral radius of $(\lambda_i I_r + A_r)$ decreases, the interpolation error increases.

From Table 3.3, it is observed that TL-IRKA performs better than IRKA in satisfying the $H_2(\tau)$ optimality conditions. The relative interpolation errors are negligible for the shorter interval ($\tau = 0.1$ s). The errors are considerably more significant for the second time interval ($\tau = 2$ s). The data in Table 3.2 and Table 3.3 support the theoretical results from Theorem 3.3.1.

Final-Time	Algorithm	$\|\text{RTErr}\|_{\text{rel}}$	$\|\text{LTErr}\|_{\text{rel}}$	$\|\text{dErr}\|_{\text{rel}}$
$\tau = 0.1$ s	TL-IRKA	4.48×10^{-12}	4.48×10^{-12}	1.32×10^{-11}
	IRKA	0.0045	0.0045	5.6221
$\tau = 2$ s	TL-IRKA	0.0028	0.0028	0.0187
	IRKA	0.0804	0.0804	8.3027

Table 3.3: Relative error in the optimality conditions for Beam example

3.6.2 Example 2

The second example is an artificial system of order 1006, introduced in [70]. It is a purely theoretical example and is commonly used as a benchmark example in literature[1, 4, 43, 69]. The system matrices for this LTI model are as follows

$$A = \begin{bmatrix} A_1 & & & \\ & A_2 & & \\ & & A_3 & \\ & & & A_4 \end{bmatrix}, \quad \text{where} \quad A_1 = \begin{bmatrix} -1 & 100 \\ -100 & -1 \end{bmatrix}, A_2 = \begin{bmatrix} -1 & 200 \\ -200 & -1 \end{bmatrix},$$

$$A_3 = \begin{bmatrix} -1 & 400 \\ -400 & -1 \end{bmatrix}, A_4 = -\text{diag}(1, 2, \cdots, 1000), B = \begin{bmatrix} 10e_6 \\ e_{1000} \end{bmatrix}, C = B^T,$$

where $e_i \in \mathbb{R}^{i\times 1}$ is the vector with entry equal to 1.

Reduced models of order $r = 20$ are obtained for the time intervals $[0, 0.2]$ s and $[0, 2]$ s. The iterative algorithms are stopped when the change in the eigenvalues of A_r is less than 10^{-5}. The algorithms TL-IRKA and TL-TSIA are randomly initialized. They converge for both time intervals considered. The impulse responses of the original and the reduced-order systems obtained by various model reduction algorithms are compared in Figure 3.5 for $[0, 0.2]$ s and in Figure 3.7 for $[0, 2]$ s. Similarly, the errors $\text{AbsErr}(t)$ between the original and the reduced-order models are plotted in Figure 3.6 for $[0, 0.2]$ s and in Figure 3.8 for $[0, 2]$ s. The figures indicate the good performance of the proposed TL-IRKA algorithm compared to the other model reduction algorithms.

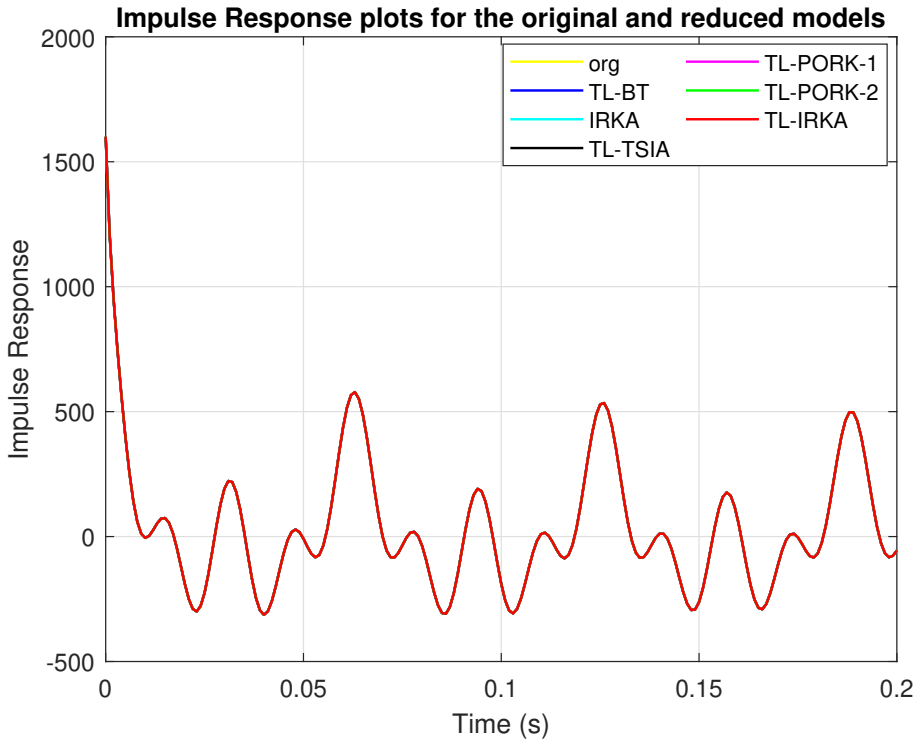

Figure 3.5: FOM example: Impulse response plots for final time $\tau = 0.2$ s

Algorithm	TL-BT	TL-IRKA	TL-TSIA	IRKA	TL-PORK-1	TL-PORK-2
$\text{Rel}\|\text{Err}\|_{H_2(\tau)}$ $\tau = 0.2$ s	5.79×10^{-9}	5.59×10^{-12}	5.59×10^{-12}	3.01×10^{-7}	3.14×10^{-7}	3.01×10^{-7}
$\text{Rel}\|\text{Err}\|_{H_2(\tau)}$ $\tau = 2$ s	1.06×10^{-8}	6.31×10^{-9}	6.31×10^{-9}	2.05×10^{-7}	1.05×10^{-8}	2.05×10^{-7}

Table 3.4: Relative $H_2(\tau)$ Errors in FOM example.

Comparing the relative $H_2(\tau)$ errors listed in Table 3.4, it is observed that TL-IRKA and TL-TSIA perform better than the other algorithms for both time intervals. In Table 3.5, interpolation errors for $\tau = 0.2$ s are recorded. Similarly, interpolation errors for $\tau = 2$ s are recorded in Table 3.6. The interpolation errors are negligible for interpolation points with $\text{Re}(\lambda_i)\tau \ll -1$ and with high values of the spectral radius of $(\lambda_i I_r + A_r)$. The errors increase as $\text{Re}(\lambda_i)\tau$ increases and the spectral radius of $(\lambda_i I_r + A_r)$ decreases.

The relative interpolation errors of TL-IRKA and IRKA for both time intervals are compared in Table 3.7. The relative interpolation errors due to TL-IRKA for $[0, 0.2]$ s are smaller than those for $[0, 2]$ s. Further, for both time intervals, TL-IRKA approximates the $H_2(\tau)$ optimality conditions more accurately than IRKA.

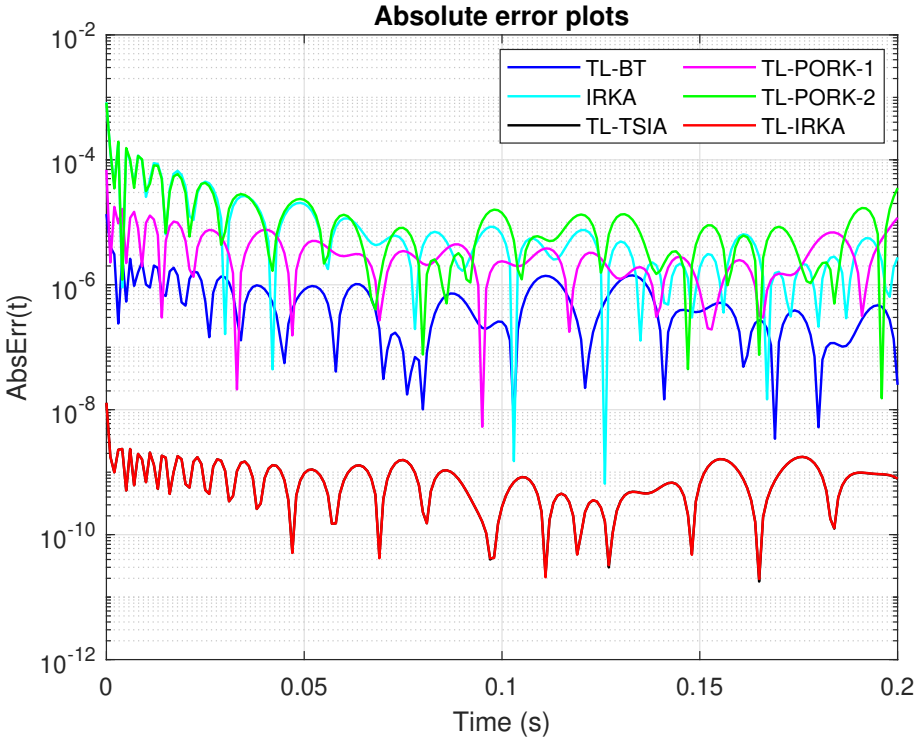

Figure 3.6: FOM example: Error plots for final time $\tau = 0.2$ s

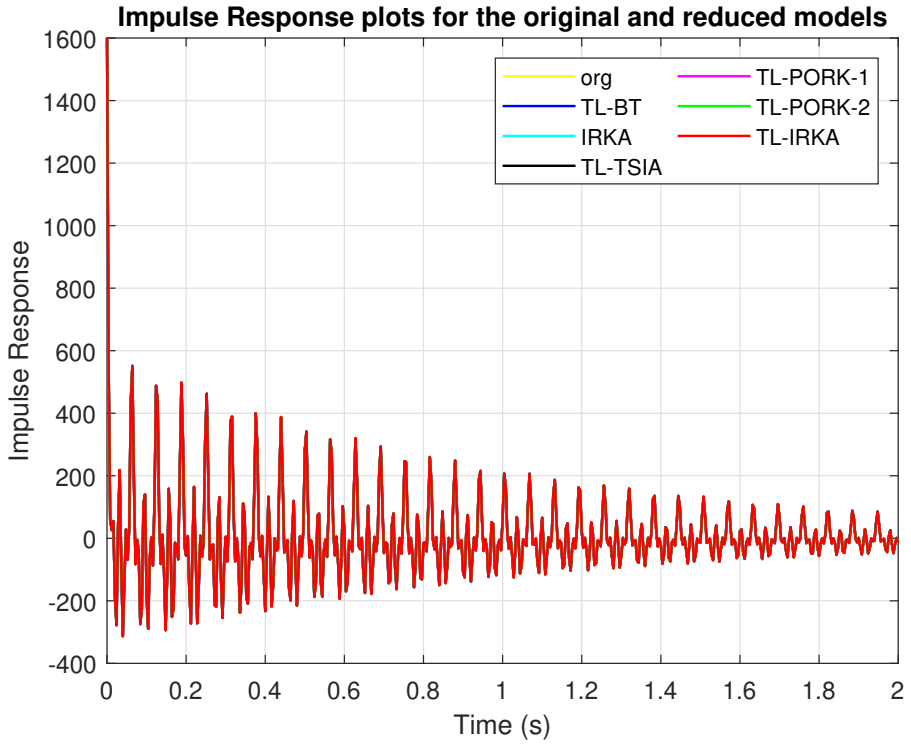

Figure 3.7: FOM example: Plots of impulse responses for $\tau = 2$ s

Final-Time	i	$\mathrm{Re}(\lambda_i)\tau$	$\rho(\lambda_i I_r + A_r)$	RTerr(i)	LTerr(i)	derr(i)
$\tau = 0.2$ s	1	-192.8	1928.6	1.5×10^{-15}	1.5×10^{-15}	1.3×10^{-18}
	2	-166.1	1795.0	1.1×10^{-15}	1.1×10^{-15}	1.7×10^{-18}
	3	-130.5	1617.0	2.4×10^{-15}	2.4×10^{-15}	2.6×10^{-18}
	4	-0.2	1044.9	5.5×10^{-12}	5.5×10^{-12}	3.9×10^{-11}
	6	-96.4	1446.1	1.8×10^{-15}	1.8×10^{-15}	2.6×10^{-18}
	7	-68.4	1306.3	3.5×10^{-15}	3.5×10^{-15}	8.7×10^{-18}
	8	-0.2	985.8	2.3×10^{-11}	2.3×10^{-11}	6.3×10^{-12}
	10	-47.3	1201.0	2.7×10^{-15}	2.7×10^{-15}	1.2×10^{-17}
	11	-0.2	970.5	1.3×10^{-11}	1.3×10^{-11}	1.3×10^{-11}
	13	-32.1	1124.8	7.5×10^{-15}	7.5×10^{-15}	1.2×10^{-17}
	14	-21.3	1071.0	4×10^{-15}	4×10^{-15}	3.2×10^{-17}
	15	-13.8	1033.5	8.9×10^{-15}	8.9×10^{-15}	5.2×10^{-17}
	16	-8.6	1007.5	8×10^{-15}	8×10^{-15}	4.3×10^{-18}
	17	-5.1	989.6	9.77×10^{-15}	9.77×10^{-15}	3.3×10^{-15}
	18	-2.6	977.6	2.0×10^{-13}	2.0×10^{-13}	4.7×10^{-14}
	19	-0.3	965.8	2.6×10^{-12}	2.6×10^{-12}	5.6×10^{-13}
	20	-1.1	969.9	1.08×10^{-12}	1.08×10^{-12}	2.5×10^{-13}

Table 3.5: Interpolation errors for $\tau = 0.2$ s for FOM Example

Final-Time	i	$\mathrm{Re}(\lambda_i)\tau$	$\rho(\lambda_i I_r + A_r)$	RTerr(i)	LTerr(i)	derr(i)
$\tau = 2$ s	1	-1871.1	1871.1	2.2×10^{-15}	2.2×10^{-15}	2.4×10^{-18}
	2	-1440.1	1655.6	3.8×10^{-15}	3.8×10^{-15}	4.1×10^{-18}
	3	-967.6	1419.4	4.4×10^{-15}	4.4×10^{-15}	6.1×10^{-18}
	4	-2	1018.4	2.2×10^{-15}	2.2×10^{-15}	4.3×10^{-9}
	6	-604.5	1237.8	2.2×10^{-15}	2.2×10^{-15}	8.7×10^{-18}
	7	-2	957.7	4.1×10^{-9}	4.1×10^{-9}	9.6×10^{-9}
	9	-364.3	1117.7	7.6×10^{-11}	7.6×10^{-11}	3.5×10^{-10}
	10	-2	941.9	2.2×10^{-15}	2.2×10^{-15}	1.5×10^{-18}
	12	-215.4	1043.3	2.2×10^{-15}	2.2×10^{-15}	1.5×10^{-18}
	13	-125.8	998.5	2.2×10^{-15}	2.2×10^{-15}	1.5×10^{-18}
	14	-72.9	972.0	2.2×10^{-15}	2.2×10^{-15}	1.5×10^{-18}
	15	-41.8	956.5	2.2×10^{-15}	2.2×10^{-15}	1.5×10^{-18}
	16	-23.8	947.5	2.2×10^{-15}	2.2×10^{-15}	1.5×10^{-18}
	17	-13.4	942.3	2.2×10^{-15}	2.2×10^{-15}	1.5×10^{-18}
	18	-7.5	939.3	2.2×10^{-15}	2.2×10^{-15}	1.5×10^{-18}
	19	-2.0	936.6	2.2×10^{-15}	2.2×10^{-15}	1.5×10^{-18}
	20	-4.2	937.7	2.2×10^{-15}	2.2×10^{-15}	1.5×10^{-18}

Table 3.6: Interpolation errors for $\tau = 2$ s for FOM Example

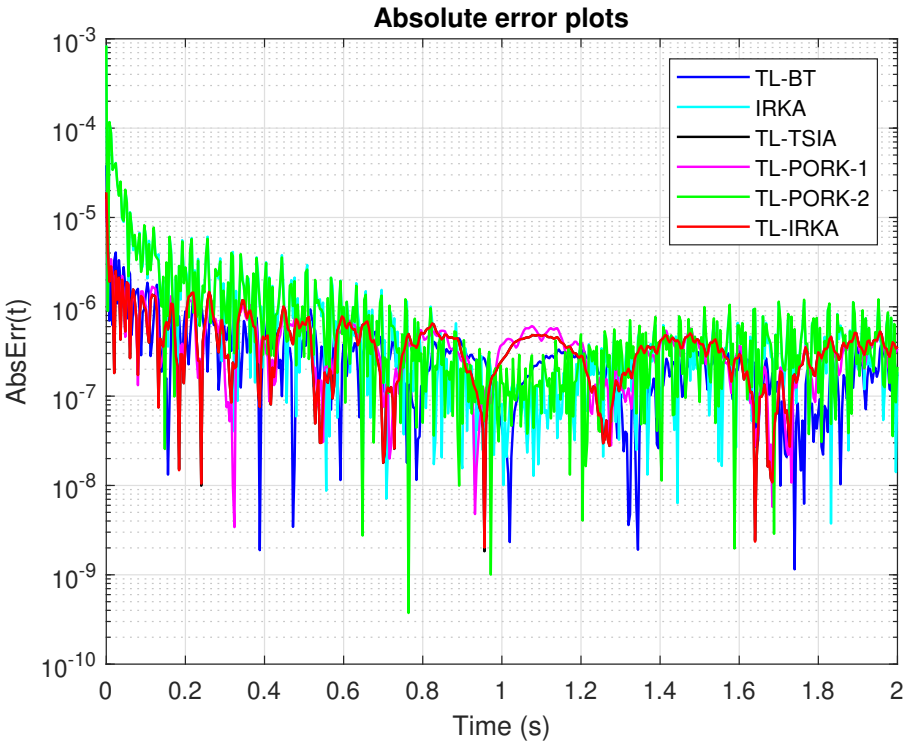

Figure 3.8: FOM example: Plots of absolute errors for $\tau = 2$ s

Final-Time	Algorithm	$\|\text{RTErr}\|_{\text{rel}}$	$\|\text{LTErr}\|_{\text{rel}}$	$\|\text{dErr}\|_{\text{rel}}$
$\tau = 0.2$ s	TL-IRKA	2.03×10^{-12}	2.03×10^{-12}	1.23×10^{-10}
	IRKA	2.60×10^{-8}	2.60×10^{-8}	1.02×10^{-5}
$\tau = 2$ s	TL-IRKA	4.24×10^{-10}	4.24×10^{-10}	1.35×10^{-8}
	IRKA	1.07×10^{-9}	1.07×10^{-9}	3.20×10^{-5}

Table 3.7: Relative error in the optimality conditions for FOM example

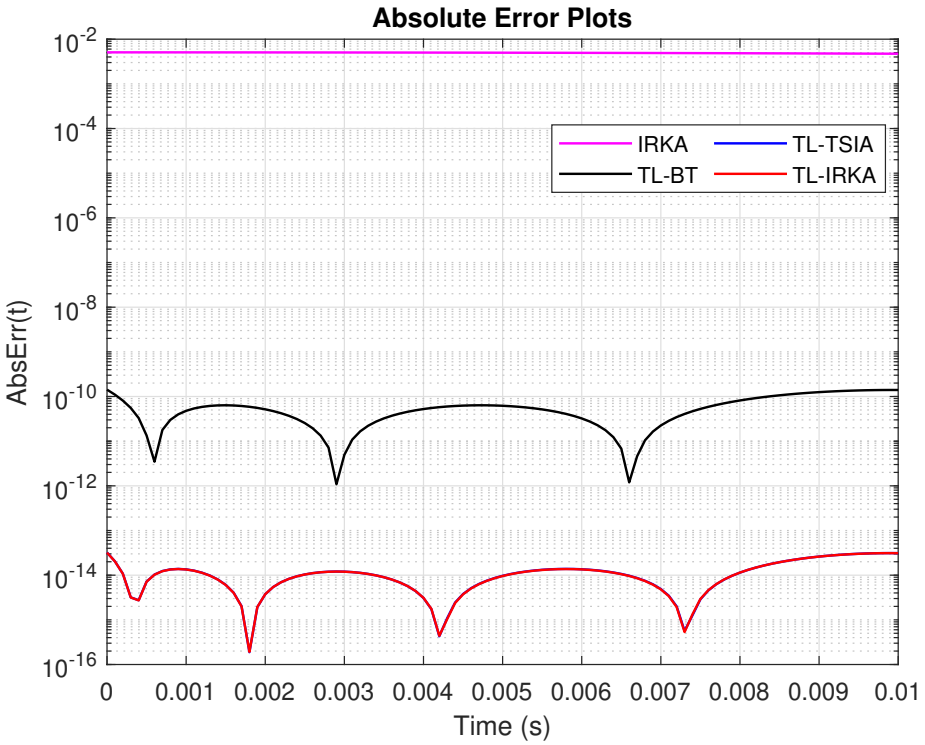

Figure 3.9: ISS Example: Error plots for final time $\tau = 0.01$ s.

3.6.3 Example 3

The third example is the ISS model, discussed in Chapter 1. Reduced models of order $r = 12$ are obtained for the time intervals $[0, 0.01]$ s, $[0, 0.1]$ s and $[0, 1]$ s. The stopping criteria for the iterative algorithms is the change in the eigenvalues of A_r becoming less than 10^{-8}. The initial interpolation points and tangential directions for TL-IRKA and state matrices for TL-TSIA are randomly chosen. The algorithms converge for all the time intervals. The error norm, i.e., AbsErr(t), between the original and the reduced-order models obtained by the different model algorithms are displayed in Figure 3.9 for $[0, 0.01]$ s, Figure 3.10 for $[0, 0.1]$ s and Figure 3.11 for $[0, 1]$ s.

Algorithm	TL-BT	TL-IRKA	TL-TSIA	IRKA
$\text{Rel}\|\text{Err}\|_{H_2(\tau)}$ $\tau = 0.01$ s	9.84×10^{-9}	2.0319×10^{-12}	2.0332×10^{-12}	0.6940
$\text{Rel}\|\text{Err}\|_{H_2(\tau)}$ $\tau = 0.1$ s	2.99×10^{-4}	2.9962×10^{-4}	2.9923×10^{-4}	0.8657
$\text{Rel}\|\text{Err}\|_{H_2(\tau)}$ $\tau = 1$ s	0.1946	0.1685	0.1684	0.8774

Table 3.8: Relative $H_2(\tau)$ Errors in ISS example.

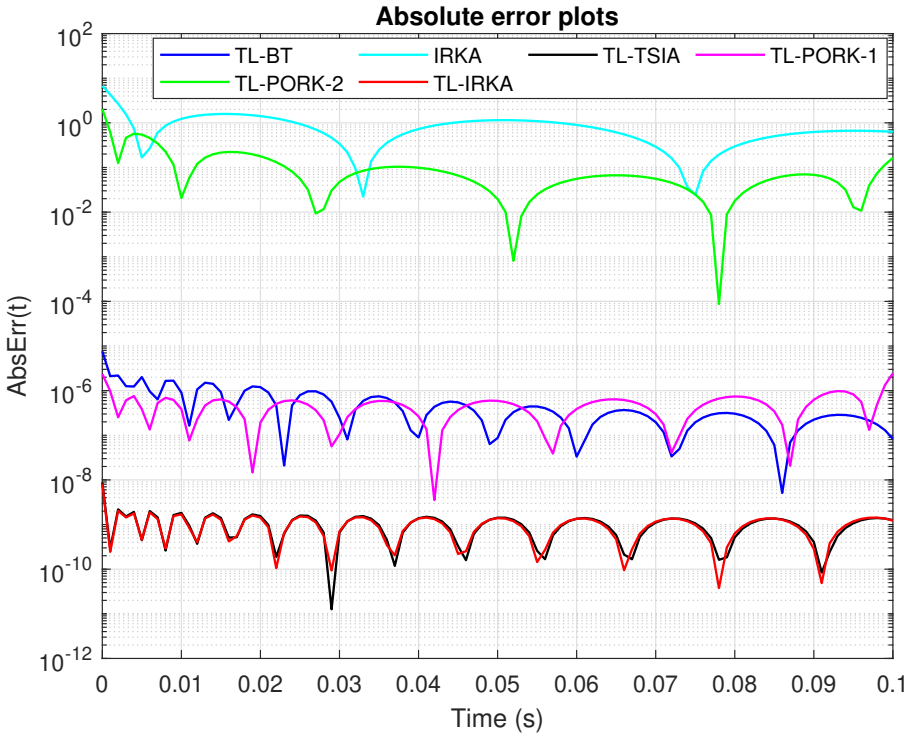

Figure 3.10: ISS Example: Error plots for final time $\tau = 0.1$ s.

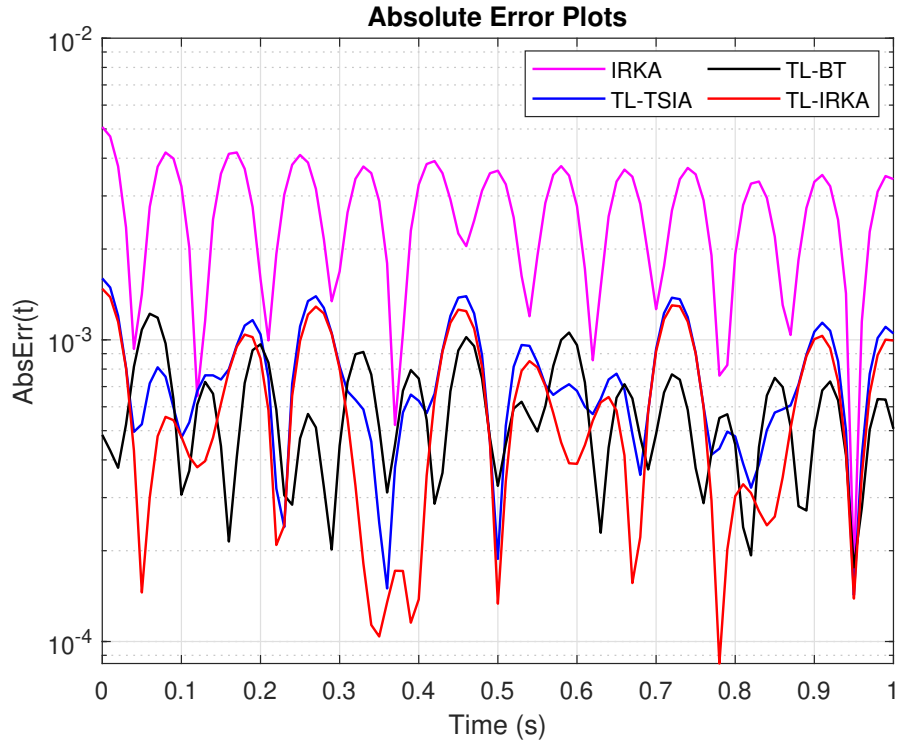

Figure 3.11: ISS Example: Error plots for final time $\tau = 1$ s.

Final-Time	i	$\mathrm{Re}(\lambda_i)\tau$	$\rho(\lambda_i I_r + A_r)$	RTerr(i)	LTerr(i)	derr(i)
$\tau = 0.01$ s	1	-0.0057	95.1	2.1×10^{-20}	6.4×10^{-18}	1.2×10^{-21}
	3	-0.0056	94.9	1.7×10^{-20}	6.3×10^{-18}	2.0×10^{-21}
	5	-0.0043	85.9	1.1×10^{-19}	2×10^{-17}	4.2×10^{-19}
	7	-0.2511	54.0	3.1×10^{-20}	2.3×10^{-18}	2.9×10^{-23}
	8	-0.0306	47.7	7.6×10^{-20}	2.5×10^{-17}	3.3×10^{-22}
	9	-0.0112	62.8	2.7×10^{-20}	9.0×10^{-18}	3.4×10^{-21}
	11	-0.0109	62.4	2.1×10^{-20}	7.3×10^{-18}	2.3×10^{-21}
$\tau = 0.1$ s	1	4.1911	83.8	1.9×10^{-11}	2.8×10^{-9}	4.1×10^{-15}
	2	0.0626	97.8	1.9×10^{-11}	9.2×10^{-9}	6.3×10^{-13}
	4	0.0726	97.7	1.5×10^{-11}	7.2×10^{-9}	4.0×10^{-13}
	6	-0.0579	86.9	5.6×10^{-11}	8.6×10^{-9}	2.8×10^{-12}
	8	-0.0250	48.9	3.9×10^{-11}	9.4×10^{-9}	2.3×10^{-12}
	9	-0.6629	67.5	1.3×10^{-11}	7.5×10^{-9}	9.9×10^{-13}
	11	-0.7256	67.4	1.0×10^{-11}	5.9×10^{-9}	8.3×10^{-13}
$\tau = 1$ s	1	-0.3309	95.7	2.4×10^{-9}	9.4×10^{-7}	5.2×10^{-10}
	3	-0.2036	85.9	7.3×10^{-8}	1.3×10^{-5}	4.9×10^{-8}
	5	-0.1182	69.4	4.4×10^{-9}	1.3×10^{-6}	1.1×10^{-9}
	7	-0.5855	49.1	8.5×10^{-9}	2.9×10^{-6}	2.7×10^{-9}
	9	-0.2674	56.9	1.5×10^{-8}	6.5×10^{-6}	6.6×10^{-9}
	11	-0.0405	56.3	7.9×10^{-9}	3×10^{-6}	1.1×10^{-8}

Table 3.9: Interpolation errors for various time intervals for ISS Example

Final-Time	Algorithm	$\|\text{RTErr}\|_{\text{rel}}$	$\|\text{LTErr}\|_{\text{rel}}$	$\|\text{dErr}\|_{\text{rel}}$
$\tau = 0.01$ s	TL-IRKA	1.84×10^{-12}	1.83×10^{-12}	1.94×10^{-9}
	IRKA	2.2988	2.2991	2.2879
$\tau = 0.1$ s	TL-IRKA	7.68×10^{-4}	8.69×10^{-4}	0.0021
	IRKA	1.5786	1.5451	9.4650
$\tau = 1$ s	TL-IRKA	0.0575	0.0608	0.1398
	IRKA	0.3206	0.4175	0.4214

Table 3.10: Relative error in the optimality conditions for ISS example

Table 3.8 lists the relative $H_2(\tau)$ errors corresponding to different model reduction algorithms. TL-IRKA and TL-TSIA perform better than TL-BT and IRKA for the smallest time interval $[0, 0.01]$ s. TL-IRKA has comparable results with TL-BT and TL-TSIA and better performance than IRKA for the other time intervals.

Table 3.9 contains the interpolation errors corresponding to various interpolation points. From the table, it is evident that $|\text{Re}(\lambda_i)\tau| < 3$ and the spectral radius of $(\lambda_i I_r + A_r)$ varies between 49 and 100 for all the interpolation points. Hence, these terms do not contribute significantly to the interpolation errors. Instead, the final time τ determines the error magnitudes. The errors corresponding to $\tau = 0.01$ s are negligible and increase by several orders of magnitude for $\tau = 0.1$ s and $\tau = 1$ s. Table 3.10 compares the relative interpolation errors for TL-IRKA and IRKA. TL-IRKA performs better than IRKA for every time interval. The error due to TL-IRKA is negligible compared to IRKA for the smallest time interval $[0, 0.01]$ s.

The data in Tables 3.1, 3.4, and 3.8 imply that TL-IRKA performs better than TL-BT for the shortest time interval. However, their performance is comparable for the other time intervals. Further, TL-IRKA and TL-TSIA have similar relative error magnitudes for all time intervals considered in all three examples.

In the examples discussed above, the proposed iterative algorithm TL-IRKA produces good reduced models (with respect to the $H_2(\tau)$ error norm) for random initial conditions. As discussed in Subsection 3.4.2 of this chapter, the implementation technique used for TL-IRKA is computationally expensive. This is a disadvantage of TL-IRKA, which restricts its applicability to medium-scale systems (with dimensions less than 1000) and makes it computationally expensive for large-scale systems (with dimensions greater than 1000).

3.7 Summary

In this chapter, a $H_2(\tau)$ optimal model reduction algorithm called TL-IRKA has been proposed. As the name suggests, this algorithm is a finite horizon extension of IRKA. An alternative way of deriving the interpolation-based $H_2(\tau)$ optimality conditions has been presented in this chapter. Based on these conditions, TL-IRKA has been proposed. The reduced-order models obtained by TL-IRKA satisfy the $H_2(\tau)$ optimality conditions approximately. The interpolation errors for these reduced-order models have been obtained. They are determined predominantly by the poles of the interpolating model and the time interval $[0, \tau]$. This has been verified from several simulation results. Finally, the performance of TL-IRKA has been verified through various numerical simulations.

Chapter 4

H_2 optimal model order reduction over a finite time interval

The majority of the finite horizon MOR reduction algorithms for LTI systems discussed in the previous chapters, such as TL-BT and TL-TSIA are projection-based algorithms. The algorithm TL-IRKA, proposed in Chapter 3 of the thesis, is a projection-based $H_2(\tau)$ optimal MOR algorithm. The reduced models obtained using such methods don't exactly satisfy the $H_2(\tau)$ optimality conditions. The distance to optimality for TL-TSIA is improved by using gradient-based $H_2(\tau)$ optimal model reduction techniques. To the best of the authors' knowledge, [94] is the only work that proposes a gradient-based method for $H_2(\tau)$ optimal model reduction. However, the numerical method proposed here is valid only for SISO systems, and the gradients are obtained using an interpolation framework. The primary contribution of this chapter is a gradient-based $H_2(\tau)$ optimization method, which is applicable for both SISO and MIMO systems.

In this chapter, the analytical expressions of the gradients of the $H_2(\tau)$ error norm are obtained using a gramian-based framework, unlike the interpolation-based framework used in [94]. Using the gradient expressions with a standard quasi-Newton solver, state-space parameters minimizing the $H_2(\tau)$ error norm are obtained. As previously mentioned, the $H_2(\tau)$ optimization problem is non-convex. Hence, reduced-order models obtained from the projection-based methods TL-BT and TL-TSIA are used to initialize the quasi-Newton solver. The reduced-order models obtained are locally $H_2(\tau)$ optimal. Lyapunov-based conditions for $H_2(\tau)$ optimality are obtained by equating the gradient expressions to zero. Further, the proposed gradient-based method is also verified using numerical examples.

This chapter is organised as follows. In Section 4.1, the $H_2(\tau)$ optimal model reduction problem is expressed using a gramian framework. The gradients of the $H_2(\tau)$ error norm are obtained in Section 4.2. A numerical method for $H_2(\tau)$ optimal model reduction is proposed in Section 4.3, and its computational complexity is also discussed. Three numerical examples are presented in Section 4.4, and the chapter is concluded in Section 4.5.

4.1 $H_2(\tau)$ optimal model reduction problem

In this section, the $H_2(\tau)$ norm and the $H_2(\tau)$ error norm, introduced in Chapter 2, are represented using a gramian-based framework. The representation is used to derive the gradients of the $H_2(\tau)$ error norm, which is further used to obtain Lyapunov-based conditions for $H_2(\tau)$ optimality.

4.1.1 Expressing the $H_2(\tau)$ norm using a gramian framework

The $H_2(\tau)$ norm of the system Σ, given by the state-space representation (2.1), is defined in (2.7). It can be expressed using the finite horizon system gramians [30]. The square of the $H_2(\tau)$ norm can be expressed in terms of the finite horizon controllability gramian P_τ, given by (2.13), as follows:

$$\|\Sigma\|^2_{H_2(\tau)} = \text{Tr } CP_\tau C^T. \tag{4.1}$$

Similarly, the square of the $H_2(\tau)$ norm can be expressed in terms of the finite horizon observability gramian Q_τ, given by (2.14), as follows:

$$\|\Sigma\|^2_{H_2(\tau)} = \text{Tr } B^T Q_\tau B. \tag{4.2}$$

Since the $H_2(\tau)$ norm is defined over a finite time interval, the LTI system Σ need not be asymptotically stable to have a finite $H_2(\tau)$ norm.

4.1.2 Expressing the $H_2(\tau)$ error norm using a gramian framework

The $H_2(\tau)$ model reduction problem involves finding a reduced-order system Σ_r, which solves the optimization problem given by (2.47).

The error system $(\Sigma - \Sigma_r)$ can be realized by the following state-space realization:

$$\{A_e, B_e, C_e\} = \left\{ \begin{bmatrix} A & 0 \\ 0 & A_r \end{bmatrix}, \begin{bmatrix} B \\ B_r \end{bmatrix}, \begin{bmatrix} C & -C_r \end{bmatrix} \right\}. \tag{4.3}$$

The square of the $H_2(\tau)$ norm of the above realization is given by,

$$\begin{aligned} \|\Sigma - \Sigma_r\|^2_{H_2(\tau)} &= \int_0^\tau \text{Tr}\left((C_e e^{A_e t} B_e)(C_e e^{A_e t} B_e)^T\right) dt \\ &= \int_0^\tau \text{Tr}\left((C_e e^{A_e t} B_e)^T (C_e e^{A_e t} B_e)\right) dt. \end{aligned}$$

The above norm can also be expressed as,

$$\|\Sigma - \Sigma_r\|^2_{H_2(\tau)} = \text{Tr}({B_e}^T Q_{e,\tau} B_e) = \text{Tr}(C_e P_{e,\tau} {C_e}^T). \tag{4.4}$$

Here, $P_{e,\tau}$ and $Q_{e,\tau}$ are the time-limited controllability and observability gramians of the system $(\Sigma - \Sigma_r)$. They satisfy the following Lyapunov equations,

$$A_e P_{e,\tau} + P_{e,\tau} {A_e}^T + B_e {B_e}^T - e^{A_e \tau} B_e {B_e}^T e^{{A_e}^T \tau} = 0, \quad \text{and} \tag{4.5}$$

$${A_e}^T Q_{e,\tau} + Q_{e,\tau} A_e + {C_e}^T C_e - e^{{A_e}^T \tau} {C_e}^T C_e e^{A_e \tau} = 0. \tag{4.6}$$

The gramians $P_{e,\tau}$ and $Q_{e,\tau}$ can be partitioned as follows,

$$P_{e,\tau} = \begin{pmatrix} P_\tau & X_\tau \\ X_\tau^T & P_{r,\tau} \end{pmatrix} \quad \text{and} \quad Q_{e,\tau} = \begin{pmatrix} Q_\tau & Y_\tau \\ Y_\tau^T & Q_{r,\tau} \end{pmatrix}.$$

Further, the matrix exponential $e^{A_e\tau}$ can also partitioned as follows,

$$e^{A_e\tau} = \begin{bmatrix} e^{A\tau} & 0 \\ 0 & e^{A_r\tau} \end{bmatrix}.$$

Substituting the above expressions in (4.5) and (4.6) results in the following time-limited Lyapunov and Sylvester equations,

$$AP_\tau + P_\tau A^T + BB^T - e^{A\tau}BB^T e^{A^T\tau} = 0, \tag{4.7}$$

$$AX_\tau + X_\tau {A_r}^T + B{B_r}^T - e^{A\tau}B{B_r}^T e^{{A_r}^T\tau} = 0, \tag{4.8}$$

$$A_r P_{r,\tau} + P_{r,\tau}{A_r}^T + B_r {B_r}^T - e^{A_r\tau}B_r{B_r}^T e^{{A_r}^T\tau} = 0, \tag{4.9}$$

$$A^T Q_\tau + Q_\tau A + C^T C - e^{A^T\tau}C^T C e^{A\tau} = 0, \tag{4.10}$$

$$A^T Y_\tau + Y_\tau A_r - C^T C_r + e^{A^T\tau}C^T C_r e^{A_r\tau} = 0 \quad \text{and} \tag{4.11}$$

$${A_r}^T Q_{r,\tau} + Q_{r,\tau}A_r + {C_r}^T C_r - e^{A_r^T\tau}{C_r}^T C_r e^{A_r\tau} = 0. \tag{4.12}$$

Further, equation (4.4) can be re-written as follows,

$$\|\Sigma - \Sigma_r\|^2_{H_2(\tau)} = \mathrm{Tr}\left(CP_\tau C^T - 2CX_\tau C_r^T + C_r P_{r,\tau} C_r^T\right), \tag{4.13}$$

$$= \mathrm{Tr}\left(B^T Q_\tau B + 2B^T Y_\tau B_r + B_r^T Q_{r,\tau} B_r\right). \tag{4.14}$$

4.2 Gradients of the $H_2(\tau)$ error norm

Consider the $H_2(\tau)$ optimization problem given by (2.47), where the cost function is the $H_2(\tau)$ error given by (4.13) or (4.14). For the reduced-order model, given by (2.17), to be optimal, the gradients of the cost function with respect to A_r, B_r and C_r should be zero. Therefore, a closed-form expression for these gradients is derived in this section using the Fréchet derivative of a matrix exponential [2]. These expressions are necessary for the model reduction method proposed in the next section.

Given the matrix exponential $f(X) = e^X$, its Fréchet derivative for a perturbation matrix Y is given by,

$$L(X,Y) = \int_0^1 e^{X(1-s)} Y e^{Xs} ds. \tag{4.15}$$

For a real-valued function $f : \mathbb{R}^{m\times n} \to \mathbb{R}$, the gradient at $M \in \mathbb{R}^{m\times n}$ is a matrix $\bigtriangledown_M f(M) \in \mathbb{R}^{m\times n}$ defined as,

$$[\bigtriangledown_M f(M)]_{i,j} = \frac{d}{dM_{i,j}} f(M), \quad i = 1,\ldots,m, j = 1,\ldots,p. \tag{4.16}$$

Given a perturbation $\Delta \in \mathbb{R}^{m\times n}$, the Taylor series expansion of the real-valued function $f(M+\Delta)$ is given by,

$$f(M+\triangle) = f(M) + \langle \bigtriangledown_M f(M), \triangle\rangle + O(\|\triangle\|^2),$$

where $\langle A, B\rangle = \mathrm{Tr}(A^T B)$.

Before deriving the expression for the gradients, the following lemma, which is used in the derivation, is stated.

Lemma 4.2.1 ([98], Lemma 3.2). *For $A \in \mathbb{R}^{n\times n}$, $B \in \mathbb{R}^{m\times m}$, $C \in \mathbb{R}^{n\times m}$, and $D \in \mathbb{R}^{m\times n}$, let $M \in \mathbb{R}^{n\times m}$ and $N \in \mathbb{R}^{m\times n}$ be the solutions of the matrix equations $AM + MB + C = 0$ and $NA + BN + D = 0$, respectively. Then, $\mathrm{Tr}(CN) = \mathrm{Tr}(DM)$.*

Theorem 4.2.2. *Let $\nabla_{A_r} J$, $\nabla_{B_r} J$ and $\nabla_{C_r} J$ be the gradients of the square of the $H_2(\tau)$ error norm $J = \|G - G_r\|^2_{H_2(\tau)}$ with respect to A_r, B_r and C_r. They are given by*

$$\nabla_{A_r} J = 2(Q_{r,\tau} P_r + Y_\tau^T X + \tau(L(A_r\tau, S_\tau)^T)), \tag{4.17}$$

$$\nabla_{B_r} J = 2(Q_{r,\tau} B_r + Y_\tau^T B), \quad \textit{and} \tag{4.18}$$

$$\nabla_{C_r} J = 2(C_r P_{r,\tau} - C X_\tau), \tag{4.19}$$

where $P_{r,\tau}$, $Q_{r,\tau}$, X_τ, and Y_τ are the solutions of the matrix equations (4.9), (4.12), (4.8), and (4.11), respectively. The terms P_r and X are obtained by solving the following matrix equations,

$$P_r A_r^T + A_r P_r + B_r B_r^T = 0, \quad \textit{and} \tag{4.20}$$

$$X^T A^T + A_r X^T + B_r B^T = 0. \tag{4.21}$$

In (4.17), the term $L(A_r\tau, S_\tau)$ is the Fréchet derivative of the matrix exponential $f(A_r\tau) = e^{A_r\tau}$ along the direction S_τ, given by (4.15), where

$$S_\tau = \left(X^T e^{A^T\tau} C^T C_r - P_r e^{A_r^T\tau} C_r^T C_r \right). \tag{4.22}$$

Proof. This theorem is proved using the first-order perturbation techniques given in [10, 98]. Consider the expression of the $H_2(\tau)$ error norm given by (4.14). For a perturbation Δ_{A_r} in A_r, the corresponding first-order perturbation $\Delta_J^{A_r}$ in J is given by,

$$\begin{aligned} \Delta_J^{A_r} &= \mathrm{Tr}\left(2B^T \Delta_{Y_\tau} B_r + B_r^T \Delta_{Q_{r,\tau}} B_r\right) \\ &= \mathrm{Tr}\left(2B_r B^T \Delta_{Y_\tau} + B_r B_r^T \Delta_{Q_{r,\tau}}\right), \end{aligned} \tag{4.23}$$

where Δ_{Y_τ}, $\Delta_{Q_{r,\tau}}$ and $\Delta_{e^{A_r\tau}}$ are the corresponding perturbations in Y_τ, $Q_{r,\tau}$ and $e^{A_r\tau}$, respectively. The term $\Delta_{e^{A_r\tau}}$ can be expressed as,

$$\begin{aligned} \Delta_{e^{A_r\tau}} &= L\left(e^{A_r\tau}, \tau\Delta_{A_r}\right) \\ &= \tau \int_0^1 e^{A_r\tau(1-s)} \Delta_{A_r} e^{A_r\tau s} ds \\ &= \tau L\left(e^{A_r\tau}, \Delta_{A_r}\right). \end{aligned} \tag{4.24}$$

The matrix equation (4.11) gives rise to the following relation between the perturbations Δ_{Y_τ} and Δ_{A_r}.

$$\begin{aligned} &\Delta_{A^T Y_\tau} + \Delta_{Y_\tau A_r} - \Delta_{C^T C_r} + \Delta_{e^{A^T\tau} C^T C_r e^{A_r\tau}} = 0 \\ \Rightarrow\ & A^T \Delta_{Y_\tau} + \Delta_{Y_\tau} A_r + Y_\tau \Delta_{A_r} + e^{A^T\tau} C^T C_r \Delta_{e^{A_r\tau}} = 0. \end{aligned} \tag{4.25}$$

The terms not dependent on A_r are unaffected by the perturbation Δ_{A_r} and behave as constants. Similarly, due to the matrix equation (4.12), the relation between the perturbations $\Delta_{Q_{r,\tau}}$ and Δ_{A_r} is obtained as follows,

$$\begin{aligned}
&\Delta_{A_r{}^T Q_{r,\tau}} + \Delta_{Q_{r,\tau}A_r} + \Delta_{C_r{}^T C_r} + \Delta_{e^{A_r^T{}^\tau C_r{}^T C_r e^{A_r\tau}}} = 0 \\
\Rightarrow\ & A_r^T\Delta_{Q_{r,\tau}} + \Delta_{Q_{r,\tau}}A_r + \Delta_{A_r}^T Q_{r,\tau} + Q_{r,\tau}\Delta_{A_r} - \Delta_{e^{A_r\tau}}^T C_r^T C_r e^{A_r\tau} - e^{A_r^T} C_r^T C_r \Delta_{e^{A_r\tau}} = 0. \quad (4.26)
\end{aligned}$$

Applying Lemma 4.2.1 for the matrix equations (4.21) and (4.25) results in the following

$$\begin{aligned}
\mathrm{Tr}\left(B_r B^T \Delta_{Y_\tau}\right) &= \mathrm{Tr}\left(Y_\tau \Delta_{A_r} X^T + e^{A^T{}^\tau} C^T C_r \Delta_{e^{A_r\tau}} X^T\right) \\
&= \mathrm{Tr}\left(X^T Y_\tau \Delta_{A_r} + X^T e^{A^T{}^\tau} C^T C_r \Delta_{e^{A_r\tau}}\right). \quad (4.27)
\end{aligned}$$

Similarly, considering the matrix equations (4.20) and (4.26) and using Lemma 4.2.1 gives

$$\begin{aligned}
&\mathrm{Tr}\left(B_r B_r^T \Delta_{Q_{r,\tau}}\right) \\
&= \mathrm{Tr}\left(\Delta_{A_r}^T Q_{r,\tau} P_r + Q_{r,\tau}\Delta_{A_r} P_r - \Delta_{e^{A_r\tau}}^T C_r^T C_r e^{A_r\tau} P_r - e^{A_r^T{}^\tau} C_r^T C_r \Delta_{e^{A_r\tau}} P_r\right) \\
&= \mathrm{Tr}\left((Q_{r,\tau}P_r)^T \Delta_{A_r} + P_r Q_{r,\tau}\Delta_{A_r} - (C_r^T C_r e^{A_r\tau} P_r)^T \Delta_{e^{A_r\tau}} - P_r e^{A_r^T{}^\tau} C_r^T C_r \Delta_{e^{A_r\tau}}\right) \\
&= 2\mathrm{Tr}\left(P_r Q_{r,\tau}\Delta_{A_r} - P_r e^{A_r^T{}^\tau} C_r^T C_r \Delta_{e^{A_r\tau}}\right). \quad (4.28)
\end{aligned}$$

Substituting the right hand side of equations (4.27) and (4.28) in the expression (4.23) results in

$$\begin{aligned}
\Delta_J^{A_r} &= \mathrm{Tr}\left(2B_r B^T \Delta_{Y_\tau}\right) + \mathrm{Tr}\left(B_r B_r^T \Delta_{Q_{r,\tau}}\right) \\
&= 2\mathrm{Tr}\left(X^T Y_\tau \Delta_{A_r} + X^T e^{A^T{}^\tau} C^T C_r \Delta_{e^{A_r\tau}}\right) + 2\mathrm{Tr}\left(P_r Q_{r,\tau}\Delta_{A_r} - P_r e^{A_r^T{}^\tau} C_r^T C_r \Delta_{e^{A_r\tau}}\right) \\
&= 2\mathrm{Tr}\left(\left(X^T Y_\tau + P_r Q_{r,\tau}\right)\Delta_{A_r}\right) + 2\mathrm{Tr}\left(\left(X^T e^{A^T{}^\tau} C^T C_r - P_r e^{A_r^T{}^\tau} C_r^T C_r\right)\Delta_{e^{A_r\tau}}\right) \\
&= 2\mathrm{Tr}\left(\left(X^T Y_\tau + P_r Q_{r,\tau}\right)\Delta_{A_r}\right) + 2\ \mathrm{Tr}\left(S_\tau \Delta_{e^{A_r\tau}}\right). \quad (4.29)
\end{aligned}$$

The above expression is obtained using (4.22). Using (4.15) and (4.24) gives the following result.

$$\begin{aligned}
2\ \mathrm{Tr}\left(S_\tau \Delta_{e^{A_r\tau}}\right) &= 2\ \mathrm{Tr}\left(S_\tau \int_0^1 e^{A_r\tau(1-s)}(\Delta_{A_r}\tau)e^{A_r\tau s} ds\right) \\
&= 2\tau\ \mathrm{Tr}\left(\int_0^1 e^{A_r\tau s} S_\tau e^{A_r\tau(1-s)} ds(\Delta_{A_r})\right) \\
&= 2\tau\ \mathrm{Tr}\left(\int_0^1 e^{A_r\tau(1-s)} S_\tau e^{A_r\tau(s)} ds(\Delta_{A_r})\right) \\
&= 2\tau\ \mathrm{Tr}\left(L(A_r\tau, S_\tau)\Delta_{A_r}\right).
\end{aligned}$$

Using the above expression, (4.29) can be rewritten as follows

$$\begin{aligned}
\Delta_J^{A_r} &= 2\ \mathrm{Tr}\left(\left(X^T Y_\tau + P_r Q_{r,\tau}\right)\Delta_{A_r}\right) + 2\tau\mathrm{Tr}\ \left(L(A_r\tau, S_\tau)\Delta_{A_r}\right) \\
&= 2\mathrm{Tr}\left(\left(X^T Y_\tau + P_r Q_{r,\tau} + \tau\left(L(A_r\tau, S_\tau)\right)\right)\Delta_{A_r}\right) \\
&= \langle 2(Y_\tau{}^T X + Q_{r,\tau}P_r + \tau(L(A_r\tau, S_\tau)^T)), \Delta_{A_r}\rangle. \quad (4.30)
\end{aligned}$$

As Δ_{A_r} is arbitrary, comparing $\Delta_J^{A_r} = \langle \nabla_{A_r} J, \Delta_{A_r}\rangle$ with (4.30) gives rise to

$$\nabla_{A_r} J = 2(Y_\tau{}^T X + Q_{r,\tau}P_r + \tau(L(A_r\tau, S_\tau)^T)).$$

When B_r in (4.14) is perturbed by Δ_{B_r}, the corresponding first-order perturbation $\nabla_{B_r} J$ in J is given by

$$\begin{aligned}\Delta_J^{B_r} &= \mathrm{Tr}\left(2B^T Y_\tau \Delta_{B_r} + \Delta_{B_r}^T Q_{r,\tau} B_r + B_r^T Q_{r,\tau} \Delta_{B_r}\right) \\ &= \mathrm{Tr}\left(2B^T Y_\tau \Delta_{B_r} + (Q_{r,\tau} B_r)^T \Delta_{B_r} + B_r^T Q_{r,\tau} \Delta_{B_r}\right) \\ &= 2\mathrm{Tr}\left(\left(B^T Y_\tau + B_r^T Q_{r,\tau}\right) \Delta_{B_r}\right) \\ &= \langle 2\left(Y_\tau^T B + Q_{r,\tau} B_r\right), \Delta_{B_r} \rangle. \end{aligned} \tag{4.31}$$

As Δ_{B_r} is arbitrary, comparing the above relation with $\Delta_J^{B_r} = \langle \nabla_{B_r} J, \Delta_{B_r} \rangle$ results in

$$\nabla_{B_r} J = 2\left(Y_\tau^T B + Q_{r,\tau} B_r\right).$$

Consider the expression of J given by (4.13). Due to perturbation Δ_{C_r} of C_r, the first order perturbation in J is as follows,

$$\begin{aligned}\Delta_J^{C_r} &= \mathrm{Tr}\left(-2CX_\tau \Delta_{C_r}^T + \Delta_{C_r} P_{r,\tau} C_r^T + C_r P_{r,\tau} \Delta_{C_r}^T\right) \\ &= \mathrm{Tr}\left(P_{r,\tau} C_r^T \Delta_{C_r} + (C_r P_{r,\tau})^T \Delta_{C_r} - 2(CX_\tau)^T \Delta_{C_r}\right) \\ &= \mathrm{Tr}\left(2\left(C_r P_{r,\tau} - CX_\tau\right)^T \Delta_{C_r}\right)\right) \\ &= \langle 2\left(C_r P_{r,\tau} - CX_\tau\right), \Delta_{C_r} \rangle. \end{aligned} \tag{4.32}$$

As Δ_{C_r} is arbitrary, comparing the above expression with $\Delta_J^{C_r} = \langle \nabla_{C_r} J, \Delta_{C_r} \rangle$ gives the following result

$$\nabla_{C_r} J = 2\left(C_r P_{r,\tau} - CX_\tau\right).$$

□

Corollary 4.2.3. *Let the reduced-order system Σ_r, given by the state space representation (2.17), be a local $H_2(\tau)$ optimal approximation of order r for the full order system Σ, given by the state space representation (2.1). Then,*

$$Q_{r,\tau} P_r + Y_\tau^T X + \tau(L(A_r\tau, S_\tau)^T) = 0, \tag{4.33}$$

$$Q_{r,\tau} B_r + Y_\tau^T B = 0, \text{ and} \tag{4.34}$$

$$C_r P_{r,\tau} - CX_\tau = 0, \tag{4.35}$$

where the quantities $P_{r,\tau}$, $Q_{r,\tau}$, X_τ, Y_τ, X, P_r and $L(A_r\tau, S_\tau)$ have been explained in Theorem 4.2.2.

As the $H_2(\tau)$ optimality conditions given by (4.33–4.35) are obtained using a gramian-based framework, they are referred to as Lyapunov-based $H_2(\tau)$ optimality conditions. Further, if A_r is diagonalizable, then the Lyapunov-based optimality conditions obtained here are equivalent to the interpolation-based $H_2(\tau)$ optimality conditions mentioned in Theorem 3.2.2. This is established in Appendix A.

4.3 A gradient-based numerical method for $H_2(\tau)$ optimal model reduction

This section proposes a model reduction scheme using the gradient expressions of the $H_2(\tau)$ error norm derived in the previous section. Additionally, the computational cost of the proposed model reduction scheme is discussed.

4.3.1 TL-H_2Opt model order reduction method

Due to the non-convex nature of the $H_2(\tau)$ optimization problem given by (2.47), finding global minimizers is difficult. Hence, local minimizers are obtained using standard nonlinear optimization techniques with good initial conditions [67]. The initial lower-order models are obtained by solving TL-TSIA and TL-BT. A quasi-Newton algorithm known as Broyden-Flectcher-Goldfarb-Shanno (BFGS) is used for solving the $H_2(\tau)$ optimization problem. For using the BFGS algorithm, the MATLAB function 'fminunc' is used. The closed-form expression of the gradients, given by (4.17–4.19), are used during the implementation of BFGS. The iterations are stopped when the convergence criteria are less than a preset error tolerance. The proposed model reduction scheme is called TL-H_2Opt.

4.3.2 Computational cost of TL-H_2Opt

The MATLAB function 'lyap' is used for solving the matrix equations (4.7) and (4.10) to obtain P_τ and Q_τ, respectively. The computational complexity of the underlying algorithm for 'lyap' is $\mathcal{O}(n^3)$. These terms are independent of the optimization variables A_r, B_r and C_r and must be computed only once at the start of the optimization process. $P_{r,\tau}$ and $Q_{r,\tau}$ are obtained by solving the matrix equations (4.9) and (4.12), respectively, using the 'lyap' function. The corresponding computational cost is $\mathcal{O}(n_r^3)$. These terms have to be computed at every iteration of the optimization. Since $n_r \ll n$, calculating the reduced-order gramians are not computationally heavy. The exponential term $e^{A\tau}$ is computed with the MATLAB function 'expm'. It has a computation complexity of $\mathcal{O}(n^3)$. However, this term has to be computed only once at the start of the optimization. $e^{A_r\tau}$ and $L(e^{A_r\tau}, S_\tau)$ are computed in every iteration of the optimization process using Algorithm 3 of [2]. This has a computational cost of $\mathcal{O}(n_r^3)$.

The terms Y_τ, X_τ and X are used for calculating the $H_2(\tau)$ error norm as well as the gradients of the error norm. Hence, they have to be computed at every iteration of the optimization. These terms are obtained by solving the matrix equations (4.11), (4.8) and (4.21), respectively, using the 'lyap' function in MATLAB. This has a computational cost of $\mathcal{O}(n^3)$. The computational cost can be reduced using Algorithm 3 of [14]. In this case, if the matrix A is diagonal or has some sparse structure, the cost of solving the time-limited Sylvester equations is much less than $\mathcal{O}(n^3)$.

4.4 Numerical examples

In this section, the performance of TL-H_2Opt is investigated using three numerical examples. The first two examples are asymptotically stable systems. The third example is a randomly generated

unstable SISO system. The TL-H_2Opt algorithm is initialized by the lower-order models obtained by solving the algorithms TL-TSIA and TL-BT, which are discussed in Section 2.4. The reduced models obtained by TL-H_2Opt are expected to have reduced $H_2(\tau)$ errors compared to the reduced models obtained by TL-TSIA and TL-BT. The improved performance of TL-H_2Opt is validated by comparing the $H_2(\tau)$ errors of the reduced models. Additionally, the improvement in performance is also assessed using $\Delta\text{Err}_{\text{Alg}}\%$, which is defined as follows:

$$\Delta\text{Err}_{\text{Alg}}\% = \frac{\text{Err}_{\text{Alg}}\text{-Err}_{\text{Opt}}}{\text{Err}_{\text{Alg}}} \times 100, \tag{4.36}$$

where Err_{Alg} and Err_{Opt} are the $H_2(\tau)$ errors obtained by the algorithm Alg and TL-H_2Opt with Alg initialization. In this case, Alg may refer to TL-TSIA or TL-BT. The simulations are done in MATLAB version 8.3.0.532(R2014a) on an Intel(R) Core(TM) i5-6500 CPU @ 3.20GHz system with 16 GB RAM.

4.4.1 Beam example

The first example is the cantilever beam model, discussed in Chapter 1. The aim is to obtain a reduced-order model that approximates the transient response of the full-order beam model for the time interval of $[0, 1]$ s. Reduced-order approximations are obtained for orders ranging from $r = 2$ to $r = 21$ with increments of 1 using TL-TSIA and TL-BT. Then, these reduced models are used for initializing the TL-H_2Opt algorithm.

Figure 4.1 compares the $H_2(\tau)$ errors for the reduced order models obtained with TL-TSIA and TL-H_2Opt with TL-TSIA initialization. The corresponding performance improvement $\Delta\text{Err}_{\text{TL-TSIA}}\%$ is listed in Table 4.1. Similarly, Figure 4.2 shows the $H_2(\tau)$ errors for the reduced order models obtained with TL-BT and TL-H_2Opt with TL-BT initialization. Table 4.2 lists the corresponding performance improvement $\Delta\text{Err}_{\text{TL-BT}}\%$.

The $H_2(\tau)$ approximation errors for TL-H_2Opt with TL-TSIA and TL-BT initializations are significantly lower than corresponding TL-TSIA and TL-BT reduced-order models. This is evident from Figure 4.1 and Figure 4.2 as well as Table 4.1 and Table 4.2. For $r = 4, 18, 20$, the $H_2(\tau)$ approximation error due to TL-TSIA is high or doesn't converge. Hence, errors corresponding to those orders are not included in Figure 4.1. For $r < 16$, some of the reduced order models show good improvement in the $H_2(\tau)$ errors; for example, $r = 5, 9$ and 10 show an improvement of more than 70%. This is evident from Table 4.1. For TL-BT initialization, Table 4.2 shows that $H_2(\tau)$ errors for $r = 5, 8, 9$ and 14 is reduced by more than 70%. Beyond $r \geq 16$, the optimization algorithm doesn't significantly improve the $H_2(\tau)$ approximation errors for TL-TSIA and TL-BT initializations.

4.4.2 ISS example

The second example is a MIMO model of the International Space Station (ISS), described in Chapter 1. Here, the aim is to derive lower-order models which approximate the input-output behaviour of the original model in the time interval $[0, 0.5]$ s. This time interval is less than the settling time of the system. Reduced-order models are obtained for orders ranging from $r = 2$ to $r = 42$ with increments of 2 using TL-TSIA and TL-BT. They are used for initializing TL-H_2Opt.

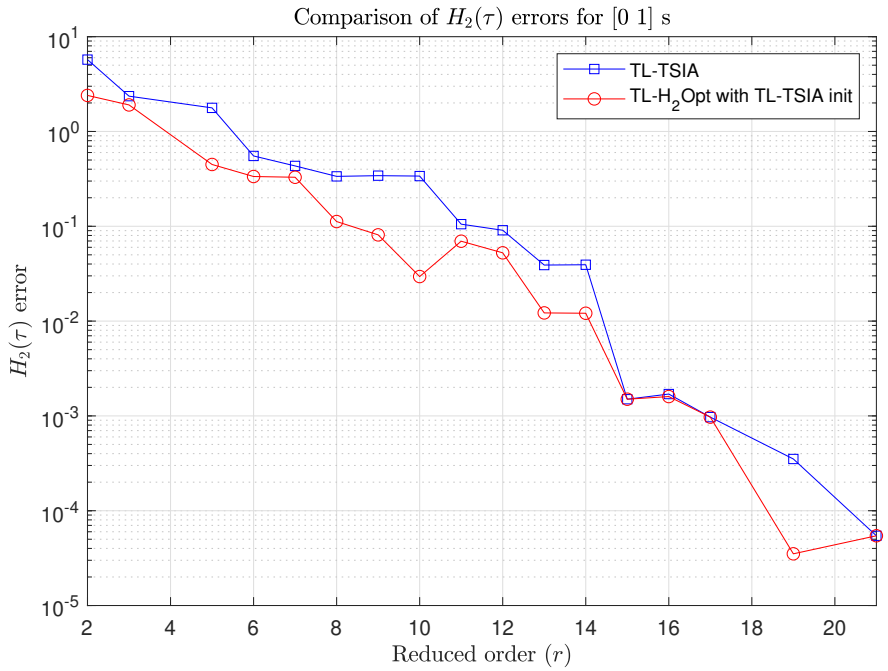

Figure 4.1: TL-TSIA vs TL-H_2Opt with TL-TSIA initialization for beam example

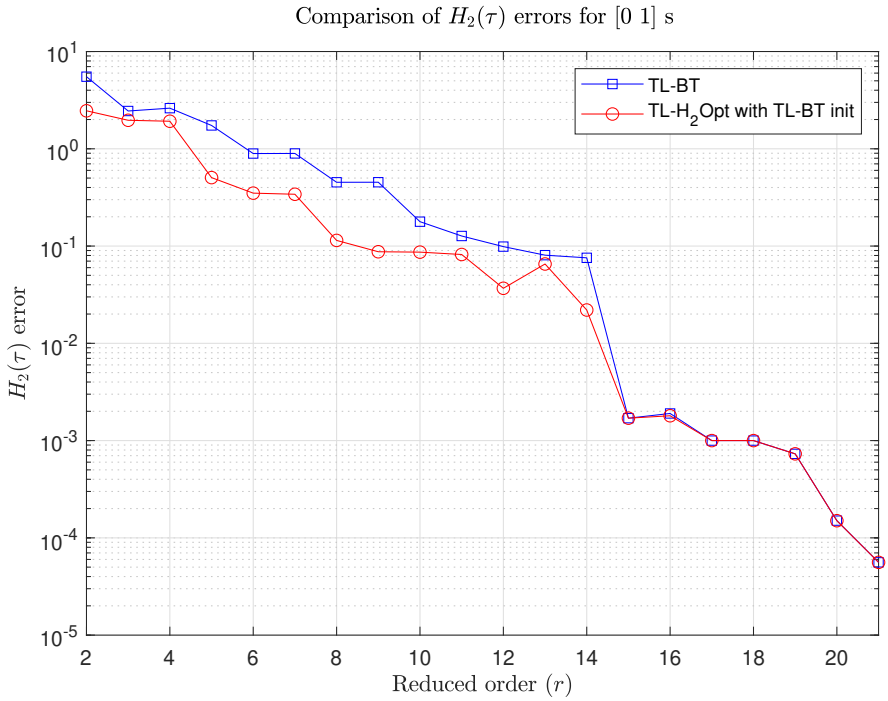

Figure 4.2: TL-BT vs TL-H_2Opt with TL-BT initialization for beam example

r	ΔErr(%)	r	ΔErr(%)	r	ΔErr(%)	r	ΔErr(%)
2	58.10	7	24.05	12	42.18	17	0.0021
3	19.18	8	66.62	13	68.72	18	
4	79.82	9	76.26	14	69.21	19	0.0626
5	74.71	10	91.28	15	0	20	
6	39.31	11	33.90	16	5.88	21	0

Table 4.1: Performance improvement of TL-H_2Opt with TL-TSIA initialization for beam example.

r	ΔErr(%)	r	ΔErr(%)	r	ΔErr(%)	r	ΔErr(%)
2	55.40	7	61.94	12	62.71	17	0
3	19.71	8	74.74	13	18.86	18	0
4	26.62	9	80.71	14	70.94	19	0.0014
5	70.90	10	51.37	15	0	20	0.1730
6	60.83	11	35.46	16	5.26	21	0

Table 4.2: Performance improvement of TL-H_2Opt with TL-BT initialization for beam example.

The $H_2(\tau)$ errors for the reduced-order models obtained using TL-TSIA and TL-H_2Opt with TL-TSIA initialization are displayed in Figure 4.3. The performance improvement $\Delta\text{Err}_{\text{TL-TSIA}}\%$ is shown in Table 4.3. Similarly, the $H_2(\tau)$ errors for TL-BT and TL-H_2Opt with TL-BT initialization are compared in Figure 4.4. The performance improvement $\Delta\text{Err}_{\text{TL-BT}}\%$ is listed in Table 4.4.

It is observed that for $r \leq 38$, the $H_2(\tau)$ errors are significantly reduced. There is no substantial error reduction for $r > 38$. For $r = 4$ and $r = 12$ obtained by TL-TSIA, the $H_2(\tau)$ approximation errors are high. Hence, they are not shown in Figure 4.3. For $r = 22, 26, 28, 30, 32$ the performance improvement $\Delta\text{Err}_{\text{TL-TSIA}}\%$ is more than 70% (evident from Table 4.3). The improvement $\Delta\text{Err}_{\text{TL-BT}}\%$ for $r = 18, 20, 22, 24, 26, 28, 32$ is more than 70% (evident from Table 4.4).

4.4.3 Unstable model

The third example is an artificially constructed unstable SISO model, which is inspired by the unstable example considered in [94]. This model is of order 402 and has 400 stable poles and 2 unstable poles. In this example, the finite time interval considered for model reduction is $[0, 0.5]$.

r	ΔErr(%)	r	ΔErr(%)	r	ΔErr(%)	r	ΔErr(%)
2	6.25	12	100	22	77.88	32	73.15
4	99.75	14	39.83	24	65.54	34	60.93
6	14.71	16	60.80	26	89.88	36	44.32
8	22.86	18	54.95	28	71.62	38	0.008
10	30.39	20	44.49	30	72.87	40	0

Table 4.3: Performance improvement of TL-H_2Opt with TL-TSIA for ISS example.

r	ΔErr(%)	r	ΔErr(%)	r	ΔErr(%)	r	ΔErr(%)
2	6.25	12	10.39	22	87.30	32	89.69
4	23.08	14	11.40	24	97.57	34	68.50
6	37.85	16	66.26	26	92.17	36	47.19
8	41.24	18	83.15	28	86.29	38	0
10	56.82	20	92.21	30	65.89	40	0

Table 4.4: Performance improvement of TL-H_2Opt with TL-BT for ISS example.

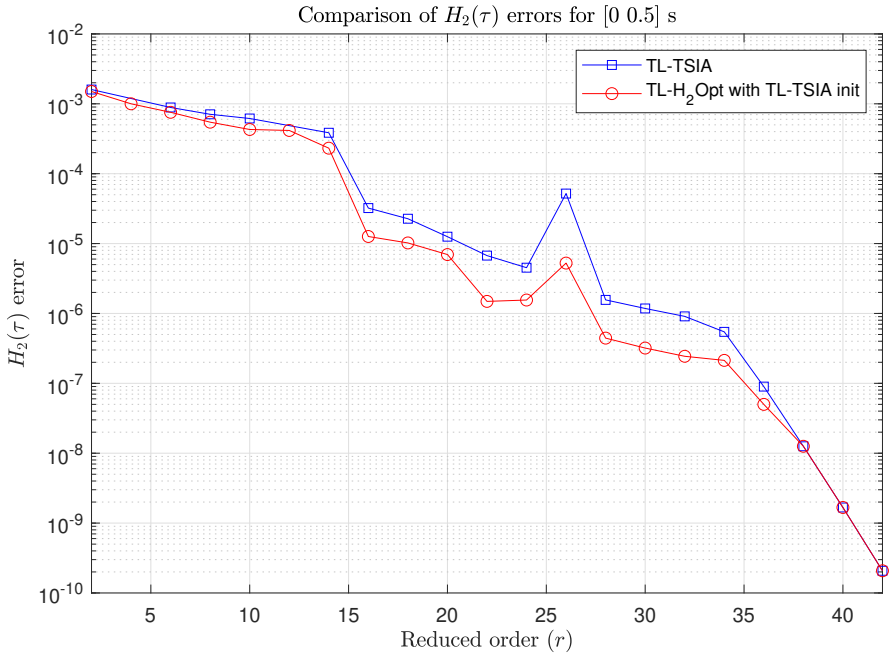

Figure 4.3: TL-TSIA vs TL-H_2Opt with TL-TSIA initialization for ISS example

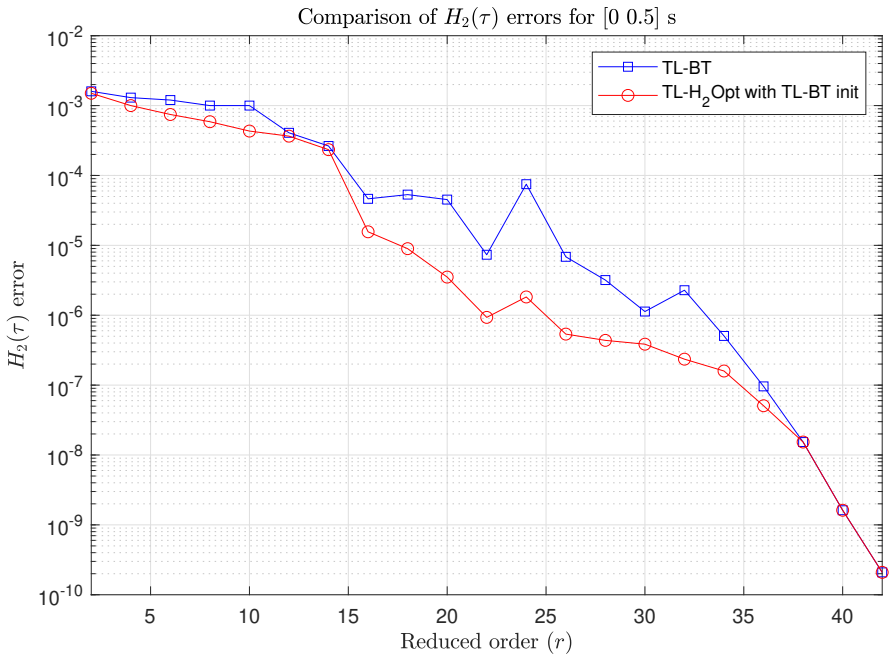

Figure 4.4: TL-BT vs TL-H_2Opt with TL-BT initialization for ISS example

Reduced models of orders ranging from $r = 2$ to $r = 12$ with increments of 1 are obtained using TL-TSIA and TL-BT. They are then used for initializing TL-H_2Opt.

The $H_2(\tau)$ approximation errors of TL-TSIA and TL-H_2Opt with TL-TSIA initialization are displayed in Figure 4.5. Similarly, Figure 4.6 compares the approximation errors for the TL-BT case. Table 4.5 and Table 4.6 list the performance improvements $\Delta\text{Err}_{\text{TL-TSIA}}\%$ and $\Delta\text{Err}_{\text{TL-BT}}\%$, respectively.

r	ΔErr	r	ΔErr	r	ΔErr	r	ΔErr
2	79.57	5	34.38	8	0.57	11	0.023
3	52.51	6	3.85	9	0	12	5.35
4	16.53	7	2.44	10	0		

Table 4.5: Performance improvement of TL-H_2Opt with TL-TSIA for unstable example.

r	ΔErr	r	ΔErr	r	ΔErr	r	ΔErr
2	32.74	5	77.22	8	69.13	11	0
3	73.32	6	81.82	9	37.64	12	0
4	7.58	7	43.48	10	0		

Table 4.6: Performance improvement of TL-H_2Opt with TL-BT for unstable example.

For $r = 2, 3$, the performance improvement for the TL-TSIA case is more than 50% as evident from Table 4.5. Table 4.6 shows that for $r = 3, 5, 6, 8$, the performance improvement for the TL-BT case is more than 50%.

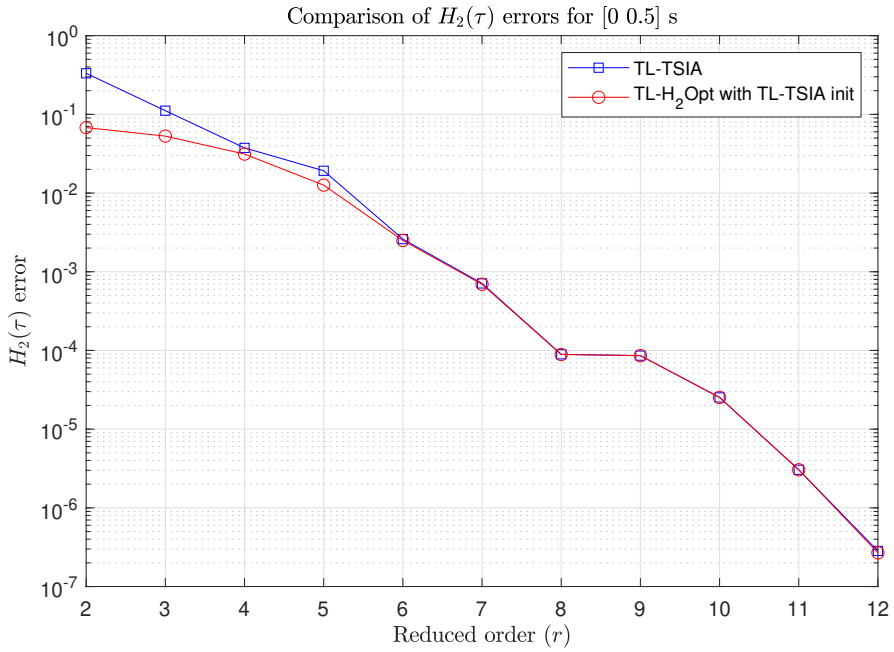

Figure 4.5: TL-TSIA vs TL-H_2Opt with TL-TSIA initialization for unstable example.

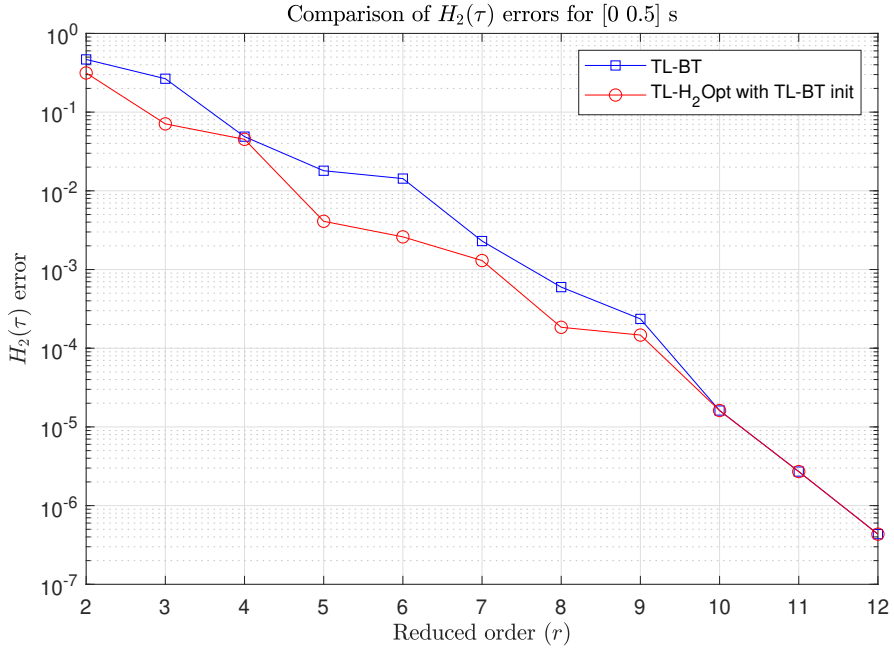

Figure 4.6: TL-BT vs TL-H_2Opt with TL-BT initialization for unstable example.

In all the examples discussed above, it is observed that TL-H_2Opt requires good reduced-order models (which are obtained by TL-TSIA and TL-BT) as initial conditions. As discussed in Section 4.3.2, TL-H_2Opt is computationally expensive, and the requirement of good initial conditions causes additional computational burden. This is a disadvantage of TL-H_2Opt and the other existing descent-based method in [94] compared to the projection-based methods. However, the superior performance of TL-H_2Opt (with respect to the $H_2(\tau)$ error norm) is validated by the above numerical examples.

4.5 Summary

A gradient-based method for obtaining $H_2(\tau)$ optimal reduced-order models, applicable for both SISO and MIMO systems, has been proposed in this chapter. The analytical expressions of the gradients of the $H_2(\tau)$ error norm have been derived. The gradients have been used with a standard quasi-Newton algorithm for minimizing the $H_2(\tau)$ error norm. The model reduction method has to be carried out in two steps. The first step involves obtaining a reduced-order model via TL-TSIA or TL-BT. In the second step, the reduced-order model is used for initializing a quasi-Newton algorithm. Finally, numerical examples have been used to demonstrate that the TL-H_2Opt algorithm performs better than TL-TSIA and TL-BT in obtaining locally $H_2(\tau)$ optimal reduced models.

Chapter 5

On the computation of gramians and a finite-horizon norm of an LTV system

System gramians and system norms play an important role in model order reduction (MOR) of LTI systems. For example, $H_2(\tau)$ norm-based MOR methods are developed in Chapter 3 and Chapter 4. Further, a gramian-based framework is used to propose the MOR method in Chapter 4. Similar to LTI systems, system norms and gramians also play an important role in the MOR of LTV systems. Due to the inherent connection of system gramians with reachability and observability maps of LTV systems, they can be computed using state trajectories. This motivates the computation of system gramians for LTV systems using system trajectory information. This is the focus of the first half of this chapter. The second half of this chapter focuses on a finite horizon system norm for continuous-time LTV systems. This norm is used in Chapter 6 as a performance measure for obtaining reduced-order models of continuous-time LTV systems over a finite time interval.

The first systematic presentation of the computation of gramians using empirical methods is given in [52]. It is extended to affine and non-affine control systems in [52, 53, 36, 37, 38]. [102] computes low-rank approximations of the empirical controllability and observability gramians for large-scale LTI systems using the method of snapshots ([95]). [80] uses modified empirical methods for evaluating the gramians of large-scale LTI systems. A finite time empirical observability gramian for an uncontrolled nonlinear system is defined in [49]. It is modified to include the control input in [75]. For control-affine nonlinear systems with a constant-input vector, gramians are computed and used for model order reduction in [46, 47].

Because of structural differences, the empirical computation methods of LTI and LTV reachability gramians are not identical. In [71, 72], system trajectory information of an LTV system is used to compute the state transition matrix, which is then used to compute the gramians of LTV systems. In the first half of this chapter, three methods are presented for calculating the finite horizon reachability gramian of LTV systems. Unlike Perev's work [71, 72], the proposed methods do not explicitly compute the state transition matrix. The first two methods use final

state information for shifted impulse and piecewise constant inputs, and the third method uses zero-input responses of a modified adjoint system to compute the reachability gramian.

System norms are used to quantify the input-to-output gain of a linear dynamical system. They are also essential in solving computational problems. The utility of the H_2 system norm for input-output analysis of LTI systems is well-documented. The H_2 and H_∞ norm are used as performance indices in analysis and design problems [108]. Hankel norm-based bounds appear in model reduction problems of continuous-time LTV systems [87]; a H_2-like norm is used for model order reduction of discrete-time LTV systems [60, 61].

The finite horizon system norm discussed in the second half of this chapter is referred to as the finite horizon H_2 norm. The norm is defined using a double integral of the impulse response matrix of the LTV system over finite time intervals. It is shown to be an upper bound of the induced system norm from the input space $L_2^m[t_0, t_f]$ to the output space $L_2^p[t_0, t_f]$. Further, a trace formula of the norm in terms of the reachability or the observability gramian is also obtained. Finally, using the concept of the modified adjoint of an LTV system [45], it is shown that the finite horizon H_2 norms of the original and the modified adjoint LTV system are equal. The trace formulas of the finite horizon H_2 norm are similar to those of a 2-norm defined in [31](Page 93, Chapter 3). However, the definitions of the norms are different, and the method of obtaining the trace formulas is also distinct. The formulas follow directly from the norm definition in this thesis, whereas in [31], they are derived using the gramian definitions.

The rest of the chapter is structured as follows. Some issues related to the computation of the reachability gramian are discussed in Section 5.1. In Section 5.2, two methods for computing the reachability gramian of LTV systems over a finite time interval are proposed. Section 5.3 introduces the adjoint and modified adjoint of an LTV system and proposes a third method for computing the reachability gramian. Section 5.4 discusses a finite horizon H_2 system norm for LTV systems and its relation with the system gramians. The chapter is concluded in Section 5.5.

5.1 Computation issues of the reachability gramian of an LTV system

The reachability gramian of the continuous-time LTV system, given by (2.72), is defined by (2.82). For $t = t_f$, the gramian is as follows:

$$P(t_f, t_0) = \int_{t_0}^{t_f} \phi(t_f, t) B(t) (B(t))^T (\phi(t_f, t))^T dt.$$

The gramian can be computed by evaluating the above integral expression. This requires the computation of the state transition matrix $\phi(t_f, t)$ in terms of t_f and t. The gramian can also be computed by solving the forward differential Lyapunov equation, given by (2.83). Computing the gramian using the above methods has the following drawbacks:

- For any arbitrary state matrix $A(t)$, deriving an analytical expression of the state transition matrix $\phi(t_f, t)$ is not straightforward.

- For systems with a large number of states, solving the matrix differential Lyapunov equation given by (2.83) becomes a computational burden.

For the reasons listed above, different approaches to determining the reachability of a gramian over a finite time interval are investigated in the later sections. This section briefly states Moore's method for computing the controllability gramian for LTI systems.

Moore's method [64]: Assuming $t_0 = 0$, the input $u(t) = e_1\delta(t)$ is applied for the initial condition, $x(0) = 0$, and the LTI system is simulated. The system response obtained is $x_j(t) = e^{At}Be_1$. In a similar way, the inputs $e_2\delta(t), e_3\delta(t), \cdots, e_m\delta(t)$ are applied and the corresponding state responses $x_2(t), x_3(t), \cdots, x_m(t)$ are obtained. The impulse response information over $[0, t_f]$ is used to compute the reachability gramian as follows,

$$P(t_f, 0) = \int_0^{t_f} [x^1(t) \cdots x^m(t)][x^1(t) \cdots x^m(t)]^T dt.$$

The finite interval controllability gramian computed using Moore's technique is inaccurate for LTV systems. This is demonstrated with the help of a numerical example. Consider the LTV system shown below,

$$\dot{x}(t) = \begin{bmatrix} 0 & 0 \\ 0 & -1 \end{bmatrix} x(t) + \begin{bmatrix} 1 \\ e^{-2t} \end{bmatrix} u(t).$$

The reachability gramian, computed by solving the forward matrix differential Lyapunov equation given by (2.83) is,

$$P_1(5, 0) = \begin{bmatrix} 5.0000 & 0.0067 \\ 0.0067 & 2.2600 \times 10^{-5} \end{bmatrix}.$$

The same gramian computed by the empirical Moore's method for the same time interval is,

$$P_2(5, 0) = \begin{bmatrix} 4.5185 & 0.3400 \\ 0.3400 & 0.0597 \end{bmatrix}.$$

Note that $P_1(5, 0)$ and $P_2(5, 0)$ are different. Thus, Moore's method is inaccurate for computing the reachability gramian of LTV systems.

5.2 Computing the reachability gramian using system trajectory information

In this section, two numerical methods for computing the finite horizon reachability gramian of an LTV system are proposed. These methods use system trajectory information for gramian computation.

5.2.1 Gramian computation using recurring time-shifted impulse inputs

In this approach, the time interval $[0, t_f]$ is divided into equal-sized sub-intervals. At the start of each sub-interval, impulse inputs are applied, and the final state data at $t = t_f$ is used to build the gramian matrix as given in Algorithm 8.

Algorithm 8: Computing $P(t_f, 0)$ using shifted impulse inputs

Input: $\epsilon, N, [0, t_f]$

Output: $D(n)$

Initialize: $n = 1, M(n) = 2^{n-1}N, D(0) = 0$;

while $\|D(n) - D(n-1)\| > \epsilon$ **do**

1. The interval $[0, t_f]$ is divided into $M(n)$ sub-intervals of length, $\Delta t = \frac{t_f}{M(n)}$;
2. For $i = 0$, apply input $\delta(t - i\Delta t)$ to the LTV system. Let $x(t_f, i\Delta t)$ be the final state vector. This is repeated for $i = 1, 2, \cdots, M(n)$;
3. The $n \times (M(n) + 1)$ matrix of final state vectors is stored as $L(n)$,

$$L(n) = \begin{bmatrix} x(t_f, 0) & x(t_f, \Delta t) & \dots & x(t_f, M(n)\Delta t) \end{bmatrix};$$

4. Compute $D(n) = L(n) \times (L(n))^T \times \Delta t$;
5. Update $n = n + 1$;

end

The initial state of the LTV system is assumed to be zero. For smaller values of ϵ, the gramians computed are more accurate, but the computation cost is high. Thus, depending on the accuracy of the gramian approximation, the value of ϵ is chosen.

Remark 6. For each iteration, previous iteration samples can be reused. For example, $L(1)$ can be constructed using $M(1) + 1 = N + 1$ samples. The matrix $L(2)$ computed in the second iteration is given by

$$\begin{bmatrix} x(t_f, 0) & x(t_f, \frac{\Delta t}{2}) & x(t_f, 2\frac{\Delta t}{2}) & \cdots & x(t_f, 2N\frac{\Delta t}{2}) \end{bmatrix}.$$

Among the above samples, $L(1)$ already contains the set: $\{x(t_f, 0), x(t_f, 2\frac{\Delta t}{2}), \cdots, x(t_f, N\frac{\Delta t}{2})\}$. The rest of the samples $\{x(t_f, \frac{\Delta t}{2}), x(t_f, 3\frac{\Delta t}{2}), \cdots, x(t_f, (2N-1)\frac{\Delta t}{2})\}$, can be obtained using N simulations. Similarly, $\frac{M(n)}{2}$ samples instead of $M(n) + 1$ is used for every iteration excluding the first.

Theorem 5.2.1. *As $n \to \infty$, the matrix $D(n)$ transforms to $\int_0^{t_f} \phi(t_f, t)B(t)(B(t))^T (\phi(t_f, t))^T dt$.*

Proof. For the input $u(\tau) = \delta(\tau - z)$ to the LTV system, given by (2.72), the final state obtained at $t = t_f$ is

$$x(t_f, z) = \phi(t_f, z)B(z).$$

For a fixed value of N, the size of the interval Δt at the n^{th} iteration is $\frac{t_f - t_0}{M(n)} = \frac{t_f - t_0}{2^{n-1}N}$. The matrix $L(n)$ is as follows,

$$L(n) = \begin{bmatrix} x(t_f, 0) & x(t_f, \Delta t) & \cdots & x(t_f, M(n)\Delta t) \end{bmatrix}$$

Substituting $L(n)$ in $D(n)$ results in,

$$\begin{aligned} D(n) &= \sum_{i=0}^{M(n)} x(t_f, i\Delta t)(x(t_f, i\Delta t))^T \Delta t \\ &= \sum_{i=0}^{M(n)} \phi(t_f, i\Delta t)B(i\Delta t)(B(i\Delta t))^T(\phi(t_f, i\Delta t))^T \Delta t \end{aligned}$$

As $n \to \infty$, $\Delta t \to 0$ and thus $D(n) \to \int_0^{t_f} \phi(t_f, t)B(t)(B(t))^T \left(\phi(t_f, t)\right)^T dt$. □

5.2.2 Gramian computation using recurring time-shifted pulse inputs

The time interval $[0, t_f]$ is divided into sub-intervals. A time-shifted pulse with a width equal to the sub-interval length and unit height is applied as input to the LTV system for each sub-interval. Using the final states obtained, the gramian matrix is calculated. This is outlined in Algorithm 9. Similar to Algorithm 8, it is considered that the initial state of the LTV system is zero.

Algorithm 9: Computing $P(t_f, 0)$ using shifted pulse inputs

Input: $\epsilon, N, [0, t_f]$

Output: $D(n)$

Initialize: $n = 1, M(n) = 2^{n-1}N, D(0) = 0$;

while $\|D(n) - D(n-1)\| > \epsilon$ **do**

1. Divide $[0, t_f]$ into $M(n)$ sub-intervals of length, $\Delta t = \frac{t_f}{M(n)}$;
2. Apply $M(n)$ input trajectories defined as,

$$u_i(t) = \begin{cases} 1, & t \in [i\Delta t, (i+1)\Delta t] \\ 0, & t \in [t_0, t_f] \backslash [i\Delta t, (i+1)\Delta t] \end{cases} \tag{5.1}$$

for $i = 0, 1, \cdots, M(n) - 1$ to the LTV system given by (2.72). $x_i(t_f)$ is the final state vector for the input $u_i(t)$;

3. The final state vectors are stored in a matrix $L(n)$,

$$L(n) = \begin{bmatrix} x_0(t_f) & x_1(t_f) & \dots & x_{(M(n)-1)}(t_f) \end{bmatrix};$$

4. Compute $D(n) = \frac{L(n) \times (L(n))^T}{\Delta t}$;
5. Update $n = n + 1$;

end

The matrix $D(n)$ approximates the reachability gramian over $[0, t_f]$. The value of ϵ is set depending on how precisely the gramian is to be computed.

Theorem 5.2.2. *As $n \to \infty$, the matrix $D(n)$ transforms to $\int_0^{t_f} \phi(t_f, t)B(t)(B(t))^T \left(\phi(t_f, t)\right)^T dt$.*

Proof. For the input $u_i(t)$ given by (5.1), the final state of the LTV system given by (2.72) is,

$$x_i(t_f) = \int_0^{t_f} \phi(t_f, \tau)B(\tau)u_i(\tau)d\tau.$$

The above expression can be reframed as,

$$x_i(t_f) = \int_0^{i\Delta t} \phi(t_f, \tau)B(\tau)u_i(\tau)d\tau + \int_{i\Delta t}^{(i+1)\Delta t} \phi(t_f, \tau)B(\tau)u_i(\tau)d\tau + \int_{(i+1)\Delta t}^{t_f} \phi(t_f, \tau)B(\tau)u_i(\tau)d\tau.$$

In the above expression, the first and third terms are zero, so $x_i(t_f)$ becomes

$$x_i(t_f) = \int_{i\Delta t}^{(i+1)\Delta t} \phi(t_f, \tau)B(\tau)d\tau.$$

For small Δt, $x_i(t_f)$ can be approximated as

$$x_i(t_f) \approx \phi(t_f, i\Delta t)B(i\Delta t)\Delta t.$$

Replacing $x_i(t_f)$ in $L(n) \times (L(n))^T$ results in

$$\begin{aligned} L(n) \times (L(n))^T &= \sum_{i=1}^{M(n)} x_i(t_f)(x_i(t_f))^T \\ &\approx \sum_{i=1}^{M(n)} \phi(t_f, i\Delta t)B(i\Delta t)(\phi(t_f, i\Delta t)B(i\Delta t))^T(\Delta t)^2. \end{aligned}$$

The following is obtained by dividing both sides of the above expression by Δt.

$$\begin{aligned} D(n) &= \frac{(L(n) \times (L(n))^T)}{\Delta t} \\ &\approx \sum_{i=1}^{N} \phi(t_f, i\Delta t)B(i\Delta t)(\phi(t_f, i\Delta t)B(i\Delta t))^T \Delta t. \end{aligned}$$

As $n \to \infty$, $\Delta t \to 0$. Thus, $D(n)$ transforms to $\int_0^{t_f} \phi(t_f, t)B(t)(B(t))^T \left(\phi(t_f, t)\right)^T dt$. □

Remark 7. For a fixed value of N, Algorithm 9 requires less number of iterations (n) compared to Algorithm 8 for computation of the reachability gramian with a desired level of accuracy.

5.2.3 Gramian computation for multi-input systems

Algorithm 8 and Algorithm 9 can be extended to MIMO systems as follows

$$\begin{aligned} P(t_f, 0) &= \int_0^{t_f} \phi(t_f, t)B(t)(B(t))^T(\phi(t_f, t))^T dt \\ &= \int_0^{t_f} \phi(t_f, t) \sum_{i=1}^{m} B_i(t)(B_i(t))^T(\phi(t_f, t))^T dt \\ &= \sum_{i=1}^{m} \int_0^{t_f} \phi(t_f, t)B_i(t)(B_i(t))^T(\phi(t_f, t))^T dt \\ &= \sum_{i=1}^{m} P_i(t_f, 0), \end{aligned}$$

where $u_1, u_2, \ldots, u_m$ are m inputs of the system. The columns of the input matrix $B(t)$ are $B_1(t), B_2(t), \ldots, B_m(t)$. For the i^{th} input u_i, let the corresponding reachability gramian component be $P_i(t_f, 0)$. To compute $P_1(t_f, 0)$, the remaining inputs are set to zero i.e. $u_i \equiv 0, i = 2, \ldots, m$. Applying a set of recurring inputs to u_1 as given by Algorithm 8 or 9, the gramian component is calculated. Similarly, for the remaining components, all the remaining inputs except the corresponding input are set to zero and applying recurring inputs to the non-zero input, the gramian component is computed. The gramian components, when added up, give the reachability gramian $P(t_f, 0)$.

Remark 8. For both Algorithm 8 and Algorithm 9, the time interval $[0, t_f]$ is split into $M(n) = 2^{n-1}N$ sub-intervals of length Δt at a particular iteration. Further, Algorithm 8 requires $M(n)+1$ simulations of the LTV system for gramian computation, whereas Algorithm 9 requires $M(n)$ simulations for the same. The gramian is better approximated for a large value of N, but the computational cost increases.

5.2.4 Numerical example

Consider the following LTV system,

$$\frac{dx(t)}{dt} = \begin{bmatrix} -1 + 0.5cos^2(t) & 1 - 0.5sin(t)cos(t) \\ -1 - 0.5sin(t)cos(t) & -1 + 0.5sin^2(t) \end{bmatrix} x(t) + \begin{bmatrix} 1 \\ 1 \end{bmatrix} u(t)$$
$$y(t) = \begin{bmatrix} 1 & 1 \end{bmatrix} x(t). \tag{5.2}$$

The reachability gramian of the above system is computed using Algorithm 8 and Algorithm 9 for the time interval $[0, 5]$ s. The results are compared with the reachability gramian computed by solving the differential Lyapunov equation, given by (2.83).

Solving the differential Lyapunov equation (2.83) from $t_0 = 0$ s to $t_f = 5$ s with zero initial condition results in

$$P_1(5, 0) = \begin{bmatrix} 0.7938 & 0.3662 \\ 0.3662 & 0.5428 \end{bmatrix}. \tag{5.3}$$

Setting $N = 5$, the reachability gramian is computed over the time interval $[0, 5]$ s using Algorithm 8 for various values of n. For $n = 1$, the result is

$$P_2(5, 0) = \begin{bmatrix} 0.2787 & -0.0093 \\ -0.0093 & 0.2779 \end{bmatrix}.$$

For $n = 2$, the result is

$$P_2(5, 0) = \begin{bmatrix} 0.5367 & 0.1441 \\ 0.1441 & 0.3541 \end{bmatrix}.$$

For $n = 5$, the result is

$$P_2(5, 0) = \begin{bmatrix} 0.7683 & 0.3421 \\ 0.3421 & 0.5199 \end{bmatrix}.$$

Similarly, setting $N = 5$, the reachability gramian is again computed over the time interval $[0, 5]$ s using Algorithm 9 for different values of n. For $n = 1$, the result is

$$P_2(5, 0) = \begin{bmatrix} 0.7388 & 0.3030 \\ 0.3030 & 0.4216 \end{bmatrix}.$$

For $n = 2$, the result is

$$P_2(5, 0) = \begin{bmatrix} 0.7590 & 0.3417 \\ 0.3417 & 0.5029 \end{bmatrix}.$$

Comparing the results, it is observed that Algorithm 8 approximates the reachability gramian quite well for $n = 5$ whereas Algorithm 9 does the same for $n = 2$. For both methods, increasing n gives more accurate results. However, for a fixed N, Algorithm 9 approximates the reachability gramian better than Algorithm 8 for smaller values of n.

5.3 Computing the reachability gramian using the system adjoint

Adjoint models are widely used in computational mathematics, optimization theory, and system and circuit theory, particularly in analyzing the sensitivity of a cost function or system behaviour to

parameter variations [19, 76, 48]. This section will focus on the duality concept and discuss adjoint and modified adjoint systems for LTV systems. Further, the modified adjoint of LTV systems is used to propose an alternate method for computing the finite horizon reachability gramian of LTV systems.

5.3.1 Adjoint and modified adjoint of a continuous-time LTV system

The adjoint dynamical system Σ_a associated with the LTV system given by the state-space representation (2.72), with its operation restricted to the finite time interval $[t_0, t_f]$, is a finite-dimensional state-space realization of order n and is given by

$$\begin{aligned} \dot{x_a}(t) &= -A^T(t)x_a(t) - C^T(t)u_a(t), \\ y_a(t) &= B^T(t)x_a(t), \end{aligned} \tag{5.4}$$

with t varying from $t = t_f$ to $t = t_0$. For $t \geq \tau$, let $\phi_a(t, \tau)$ and $h_a(t, \tau)$ be the state transition matrix and the impulse response matrix, respectively, of the adjoint system.

For simulating the adjoint system, the "modified adjoint system", denoted by Σ_{ma}, is used in [45]. This system has a finite-dimensional state-space realization of order n, and t varies from t_0 to t_f, similar to the original system Σ. For the finite time horizon $[t_0, t_f]$, the modified adjoint is defined as

$$\begin{aligned} \dot{x}_{ma}(t) &= (A(t_0 + t_f - t))^T x_{ma}(t) + (C(t_0 + t_f - t))^T u_{ma}(t), \\ y_{ma}(t) &= (B(t_0 + t_f - t))^T x_{ma}(t). \end{aligned} \tag{5.5}$$

For $t \geq \tau$, let $\phi_{ma}(t, \tau)$ and $h_{ma}(t, \tau)$ be the state transition matrix and impulse response matrix, respectively, of the modified adjoint system.

The following proposition establishes the relation between the state transition matrices of the original LTV system and its adjoint.

Proposition 5.3.1. *If $\phi_a(t, \tau)$ is the state transition matrix of the LTV system Σ_a, the adjoint of the LTV system Σ, with state transition matrix $\phi(t, \tau)$, then*

$$\phi_a(t, \tau) = (\phi(\tau, t))^T. \tag{5.6}$$

Proof. For $u \equiv 0$, the differential equation of the LTV system Σ becomes,

$$\frac{d}{dt}x(t) = A(t)x(t), \tag{5.7}$$

Let $x(t_0)$ be the initial condition. For $t \geq t_0$, $x(t) = \phi(t, t_0)x(t_0)$.

Similarly, for $u_a \equiv 0$, the differential equation of the adjoint LTV system Σ_a becomes,

$$\frac{d}{dt}y(t) = -(A(t))^T y(t), \tag{5.8}$$

Let $x(t_f)$ be the final condition. For $t \leq t_f$, $x(t) = \phi_a(t, t_f)x(t_f)$. Using (5.7) and (5.8), the following result is obtained.

$$\begin{aligned} \frac{d}{dt}\left((x(t))^T y(t)\right) &= \left(\frac{d}{dt}x(t)\right)^T y(t) + (x(t))^T \frac{d}{dt}y(t) \\ &= (x(t))^T (A(t))^T y(t) - (x(t))^T (A(t))^T y(t) \\ &= 0. \end{aligned}$$

This shows that the inner product of $x(t)$ and $y(t)$ is constant for all t. Let $k \in \mathbb{R}$ be the constant. Then,

$$\begin{aligned}&(x(t))^T y(t) = k\\ &\Rightarrow (x(t_0))^T(\phi(t,t_0))^T\phi_a(t,t_f)x_a(t_f) = k. \quad \forall\, t \in [t_0, t_f]\end{aligned}$$

The above expression is true if

$$(\phi(t,t_0))^T\phi_a(t,t_f) = M, \tag{5.9}$$

where M is a constant matrix for all t. M is obtained by evaluating $(\phi(t,t_0))^T\phi_a(t,t_f)$ at $t = t_0$ as follows,

$$\begin{aligned}M &= (\phi(t_0,t_0))^T\phi_a(t_0,t_f)\\ &= \phi_a(t_0,t_f).\end{aligned}$$

Substituting the above expression for M in (5.9) results in

$$\begin{aligned}&(\phi(t,t_0))^T\phi_a(t,t_f) = \phi_a(t_0,t_f)\\ &\Rightarrow \phi_a(t,t_f)\left(\phi_a(t_0,t_f)\right)^{-1} = (\phi(t,t_0))^{-T}\\ &\Rightarrow \phi_a(t,t_f)\phi_a(t_f,t_0) = (\phi(t,t_0))^{-T}\\ &\Rightarrow \phi_a(t,t_0) = (\phi(t,t_0))^{-T}.\end{aligned}$$

Using the above result, $\phi_a(t,\tau)$ is obtained as follows,

$$\begin{aligned}\phi_a(t,\tau) &= \phi_a(t,t_0)\phi_a(t_0,\tau)\\ &= (\phi(t,t_0))^{-T}\left(\phi_a(\tau,t_0)\right)^{-1}\\ &= (\phi(t,t_0))^{-T}\left(\phi(\tau,t_0)\right)^{T}\\ &= (\phi(t,t_0)\phi(t_0,\tau))^{-T}\\ &= (\phi(t,\tau))^{-T}.\end{aligned}$$

□

Using the above proposition, the relation between the state transition matrices of the original LTV and the modified adjoint LTV system is established.

Proposition 5.3.2. *If $\phi_{ma}(t,\tau)$ is the state transition matrix of the LTV system Σ_{ma}, the modified adjoint of the LTV system Σ, with state transition matrix $\phi(t,\tau)$, then*

$$\phi_{ma}(t,\tau) = (\phi(t_0 + t_f - \tau, t_0 + t_f - t))^T. \tag{5.10}$$

Proof. Let $x_a(t)$ and $x_{ma}(t)$ be the state vectors for the adjoint system Σ_a and the modified adjoint system Σ_{ma}, respectively. For $t \in [t_0, t_f]$, the state vectors are related as,

$$x_{ma}(t) = x_a(t_0 + t_f - t)$$

For $t = t_0$, $x_{ma}(t_0) = x_a(t_f)$. The above expression can be expressed in terms of the state transition matrices of the adjoint and modified adjoint systems as follows,

$$\begin{aligned}&\phi_{ma}(t,t_0)x_{ma}(t_0) = \phi_a(t_0+t_f-t,t_f)x_a(t_f)\\ &\Rightarrow \left(\phi_{ma}(t,t_0) - \phi_a(t_0+t_f-t,t_f)\right)x_{ma}(t_0) = 0.\end{aligned}$$

As the above expression is true for arbitrary value of $x_{ma}(t_0)$, it follows that

$$\phi_{ma}(t,t_0) = \phi_a(t_0+t_f-t,t_f).$$

Using the above expression, the state transition matrix of the modified adjoint system for $t \geq \tau$ is given by,

$$\begin{aligned}\phi_{ma}(t,\tau) &= \phi_{ma}(t,t_0)\left(\phi_{ma}(\tau,t_0)\right)^{-1}\\ &= \phi_a(t_0+t_f-t,t_f)\left(\phi_a(t_0+t_f-\tau,t_f)\right)^{-1}\\ &= \phi_a(t_0+t_f-t,t_f)\phi_a(t_f,t_0+t_f-\tau)\\ &= \phi_a(t_0+t_f-t,t_0+t_f-\tau).\end{aligned}$$

The following result is obtained using (5.6) in the above expression.

$$\begin{aligned}\phi_{ma}(t,\tau) &= \left(\phi(t_0+t_f-t,t_0+t_f-\tau)\right)^{-T}\\ &= \left(\phi(t_0+t_f-\tau,t_0+t_f-t)\right)^{T}.\end{aligned}$$

□

5.3.2 Gramians of the modified adjoint of a continuous-time LTV system

In the previous subsection, the connection between the state transition matrices of the original LTV system and the modified adjoint of the system is established. This subsection explores the connection of the system gramians of the modified adjoint system Σ_{ma} and the original LTV system Σ.

Theorem 5.3.3. *For $t \in [t_0, t_f]$, the reachability gramian $P_{ma}(t,t_0)$ and the observability gramian $Q_{ma}(t_f,t)$ of the modified adjoint system Σ_{ma}, with state-space representation (5.5), is related to the observability gramian $Q(t_f,t)$ and reachability gramian $P(t,t_0)$ of the original system Σ, with state-space representation (2.72), as follows:*

$$P_{ma}(t,t_0) = Q(t_f,t_0+t_f-t) \quad \textit{and} \tag{5.11}$$

$$Q_{ma}(t_f,t) = P(t_0+t_f-t,t_0). \tag{5.12}$$

Proof. The reachability gramian of the modified adjoint system Σ_{ma} is given by

$$P_{ma}(t,t_0) = \int_{t_0}^{t} \phi_{ma}(t,\tau)B_{ma}(\tau)(B_{ma}(\tau))^T(\phi_{ma}(t,\tau))^T d\tau. \tag{5.13}$$

Replacing the state transition matrix of the modified adjoint system with the expression, obtained in (5.10), and replacing $B_{ma}(\tau)$ with $(C(t_0+t_f-\tau))^T$, the integrand of the integral in (5.13) can

be expressed as

$$\begin{aligned}&\phi_{ma}(t,\tau)B_{ma}(\tau)(B_{ma}(\tau))^T(\phi_{ma}(t,\tau))^T\\&=((\phi(t_0+t_f-\tau,t_0+t_f-t))^T\,(C(t_0+t_f-\tau))^T\,C(t_0+t_f-\tau)\phi(t_0+t_f-\tau,t_0+t_f-t).\end{aligned}$$

Replacing the above expression for the integrand in (5.13) and changing the variable of integration to $z = t_f + t_0 - \tau$ results in

$$\begin{aligned}P_{ma}(t,t_0)&=\int_{t_0+t_f-t}^{t_f}((\phi(z,t_0+t_f-t))^T\,(C(z))^T\,C(z)\phi(z,t_0+t_f-t)dz\\&=Q(t_f,t_0+t_f-t).\end{aligned}$$

The observability gramian of the modified adjoint system Σ_{ma} is given by,

$$Q_{ma}(t_f,t)=\int_t^{t_f}(\phi_{ma}(t,\tau))^T(C_{ma}(t))^TC_{ma}(t)\phi_{ma}(t,\tau)d\tau.$$

Similar to the first case, substituting the state transition matrix for the modified adjoint system given by (5.10) and replacing $C_{ma}(\tau)$ as $(B(t_0+t_f-\tau))^T$ gives the following result.

$$\begin{aligned}&Q_{ma}(t_f,t)\\&=\int_t^{t_f}(\phi_{ma}(\tau,t))^T(C_{ma}(\tau))^TC_{ma}(\tau)\phi_{ma}(\tau,t)d\tau\\&=\int_t^{t_f}\phi(t_0+t_f-t,t_0+t_f-\tau)B(t_0+t_f-\tau)(B(t_0+t_f-\tau))^T(\phi(t_0+t_f-t,t_0+t_f-\tau))^Td\tau\\&=\int_{t_0}^{t_0+t_f-t}\phi(t_0+t_f-t,z)B(z)(B(z))^T(\phi(t_0+t_f-t,z))^Tdz\\&=P(t_0+t_f-t,t_0).\end{aligned}$$

□

Corollary 5.3.4. *For the time interval $[t_0,t_f]$, the system gramians of the original LTV system Σ and its modified adjoint Σ_{ma} are related as*

$$P_{ma}(t_f,t_0)=Q(t_f,t_0)\quad \textit{and} \tag{5.14}$$

$$Q_{ma}(t_f,t_0)=P(t_f,t_0). \tag{5.15}$$

Proof. Substituting $t = t_f$ in equation (5.11) derived in Lemma 5.3.3, equation (5.14) is obtained. Similarly, substituting $t = t_0$ in equation (5.12) of the same lemma, equation (5.15) is obtained. □

5.3.3 Gramian computation using zero-input trajectories of the modified adjoint system

Various numerical methods exist in the literature for computing the observability gramian $Q(t_f,t_0)$. However, few methods exist for computing the reachability gramian $P(t_f,t_0)$. Using the equivalence between $P(t_f,t_0)$ and $Q_{ma}(t_f,t_0)$, established in Lemma 5.3.4, numerical techniques for computing the observability gramian can be used to calculate the reachability gramian. In Algorithm 10, the observability gramian computation method given in [46, 52] is used to compute the finite horizon reachability gramian of a continuous-time LTV system.

Algorithm 10: Computing $P(t_f, t_0)$ using modified-adjoint system

Input: System matrices $(A(t), B(t), C(t))$ belonging to an LTV system of order n;
Finite time horizon $[t_0, t_f]$;
Sampling period Δ;

Output: $P(t_f, t_0)$;

Procedure:

1. Obtain the modified adjoint of the original system for the finite time horizon $[t_0, t_f]$ as given by (5.5).
2. Divide $[t_0, t_f]$ into N intervals using the sampling period Δ, i.e., $\Delta = \frac{t_f - t_0}{N}$. The sampling instants are given by $t_k = (k-1)\Delta$ for $k = 1, \ldots, N$.
3. For the initial condition $x_{ma1}(t_0) = e_1$, input $u \equiv 0$ and sampling period Δ, the modified adjoint system is simulated, and the output is stored as $y_{ma1}(k)$, $k = 1, \ldots, N$.
4. The above step is repeated $(n-1)$ times for initial conditions $x_{ma2} = e_2$, …, $x_{man} = e_n$. For each simulation, the output is stored as $y_{ma2}(t_k)$, …, $y_{man}(t_k)$, $k = 1, 2, \ldots, N$.
5. The matrix $Y_{ma}(t_1)$ is constructed as follows:

$$Y_{ma}(t_1) = \left[y_{ma1}(t_1) \ldots y_{man}(t_1) \right]; \tag{5.16}$$

Similarly, matrices $Y_{ma}(t_2)$, …, $Y_{ma}(t_N)$ are constructed.

6. The gramian is calculated as follows:

$$P(t_f, t_0) = O_{ma}(t_f, t_0) = \sum_{k=1}^{N} \left(Y_{ma}(t_k) \right)^T Y_{ma}(t_k) \Delta; \tag{5.17}$$

Remark 9. The above method computes a finite horizon reachability gramian over $[t_0, t_f]$. For computing the gramian over a different interval $[t_{0_1}, t_{f_1}]$, the new modified adjoint of the original LTV system is initially constructed. The observability gramian of this new adjoint system gives the reachability gramian of the original system over $[t_{0_1}, t_{f_1}]$. This technique requires n (dimension) simulations of the original LTV system. Thus, it will be computationally expensive for large-scale systems with many states.

5.3.4 Numerical example

This subsection presents an example that numerically verifies the results obtained in the previous subsection, particularly Lemma 5.3.3 and Corollary 5.3.4.

Example 1

Consider the LTV system given by (5.2). The modified adjoint of the LTV system for the finite time horizon $[0, 5]$ s is given by

$$\frac{dx_{ma}(t)}{dt} = \begin{bmatrix} -1 + 0.5cos^2(5-t) & 1 - 0.5sin(5-t)cos(5-t) \\ -1 - 0.5sin(5-t)cos(5-t) & -1 + 0.5sin^2(5-t) \end{bmatrix} x_{ma}(t) + \begin{bmatrix} 1 \\ 1 \end{bmatrix} u_{ma}(t).$$

For a time interval $[0, 5]$ s and a sampling time $\Delta = 0.001$ s, the observability gramian $Q_{ma}(5, 0)$ computed using Algorithm 10 is as follows,

$$Q_{ma}(5,0) = \begin{bmatrix} 0.7939 & 0.3673 \\ 0.3673 & 0.5446 \end{bmatrix}.$$

The reachability gramian of the original LTV system is denoted as $P_1(5, 0)$. It is computed by solving the differential Lyapunov equation (2.83) and is given by (5.3). Comparing the gramians, it is seen that the observability gramian of the modified adjoint system $Q_{ma}(5, 0)$ equals the reachability gramian of the original LTV system $P_1(5, 0)$.

For the same interval $[0, 5]$ s and sampling time $\Delta = 0.001$ s, the reachability gramian of the original LTV system $P(3, 0)$, obtained by solving the differential Lyapunov equation (2.83) is given by

$$P(3,0) = \begin{bmatrix} 1.3080 & 0.2978 \\ 0.2978 & 0.2577 \end{bmatrix}.$$

Setting $t_0 = 2$, the observability gramian of the modified adjoint system given above is as follows,

$$Q_{ma}(5,2) = \begin{bmatrix} 1.3086 & 0.2983 \\ 0.2983 & 0.2522 \end{bmatrix}.$$

Comparing the gramians, it is observed that $Q_{ma}(5, 2) = P(5 - 2, 0) = P(3, 0)$.

5.4 A system norm for continuous-time LTV systems

For LTI systems, system norms such as H_2 and H_∞ norm are defined using the system transfer function - a frequency domain representation. Unlike LTI systems, the frequency domain representation for finite horizon LTV systems is not well established. Hence, a time-domain representation is used to generalise the notion of norms to such systems.

In the case of LTI systems with m inputs, a deterministic interpretation of the square of the H_2 norm is given in Section 4.3 of [108]. It is the sum of the squared L_2 norms of the impulse responses for m impulse inputs given by $u_i(t) = \delta(t)e_i$ for $i = 1, \ldots, m$. In this section, a system norm for finite horizon LTV systems, which is a generalization of the H_2 norm of the LTI system, is discussed. The norm is defined using the impulse response matrix of the LTV system, and a trace formula involving the reachability or the observability gramians is obtained.

5.4.1 A finite horizon H_2 system norm

For an admissible input $u(t)$, the output $y(t)$ of the LTV system given by (2.72) is,

$$y(t) = \int_{t_0}^{t} h(t, \tau)u(t)dt. \tag{5.18}$$

Taking norm and squaring both sides of (5.18) results in

$$\begin{aligned}
\|y(t)\|^2 &= \left\| \int_{t_0}^{t} h(t,\tau)u(\tau)d\tau \right\|^2 \\
&\leq \left(\int_{t_0}^{t} \|h(t,\tau)u(\tau)\| \, d\tau \right)^2 \\
&\leq \left(\int_{t_0}^{t} \|h(t,\tau)\|_F \, \|u(\tau)\| \, d\tau \right)^2 \qquad (5.19) \\
&\leq \left(\int_{t_0}^{t} \|h(t,\tau)\|_F^2 \, d\tau \right) \left(\int_{t_0}^{t} \|u(\tau)\|^2 \, d\tau \right) \qquad (5.20) \\
&\leq \left(\int_{t_0}^{t} \|h(t,\tau)\|_F^2 \, d\tau \right) \left(\int_{t_0}^{t_f} \|u(\tau)\|^2 \, d\tau \right), \qquad (5.21)
\end{aligned}$$

where (5.20) is obtained from (5.19) by applying Cauchy-Schwarz inequality. Integrating both sides of the inequality (5.21) over the time-interval $[t_0, t_f]$ and taking the positive square-roots gives

$$\begin{aligned}
&\left(\int_{t_0}^{t_f} \|y(t)\|^2 \, dt \right)^{\frac{1}{2}} \leq \left(\int_{t_0}^{t_f} \int_{t_0}^{t} \|h(t,\tau)\|_F^2 \, d\tau dt \right)^{\frac{1}{2}} \left(\int_{t_0}^{t_f} \|u(\tau)\|^2 \, d\tau \right)^{\frac{1}{2}} \\
&\Rightarrow \|y\|_{L_2^p[t_0,t_f]} \leq \left(\int_{t_0}^{t_f} \int_{t_0}^{t} \|h(t,\tau)\|_F^2 \, d\tau dt \right)^{\frac{1}{2}} \|u\|_{L_2^m[t_0,t_f]} . \qquad (5.22)
\end{aligned}$$

The term $\left(\int_{t_0}^{t_f} \int_{t_0}^{t} \|h(t,\tau)\|_F^2 \, d\tau dt \right)^{\frac{1}{2}}$ is referred to as the finite horizon H_2 norm of the LTV system. It is also denoted by $\|\Sigma\|_{H_2[t_0,t_f]}$. It is evident from (5.22) that when the LTV system Σ is viewed as an input-output operator, the system norm $\|\Sigma\|_{H_2[t_0,t_f]}$ is an upper bound of the induced norm from the input space $L_2^m[t_0,t_f]$ to the output space $L_2^p[t_0,t_f]$.

For LTI and LTP systems, the H_2 norm is related to the respective systems' controllability and observability gramians. The following proposition shows that the finite horizon H_2 norm can be expressed as a trace formula involving the system gramians.

Lemma 5.4.1. *The square of the finite horizon H_2 norm of the LTV system Σ, given by (2.72) can be expressed using the reachability gramian $P(t,t_0)$ as follows,*

$$\|\Sigma\|_{H_2[t_0,t_f]}^2 = \int_{t_0}^{t_f} Tr\left(C(t)P(t,t_0)C^T(t)\right) dt. \qquad (5.23)$$

The square of the norm can also be expressed using the observability gramian $Q(t_f,t)$ as follows,

$$\|\Sigma\|_{H_2[t_0,t_f]}^2 = \int_{t_0}^{t_f} Tr\left(B^T(t)Q(t_f,t)B(t)\right) dt. \qquad (5.24)$$

Proof. The square of the finite horizon H_2 norm, i.e. $\|\Sigma\|_{H_2[t_0,t_f]}^2$ can be simplified as follows,

$$\begin{aligned}
\|\Sigma\|_{H_2[t_0,t_f]}^2 &= \int_{t_0}^{t_f} \int_{t_0}^{t} \mathrm{Tr}\left(h(t,\tau)(h(t,\tau))^T\right) d\tau dt \\
&= \int_{t_0}^{t_f} \mathrm{Tr}\left(C(t) \left(\int_{t_0}^{t} \phi(t,\tau)B(\tau)(B(\tau))^T(\phi(t,\tau))^T d\tau \right) (C(t))^T \right) dt \\
&= \int_{t_0}^{t_f} \mathrm{Tr}\left(C(t)P(t,t_0)(C(t))^T\right) dt,
\end{aligned}$$

where the definition of $P(t,t_0)$ is given by (2.82).

The finite horizon H_2 norm expression involves double integration. Exchanging the order of integration of the variables t and τ results in

$$\begin{aligned}\|\Sigma\|^2_{H_2[t_0,t_f]} &= \int_{t_0}^{t_f}\int_{t_0}^{t} \mathrm{Tr}\left(h(t,\tau)(h(t,\tau))^T\right) d\tau dt d\tau dt \\ &= \int_{t_0}^{t_f}\int_{\tau}^{t_f} \mathrm{Tr}\left((h(t,\tau))^T h(t,\tau)\right) dt d\tau \\ &= \int_{t_0}^{t_f} \mathrm{Tr}\left(B^T(\tau)\left(\int_{\tau}^{t_f}(\phi(t,\tau))^T C^T(\tau)C(\tau)\phi(t,\tau)dt\right)B(\tau)\right) d\tau \\ &= \int_{t_0}^{t_f} \mathrm{Tr}\left(B^T(\tau)Q(t_f,\tau)B(\tau)\right) d\tau,\end{aligned}$$

where the definition of $Q(t_f,\tau)$ is given by (2.84). □

The finite horizon H_2 norm of the original system Σ and the modified adjoint system Σ_{ma} are the same. The following theorem proves this.

Theorem 5.4.2. *The LTV systems Σ and Σ_{ma} given by the state space representations (2.72) and (5.5), respectively, have the same finite horizon H_2 norm, i.e., $\|\Sigma\|_{H_2[t_0,t_f]} = \|\Sigma_{ma}\|_{H_2[t_0,t_f]}$.*

Proof. For the modified adjoint system Σ_{ma}, the input and the output matrices are $B_{ma}(t) = (C(t_0+t_f-t))^T$ and $C_{ma}(t) = (B(t_0+t_f-t))^T$, respectively. Using these expressions and the relation (5.11), the square of the finite horizon H_2 norm of the modified adjoint system can be simplified as follows,

$$\begin{aligned}\|\Sigma_{ma}\|^2_{H_2[t_0,t_f]} &= \int_{t_0}^{t_f} \mathrm{Tr}\left(C_{ma}(t)P_{ma}(t,t_0)(C_{ma}(t))^T\right) dt \\ &= \int_{t_0}^{t_f} \mathrm{Tr}\left((B(t_0+t_f-t))^T Q(t_f,t_0+t_f-t)B(t_0+t_f-t)\right) dt \\ &= \int_{t_0}^{t_f} \mathrm{Tr}\left((B(z))^T Q(t_f,z)B(z)\right) dz \\ &= \|\Sigma\|^2_{H_2[t_0,t_f]}. \end{aligned} \tag{5.25}$$

Taking the positive square root of (5.25), $\|\Sigma\|_{H_2[t_0,t_f]} = \|\Sigma_{ma}\|_{H_2[t_0,t_f]}$ is obtained. □

5.4.2 Numerical example

This subsection computes the finite horizon H_2 norm of an LTV system for a given time interval. Through this example, it is verified that the area under the graphs of $\mathrm{Tr}\left(C(t)P(t,t_0)(C(t))^T\right)$ and $\mathrm{Tr}\left((B(t))^T Q(t_f,t)B(t)\right)$ for the time interval $[t_0,t_f]$ are equal (as shown in Proposition 5.4.1).

Similar to the previous examples of this chapter, the LTV system given by (5.2) is considered. Assume a time interval of $[-0.5,1]$ s. The reachability gramian $P(t,-0.5)$ is computed by solving the differential Lyapunov equation given by (2.83). Further, the observability gramian $Q(1,t)$ is computed by solving the differential Lyapunov equation (2.85). The plots of $\mathrm{Tr}\left(C(t)P(t,-0.5)(C(t))^T\right)$ and $\mathrm{Tr}\left((B(t))^T Q(1,t)B(t)\right)$ for the time interval $[-0.5,1]$ s are displayed in Figure 5.1.

The area under the integrand involving the reachability gramian is

$$\int_{-0.5}^{1} \mathrm{Tr}\left(C(t)P(t,-0.5)(C(t))^T\right) dt = 1.1921. \tag{5.26}$$

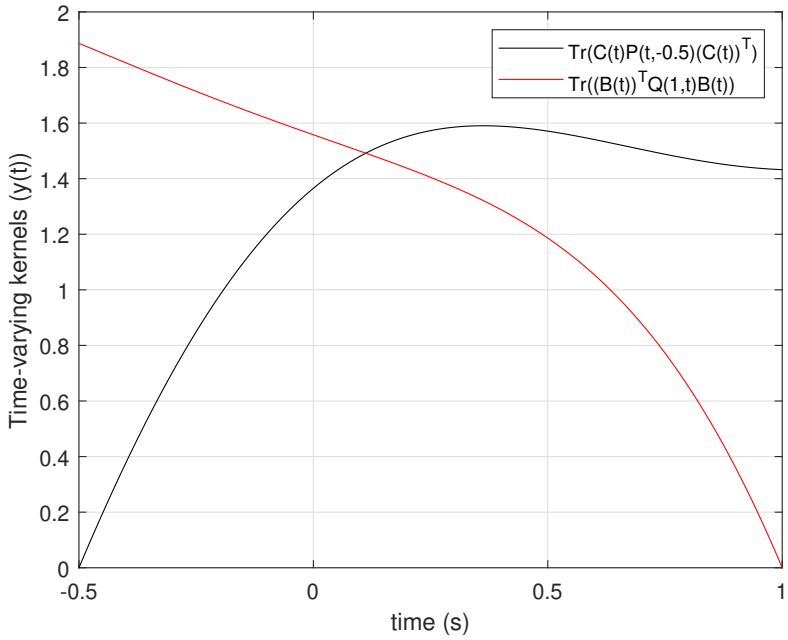

Figure 5.1: Plots of the integrands of the squared finite horizon H_2 norm, $\|\Sigma\|^2_{H_2[-0.5,1]}$

.

Similarly, the area under the integrand involving the observability gramian is

$$\int_{-0.5}^{1} \mathrm{Tr}\left((B(t))^T Q(1,t)B(t)\right) dt = 1.1921. \tag{5.27}$$

Comparing (5.26) and (5.27) results in

$$\int_{-0.5}^{1} \mathrm{Tr}\left(C(t)P(t,-0.5)(C(t))^T\right) dt = \int_{-0.5}^{1} \mathrm{Tr}\left((B(t))^T Q(1,t)B(t)\right) dt.$$

The $H_2[-0.5,1]$ norm of the LTV system is as follows

$$\begin{aligned}\|\Sigma\|_{H_2[-0.5,1]} &= \left(\int_{-0.5}^{1} \mathrm{Tr}\left(C(t)P(t,-0.5)(C(t))^T\right) dt\right)^{\frac{1}{2}} \\ &= \left(\int_{-0.5}^{1} \mathrm{Tr}\left((B(t))^T Q(1,t)B(t)\right) dt\right)^{\frac{1}{2}} \\ &= 1.3828.\end{aligned}$$

5.5 Summary

In this chapter, numerical methods for computing the finite horizon reachability gramian have been proposed, and a finite horizon system norm for a continuous-time LTV system has been discussed. Three methods for numerical computation of the gramian have been proposed. The first two methods use system trajectory information for recurring impulse and pulse inputs. The third method uses the modified adjoint of the original LTV system for computing the gramian. A finite horizon H_2 norm for continuous-time LTV systems has been discussed. A trace formula of the norm in terms of the reachability and the observability gramian has been obtained.

Chapter 6

Finite horizon MOR of LTV systems based on error norm minimization

MOR algorithms for LTI systems cannot be directly applied to LTV systems. The literature in the area of MOR of LTV systems is comparatively scarce. The BT algorithm for infinite horizon MOR of LTI systems is extended to the finite horizon MOR problem for LTI systems as TL-BT. It is further extended to both continuous as well as discrete-time LTV systems in [99, 91, 92]. Unlike BT and TL-BT, the $H_2(\tau)$ optimal model reduction problems considered in Chapter 3 and Chapter 4 are based on minimizing a well-defined error criterion. Such an error criterion-based finite horizon MOR scheme for discrete-time LTV systems is proposed in [60, 61]. Based on the LTV system norm discussed in Chapter 5, a similar error-criterion-based finite horizon model reduction problem for continuous-time LTV systems is proposed in this chapter.

The principal contribution of this chapter is an iterative algorithm for finite horizon model order reduction of continuous-time LTV systems. Firstly, it is shown that the finite horizon H_2 norm, proposed in the previous chapter, can be considered as a performance measure for the model order reduction of LTV systems. Next, closed-form expressions of the functional derivatives of the error norm with respect to the state-space parameters of the reduced-order systems are obtained. Using these expressions, conditions for optimality of the error norm are obtained. Finally, the optimality conditions are formulated as a projection problem and based on it, an iterative algorithm is proposed. The algorithm is validated with the help of two numerical examples.

The chapter is organised as follows. A finite horizon H_2 error norm for continuous-time LTV systems is introduced in Section 6.1. In Section 6.2, the functional derivatives are determined, conditions for optimality of the error norm with respect to the state-space matrices of the reduced-order LTV system are obtained, and several identities related to the optimality conditions are established. Based on the identities, Section 6.3 proposes a projection-based iterative algorithm for obtaining reduced-order systems which satisfy the optimality conditions. The performance of the proposed model reduction algorithm is verified with two numerical examples in Section 6.4.

The chapter is summarized in Section 6.5.

6.1 A finite horizon H_2 error norm

Consider the reduced-order LTV approximation Σ_r of the full-order LTV system Σ. Let Σ_r and Σ be given by (2.86) and (2.72), respectively. Let $\phi_r(t,\tau)$ be the state-transition matrix of the reduced-order system described by the map $\phi_r(\cdot,\cdot) : [t_0,t_f]\times[t_0,t_f] \to \mathbb{R}^{r\times r}$. The impulse response of Σ_r is given by $h_r(t,\tau) = C_r(t)\phi_r(t,\tau)B_r(\tau)$.

For the finite time horizon $[t_0,t_f]$, the modified adjoint of the reduced-order system Σ_r is given by,

$$\begin{aligned} \dot{x}_{rma}(t) &= A_{rma}(t)x_{rma}(t) + B_{rma}(t)u_{ma}(t), \\ y_{rma}(t) &= C_{rma}(t)x_{rma}(t), \end{aligned} \tag{6.1}$$

where $A_{rma}(t) = (A_r(t_0+t_f-t))^T$, $B_{rma}(t) = (C_r(t_0+t_f-t))^T$ and $C_{rma}(t) = (B_r(t_0+t_f-t))^T$. For $t \geq \tau$, let $\phi_{rma}(t,\tau)$ and $h_{rma}(t,\tau)$ be the state transition matrix and the impulse response matrix, respectively, of the modified adjoint system.

For a permissible input $u(t)$, the output $y(t)$ of the full-order system Σ is $y(t) = \int_{t_0}^{t} h(t,\tau)u(\tau)d\tau$ and the output $y_r(t)$ of the reduced-order system Σ_r is given by $y_r(t) = \int_{t_0}^{t} h_r(t,\tau)u(\tau)d\tau$. The norm of the error $e(t)$ between the two outputs is given by,

$$\begin{aligned} \|e(t)\|_2 &= \|y(t) - y_r(t)\|_2 \\ &= \left\| \int_{t_0}^{t} \left(h(t,\tau) - h_r(t,\tau)\right) u(\tau)d\tau \right\|_2 . \end{aligned}$$

Similar to the derivation of the inequality (5.22) in Subsection 5.4.1 of Chapter 5, the following inequality is obtained.

$$\|e\|_{L_2^p[t_0,t_f]} \leq \left(\int_{t_0}^{t_f} \int_{t_0}^{t} \|h(t,\tau) - h_r(t,\tau)\|_F^2 \, d\tau dt \right)^{\frac{1}{2}} \|u\|_{L_2^m[t_0,t_f]} . \tag{6.2}$$

From the above inequality, it is observed that minimizing $\left(\int_{t_0}^{t_f} \int_{t_0}^{t} \|h(t,\tau) - h_r(t,\tau)\|_F \, d\tau dt \right)^{\frac{1}{2}}$ ensures that $y_r(t)$ is a good approximation of $y(t)$ over the time-interval $[t_0,t_f]$. This error norm, denoted by $\|\Sigma - \Sigma_r\|_{H_2[t_0,t_f]}$, is referred to as the finite horizon H_2 error norm between the LTV systems Σ and Σ_r. This chapter uses the error norm to propose a model order reduction algorithm for continuous-time LTV systems.

Let $[t_0,t_f]$ be the time interval for analysing the systems Σ and Σ_r. Given initial time t_0, the reachability gramian of the reduced-order system at time-instant t, denoted by $P_r(t,t_0)$, is given by

$$P_r(t,t_0) = \int_{t_0}^{t} \phi_r(t,\tau)B_r(\tau)(B_r(\tau))^T(\phi_r(t,\tau))^T d\tau. \tag{6.3}$$

Further, given initial time t_0 and a time-instant t, the matrices $X(t,t_0)$, $X_{ma}(t,t_0)$ and $P_{rma}(t,t_0)$

are given by

$$X(t,t_0) = \int_{t_0}^{t} \phi(t,\tau)B(\tau)(B_r(\tau))^T(\phi_r(t,\tau))^T d\tau, \tag{6.4}$$

$$X_{ma}(t,t_0) = \int_{t_0}^{t} \phi_{ma}(t,\tau)B_{ma}(\tau)(B_{r,ma}(\tau))^T(\phi_{r,ma}(t,\tau))^T d\tau, \tag{6.5}$$

$$P_{rma}(t,t_0) = \int_{t_0}^{t} \phi_{rma}(t,\tau)B_{rma}(\tau)(B_{rma}(\tau))^T(\phi_{rma}(t,\tau))^T d\tau. \tag{6.6}$$

Note that $P_{rma}(t,t_0)$ is the reachability gramian of the reduced-order modified adjoint system Σ_{rma}.

Differentiating $P_r(t,t_0)$ with respect to t using Leibniz integral rule results in

$$\begin{aligned}
&\frac{d}{dt}P_r(t,t_0)\\
&= \frac{d}{dt}\int_{t_0}^{t} \phi_r(t,\tau)B_r(\tau)(B_r(\tau))^T(\phi_r(t,\tau))^T d\tau.\\
&= \phi_r(t,t)B_r(t)(B_r(t))^T(\phi_r(t,t))^T + \int_{t_0}^{t}\left(\frac{\partial}{\partial t}\phi_r(t,\tau)\right)B_r(\tau)(B_r(\tau))^T(\phi_r(t,\tau))^T d\tau +\\
&+ \int_{t_0}^{t} \phi_r(t,\tau)B_r(\tau)(B_r(\tau))^T\left(\frac{\partial}{\partial t}\phi_r(t,\tau)\right)^T d\tau
\end{aligned}$$

By using (2.77), the above expression simplifies to

$$\begin{aligned}
\frac{d}{dt}P_r(t,t_0) &= B_r(t)(B_r(t))^T + A(t)\int_{t_0}^{t} \phi_r(t,\tau)B_r(\tau)(B_r(\tau))^T(\phi_r(t,\tau))^T d\tau +\\
&+ \int_{t_0}^{t} \phi_r(t,\tau)B_r(\tau)(B_r(\tau))^T(\phi_r(t,\tau))^T d\tau(A(t))^T\\
&= A_r(t)P_r(t,t_0) + P_r(t,t_0)(A_r(t))^T + B_r(t)(B_r(t))^T.
\end{aligned} \tag{6.7}$$

Thus, $P_r(t,t_0)$ can be computed by solving the matrix differential equation (6.7) with initial condition $P_r(t_0,t_0) = 0_{r\times r}$.

Similarly, differentiating the matrices $X(t,t_0)$, $X_{ma}(t,t_0)$ and $P_{rma}(t,t_0)$ with respect to t by applying Leibniz integral rule and using (2.77), the following matrix differential equations are obtained.

$$\frac{d}{dt}X(t,t_0) = A(t)X(t,t_0) + X(t,t_0)(A_r(t))^T + B(t)(B_r(t))^T, \tag{6.8}$$

$$\frac{d}{dt}X_{ma}(t,t_0) = A_{ma}(t)X_{ma}(t,t_0) + X_{ma}(t,t_0)(A_{rma}(t))^T(t) + B_{ma}(t)(B_{rma}(t))^T, \tag{6.9}$$

$$\frac{d}{dt}P_{rma}(t,t_0) = A_{rma}(t)P_{rma}(t,t_0) + P_{rma}(t,t_0)(A_{rma}(t))^T + B_{rma}(t)(B_{rma}(t))^T. \tag{6.10}$$

Hence, $X(t,t_0)$, $X_{ma}(t,t_0)$ and $P_{rma}(t,t_0)$ are computed by solving the matrix differential equations (6.8), (6.9) and (6.10) with initial conditions $X(t_0,t_0) = 0_{n\times r}$, $X_{ma}(t_0,t_0) = 0_{n\times r}$ and $P_{rma} = 0_{r\times r}$, respectively.

Similarly, given final time t_f, the observability gramian of the system Σ_r at time-instant t, denoted by $Q_r(t_f,t)$, is given by

$$Q_r(t_f,t) = \int_{t}^{t_f} (\phi_r(\tau,t))^T(C_r(\tau))^T C_r(\tau)\phi_r(\tau,t)d\tau. \tag{6.11}$$

Additionally, given final time t_f and a time-instant t, the matrix $Y(t_f,t)$ is given by,

$$Y(t_f,t)=\int_t^{t_f}(\phi_r(\tau,t))^T(C_r(\tau))^TC(\tau)\phi(\tau,t)d\tau. \tag{6.12}$$

Differentiating the matrices $Y(t_f,t)$ and $Q_r(t_f,t)$ with respect to t using Leibniz integral rule and substituting $\frac{\partial}{\partial t}\phi(\tau,t)=-\phi(\tau,t)A(t)$, the following matrix differential equations are obtained.

$$-\frac{d}{dt}Y(t_f,t)=(A(t))^TY(t_f,t)+Y(t_f,t)A_r(t)+(C(t))^TC_r(t), \tag{6.13}$$

$$-\frac{d}{dt}Q_r(t_f,t)=(A_r(t))^TQ_r(t_f,t)+Q_r(t_f,t)A_r(t)+(C_r(t))^TC_r(t). \tag{6.14}$$

Thus, the matrices $Y(t_f,t)$ and $Q_r(t_f,t)$ can be computed by solving the matrix differential equations (6.13) and (6.14), respectively, with final conditions $Y(t_f,t_f)=0_{n\times r}$ and $Q_r(t_f,t_f)=0_{r\times r}$.

Lemma 6.1.1. *$P_{rma}(t,t_0)$ and $Q_r(t_f,t)$, given by (6.6) and (6.11), respectively, are related as,*

$$P_{rma}(t,t_0)=Q_r(t_f,t_0+t_f-t). \tag{6.15}$$

Similarly, $X_{ma}(t,t_0)$ and $Y(t_f,t)$, given by (6.5) and (6.12), respectively, are related as,

$$X_{ma}(t,t_0)=Y(t_f,t_0+t_f-t). \tag{6.16}$$

Proof. Substituting $\phi_{rma}(t,\tau)=(\phi_r(t_0+t_f-\tau,t_0+t_f-t))^T$ (using Proposition 5.3.2) and $B_{rma}(\tau)=(C_r(t_0+t_f-\tau))^T$ in (6.6) gives

$$\begin{aligned}&P_{rma}(t,t_0)\\&=\int_{t_0}^{t}\phi_{rma}(t,\tau)B_{rma}(\tau)(B_{rma}(\tau))^T(\phi_{rma}(t,\tau))^Td\tau\\&=\int_{t_0}^{t}(\phi_r(t_0+t_f-\tau,t_0+t_f-t))^T(C_r(t_0+t_f-\tau))^TC_r(t_0+t_f-\tau)\phi_r(t_0+t_f-\tau,t_0+t_f-t)d\tau\end{aligned}$$

Changing the variable of integration to $z=t_0+t_f-\tau$ results in

$$\begin{aligned}P_{rma}(t,t_0)&=\int_{t_0+t_f-t}^{t_f}(\phi_r(z,t_0+t_f-t))^T(C_r(z))^TC_r(z)\phi_r(z,t_0+t_f-t)dz\\&=Q_r(t_f,t_0+t_f-t).\end{aligned}$$

Similarly, substituting $\phi_{ma}(t,\tau)=(\phi(t_0+t_f-\tau,t_0+t_f-t))^T$, $\phi_{rma}(t,\tau)=(\phi_r(t_0+t_f-\tau,t_0+t_f-t))^T$, $B_{ma}(\tau)=(C(t_0+t_f-\tau))^T$ and $C_{rma}(\tau)=(B_r(t_0+t_f-\tau))^T$ in (6.5), results in the following

$$\begin{aligned}&X_{ma}(t,t_0)=\int_{t_0}^{t}\phi_{ma}(t,\tau)B_{ma}(\tau)(B_{rma}(\tau))^T(\phi_{rma}(t,\tau))^Td\tau\\&=\int_{t_0}^{t}(\phi(t_0+t_f-\tau,t_0+t_f-t))^T(C(t_0+t_f-\tau))^TC_r(t_0+t_f-\tau)\phi_r(t-0+t_f-\tau,t_0+t_f-t)d\tau.\end{aligned}$$

Changing the variable of integration to $z=t_0+t_f-\tau$ gives

$$\begin{aligned}X_{ma}(t,t_0)&=\int_{t_0+t_f-t}^{t_f}(\phi(z,t_0+t_f-t))^T(C(z))^TC_r(z)\phi_r(z,t_0+t_f-t)dz\\&=Y(t_f,t_0+t_f-t).\end{aligned}$$

□

Proposition 6.1.2. *The square of the finite horizon H_2 error norm is expressed using the reachability gramians of Σ and Σ_r as follows,*

$$\begin{aligned}&\|\Sigma-\Sigma_r\|^2_{H_2[t_0,t_f]}\\&=\int_{t_0}^{t_f} Tr\left(C(t)P(t,t_0)(C(t))^T-2C(t)X(t,t_0)(C_r(t))^T+C_r(t)P_r(t,t_0)(C_r(t))^T\right)dt.\end{aligned}\tag{6.17}$$

Similarly, the square of the finite horizon H_2 error norm is expressed using the observability gramians of Σ and Σ_r as follows,

$$\begin{aligned}&\|\Sigma-\Sigma_r\|^2_{H_2[t_0,t_f]}\\&=\int_{t_0}^{t_f} Tr((B(t))^TQ(t_f,t)B(t)-2(B(t))^TY(t_f,t)B_r(t)+(B_r(t))^TQ_r(t_f,t)B_r(t))dt.\end{aligned}\tag{6.18}$$

$$\begin{aligned}&=\int_{t_0}^{t_f} Tr(C_{ma}(t)P_{ma}(t,t_0)(C_{ma}(t))^T-2C_{ma}(t)X_{ma}(t,t_0)(C_{rma}(t))^T+\\&C_{rma}(t)P_{rma}(t,t_0)(C_{rma}(t))^T)dt.\end{aligned}\tag{6.19}$$

Proof. The error norm $\|\Sigma-\Sigma_r\|^2_{H_2[t_0,t_f]}$ involves doubles integration and can be expressed as follows,

$$\|\Sigma-\Sigma_r\|^2_{H_2[t_0,t_f]}=\int_{t_0}^{t_f}\int_{t_0}^{t}\|h(t,\tau)-h_r(t,\tau)\|_F^2\,d\tau dt\tag{6.20}$$

$$=\int_{t_0}^{t_f}\int_{\tau}^{t_f}\|h(t,\tau)-h_r(t,\tau)\|_F^2\,dtd\tau.\tag{6.21}$$

The integrand of the double integral in (6.20) can be expressed as,

$$\begin{aligned}&\|h(t,\tau)-h_r(t,\tau)\|_F^2\\&=\mathrm{Tr}\left((h(t,\tau)-h_r(t,\tau))\,(h(t,\tau)-h_r(t,\tau))^T\right)\\&=\mathrm{Tr}\left((C(t)\phi(t,\tau)B(\tau)-C_r(t)\phi_r(t,\tau)B_r(\tau))\,((B(\tau))^T(\phi(t,\tau))^T(C(t))^T-(B_r(\tau))^T(\phi_r(t,\tau))^T(C_r(t))^T)\right)\\&=\underbrace{\mathrm{Tr}\left(C(t)\phi(t,\tau)B(\tau)(B(\tau))^T(\phi(t,\tau))^T(C(t))^T\right)}_{\text{I}}-\underbrace{\mathrm{Tr}\left(C_r(t)\phi_r(t,\tau)B_r(\tau)(B(\tau))^T(\phi(t,\tau))^T(C(t))^T\right)}_{\text{II}}-\\&\underbrace{\mathrm{Tr}\left(C(t)\phi(t,\tau)B(\tau)(B_r(\tau))^T(\phi_r(t,\tau))^T(C_r(t))^T\right)}_{\text{III}}+\underbrace{\mathrm{Tr}\left(C_r(t)\phi_r(t,\tau)B_r(\tau)(B_r(\tau))^T(\phi_r(t,\tau))^T(C_r(t))^T\right)}_{\text{IV}}\end{aligned}\tag{6.22}$$

Letting $A=C(t)\phi(t,\tau)B(\tau)$ and $B=C_r(t)\phi_r(t,\tau)B_r(\tau)$ and using the property $\mathrm{Tr}(AB)=\mathrm{Tr}(BA)$, it follows that the terms (II) and (III) of (6.22) are equal. Applying the double integral $\int_{t_0}^{t_f}\int_{t_0}^{t}(\cdot)d\tau dt$ on term (I) of (6.22) and exchanging the position of the trace and the inner integral operator $\int_{t_0}^{t}(\cdot)d\tau$ results in

$$\begin{aligned}&\int_{t_0}^{t_f}\mathrm{Tr}\left(C(t)\left(\int_{t_0}^{t}\phi(t,\tau)B(\tau)(B(\tau))^T(\phi(t,\tau))^Td\tau\right)(C(t))^T\right)dt\\&=\int_{t_0}^{t_f}\mathrm{Tr}\left(C(t)P(t,t_0)(C(t))^T\right)dt.\end{aligned}\tag{6.23}$$

A similar operation on (II) of (6.22) gives,

$$\int_{t_0}^{t_f} \mathrm{Tr}\left(C(t)\left(\int_{t_0}^{t}\phi(t,\tau)B(\tau)(B_r(\tau))^T(\phi_r(t,\tau))^T d\tau\right)(C_r(t))^T\right)dt$$
$$= \int_{t_0}^{t_f} \mathrm{Tr}\left(C(t)X(t,t_0)(C_r(t))^T\right)dt. \tag{6.24}$$

Repeating the same steps on (IV) of (6.22) gives,

$$\int_{t_0}^{t_f} \mathrm{Tr}\left(C_r(t)\left(\int_{t_0}^{t}\phi_r(t,\tau)B_r(\tau)(B_r(\tau))^T(\phi_r(t,\tau))^T d\tau\right)(C_r(t))^T\right)dt$$
$$= \int_{t_0}^{t_f} \mathrm{Tr}\left(C_r(t)P_r(t,t_0)(C_r(t))^T\right)dt. \tag{6.25}$$

Adding (6.23), (6.24) and (6.25), (6.20) can be expressed as

$$\|\Sigma-\Sigma_r\|^2_{H_2[t_0,t_f]}$$
$$= \int_{t_0}^{t_f} \mathrm{Tr}\left(C(t)P(t,t_0)(C(t))^T - 2C(t)X(t,t_0)(C_r(t))^T + C_r(t)P_r(t,t_0)(C_r(t))^T\right)dt.$$

The integrand of the double integral in (6.21) can be written as,

$$\begin{aligned}
&\|h(t,\tau)-h_r(t,\tau)\|_F^2\\
&= \mathrm{Tr}\left((h(t,\tau)-h_r(t,\tau))^T(h(t,\tau)-h_r(t,\tau))\right)\\
&= \mathrm{Tr}\left(((B(\tau))^T(\phi(t,\tau))^T(C(t))^T-(B_r(\tau))^T(\phi_r(t,\tau))^T(C_r(t))^T)(C(t)\phi(t,\tau)B(\tau)-C_r(t)\phi_r(t,\tau)B_r(\tau))\right)\\
&= \underbrace{\mathrm{Tr}\left((B(\tau))^T(\phi(t,\tau))^T(C(t))^TC(t)\phi(t,\tau)B(\tau)\right)}_{\text{I}} - \underbrace{\mathrm{Tr}\left((B(\tau))^T(\phi(t,\tau))^T(C(t))^TC_r(t)\phi_r(t,\tau)B_r(\tau)\right)}_{\text{II}} -\\
&\underbrace{\mathrm{Tr}\left((B_r(\tau))^T(\phi_r(t,\tau))^T(C_r(t))^TC(t)\phi(t,\tau)B(\tau)\right)}_{\text{III}} + \underbrace{\mathrm{Tr}\left((B_r(\tau))^T(\phi_r(t,\tau))^T(C_r(t))^TC_r(t)\phi_r(t,\tau)B_r(\tau)\right)}_{\text{IV}}.
\end{aligned} \tag{6.26}$$

Similar to the previous case, the terms (II) and (III) of (6.26) are equal. Applying the double integral $\int_{t_0}^{t_f}\int_{\tau}^{t_f}(\cdot)dtd\tau$ on (I) of (6.26) and exchanging the position of the trace and the inner integral operator, $\int_{\tau}^{t_f}(\cdot)dt$, the term (I) of (6.26) becomes

$$\int_{t_0}^{t_f} \mathrm{Tr}\left((B(\tau))^T\left(\int_{\tau}^{t_f}(\phi(t,\tau))^T(C(t))^TC(t)\phi(t,\tau)dt\right)B(\tau)\right)d\tau$$
$$= \int_{t_0}^{t_f} \mathrm{Tr}\left((B(\tau))^TQ(t_f,\tau)B(\tau)\right)d\tau. \tag{6.27}$$

The same action on the term (II) of (6.26) gives,

$$\int_{t_0}^{t_f} \mathrm{Tr}\left((B(\tau))^T\left(\int_{\tau}^{t_f}(\phi(t,\tau))^T(C(t))^TC_r(t)\phi_r(t,\tau)dt\right)B_r(\tau)\right)d\tau$$
$$= \int_{t_0}^{t_f} \mathrm{Tr}\left((B(\tau))^TY(t_f,\tau)B_r(\tau)\right)d\tau. \tag{6.28}$$

Similar action on the term (IV) of (6.26) results in the following,

$$\int_{t_0}^{t_f} \mathrm{Tr}\left((B_r(\tau))^T\left(\int_{\tau}^{t_f}(\phi_r(t,\tau))^T(C_r(t))^TC_r(t)\phi_r(t,\tau)dt\right)B_r(\tau)\right)d\tau$$
$$= \int_{t_0}^{t_f} \mathrm{Tr}\left((B_r(\tau))^TQ_r(t_f,\tau)B_r(\tau)\right)d\tau. \tag{6.29}$$

Adding (6.27), (6.28) and (6.29), (6.21) can be denoted as

$$\|\Sigma - \Sigma_r\|^2_{H_2[t_0,t_f]}$$
$$= \int_{t_0}^{t_f} \mathrm{Tr}((B(t))^T Q(t_f,t)B(t) - 2(B(t))^T Y(t_f,t)B_r(t) + (B_r(t))^T Q_r(t_f,t)B_r(t))dt.$$

Changing the variable of integration to $z = t_0 + t_f - t$, the above equation becomes

$$\int_{t_0}^{t_f} \mathrm{Tr}\left((B(t_0+t_f-z))^T Q(t_f,t_0+t_f-z)B(t_0+t_f-z)\right)dz -$$
$$\int_{t_0}^{t_f} 2\mathrm{Tr}\left(B(t_0+t_f-z))^T Y(t_f,t_0+t_f-z)B_r(t_0+t_f-z)\right)dz +$$
$$\int_{t_0}^{t_f} \mathrm{Tr}\left(B_r(t_0+t_f-z))^T Q_r(t_f,t_0+t_f-z)B_r(t_0+t_f-z)\right)dz.$$

Substituting $C_{ma}(z) = (B(t_0+t_f-z))^T$ and $C_{rma}(z) = (B_r(t_0+t_f-z))^T$ in the above expression and using (5.11), (6.15) and (6.16) gives the following result.

$$\|\Sigma - \Sigma_r\|^2_{H_2[t_0,t_f]} = \int_{t_0}^{t_f} \mathrm{Tr}\left(C_{ma}(z)P_{ma}(z,t_0)\left(C_{ma}(z)\right)^T\right)dz +$$
$$\int_{t_0}^{t_f} 2\mathrm{Tr}\left(C_{ma}(z)X(z,t_0)\left(C_{rma}(z)\right)^T\right)dz + \int_{t_0}^{t_f} \mathrm{Tr}\left(C_{rma}(z)P_{rma}(z,t_0)\left(C_{rma}(z)\right)^T\right)dz.$$

□

6.2 Functional derivatives of the finite horizon H_2 error norm

In this section, the functional derivatives of the finite horizon H_2 error norm, defined in the previous section, are obtained with respect to the state-space matrices of the reduced-order system Σ_r. The effect of a perturbation in the state matrix on the state transition matrix of the reduced-order system is analysed in the following lemma.

Lemma 6.2.1. *Consider the reduced-order LTV system given by (2.86). Let the state matrix $A_r(t)$ be perturbed by a continuous mapping $\Delta A_r(t) : [t_0, t_f] \to \mathbb{R}^{r\times r}$. Let $(A_r(t) + \Delta A_r(t))$ be the state matrix and $\hat{\phi}_r(t,\tau)$ as the state transition matrix of the perturbed system. The perturbation in the state transition matrix induced by the perturbation in the state matrix is as follows*

$$\Delta\phi_r(t,t_0) = \hat{\phi}_r(t,t_0) - \phi_r(t,t_0) =$$
$$= \int_{t_0}^{t} \phi_r(t,\tau)\Delta A_r(\tau)\phi_r(\tau,t_0)d\tau + \int_{t_0}^{t}\int_{t_0}^{\tau} \phi_r(t,\tau)\Delta A_r(\tau)\phi_r(\tau,s)\Delta A_r(s)\hat{\phi}_r(s,t_0)ds\,d\tau. \quad (6.30)$$

Proof. For $u \equiv 0$, the LTV system Σ_r given by (2.86) becomes

$$\frac{dx_r(t)}{dt} = A_r(t)x_r(t).$$

The solution to the above differential equation for initial condition $x_r(t_0)$ is given by

$$x_r(t) = \phi_r(t,t_0)x_r(t_0). \quad (6.31)$$

Let $\hat{x}_r(t)$ be the state vector for the new state matrix $(A_r(t) + \Delta A_r(t))$. The new differential equation is as follows

$$\frac{d\hat{x}_r(t)}{dt} = (A_r(t) + \Delta A_r(t))\hat{x}_r(t).$$

Let $\hat{\phi}_r(t, s)$ be the state transition matrix for the new state matrix. For the same initial condition $x_r(t_0)$, the solution of the above differential equation is given by

$$\hat{x}_r(t) = \hat{\phi}_r(t, t_0)x_r(t_0). \tag{6.32}$$

Let $\Delta x_r(t) = \hat{x}_r(t) - x_r(t)$. Differentiating $\Delta x_r(t)$ with respect to t results in

$$\begin{aligned}\frac{d\Delta x_r(t)}{dt} &= \frac{d\hat{x}_r(t)}{dt} - \frac{dx_r(t)}{dt} \\ &= A(t)\Delta x_r(t) + \Delta A_r(t)\hat{x}_r(t).\end{aligned}$$

For $t = t_0$, $\Delta x_r(t_0) = \hat{x}_r(t_0) - x_r(t_0) = 0$. The solution of the above differential equation is given by,

$$\begin{aligned}\Delta x_r(t) &= \int_{t_0}^{t} \phi_r(t, \tau)\Delta A_r(\tau)\hat{x}_r(\tau)d\tau \\ &= \left(\int_{t_0}^{t} \phi_r(t, \tau)\Delta A_r(\tau)\hat{\phi}_r(\tau, t_0)d\tau\right) x_r(t_0).\end{aligned} \tag{6.33}$$

Subtracting (6.32) from (6.31), gives the following expression for $\Delta x_r(t)$,

$$\begin{aligned}\Delta x_r(t) &= \left(\hat{\phi}_r(t, t_0) - \phi_r(t, t_0)\right) x_r(t_0) \\ &= \Delta\phi_r(t, t_0)x_r(t_0).\end{aligned} \tag{6.34}$$

Comparing (6.33) and (6.34) results in the following

$$\Delta\phi_r(t, t_0)x_r(t_0) = \left(\int_{t_0}^{t} \phi_r(t, \tau)\Delta A_r(\tau)\hat{\phi}_r(\tau, t_0)d\tau\right) x_r(t_0).$$

Since the above expression is true for arbitrary $x_r(t_0)$,

$$\Delta\phi_r(t, t_0) = \int_{t_0}^{t} \phi_r(t, \tau)\Delta A_r(\tau)\hat{\phi}_r(\tau, t_0)d\tau \tag{6.35}$$

$$= \int_{t_0}^{t} \phi_r(t, \tau)\Delta A_r(\tau)\phi_r(\tau, t_0)d\tau + \int_{t_0}^{t} \phi_r(t, \tau)\Delta A_r(\tau)\Delta\phi_r(\tau, t_0)d\tau. \tag{6.36}$$

(6.35) yields $\Delta\phi_r(\tau, t_0) = \int_{t_0}^{\tau} \phi_r(\tau, s)\Delta A_r(s)\hat{\phi}_r(s, t_0)ds$. Using this expression in the second term on the right-hand side of (6.36) results in

$$\begin{aligned}&\int_{t_0}^{t} \phi_r(t, \tau)\Delta A_r(\tau)\Delta\phi_r(\tau, t_0)d\tau \\ &= \int_{t_0}^{t} \phi_r(t, \tau)\Delta A_r(\tau) \int_{t_0}^{\tau} \phi_r(\tau, s)\Delta A_r(s)\hat{\phi}_r(s, t_0)ds\, d\tau \\ &= \int_{t_0}^{t} \int_{t_0}^{\tau} \phi_r(t, \tau)\Delta A_r(\tau)\phi_r(\tau, s)\Delta A_r(s)\hat{\phi}_r(s, t_0)ds\, d\tau.\end{aligned}$$

Substituting the above expression in (6.36) gives the following result,

$$\Delta\phi_r(t, t_0) = \int_{t_0}^{t} \phi_r(t, \tau)\Delta A_r(\tau)\phi_r(\tau, t_0)d\tau + \int_{t_0}^{t} \int_{t_0}^{\tau} \phi_r(t, \tau)\Delta A_r(\tau)\phi_r(\tau, s)\Delta A_r(s)\hat{\phi}_r(s, t_0)ds\, d\tau.$$

□

Let $\Delta_1\phi_r(t,t_0)$ be the first-term in the right-hand side of equation (6.30). In the following corollary, it is proved that for LTI systems, $\Delta_1\phi_r(t,t_0)$ simplifies to the Fréchet derivative of the matrix exponential e^{A_rt} along the perturbation matrix ΔA_r, denoted by $L(e^{A_rt},\Delta A_r)$ (defined in Chapter 4).

Corollary 6.2.2. *If $A_r(t)=A_r$ and $\Delta A_r(t)=\Delta A_r$ $\forall t\in[t_0,t_f]$, then*

$$\Delta_1\phi_r(t,s)=L(e^{A_rt},\Delta A_r). \tag{6.37}$$

Proof. Under the given assumptions, the first-order perturbation in the state transition matrix due to transition in the state matrix becomes

$$\begin{aligned}
\Delta_1\phi_r(t,t_0) &= \int_{t_0}^{t}\phi_r(t,\tau)\Delta A_r(\tau)\phi_r(\tau,t_0)d\tau\\
&= \int_{t_0}^{t}e^{A_r(t-\tau)}\Delta A_r e^{A_r(\tau-t_0)}d\tau\\
&= \int_{0}^{t-t_0}e^{A_r(t-t_0-l)}\Delta A_r e^{A_rl}dl\\
&= \int_{0}^{t-t_0}e^{\left(A_r(t-t_0)\left(1-\frac{l}{t-t_0}\right)\right)}\Delta A_r(t-t_0)e^{A_r(t-t_0)\left(\frac{l}{t-t_0}\right)}\frac{dl}{t-t_0}\\
&= \int_{0}^{1}e^{A_rt(1-s)}\Delta A_r e^{A_rts}ds\\
&= L(e^{A_rt},\Delta A_r).
\end{aligned}$$

□

Lemma 6.2.1 plays a crucial role in the derivation of the functional derivatives of the error norm $\|\Sigma-\Sigma_r\|^2_{H_2[t_0,t_f]}$ with respect to the state-space matrices of the reduced-order system Σ_r. Let $M_i=\{f_i|f_i:[t_0,t_f]\to\mathbb{R}^{m_i\times n_i}$ is continuous and bounded$\}$ for $i=1,2,\ldots,k$. Consider F as $F:M_1\times M_2\times\ldots\times M_k\to\mathbb{R}$.

Definition 6.2.3 ([68], Appendix A)**.** The functional derivative of F with respect to $f_i\in M_i$ is a function given by $\frac{\partial F}{\partial f_i}:[t_0,t_f]\to\mathbb{R}^{m\times n}$ which satisfies

$$\begin{aligned}
\left\langle\frac{\partial F}{\partial f_i},\Delta f_i\right\rangle &= \int_{t_0}^{t_f}\mathrm{Tr}\left(\left(\frac{\partial F}{\partial f_i}(t)\right)^T\Delta f_i(t)\right)dt\\
&= \lim_{\epsilon\to0}\frac{F[f_i+\epsilon\Delta f_i]-F[f_i]}{\epsilon},
\end{aligned} \tag{6.38}$$

where ϵ is a scalar and $\Delta f_i:[t_0,t_f]\to\mathbb{R}^{m_i\times n_i}$ is an function in M_i.

Thus, given $\Delta f_i\in M_i$, the functional derivative of F with respect to f_i is the function for which the inner product between $\frac{\partial F}{\partial f_i}$ and Δf_i is the directional derivative of the functional F in the direction of Δf_i.

Theorem 6.2.4. *Consider $J[A_r,B_r,C_r]=\|\Sigma-\Sigma_r\|^2_{H_2[t_0,t_f]}$ where $A_r(t)$, $B_r(t)$ and $C_r(t)$ are given by (2.86). The functional derivatives of J with respect to $A_r(t)$, $B_r(t)$ and $C_r(t)$, respectively,*

are as follows:

$$\frac{\partial J}{\partial A_r}(t) = 2(Q_r(t_f,t)P_r(t,t_0) - (Y(t_f,t))^T X(t,t_0)), \tag{6.39}$$

$$\frac{\partial J}{\partial B_r}(t) = 2(Q_r(t_f,t)B_r(t) - (Y(t_f,t))^T B(t)) \quad \textit{and} \tag{6.40}$$

$$\frac{\partial J}{\partial C_r}(t) = 2(C_r(t)P_r(t,t_0) - C(t)X(t,t_0)). \tag{6.41}$$

Proof. The inner product between $\frac{\partial J}{\partial B_r}$ and an arbitrary matrix-valued perturbation $\Delta B_r : [t_0, t_f] \to \mathbb{R}^{r\times m}$ is as follows:

$$\begin{aligned}\left\langle \frac{\partial J}{\partial B_r}, \Delta B_r \right\rangle &= \int_{t_0}^{t_f} \mathrm{Tr}\left(\left(\frac{\partial J}{\partial B_r}(t) \right)^T \Delta B_r(t) \right) dt \\ &= \lim_{\epsilon \to 0+} \frac{1}{\epsilon} \left(J[A_r, B_r + \epsilon \Delta B_r, C_r] - J[A_r, B_r, C_r] \right).\end{aligned} \tag{6.42}$$

Considering the expression of J given by (6.18) results in the following

$$\begin{aligned}&J[A_r, B_r + \epsilon\Delta B_r, C_r] - J[A_r, B_r, C_r] \\ &= -2\epsilon \int_{t_0}^{t_f} \mathrm{Tr}\left(B^T(\tau) Y(t_f,\tau) \Delta B_r(\tau) \right) d\tau + \epsilon \int_{t_0}^{t_f} \mathrm{Tr}\left(\Delta B_r^T(\tau) Q_r(t_f,\tau) B_r(\tau) \right) d\tau + \\ &\epsilon \int_{t_0}^{t_f} \mathrm{Tr}\left(B_r^T(\tau) Q_r(t_f,\tau) \Delta B_r(\tau) \right) d\tau + \epsilon^2 \int_{t_0}^{t_f} \mathrm{Tr}\left(\Delta B_r^T(\tau) Q_r(t_f,\tau) \Delta B_r(\tau) \right) d\tau.\end{aligned}$$

Dividing the above expression by ϵ gives

$$\begin{aligned}&\lim_{\epsilon \to 0+} \frac{1}{\epsilon} \left(J[A_r, B_r + \epsilon\Delta B_r, C_r] - J[A_r, B_r, C_r] \right) \\ &= -2 \int_{t_0}^{t_f} \mathrm{Tr}\left(B^T(\tau) Y(t_f,\tau) \Delta B_r(\tau) \right) d\tau + \int_{t_0}^{t_f} \mathrm{Tr}\left(\Delta B_r^T(\tau) Q_r(t_f,\tau) B_r(\tau) \right) d\tau + \\ &\int_{t_0}^{t_f} \mathrm{Tr}\left(B_r^T(\tau) Q_r(t_f,\tau) \Delta B_r(\tau) \right) d\tau + \epsilon \int_{t_0}^{t_f} \mathrm{Tr}\left(\Delta B_r^T(\tau) Q_r(t_f,\tau) \Delta B_r(\tau) \right) d\tau.\end{aligned}$$

Taking the limit of the above expression as $\epsilon \to 0+$ and using the identity $Tr(A^T B) = Tr(B^T A)$ results in

$$\begin{aligned}&\lim_{\epsilon \to 0+} \frac{1}{\epsilon} \left(J[A_r, B_r + \epsilon\Delta B_r, C_r] - J[A_r, B_r, C_r] \right) \\ &= -2 \int_{t_0}^{t_f} \mathrm{Tr}\left(B^T(\tau) Y(t_f,\tau) \Delta B_r(\tau) \right) d\tau + 2 \int_{t_0}^{t_f} \mathrm{Tr}\left(B_r^T(\tau) Q_r(t_f,\tau) \Delta B_r(\tau) \right) d\tau \\ &= 2 \int_{t_0}^{t_f} \mathrm{Tr}\left(\left(Q_r(t_f,\tau) B_r(\tau) - (Y(t_f,\tau))^T B(\tau) \right)^T \Delta B_r(\tau) \right) d\tau \\ &= \langle 2 \left(Q_r(t_f,\tau) B_r(\tau) - (Y(t_f,\tau))^T B(\tau) \right), \Delta B_r(\tau) \rangle.\end{aligned}$$

Since ΔB_r is arbitrary, the following result is obtained when comparing the above expression with (6.42).

$$\frac{\partial J}{\partial B_r}(t) = 2 \left(Q_r(t_f,t) B_r(t) - (Y(t_f,t))^T B(t) \right).$$

The inner product between $\frac{\partial J}{\partial C_r}$ and an arbitrary matrix-valued perturbation $\Delta C_r : [t_0, t_f] \to$

$\mathbb{R}^{p\times r}$ is given by

$$\left\langle \frac{\partial J}{\partial C_r}, \Delta C_r \right\rangle = \int_{t_0}^{t_f} \mathrm{Tr}\left(\left(\frac{\partial J}{\partial C_r}(t) \right)^T \Delta C_r(t) \right) dt \tag{6.43}$$
$$= \lim_{\epsilon \to 0+} \frac{1}{\epsilon} \left(J[A_r, B_r, C_r + \epsilon \Delta C_r] - J[A_r, B_r, C_r] \right).$$

Using the expression of J given by (6.17) results in the following

$$\begin{aligned}
&J[A_r, B_r, C_r + \epsilon \Delta C_r] - J[A_r, B_r, C_r] \\
&= -2\epsilon \int_{t_0}^{t_f} \mathrm{Tr}\left(C(t) X(t, t_0) (\Delta C_r(t))^T \right) dt + \epsilon \int_{t_0}^{t_f} \mathrm{Tr}\left(\Delta C_r(t) P_r(t, t_0) (C_r(t))^T \right) dt + \\
&\epsilon \int_{t_0}^{t_f} \mathrm{Tr}\left(C_r(t) P_r(t, t_0) (\Delta C_r(t))^T \right) dt + \epsilon^2 \int_{t_0}^{t_f} \mathrm{Tr}\left(\Delta C_r(t) P_r(t, t_0) (\Delta C_r(t))^T \right) dt.
\end{aligned}$$

Dividing the above expression by ϵ, taking the limit as $\epsilon \to 0+$ and using the identity $\mathrm{Tr}(A^T B) = \mathrm{Tr}(B^T A)$ gives

$$\begin{aligned}
&\lim_{\epsilon \to 0+} \frac{1}{\epsilon} \left(J[A_r, B_r, C_r + \epsilon \Delta C_r] - J[A_r, B_r, C_r] \right) \\
&= -2 \int_{t_0}^{t_f} \mathrm{Tr}\left(C(t) X(t, t_0) (\Delta C_r(t))^T \right) dt + \int_{t_0}^{t_f} \mathrm{Tr}\left(\Delta C_r(t) P_r(t, t_0) (C_r(t))^T \right) dt + \\
&\int_{t_0}^{t_f} \mathrm{Tr}\left(C_r(t) P_r(t, t_0) (\Delta C_r(t))^T \right) dt. \\
&= 2 \int_{t_0}^{t_f} \mathrm{Tr}\left(\left(C_r(t) P_r(t, t_0) - C(t) X(t, t_0) \right) (\Delta C_r(t))^T \right) dt \\
&= 2 \int_{t_0}^{t_f} \mathrm{Tr}\left(\left(C_r(t) P_r(t, t_0) - C(t) X(t, t_0) \right)^T \Delta C_r(t) \right) dt.
\end{aligned}$$

Since ΔC_r is arbitrary, comparing the above expression with (6.43) results in

$$\frac{\partial J}{\partial C_r}(t) = 2(C_r(t) P_r(t, t_0) - C(t) X(t, t_0)).$$

The inner product between $\frac{\partial J}{\partial A_r}$ and an arbitrary matrix-valued perturbation $\Delta A_r : [t_0, t_f] \to \mathbb{R}^{r\times r}$ is given by

$$\left\langle \frac{\partial J}{\partial A_r}, \Delta A_r \right\rangle = \int_{t_0}^{t_f} \mathrm{Tr}\left(\left(\frac{\partial J}{\partial A_r}(t) \right)^T \Delta A_r(t) \right) dt \tag{6.44}$$
$$= \lim_{\epsilon \to 0+} \frac{1}{\epsilon} \left(J[A_r + \epsilon \Delta A_r, B_r, C_r] - J[A_r, B_r, C_r] \right).$$

Let $\hat{\phi}_r(t, \tau) = \phi_r(t, \tau) + \Delta\phi_r(t, \tau)$ be the state transition matrix corresponding to the perturbed state matrix $(A_r + \epsilon \Delta A_r)$. Equation (6.30) results in

$$\Delta\phi_r(t, t_0) = \epsilon \int_{t_0}^{t} \phi_r(t, \tau) \Delta A_r(\tau) \phi_r(\tau, t_0) d\tau + \epsilon^2 \phi\,. \tag{6.45}$$

where $\phi = \int_{t_0}^{t} \int_{t_0}^{\tau} \phi_r(t, \tau) \Delta A_r(\tau) \phi_r(\tau, s) \Delta A_r(s) \hat{\phi}_r(s, t_0) ds\, d\tau$. Using the expression of J given by (6.17) results in the following.

$$\begin{aligned}
&J[A_r + \epsilon \Delta A_r, B_r, C_r] - J[A_r, B_r, C_r] \\
&= \int_{t_0}^{t_f} \mathrm{Tr}\left(C_r(t) \Delta P_r(t, t_0) (C_r(t))^T \right) dt - 2 \int_{t_0}^{t_f} \mathrm{Tr}\left(C(t) \Delta X(t, t_0) (C_r(t))^T \right) dt,
\end{aligned} \tag{6.46}$$

where $\Delta P_r(t,t_0)$ and $\Delta X(t,t_0)$ are the perturbations in $P_r(t,t_0)$ and $X(t,t_0)$, respectively, due to the perturbation of the state matrix $A_r(t)$. Using the integral form of $P_r(t,t_0)$ given by (6.3), the first term on the right-hand side of the expression (6.46) can be simplified as follows,

$$\begin{aligned}
&\int_{t_0}^{t_f} \mathrm{Tr}\left(C_r(t)\int_{t_0}^{t}\Delta\phi_r(t,\tau)B_r(\tau)(B_r(\tau))^T(\phi_r(t,\tau))^T d\tau (C_r(t))^T\right)dt+\\
&\int_{t_0}^{t_f} \mathrm{Tr}\left(C_r(t)\int_{t_0}^{t}\phi_r(t,\tau)B_r(\tau)(B_r(\tau))^T(\Delta\phi_r(t,\tau))^T d\tau (C_r(t))^T\right)dt+\\
&\int_{t_0}^{t_f} \mathrm{Tr}\left(C_r(t)\int_{t_0}^{t}\Delta\phi_r(t,\tau)B_r(\tau)(B_r(\tau))^T(\Delta\phi_r(t,\tau))^T d\tau (C_r(t))^T\right)dt\\
&=2\int_{t_0}^{t_f} \mathrm{Tr}\left(C_r(t)\int_{t_0}^{t}\Delta\phi_r(t,\tau)B_r(\tau)(B_r(\tau))^T(\phi_r(t,\tau))^T d\tau (C_r(t))^T\right)dt+\\
&\int_{t_0}^{t_f} \mathrm{Tr}\left(C_r(t)\int_{t_0}^{t}\Delta\phi_r(t,\tau)B_r(\tau)(B_r(\tau))^T(\Delta\phi_r(t,\tau))^T d\tau (C_r(t))^T\right)dt.
\end{aligned}$$

Substituting $\Delta\phi_r(t,\tau)$ from (6.45) in the above expression results in

$$2\epsilon\int_{t_0}^{t_f} \mathrm{Tr}\left((C_r(t))^TC_r(t)\int_{t_0}^{t}\int_{\tau}^{t}\phi_r(t,s)\Delta A_r(s)\phi_r(s,\tau)B_r(\tau)(B_r(\tau))^T(\phi_r(t,\tau))^T ds\, d\tau\right)dt+\mathrm{Tr}(\Psi), \tag{6.47}$$

where $\mathrm{Tr}(\Psi)=\mathcal{O}(\epsilon^2)$.

Consider the first term of the expression (6.47). Exchanging the order of integration of the variables s and τ results in

$$\begin{aligned}
&2\epsilon\int_{t_0}^{t_f} \mathrm{Tr}\left((C_r(t))^TC_r(t)\int_{t_0}^{t}\int_{t_0}^{s}\phi_r(t,s)\Delta A_r(s)\phi_r(s,\tau)B_r(\tau)(B_r(\tau))^T(\phi_r(s,\tau))^T(\phi_r(t,s))^T d\tau\, ds\right)dt\\
&=2\epsilon\mathrm{Tr}\int_{t_0}^{t_f}\int_{t_0}^{t}(\phi_r(t,s))^T(C_r(t))^TC_r(t)\phi_r(t,s)\Delta A_r(s)\int_{t_0}^{s}\phi_r(s,\tau)B_r(\tau)(B_r(\tau))^T(\phi_r(s,\tau))^T d\tau\, ds\, dt\\
&=2\epsilon\mathrm{Tr}\int_{t_0}^{t_f}\int_{t_0}^{t}(\phi_r(t,s))^T(C_r(t))^TC_r(t)\phi_r(t,s)\Delta A_r(s)P_r(s,t_0)ds\, dt.
\end{aligned}$$

Further, exchanging the order of integration of the variables t and s in the above expression yields

$$\begin{aligned}
&2\epsilon\mathrm{Tr}\int_{t_0}^{t_f}\int_{s}^{t_f}(\phi_r(t,s))^T(C_r(t))^TC_r(t)\phi_r(t,s)\Delta A_r(s)P_r(s,t_0)dt\, ds\\
&=2\epsilon\mathrm{Tr}\int_{t_0}^{t_f}P_r(s,t_0)\left(\int_{s}^{t_f}(\phi_r(t,s))^T(C_r(t))^TC_r(t)\phi_r(t,s)dt\right)\Delta A_r(s)ds\\
&=2\epsilon\mathrm{Tr}\int_{t_0}^{t_f}P_r(s,t_0)Q_r(t_f,s)\Delta A_r(s)ds\\
&=2\epsilon\int_{t_0}^{t_f}\mathrm{Tr}\left((Q_r(t_f,s)P_r(s,t_0))^T\Delta A_r(s)\right)ds.
\end{aligned}$$

The expression (6.47) can be simplified as

$$2\epsilon\int_{t_0}^{t_f}\mathrm{Tr}\left((Q_r(t_f,s)P_r(s,t_0))^T\Delta A_r(s)\right)ds+\mathrm{Tr}\Psi. \tag{6.48}$$

Similarly, using the integral form of $X(t,t_0)$ and substituting $\Delta\phi_r(t,\tau)$ from (6.45), the second

term on the right-hand side of the equation (6.46) can be simplified as,

$$
\begin{aligned}
&2\int_{t_0}^{t_f} \mathrm{Tr}\left(C(t)\int_{t_0}^{t}\phi(t,\tau)B(\tau)(B_r(\tau))^T(\Delta\phi_r(t,\tau))^T d\tau (C_r(t))^T\right)dt \\
&= 2\epsilon \mathrm{Tr}\int_{t_0}^{t_f}(C_r(t))^T C(t)\int_{t_0}^{t}\phi(t,\tau)B(\tau)(B_r(\tau))^T\int_{\tau}^{t}(\phi_r(s,\tau))^T(\Delta A_r(s))^T(\phi_r(t,s))^T ds\, d\tau\, dt + \mathrm{Tr}(\eta) \\
&= 2\epsilon \mathrm{Tr}\int_{t_0}^{t_f}(C_r(t))^T C(t)\int_{t_0}^{t}\int_{\tau}^{t}\phi(t,s)\phi(s,\tau)B(\tau)(B_r(\tau))^T(\phi_r(s,\tau))^T(\Delta A_r(s))^T(\phi_r(t,s))^T ds\, d\tau\, dt \\
&+ \mathrm{Tr}(\eta), \qquad (6.49)
\end{aligned}
$$

where $\mathrm{Tr}(\eta) = \mathcal{O}(\epsilon^2)$. For the first term of the above expression, exchanging the order of integration of s and τ results in

$$
\begin{aligned}
&2\epsilon \mathrm{Tr}\int_{t_0}^{t_f}(C_r(t))^T C(t)\int_{t_0}^{t}\phi(t,s)\int_{t_0}^{s}\phi(s,\tau)B(\tau)(B_r(\tau))^T(\phi_r(s,\tau))^T d\tau(\Delta A_r(s))^T(\phi_r(t,s))^T ds\, dt \\
&= 2\epsilon \mathrm{Tr}\int_{t_0}^{t_f}\int_{t_0}^{t}(\phi_r(t,s))^T(C_r(t))^T C(t)\phi(t,s)X(s,t_0)(\Delta A_r(s))^T ds\, dt
\end{aligned}
$$

Additionally, changing the order of integration of s and t gives

$$
\begin{aligned}
&2\epsilon \mathrm{Tr}\int_{t_0}^{t_f}\int_{s}^{t_f}(\phi_r(t,s))^T(C_r(t))^T C(t)\phi(t,s)dt X(s,t_0)(\Delta A_r(s))^T ds \\
&= 2\epsilon \mathrm{Tr}\int_{t_0}^{t_f} Y(t_f,s)X(s,t_0)(\Delta A_r(s))^T ds \\
&= 2\epsilon \mathrm{Tr}\int_{t_0}^{t_f}\left(Y(t_f,s)X(s,t_0)\right)^T \Delta A_r(s) ds.
\end{aligned}
$$

Thus, the expression (6.49) simplifies to

$$
2\epsilon \mathrm{Tr}\int_{t_0}^{t_f}\left(Y(t_f,s)X(s,t_0)\right)^T \Delta A_r(s) ds + \mathrm{Tr}(\eta). \qquad (6.50)
$$

Substituting (6.48) and (6.50) in (6.46) results in

$$
\begin{aligned}
&J[A_r+\epsilon\Delta A_r, B_r, C_r] - J[A_r, B_r, C_r] \\
&= 2\epsilon\int_{t_0}^{t_f}\mathrm{Tr}\left(\left(Q_r(t_f,s)P_r(s,t_0) - Y(t_f,s)X(s,t_0)\right)^T\Delta A_r(s)\right)ds + \mathrm{Tr}(\Psi-\eta),
\end{aligned}
$$

where $\mathrm{Tr}(\Psi-\eta) = \mathcal{O}(\epsilon^2)$. Dividing the above expression by ϵ and taking limit as $\epsilon \to 0$ yields

$$
\begin{aligned}
&\lim_{\epsilon\to 0+}\frac{1}{\epsilon}\left(J[A_r+\epsilon\Delta A_r, B_r, C_r] - J[A_r, B_r, C_r]\right) \\
&= 2\int_{t_0}^{t_f}\mathrm{Tr}\left(\left(Q_r(t_f,s)P_r(s,t_0) - Y(t_f,s)X(s,t_0)\right)^T\Delta A_r(s)\right)ds.
\end{aligned}
$$

As $\Delta A_r(t)$ is arbitrary, comparing the above expression with (6.44), the following result is obtained.

$$
\frac{\partial J}{\partial A_r}(t) = 2(Q_r(t_f,t)P_r(t,t_0) - (Y(t_f,t))^T X(t,t_0)).
$$

□

The functional derivatives of the error norm obtained above are used in the following theorem.

Theorem 6.2.5. *Let the continuous time-varying matrices $\overline{A_r}(t)$, $\overline{B_r}(t)$ and $\overline{C_r}(t)$ be a stationary point of the functional $J[A_r, B_r, C_r]$. For $A_r(t) = \overline{A_r}(t)$, $B_r(t) = \overline{B_r}(t)$ and $C_r(t) = \overline{C_r}(t)$, let $\overline{P_r}(t, t_0)$, $\overline{Q_r}(t_f, t)$, $\overline{X}(t, t_0)$ and $\overline{Y}(t_f, t)$ be the solutions of the matrix differential equations (6.7), (6.14), (6.8) and (6.13), respectively. If $\overline{P_r}(t, t_0)$ and $\overline{Q_r}(t_f, t)$ are invertible at every instant $t \in [t_0, t_f]$, then*

$$\overline{A_r}(t) = (W_r(t))^T \left(A(t)V_r(t) - \frac{dV_r(t)}{dt} \right), \quad \text{or} \tag{6.51}$$

$$= \left((W_r(t))^T A(t) + \frac{d}{dt}(W_r(t))^T \right) V_r(t), \tag{6.52}$$

$$\overline{B_r}(t) = (W_r(t))^T B(t), \quad \textit{and} \tag{6.53}$$

$$\overline{C_r}(t) = C(t)V_r(t), \tag{6.54}$$

where $(W_r(t))^T V_r(t) = I_r$ with $W_r(t) = \overline{Y}(t_f, t) \left(\overline{Q_r}(t_f, t)\right)^{-1}$ and $V_r(t) = \overline{X}(t, t_0) \left(\overline{P_r}(t, t_0)\right)^{-1}$.

Proof. Let $(\overline{A_r}(t), \overline{B_r}(t), \overline{C_r}(t))$ be a stationary point of the functional $J[A_r, B_r, C_r]$. Let $\overline{\frac{\partial J}{\partial A_r}}(t) = \frac{\partial J}{\partial A_r}\Big|_{(\overline{A_r}(t), \overline{B_r}(t), \overline{C_r}(t))}$, $\overline{\frac{\partial J}{\partial B_r}}(t) = \frac{\partial J}{\partial B_r}\Big|_{(\overline{A_r}(t), \overline{B_r}(t), \overline{C_r}(t))}$ and $\overline{\frac{\partial J}{\partial C_r}}(t) = \frac{\partial J}{\partial C_r}\Big|_{(\overline{A_r}(t), \overline{B_r}(t), \overline{C_r}(t))}$. For arbitrary $\Delta A_r(t)$, $\Delta B_r(t)$ and $\Delta C_r(t)$ with appropriate dimensions, continuous over $[t_0, t_f]$, the following relations hold.

$$\left\langle \overline{\frac{\partial J}{\partial A_r}}, \Delta A_r \right\rangle = \left\langle \overline{\frac{\partial J}{\partial B_r}}, \Delta B_r \right\rangle = \left\langle \overline{\frac{\partial J}{\partial C_r}}, \Delta C_r \right\rangle = 0$$

As $\overline{\frac{\partial J}{\partial A_r}}(t)$, $\overline{\frac{\partial J}{\partial B_r}}(t)$ and $\overline{\frac{\partial J}{\partial C_r}}(t)$ are continuous in $[t_0, t_f]$, the following results is obtained.

$$\overline{\frac{\partial J}{\partial A_r}}(t) = \overline{Q_r}(t_f, t)\overline{P}_r(t, t_0) - (\overline{Y}(t_f, t))^T \overline{X}(t, t_0) = 0 \tag{6.55}$$

$$\overline{\frac{\partial J}{\partial B_r}}(t) = \overline{Q_r}(t_f, t)\overline{B_r}(t) - (\overline{Y}(t_f, t))^T B(t) = 0 \tag{6.56}$$

$$\overline{\frac{\partial J}{\partial C_r}}(t) = \overline{C_r}(t)\overline{P_r}(t, t_0) - C(t)\overline{X}(t, t_0) = 0. \tag{6.57}$$

(6.56) and (6.57) gives

$$\begin{aligned}
\overline{B_r}(t) &= \left(\overline{Q_r}(t_f, t)\right)^{-1} \left(\overline{Y}(t_f, t)\right)^T B(t) \\
&= \left(\overline{Y}(t_f, t) \left(\overline{Q_r}(t_f, t)\right)^{-1}\right)^T B(t), \quad \text{and} \\
&= (W_r(t))^T B(t) \quad \text{and} \\
\overline{C_r}(t) &= C(t)\overline{X}(t, t_0) \left(\overline{P_r}(t, t_0)\right)^{-1} = C(t)V_r(t),
\end{aligned}$$

where $W_r(t) = \overline{Y}(t_f, t) \left(\overline{Q_r}(t_f, t)\right)^{-1}$ and $V_r(t) = \overline{X}(t, t_0) \left(\overline{P_r}(t, t_0)\right)^{-1}$. The following result is obtained using (6.55).

$$\begin{aligned}
(W_r(t))^T V_r(t) &= \left(\overline{Q_r}(t_f, t)\right)^{-1} \left(\left(\overline{Y}(t_f, t)\right)^T \overline{X}(t, t_0) \right) \left(\overline{P_r}(t, t_0)\right)^{-1} \\
&= \left(\overline{Q_r}(t_f, t)\right)^{-1} \left(\overline{Q_r}(t_f, t)\overline{P_r}(t, t_0)\right) \left(\overline{P_r}(t, t_0)\right)^{-1} \\
&= I_r.
\end{aligned} \tag{6.58}$$

Left multiplying (6.8) by $(W(t))^T$, substituting $\overline{X}(t,t_0) = V_r(t)\overline{P_r}(t,t_0)$ and using (6.58) gives

$$(W_r(t))^T \frac{d}{dt}\left(V_r(t)\overline{P_r}(t,t_0)\right) = (W_r(t))^T A(t)V_r(t)\overline{P_r}(t,t_0) + (W_r(t))^T V_r(t)\overline{P_r}(t,t_0)(\overline{A_r}(t))^T + (W_r(t))^T B(t)(\overline{B_r}(t))^T$$

$$\Rightarrow (W_r(t))^T V_r(t)\frac{d}{dt}\overline{P_r}(t,t_0) + (W_r(t))^T \left(\frac{d}{dt}V_r(t)\right)\overline{P_r}(t,t_0) = (W_r(t))^T A(t)V_r(t)\overline{P_r}(t,t_0) + \overline{P_r}(t,t_0)(\overline{A_r}(t))^T + \overline{B_r}(t)(\overline{B_r}(t))^T$$

$$\Rightarrow \frac{d}{dt}\overline{P_r}(t,t_0) = \left((W_r(t))^T A(t)V_r(t) - W_r(t))^T \frac{d}{dt}V_r(t)\right)\overline{P_r}(t,t_0) + \overline{P_r}(t,t_0)(\overline{A_r}(t))^T + \overline{B_r}(t)(\overline{B_r}(t))^T.$$

Comparing the above matrix differential equation with (6.7) results in

$$\overline{A_r}(t) = \left(W_r(t))^T A(t)V_r(t) - W_r(t)\right)^T \frac{d}{dt}V_r(t).$$

Similarly, taking transpose of (6.13), right multiplying it by $V(t)$, substituting $\overline{Y}(t_f,t) = W_r(t)\overline{Q_r}(t_f,t)$, and using (6.58) gives

$$-\frac{d}{dt}(\overline{Q_r}(t_f,t))^T = (\overline{Q_r}(t_f,t))^T \left((W_r(t))^T A(t) + \frac{d}{dt}(W_r(t))^T\right)V(t) + (\overline{A_r}(t))^T(\overline{Q_r}(t_f,t))^T + (\overline{C_r}(t))^T\overline{C_r}(t).$$

The following result is obtained by comparing the above matrix differential equation with (6.14).

$$\overline{A_r}(t) = \left((W_r(t))^T A(t) + \frac{d}{dt}(W_r(t))^T\right)V(t).$$

□

Remark 10. The conditions (6.55)-(6.57) are first-order necessary conditions for optimality of the finite horizon H_2 error norm $J = \|\Sigma - \Sigma_r\|^2_{H_2[t_0,t_f]}$. As the conditions are expressed using a gramian framework, they can be considered as the LTV generalization of the Lyapunov-based H_2 optimality conditions for continuous-time LTI systems, given by (2.39)-(2.41) in Corollary 2.4.4.

6.3 A projection-based iterative algorithm

Consider the equations (6.3), (6.4), (6.11), (6.12) and (6.51),(6.53), (6.54). They can be interpreted as two coupled equations, $(X,Y,P_r,Q_r) = f(A_r,B_r,C_r)$ and $(A_r,B_r,C_r) = g(X,Y,P_r,Q_r)$. Thus, if (A_r,B_r,C_r) is a stationary point of $J[A_r,B_r,C_r]$, then it is also a fixed point as $g(f(A_r,B_r,C_r)) = (A_r,B_r,C_r)$. This motivates the following iterative procedure: $(X,Y,P_r,Q_r)_{k+1} = f(A_r,B_r,C_r)_{k+1}$ and $(A_r,B_r,C_r)_{k+1} = g(X,Y,P_r,Q_r)_k$. If the starting (initial) point of the iterative procedure is near to a fixed point, then it is supposed to converge to the fixed point.

Based on the above idea, a fixed-point iterative scheme for continuous-time LTV systems is proposed in Algorithm 11. An appropriate initial point is critical for the convergence of the iterative scheme. Hence, instead of random initialization, a reduced-order LTV model of order r, obtained by FH BT, is used to initialize the algorithm.

Let (A_r^1, B_r^1, C_r^1) be the initial reduced-order LTV model of order r. Let ${\frac{\partial J}{\partial A_r}}^1$, ${\frac{\partial J}{\partial B_r}}^1$ and ${\frac{\partial J}{\partial C_r}}^1$ be the functional derivatives with respect to (A_r^1, B_r^1, C_r^1). Also, let $J_{A_r}^1 := \max_{t\in[t_0,t_f]} \left\| {\frac{\partial J}{\partial A_r}}^1 \right\|_2$, $J_{B_r}^1 := \max_{t\in[t_0,t_f]} \left\| {\frac{\partial J}{\partial B_r}}^1 \right\|_2$ and $J_{C_r}^1 := \max_{t\in[t_0,t_f]} \left\| {\frac{\partial J}{\partial C_r}}^1 \right\|_2$. As the reduced-order model obtained by the FH BT algorithm is not optimal, $J_{A_r}^1$, $J_{B_r}^1$ and $J_{C_r}^1$ are non-zero. The following quantities are computed for every iteration of Algorithm 11.

$$\text{DerAr} := \left(\max_{t\in[t_0,t_f]} \left\| \frac{\partial J}{\partial A_r}(t) \right\|_2 \right) / J_{A_r}^1, \tag{6.59}$$

$$\text{DerBr} := \left(\max_{t\in[t_0,t_f]} \left\| \frac{\partial J}{\partial B_r}(t) \right\|_2 \right) / J_{B_r}^1, \text{and} \tag{6.60}$$

$$\text{DerCr} := \left(\max_{t\in[t_0,t_f]} \left\| \frac{\partial J}{\partial C_r}(t) \right\|_2 \right) / J_{C_r}^1 \tag{6.61}$$

In the above terms, normalization by $J_{A_r}^1$, $J_{B_r}^1$ and $J_{C_r}^1$ ensures the ease of comparing them for subsequent iterations.

Algorithm 11: Finite horizon TSIA (FH TSIA) for LTV systems

Input: $A(t), B(t), C(t)$; A finite time-interval $[t_0, t_f]$; Order of the reduced-order model (r); Initial $A_r^0(t), B_r^0(t), C_r^0(t)$, obtained by FH-BT over $[t_0, t_f]$;

Output: $A_r(t), B_r(t), C_r(t)$;

while *(not converged*)* **do**

1. Compute $X(t, t_0)$, $P_r(t, t_0)$, $Y(t_f, t)$ and $Q_r(t_f, t)$ by solving the matrix differential equations (6.8), (6.7), (6.13) and (6.14) for updated values of $A_r(t)$, $B_r(t)$ and $C_r(t)$;
2. Compute DerAr, DerBr, and DerCr as defined by (6.59), (6.60) and (6.61), respectively;
3. Compute the projection matrices: $V_r(t) = X(t, t_0)(P_r(t, t_0))^{-1}$ and $W_r(t) = Y(t_f, t)\,(Q_r(t_f, t))^{-1}$;
4. Update the reduced-order matrices using Equations (6.51), (6.53) and (6.54);

end

∗(The meaning of the term 'not converged' is explained in Remark 11.)

Remark 11. Similar to the TL-TSIA algorithm for LTI systems, a convergence proof for the proposed FH TSIA algorithm is not available. The algorithm is terminated when there is no significant change in the values of DerAr, DerBr and DerCr for successive iterations. If DerAr, DerBr and DerCr are less than 1 at termination, it indicates the closeness of the obtained reduced-order model to the optimality conditions and an improvement over the FH BT algorithm.

Remark 12. To compute $V_r(t)$, $X(t, t_0)$ and $P_r(t, t_0)$ are obtained by solving the matrix differential equations (6.8) and (6.7), respectively, with zero initial conditions from $t = t_0$ to $t = t_f$. For computing $W_r(t)$, the modified adjoint system is used to obtain $X_{ma}(t, t_0)$ and $P_{rma}(t, t_0)$ by solving the differential equations (6.9) and (6.10), respectively, from $t = t_0$ to $t = t_f$ with zero initial conditions. Then, $W_{rma}(t) = X_{ma}(t, t_0)\,(P_{rma}(t, t_0))^{-1}$ is obtained. Using (6.15) and (6.16) of Lemma 6.1.1, a time reversal operation on $W_{rma}(t)$ is applied to obtain $W_r(t)$ i.e. $W_r(t) = W_{rma}(t_0 + t_f - t)$.

Remark 13. The above algorithm is the generalization of the TSIA algorithm, proposed by [104] and stated in Algorithm 5 of Chapter 2, to continuous-time LTV systems.

The computational complexity of the proposed FH TSIA algorithm and the existing FH BT algorithm is now discussed. FH BT involves solving two differential equations with $n \times n$ matrix coefficients for the time interval $[t_0, t_f]$. Then, a pair of time-varying projection matrices are computed using Schur projection [85, 86]. In comparison, FH TSIA involves solving four differential equations, two with $n \times r$ and another two with $r \times r$ matrix coefficients for the same time interval. The solutions are used to construct a pair of time-varying projection matrices. The differential equations are solved using appropriate ordinary differential equation (ODE) solvers. Thus, the computational cost of FH BT and FH TSIA depends on the values of n and r and the time the ODE solver takes to solve the differential equations. Due to the greater number of matrix coefficients, the FH BT algorithm appears more computationally expensive. However, unlike FH BT, FH TSIA is an iterative algorithm. So, apart from the aforementioned factors, its computational cost also depends on the number of iterations required for convergence. Thus, FH BT is computationally expensive compared to FH TSIA, provided the latter requires fewer iterations for convergence.

6.4 Numerical examples

This section demonstrates the convergence of FH TSIA with the help of two numerical examples. The first example considers an artificially constructed second-order LTV model, which is approximated by a first-order LTV model. For ease of understanding, a relatively simple example is considered. The second example consists of an LTV model of a missile's pitch/yaw channel, which is approximated by a second-order and a first-order LTV model. The accuracy of a reduced-order model (ROM) is determined by computing the output error norm ($\|y - y_r\|_{L_2[t_0,t_f]}$) for a unit step input. To simplify the comparison process, the output error norms of the ROMs obtained at various iterations of FH TSIA are scaled by the output error norm of the FH BT ROM and denoted by $\|y_e\|_r$.

Example 1:

Consider the following continuous-time LTV system with initial condition $x(0) = \begin{bmatrix} 0 & 0 \end{bmatrix}^T$.

$$\begin{aligned} \frac{d}{dt}x(t) &= \begin{bmatrix} t & 2e^{-t} \\ 1 & te^{-t} \end{bmatrix} x(t) + \begin{bmatrix} 1 \\ 1 \end{bmatrix} u(t), \\ y(t) &= \begin{bmatrix} 1 & 1 \end{bmatrix} x(t), \end{aligned} \tag{6.62}$$

where $x(t) = \begin{bmatrix} x_1(t) & x_2(t) \end{bmatrix}^T$. For a time interval $[0, 2]$ s, the time-varying gramians $P(t, 0)$ and $Q(2, t)$ are computed by solving two matrix differential equations. The time-varying Hankel singular values of the above system are computed as $\text{diag}\{\sigma_1(t), \sigma_2(t)\} = (\lambda(P(t, 0)Q(2, t)))^{\frac{1}{2}}$. They are plotted in Figure 6.1. From the figure, it is clear that the first singular value $\sigma_1(t)$ almost dominates the second singular value $\sigma_2(t)$ over the time interval $[0, 2]$ s, except the first 0.08 s.

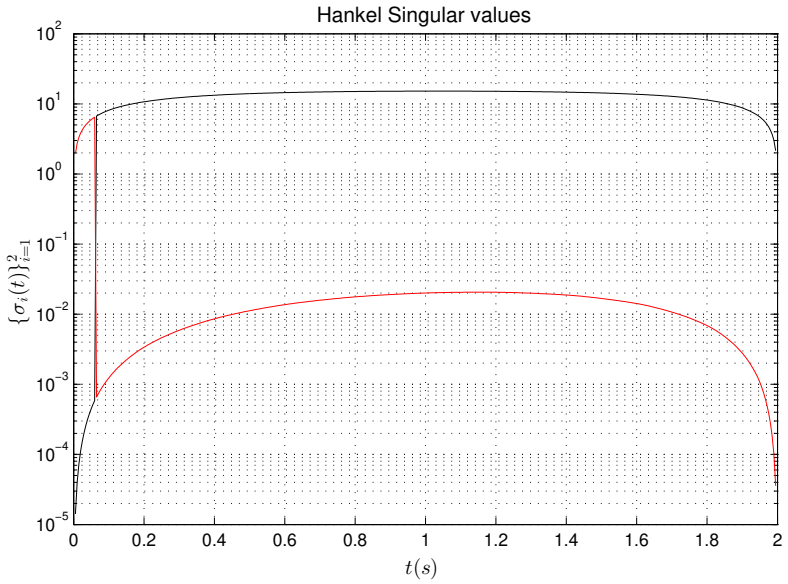

Figure 6.1: Hankel singular values of the LTV system given by (6.62) for $[0, 2]$ s.

.

For the considered time interval, a first-order approximation of the LTV system is obtained using finite horizon balanced truncation (FH BT), which is described by Algorithm 6 in Chapter 2. A first-order approximation of the LTV model is obtained using FH BT, which initialises FH TSIA. For this ROM, $J^1_{A_r} = 7.56$, $J^1_{B_r} = 136.95$, $J^1_{C_r} = 147.09$ and the output error norm is 0.35. The unit step responses of the original and the reduced-order system and the absolute error between the responses are displayed in Figure 6.2.

This ROM initialises FH TSIA. From Table 6.1, we see that there is no significant change in values of DerAr, DerBr, DerCr and $\|y_e\|_r$ beyond the sixth iteration. So, FH TSIA is terminated at the sixth iteration. The derivative and output error values indicate that the FH TSIA ROM is closer to optimality than the FH BT ROM.

Reduced-order	Iter	DerAr	DerBr	DerCr	$\|y_e\|_r$
$r = 1$	1	1.54	1.02	1.03	1.33
	2	1.48	1.02	1.04	1.31
	3	1.48	0.99	1.03	2
	4	3.37	1.06	1.09	1.38
	5	0.63	1.04	1.09	0.41
	6	0.42	1.04	1.10	0.40

Table 6.1: DerAr, DerBr, DerCr and $\|y_e\|_r$ for the first-order ROMs corresponding to iterations of FH TSIA.

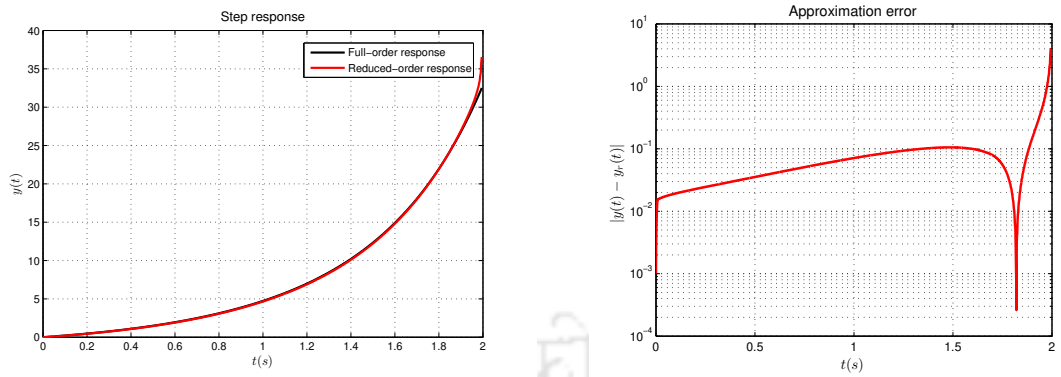

(a) (b)

Figure 6.2: (a) The step responses of the 2nd-order LTV model and a 1st-order LTV approximation obtained by FH BT. (b) The absolute value of the error between the step responses of the original model and the 1st-order approximation.

Figure 6.3 compares the step responses of the original LTV model and the reduced-order approximations and the absolute output errors between them. It also indicates that among the FH TSIA and FH BT ROMs, the unit step response of the former is closer to the unit step response of the original model.

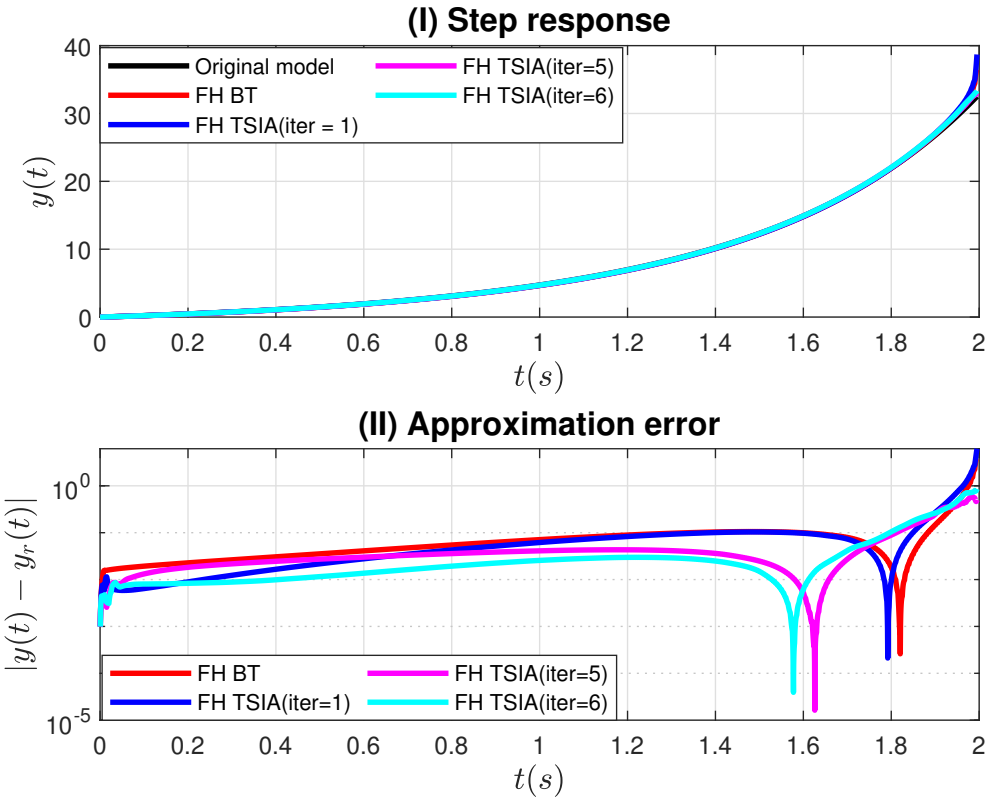

Figure 6.3: (I) Step responses for the second-order LTV model and the first-order LTV approximations achieved by FH BT and various iterations of FH TSIA, (II) Approximation errors between the step responses of the original and the reduced-order models.

Example 2:

For the second example, a linearized mathematical model of a missile's pitch/yaw channel [22],[97] is considered. The LTV model has 4 states, 2 inputs and 1 output. The inputs are the actuator deflections $\delta_y(t)$ and $\delta_z(t)$; the output is the yaw rate $\omega_y(t)$. The state-space model is given by

$$\frac{dx}{dt} = A(t)x(t) + B(t)u(t),$$

where $x = [\omega_z, \alpha, \omega_y, \beta]^T$ is the state vector and $u = [\delta_z, \delta_y]^T$ is the input vector. Here, ω_z, ω_y, α, and β are the pitch rate, the yaw rate, the attack angle and the sideslip angle, respectively. The state matrix $A(t)$ is given by

$$A(t) = \begin{bmatrix} -a_1(t) - e_1(t) & e_1(t)a_4(t) - a_2(t) & \frac{(J_z - J_x)\omega_x(t)}{57.3J_y} & \frac{e_1\omega_x(t)}{57.3} \\ 1 & -a_4(t) & 0 & -\frac{\omega_x(t)}{57.3} \\ \frac{(J_z - J_x)\omega_x(t)}{57.3J_y} & -\frac{e_2(t)\omega_x(t)}{57.3} & -b_1(t) - e_2(t) & e_2(t)b_4(t) - b_2(t) \\ 0 & \frac{w_x(t)}{57.3} & 1 & -b_4(t) \end{bmatrix}$$

where $\omega_x(t)$ is the rolling rate, J_x, J_y, and J_z are the rotary inertia of the missile corresponding to the body coordinate. The control matrix is

$$B(t) = \begin{bmatrix} -e_1(t)a_5(t) - a_3(t) & 0 \\ -a_5(t) & 0 \\ 0 & e_2(t)b_5(t) - b_3(t) \\ 0 & -b_5(t) \end{bmatrix}$$

The parameters $a_i(t)$, $b_i(t)$, $i = 1, 2, 3, 4, 5$, $e_i(t)$, $i = 1, 2$ are functions of time and varying continuously with the height and velocity of the missile. The fitting polynomials for the coefficient matrices $A(t)$ and $B(t)$ are given below

$$\begin{aligned}
a_{11}(t) &= 0.0012t^2 + 0.0342t - 1.8780 \\
a_{12}(t) &= 1.512t^2 - 8.7711t - 260.1298 \\
a_{13}(t) &= -5.2356 \\
a_{14}(t) &= 0.0067t^2 - 0.1634t + 1.9895 \\
a_{22}(t) &= -0.0017t^2 + 0.0507t - 1.5060 \\
a_{24}(t) &= -6.9808 \\
a_{31}(t) &= 5.2356 \\
a_{32}(t) &= -0.0073t^2 + 0.1759t - 2.0593 \\
a_{33}(t) &= 0.0006t^2 + 0.0478t - 1.9500 \\
a_{34}(t) &= 0.2952t^2 - 3.7314t - 25.7606 \\
a_{42}(t) &= 6.9808 \\
a_{44}(t) &= -0.0029t^2 + 0.0385t - 0.7710
\end{aligned}$$

Also, $a_{21} = a_{43} = 1$ and $a_{23} = a_{41} = 0$.

$$\begin{aligned}
b_{11}(t) &= 0.0524t^2 + 0.3368t - 185.5729 \\
b_{21}(t) &= -0.0006t^2 + 0.0139t - 0.2980 \\
b_{32}(t) &= -0.0182t^2 - 2.0279t - 159.8991 \\
b_{42}(t) &= -0.0012t^2 + 0.0186t - 0.2540
\end{aligned}$$

Also, $b_{31} = b_{41} = b_{12} = b_{22} = 0$.

The finite horizon MOR problem of the LTV model is considered for the time interval $[0, 10]$ s. The singular values $\sigma_i(t) = \lambda_i^{\frac{1}{2}}(P(t,0)Q(t_f,t))$ are plotted in Figure 6.4.

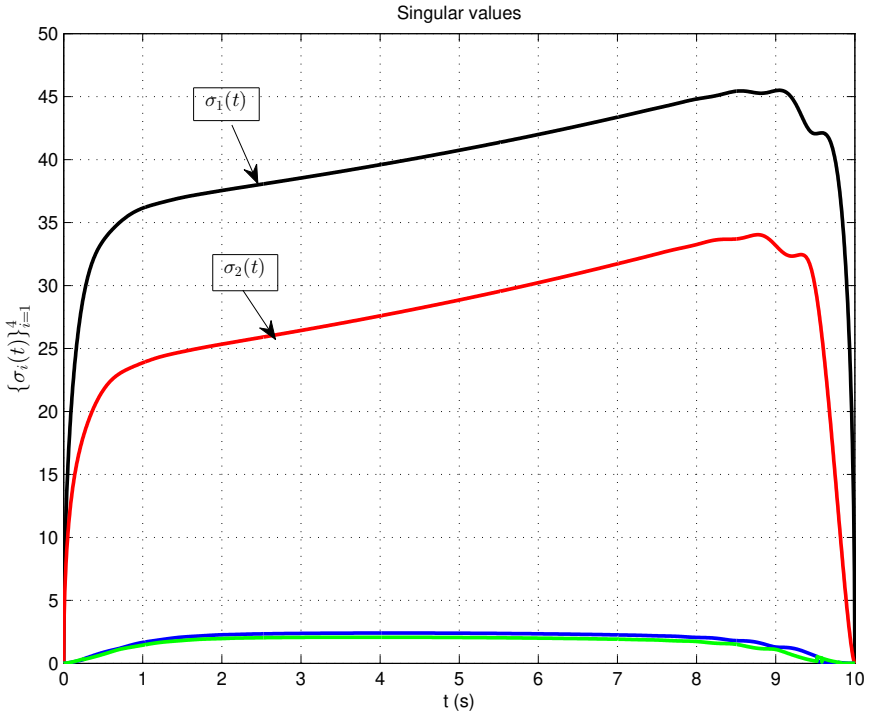

Figure 6.4: Singular values of the LTV model of a missile's pitch/yaw channel over the time interval $[0, 10]$ s.

For the time interval under consideration, the singular values $\sigma_1(t)$ and $\sigma_2(t)$ dominate. Compared to them, the singular values $\sigma_3(t)$ and $\sigma_4(t)$ are negligible. As two singular values are dominant, it is expected that two states are needed to make a good approximation. This is verified by obtaining first-order and second-order LTV approximations of the full-order LTV system using the finite horizon balanced truncation algorithm for the time interval $[0, 10]$ s and comparing the step responses of the original and the reduced-order models. The unit step responses of the original and the reduced-order models are compared in Figure 6.5 and Figure 6.6.

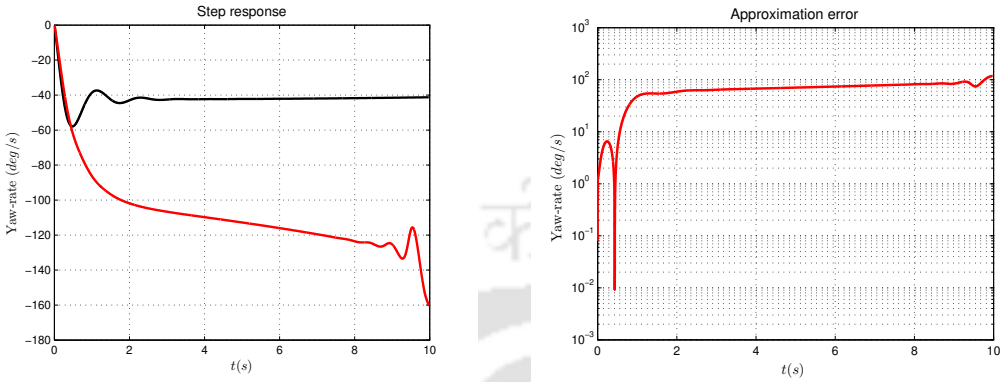

(a) (b)

Figure 6.5: (a) The step responses of the 4th-order LTV model and a first-order LTV approximation. (b) The absolute value of the error between the step responses of the original model and the 1st-order approximation.

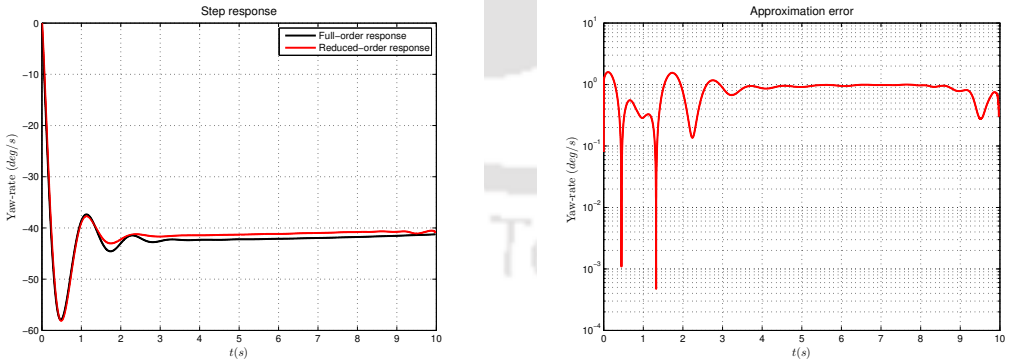

(a) (b)

Figure 6.6: (a) The step responses of the 4th-order LTV model and a second-order LTV approximation. (b) The absolute value of the error between the step responses of the original model and the 2nd-order approximation.

First-order approximation: For the first-order approximation of the LTV model obtained using FH BT, $J^1_{A_r} = 3937.9$, $J^1_{B_r} = 918.7$, $J^1_{C_r} = 748.8$ and the output error norm is 220.9. This model is used to initialize FH TSIA. Table 6.2 shows that DerAr, DerBr and DerCr and $\|y_e\|_r$ do not change significantly beyond the 15^{th} iteration. Hence, FH TSIA is terminated at the 15^{th} iteration. Step responses are applied at both inputs of the original and the reduced-order models. The outputs are compared in Figure 6.7. The FH TSIA ROM is much closer to optimality and has a considerably lesser output error norm compared to the FH BT ROM.

Reduced-order	Iter	DerAr	DerBr	DerCr	$\|y_e\|_r$
$r = 1$	3	0.73	0.76	1.43	0.53
	6	0.43	0.76	1.60	0.35
	9	0.22	0.76	1.68	0.28
	12	0.09	0.75	1.60	0.24
	15	0.03	0.75	1.60	0.22
$r = 2$	1	2.51	0.32	1	0.84
	2	2.10	0.13	1	0.96
	3	1.05	0.11	0.79	0.83

Table 6.2: DerAr, DerBr, DerCr and $\|y_e\|_r$ for various iterations of FH TSIA.

Figure 6.3 compares the step responses of the original LTV model and the reduced-order approximations and the absolute output errors between them. It also indicates that among the FH TSIA and FH BT ROMs, the unit step response of the former is closer to the unit step response of the original model.

Second-order approximation: Then, a second-order approximation of the LTV model is obtained using FH BT. For this model, $J^1_{A_r} = 29.0$, $J^1_{B_r} = 317.2$, $J^1_{C_r} = 3.21 \times 10^{-13}$ and the output error norm is 2.8. This shows that second-order FH BT ROM is a much better approximation of the original model than the first-order ROM. This model is then used to initialize FH TSIA, which converges in just three iterations, as seen from Table 6.2. Compared to the significant improvement of the FH TSIA ROM for the first-order approximation, there is only a slight improvement for the second-order approximation. This is because the second-order FH BT ROM is already close to optimality. Figure 6.8 displays the step responses of the original and the second-order ROMs and the absolute errors between them.

For both numerical examples, we observe that FH TSIA converges after a finite number of iterations and performs better than FH BT.

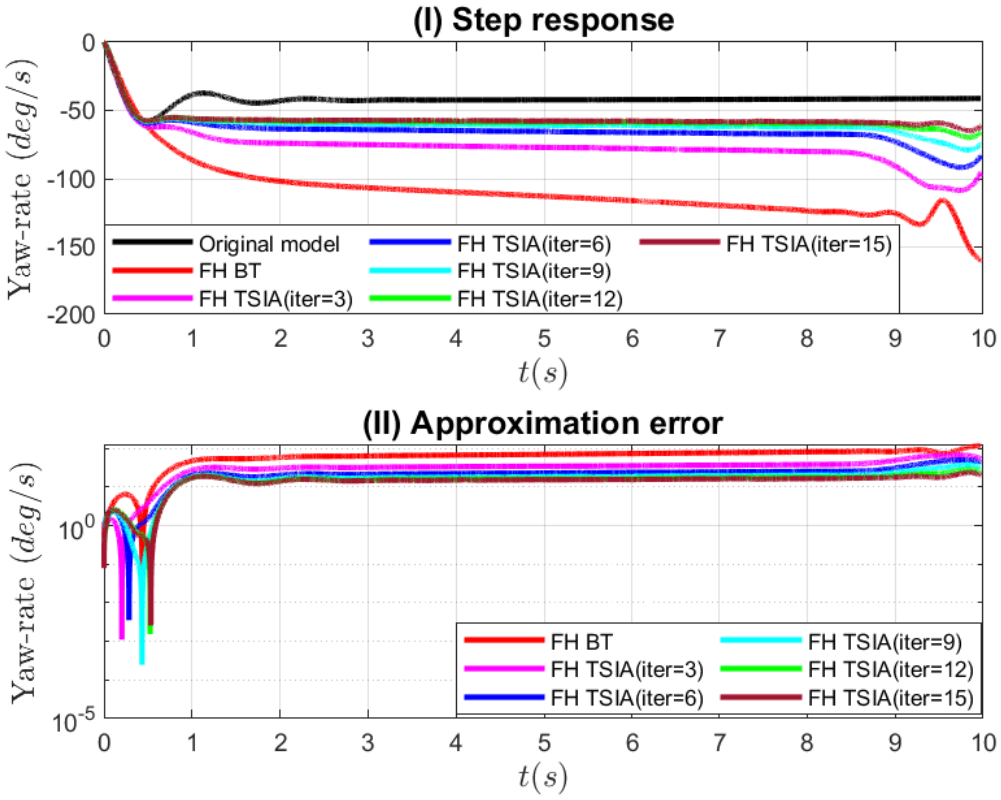

Figure 6.7: (I) Step responses for the 4^{th}-order LTV model and the first-order approximations obtained by FH BT and various iterations of FH TSIA. (II) Approximation errors between the step responses of the original and the reduced-order models.

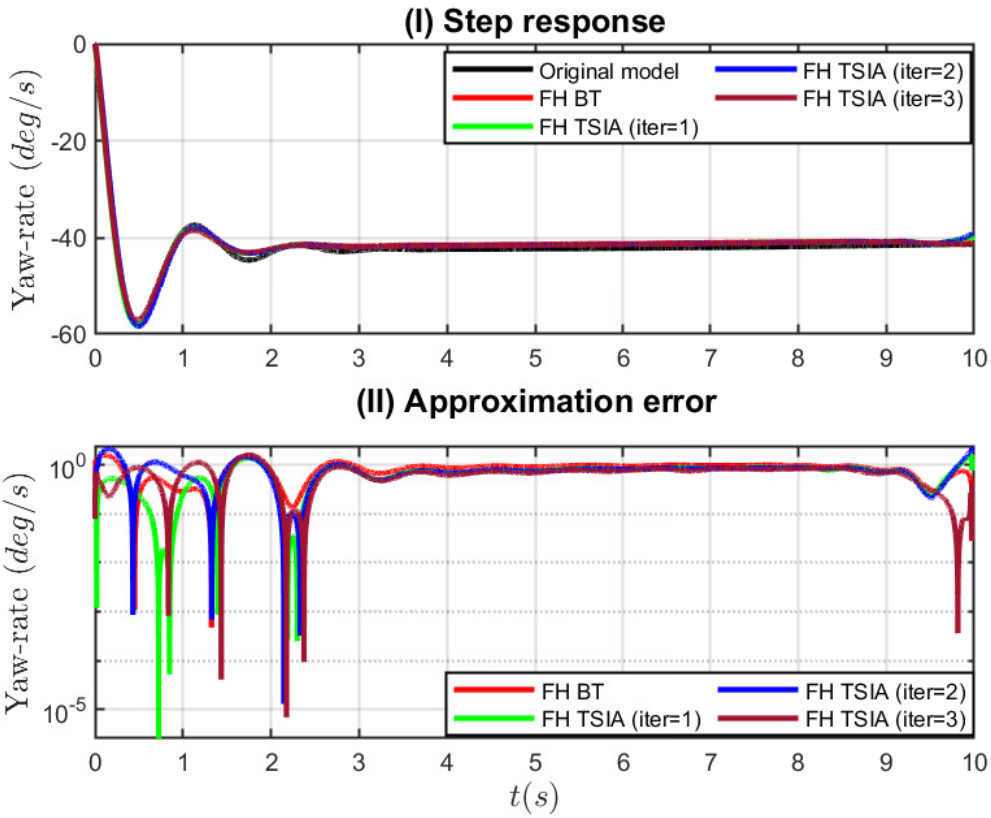

Figure 6.8: (I) Step responses for the 4^{th}-order LTV model and the second-order LTV approximations obtained by FH BT and various iterations of FH TSIA. (II) Absolute value of error between the step responses of the original and the reduced-order models.

6.5 Summary

A finite horizon H_2 optimal model order reduction algorithm for a continuous-time LTV system has been proposed in this chapter. The functional derivatives of the finite horizon H_2 error norm with respect to the state-space parameters of the reduced-order LTV system have been obtained. Further, they have been used to derive conditions for optimality of the finite horizon H_2 error norm. Based on them, the model order reduction algorithm has been proposed.

Chapter 7

Conclusions and Future Work

7.1 Conclusions

MOR techniques are used for decreasing the computational complexity or storage requirements of system models while ensuring that the input-output behaviour of the original system model is not significantly altered. Scientists and engineers use such techniques to simplify analysis, design control systems for digital twin applications, etc. The two main classes of MOR techniques are data-driven and model-based. Among the existing techniques, the category of finite horizon MOR techniques is used for capturing the behaviour of system models over a limited time interval, such as the transient period.

In this thesis, the problem of finite horizon model order reduction of LTI and LTV systems by minimizing a performance criterion is studied. For LTI systems, the criterion is a $H_2(\tau)$ error norm introduced in [30]. For such systems, a projection-based algorithm called TL-IRKA is proposed in Chapter 3 and a gradient-based algorithm called TL-H_2Opt is proposed in Chapter 4 for $H_2(\tau)$ optimal model order reduction. With regards to continuous-time LTV systems, the error criterion for model reduction is a finite horizon H_2 error norm, proposed in Chapter 6 of this thesis. Based on this error criterion, a projection-based algorithm for finite horizon model reduction of LTV systems is proposed.

For various time intervals $[0, \tau]$ s, the $H_2(\tau)$ errors of reduced-order models obtained by applying TL-IRKA and the existing finite horizon algorithms like TL-BT and TL-TSIA as well the infinite horizon algorithm IRKA are computed. Comparing the errors, it is observed that TL-IRKA performs better than TL-BT for the smaller time intervals and has similar performance for the longer time intervals. TL-IRKA also performs better than IRKA for all the time intervals considered. Further, the smaller the time interval, the better TL-IRKA's performance compared to IRKA. Finally, as $H_2(\tau)$ optimal model reduction algorithms, TL-IRKA and TL-TSIA have comparable performance for all the time intervals considered.

The projection-based algorithms TL-BT, TL-TSIA and TL-IRKA do not satisfy the $H_2(\tau)$ optimality conditions exactly. This motivates the development of a gradient-based finite horizon model order reduction method called TL-H_2Opt. Initializing TL-H_2Opt with TL-BT and TL-TSIA, reduced-order models for a range of orders are obtained. It is noted that reduced-order

models obtained by TL-H_2Opt are closer to optimality than the projection-based methods.

The implementation of TL-IRKA as well as TL-H_2Opt involves computation of the matrix exponential of the state matrix, i.e. $e^{A\tau}$. The technique used in this thesis for computing $e^{A\tau}$ has a computational cost of $\mathcal{O}(n^3)$. TL-IRKA is an iterative algorithm, and every iteration involves solving a pair of linear equations. The method employed for solving the equations has a numerical complexity of $\mathcal{O}(n^3)$. Further, every iteration of the optimization scheme TL-H_2Opt involves solving Sylvester equations. The numerical method utilized for solving them also has a $\mathcal{O}(n^3)$ complexity.

Chapter 5 and Chapter 6 deal with continuous-time LTV systems. In Chapter 5, three methods for computing the finite horizon reachability gramian of a continuous-time LTV system are presented. The methods are validated with a numerical example that involves comparing the finite horizon reachability gramian computed using a differential Lyapunov equation with the ones computed with the proposed methods. The same chapter also proposes a finite horizon H_2 norm for continuous-time LTV systems, which is used in the next chapter as a performance measure for model order reduction of continuous-time LTV systems.

The study of model order reduction for continuous-time LTV systems is less explored when compared to continuous-time LTI systems. The finite horizon balanced truncation algorithm (FH BT) is a standard method for model order reduction of LTV systems. To improve the performance of FH BT, an iterative algorithm in Chapter 6 for finite horizon model reduction of LTV systems is proposed. The algorithm aims to minimize a finite horizon H_2 error norm and is an extension of the MOR algorithm TSIA (applicable for LTI systems) to LTV systems. The proposed algorithm's performance is validated with the help of two numerical examples. It is observed that the reduced-order models (ROMs) obtained by the proposed algorithm perform better than those obtained by the FH BT algorithm.

7.2 Future work

This section discusses several aspects of the work carried out in this thesis where further research is required.

1. **Use of inexact solves for TL-IRKA:** The use of inexact solves for interpolation-based model reduction and associated perturbation effects on the IRKA model reduction algorithm has been investigated in [8, 5]. Further, it has also been proved that IRKA is robust with respect to perturbations due to the inexact solves ensuring its application for large-scale settings.

   Apart from the computation of the matrix exponential term ($e^{A\tau}$), the TL-IRKA algorithm given by Algorithm 7, proposed in Chapter 3, involves solving $2r$ linear equations for every iteration. This thesis uses the direct LU method for solving the linear equations, which has a computational cost of $\mathcal{O}(n^3)$. Similar to the studies on IRKA mentioned earlier, using inexact solves for solving the linear equations and the resulting perturbation effects on TL-IRKA can be investigated in future work.

2. **Establishing a time-limited H_2 optimal model reduction framework for bilinear**

systems: Bilinear control systems function as an interface between linear and nonlinear control systems [63, 62]. Many concepts related to model order reduction of LTI systems have been extended to bilinear systems. In [107], the H_2 norm for bilinear systems is introduced, and first-order necessary conditions for H_2 optimality based on the solutions of generalized Lyapunov equations are derived. An iterative algorithm converging to a reduced model satisfying the Lyapunov-based optimality conditions is proposed in [15]. The same work also proposes an alternate way of computing the generalized H_2 norm and, based on it, extends the algorithm IRKA to bilinear systems.

Like the infinite time case discussed above, the time-limited H_2 norm for LTI systems can be extended to bilinear systems. Lyapunov-based and interpolation-based conditions for time-limited H_2 optimality of bilinear systems can be obtained, and iterative algorithms that yield reduced-order bilinear models satisfying the optimality conditions can be proposed. Further, similar to Chapter 4, gradient-based methods for time-limited H_2 optimal model reduction of bilinear systems can also be developed using the gradients of the time-limited H_2 error norm.

3. **Extension of the H_2 optimal model reduction framework to LTV systems with piecewise-continuous parameters and time-varying state dimension:** The finite horizon H_2 norm from Chapter 5 and the model reduction framework based on minimizing the H_2 error norm from Chapter 6 assumes that the original, as well as the reduced-order LTV system, are continuous over $[t_0, t_f]$. Additionally, the reduced-order system is assumed to have a continuous state dimension over the considered time interval. However, based on the nature of the time-varying Hankel singular values, such assumptions may not produce good reduced-order models. Hence, proposing a generalized finite horizon H_2 norm and a corresponding H_2 optimal model reduction technique for LTV systems with piece-wise continuous parameters or with time-varying state dimensions is an interesting future work.

Appendix A

Equivalence of Lyapunov- and interpolation-based $H_2(\tau)$ optimality conditions

The equivalence between the interpolation-based and the Lyapunov-based H_2 optimality conditions, which are related to the H_2 optimal model reduction problem, is discussed in Chapter 2. This motivates a similar study of the equivalence between the interpolation-based and the Lyapunov-based $H_2(\tau)$ optimality conditions for the $H_2(\tau)$ optimal model reduction problem.

If the state matrix of the reduced-order system Σ_r is diagonalizable, then the interpolation-based $H_2(\tau)$ optimality conditions given in Theorem 3.2.2 and the Lyapunov-based $H_2(\tau)$ optimality conditions obtained in Theorem 4.2.2 are equivalent. This is proved in Theorem A.0.1.

Assume that the transfer function $G_r(s)$ of the LTI system Σ_r, given by (2.17), has r distinct poles. The partial fraction expansion of the transfer function matrix $G_r(s)$ is given by

$$G_r(s) = \sum_{i=1}^{r} \frac{c_i b_i^T}{s - \lambda_i}, \tag{A.1}$$

where $\lambda_i \in \mathbb{C}$, $c_i \in \mathbb{C}^p$, $b_i \in \mathbb{C}^m$. Further, assume that the set $\{\lambda_i, b_i, c_i \text{ for } i = 1, 2, \ldots, r\}$ is self conjugate. Let v_i and w_i be the right and left eigenvectors of the matrix A_r corresponding to the eigenvalue λ_i. Let

$$A_r v_i = \lambda_i v_i, \quad w_i^T A_r = \lambda_i w_i^T, \tag{A.2}$$

for $i = 1, 2, \ldots, r$. Let c_i and b_i be defined as follows,

$$c_i = C_r v_i, \quad b_i^T = w_i^T B_r. \tag{A.3}$$

For the LTI system given by (2.1), the time-limited transfer function for the time-interval $[0, \tau]$ is given by,

$$G_\tau(s) = C(sI_n - A)^{-1}(I_n - e^{-s\tau}e^{A\tau})B. \tag{A.4}$$

The time-limited transfer function $G_{r,\tau}(s)$ for the reduced-order LTI system is defined as,

$$G_{r,\tau}(s) = C_r(sI_r - A_r)^{-1}(I_r - e^{-s\tau}e^{A_r\tau})B_r. \tag{A.5}$$

Differentiating $G_\tau(s)$ and $G_{r,\tau}(s)$ with respect to s results in

$$\frac{dG_\tau}{ds}(s) = -C(sI_n - A)^{-2}(I_n - e^{-s\tau}e^{A\tau})B + \tau e^{-s\tau}C(sI_n - A)^{-1}e^{A\tau}B, \tag{A.6}$$

$$\frac{dG_{r,\tau}}{ds}(s) = -C_r(sI_r - A_r)^{-2}(I_r - e^{-s\tau}e^{A_r\tau})B_r + \tau e^{-s\tau}C_r(sI_r - A_r)^{-1}e^{A_r\tau}B_r. \tag{A.7}$$

Let $V = \begin{bmatrix} v_1 & v_2 & \dots & v_r \end{bmatrix}$, where the columns v_i's are the right eigenvectors of the matrix A_r.

Theorem A.0.1. *For $i = 1, 2, \dots, r$, $j = 1, 2, \dots, r$, $i \neq j$ and $\lambda_i \neq \lambda_j$,*

$$\frac{1}{2}\left(\nabla_{B_r}J\right)^T v_i = \left[(G_{r,\tau}(-\lambda_i^*))^T - (G_\tau(-\lambda_i^*))^T\right] c_i, \tag{A.8}$$

$$\frac{1}{2}w_i^T\left(\nabla_{C_r}J\right)^T = b_i^T\left[(G_{r,\tau}(-\lambda_i^*))^T - (G_\tau(-\lambda_i^*))^T\right], \tag{A.9}$$

$$\frac{1}{2}w_i^T\left(\nabla_{A_r}J\right)^T v_i = b_i^T\frac{d}{ds}\left[(G_\tau(s))^T - (G_{r,\tau}(s))^T\right]\Big|_{s=-\lambda_i^*} c_i \quad \textit{and} \tag{A.10}$$

$$\frac{1}{2}w_i^T\left(\nabla_{A_r}J\right)^T v_j = \frac{1}{2(\lambda_i - \lambda_j)}\left[b_i^T\left(\nabla_{B_r}J\right)^T v_j - w_i^T\left(\nabla_{C_r}J\right)^T c_j\right], \tag{A.11}$$

where $J = \|G - G_r\|^2_{H_2(\tau)}$ is the square of the $H_2(\tau)$ error norm for the time interval $[0, \tau]$, given by (4.13) or (4.14). The terms $\nabla_{A_r}J$, $\nabla_{B_r}J$ and $\nabla_{C_r}J$ are the gradients of J with respect to A_r, B_r and C_r, given by (4.17), (4.18) and (4.19), respectively. The c_i's and b_i's are the residues of the partial fraction representation of $G_r(s)$, given by (A.1). The v_i's and w_i's are the right and left eigenvectors of A_r, the state matrix of the LTI system given by (2.17).

Proof. Consider the terms X_τ, X, $P_{r,\tau}$, P_r, Y_τ and $Q_{r,\tau}$, which are the solutions of the matrix equations (4.8), (4.21), (4.9), (4.20), (4.11) and (4.12), respectively. For $i = 1, 2, \dots, r$, let $x_{i,\tau} = X_\tau w_i$, $x_i = Xw_i$, $p_{i,\tau} = P_{r,\tau}w_i$, $p_i = P_r w_i$, $y_{i,\tau} = Y_\tau v_i$ and $q_{i,\tau} = Q_{r,\tau}v_i$. Postmultiplying the matrix equation (4.8) by w_i gives

$$AX_\tau w_i + X_\tau {A_r}^T w_i + B{B_r}^T w_i - e^{A\tau}B{B_r}^T e^{{A_r}^T\tau}w_i = 0.$$

As $w_i^T A_r = \lambda_i w_i^T$ (from (A.2)), taking transpose gives ${A_r}^T w_i = \lambda_i^* w_i^T$. Multiplying the exponential $e^{A_r^T\tau}$ by w_i results in $e^{{A_r}^T}w_i = e^{\lambda_i^*\tau}w_i^T$. Making these substitutions in the above equation and using (A.3) gives the following result.

$$\begin{aligned} &Ax_{i,\tau} + \lambda_i^* X_\tau w_i + Bb_i - e^{A\tau}B{B_r}^T w_i e^{\lambda_i^*\tau} = 0 \\ &\Rightarrow Ax_{i,\tau} + \lambda_i^* x_{i,\tau} + Bb_i - e^{A\tau}Bb_i e^{\lambda_i^*\tau} = 0 \\ &\Rightarrow x_{i,\tau} = -(A + \lambda_i^* I_n)^{-1}(I_n - e^{\lambda_i^*\tau}e^{A\tau})Bb_i. \end{aligned} \tag{A.12}$$

Pre-multiplying (4.21) by w_i^T results in

$$\begin{aligned} &w_i^T X^T A^T + w_i^T A_r X^T + w_i^T B_r B^T = 0 \\ &\Rightarrow x_i^T A^T + \lambda_i w_i^T X^T + b_i^T B^T = 0 \\ &\Rightarrow x_i = -(A + \lambda_i^* I_n)^{-1}Bb_i. \end{aligned} \tag{A.13}$$

Post-multiplying (4.9) by w_i gives

$$A_r P_{r,\tau}w_i + P_{r,\tau}A_r^T w_i + B_r B_r^T w_i - e^{A_r\tau}B_r B_r^T e^{A_r^T\tau}w_i = 0.$$

Making substitutions similar to (A.12) in the above equation yields

$$\begin{aligned} & A_r p_{i,\tau} + \lambda_i^* p_{i,\tau} + B_r b_i - e^{A_r \tau} B_r b_i e^{\lambda^* \tau} = 0 \\ & \Rightarrow p_{i,\tau} = -(A_r + \lambda_i^* I_r)^{-1}(I_r - e^{\lambda_i^* \tau} e^{A_r \tau}) B_r b_i. \end{aligned} \tag{A.14}$$

Post-multiplying (4.20) by w_i gives

$$\begin{aligned} & P_r A_r^T w_i + A_r P_r w_i + B_r B_r^T w_i = 0 \\ & \Rightarrow \lambda_i^* P_r w_i + A_r p_i + B_r b_i = 0 \\ & \Rightarrow p_i = -(A_r + \lambda_i^* I_r)^{-1} B_r b_i. \end{aligned} \tag{A.15}$$

Additionally, post-multiplying (4.11) by v_i results in

$$A^T Y_\tau v_i + Y_\tau A_r v_i - C^T C_r v_i + e^{A^T \tau} C^T C_r e^{A_r \tau} v_i = 0.$$

Note that, $A_r v_i = \lambda_i v_i$ (from (A.2)) and $e^{A_r \tau} v_i = e^{\lambda_i \tau} v_i$ (from (A.3)), $c_i = C_r v_i$. Making these substitutions in the above equation gives

$$\begin{aligned} & A^T y_{i,\tau} + \lambda_i y_{i,\tau} - C^T c_i + e^{\lambda_i \tau} e^{A^T \tau} C^T c_i = 0 \\ & \Rightarrow y_{i,\tau} = (A^T + \lambda_i I_n)^{-1}(I_n - e^{\lambda_i \tau} e^{A^T \tau}) C^T c_i. \end{aligned} \tag{A.16}$$

Finally, post-multiplying (4.12) by v_i and using the same substitutions as in the previous case results in

$$\begin{aligned} & A_r^T Q_{r,\tau} v_i + Q_{r,\tau} A_r v_i + C_r^T C_r v_i - e^{A_r^T \tau} C_r^T C_r e^{A_r \tau} v_i = 0 \\ & \Rightarrow A_r^T q_{i,r} + \lambda_i q_{i,r} + C_r^T c_i - e^{\lambda_i \tau} e^{A_r^T \tau} C_r^T c_i = 0 \\ & \Rightarrow q_{i,\tau} = -(A_r^T + \lambda_i I_r)^{-1}(I_r - e^{\lambda_i \tau} e^{A_r^T \tau}) C_r^T c_i. \end{aligned} \tag{A.17}$$

Taking the transpose of $\nabla_{B_r} J$ as given by (4.18) and post-multiplying by v_i gives

$$\begin{aligned} \frac{1}{2} (\nabla_{B_r} J)^T v_i &= B_r^T Q_{r,\tau} v_i + B^T Y_\tau v_i \\ &= B_r^T q_{i,\tau} + B^T y_{i,\tau}. \end{aligned}$$

Substituting the values of $q_{i,\tau}$ and $y_{i,\tau}$ from (A.17) and (A.16), respectively, in the above expression gives

$$\begin{aligned} & \frac{1}{2} (\nabla_{B_r} J)^T v_i \\ & = -B_r^T (A_r^T + \lambda_i I_r)^{-1}(I_r - e^{\lambda_i \tau} e^{A_r^T \tau}) C_r^T c_i + B^T (A^T + \lambda_i I_n)^{-1}(I_n - e^{\lambda_i \tau} e^{A^T \tau}) C^T c_i \\ & = [G_{r,\tau}^T(-\lambda_i^*) - G_\tau^T(-\lambda_i^*)] c_i. \end{aligned}$$

Similarly, using (4.19), (A.14) and (A.12), the following result is obtained.

$$\frac{1}{2} (\nabla_{C_r} J) w_i = [H_{r,\tau}(-\lambda_i^*) - H_\tau(-\lambda_i^*)] b_i. \tag{A.18}$$

Pre-multiplying (4.17) by w_i^T and post-multiplying it by v_j and using the Fréchet derivative expression as given by (4.15) results in

$$\begin{aligned} & \frac{1}{2} w_i^T (\nabla_{A_r} J)^T v_j \\ & = w_i^T P_r Q_{r,\tau} v_j + w_i^T X^T Y_\tau v_j + w_i^T \tau(L(A_r \tau, S_\tau)) v_j \\ & = p_i^T q_{j,\tau} + x_i^T y_{j,\tau} + \int_0^1 w_i^T e^{A_r \tau (1-s)} S_\tau e^{A_r \tau s} v_j \tau ds. \end{aligned}$$

As w_i and v_j are left and right eigenvectors of A_r, $w_i^T e^{A_r\tau(1-s)} = w_i^T e^{\lambda_i\tau(1-s)}$ and $e^{A_r\tau s}v_j = e^{\lambda_i\tau s}v_j$. Making these changes in the above expression gives

$$\frac{1}{2}w_i^T\left(\nabla_{A_r}J\right)^T v_j = x_i^T y_{j,\tau} + p_i^T q_{j,\tau} + w_i^T S_\tau v_j \int_0^1 e^{\lambda_i(\tau-\tau s)}e^{\lambda_j\tau s}(\tau ds). \tag{A.19}$$

Substituting S_τ given by (4.22) and for $j = i$, the expression (A.19) becomes

$$\begin{aligned}
&\frac{1}{2}w_i^T\left(\nabla_{A_r}J\right)^T v_j \\
&= x_i^T y_{i,\tau} + p_i^T q_{i,\tau} + (w_i^T X^T e^{A^T\tau}C^T C_r v_i - w_i^T P_r e^{A_r^T\tau}C_r^T C_r v_i)\int_0^1 e^{\lambda_i(\tau-\tau s)}e^{\lambda_i\tau s}\tau ds \\
&= x_i^T y_{i,\tau} + p_i^T q_{i,\tau} + (x_i^T e^{A^T\tau}C^T c_i - p_i^T e^{A_r^T\tau}C_r^T c_i)\int_0^1 e^{\lambda_i(\tau-\tau s)}e^{\lambda_i\tau s}\tau ds.
\end{aligned} \tag{A.20}$$

Using (A.13) and (A.16), the first term on the right-hand side of (A.20) becomes

$$\begin{aligned}
x_i^T y_{i,\tau} &= \left(-b_i B^T(A^T+\lambda_i I_n)^{-1}\right)\left((A^T+\lambda_i I_n)^{-1}\left(I_n - e^{\lambda_i\tau}e^{A^T\tau}\right)C^T c_i\right) \\
&= -b_i B^T(A^T+\lambda_i I_n)^{-2}(I_n - e^{\lambda_i\tau}e^{A^T\tau})C^T c_i.
\end{aligned} \tag{A.21}$$

Using (A.14) and (A.17), the second term on the right-hand side of (A.20) becomes,

$$\begin{aligned}
p_i^T q_{i,\tau} &= \left(-b_i B_r^T(A_r^T+\lambda_i I_r)^{-1}\right)\left(-(A_r^T+\lambda_i I_r)^{-1}\left(I_r - e^{\lambda_i\tau}e^{A_r^T\tau}\right)C_r^T c_i\right) \\
&= b_i B_r^T(A_r^T+\lambda_i I_r)^{-2}(I_r - e^{\lambda_i\tau}e^{A_r^T\tau})C_r^T c_i.
\end{aligned} \tag{A.22}$$

After substituting x_i and p_i, the third term in right-hand side of the expression (A.20) becomes

$$\begin{aligned}
&(x_i^T e^{A^T\tau}C^T c_i - p_i^T e^{A_r^T\tau}C_r^T c_i)\int_0^1 e^{\lambda_i\tau}\tau ds \\
&= -\tau e^{\lambda_i\tau}b_i B^T(A^T+\lambda_i I_n)^{-1}e^{A^T\tau}C^T c_i + \tau e^{\lambda_i\tau}b_i B_r^T(A_r^T+\lambda_i I_r)^{-1}e^{A_r^T\tau}C_r^T c_i.
\end{aligned} \tag{A.23}$$

Adding (A.21), (A.22) and (A.23), rearranging the terms and using (A.6) and (A.7) gives the following result.

$$\begin{aligned}
&\frac{1}{2}w_i^T(\nabla_{A_r}J)^T v_i \\
&= -\left(b_i B^T(A^T+\lambda_i I_n)^{-2}(I_n - e^{\lambda_i\tau}e^{A^T\tau})C^T c_i + \tau e^{\lambda_i\tau}b_i B^T(A^T+\lambda_i I_n)^{-1}e^{A^T\tau}C^T c_i\right) + \\
&\left(b_i B_r^T(A_r^T+\lambda_i I_r)^{-2}(I_r - e^{\lambda_i\tau}e^{A_r^T\tau})C_r^T c_i + \tau e^{\lambda_i\tau}b_i B_r^T(A_r^T+\lambda_i I_r)^{-1}e^{A_r^T\tau}C_r^T c_i\right) \\
&= b_i\frac{d}{ds}\left[(G_\tau(s))^T - (G_{r,\tau}(s))^T\right]\Big|_{s=-\lambda_i^*} c_i.
\end{aligned}$$

For $j \neq i$, the expression (A.19) becomes

$$\begin{aligned}
\frac{1}{2}w_i^T\left(\nabla_{A_r}J\right)^T v_j &= x_i^T y_{j,\tau} + p_i^T q_{j,\tau} + w_i^T S_\tau v_j e^{\lambda_i\tau}\int_0^1 e^{(\lambda_j-\lambda_i)\tau s}\tau ds \\
&= x_i^T y_{j,\tau} + p_i^T q_{j,\tau} + w_i^T S_\tau v_j\left(\frac{e^{\lambda_i\tau} - e^{\lambda_j\tau}}{\lambda_i - \lambda_j}\right).
\end{aligned} \tag{A.24}$$

Using the identity $\left(A^T+\lambda_i I_n\right)^{-1}\left(A^T+\lambda_j I_n\right)^{-1} = \frac{1}{\lambda_i-\lambda_j}\left[\left(A^T+\lambda_j I_n\right)^{-1} - \left(A^T+\lambda_i I_n\right)^{-1}\right]$ and (A.13), (A.16), the first term on the right-hand side of (A.24) becomes,

$$\begin{aligned}
x_i^T y_{j,\tau} &= -b_i B^T(A^T+\lambda_i I_n)^{-1}(A^T+\lambda_j I_n)^{-1}(I_n - e^{\lambda_j\tau}e^{A^T\tau})C^T c_j \\
&= -\frac{1}{\lambda_i-\lambda_j}b_i B^T\left[\left(A^T+\lambda_j I_n\right)^{-1} - \left(A^T+\lambda_i I_n\right)^{-1}\right]\left(I_n - e^{\lambda_j\tau}e^{A^T\tau}\right)C^T c_j.
\end{aligned} \tag{A.25}$$

Similarly, the second term on the right-hand side of (A.24) becomes,

$$\begin{aligned} p_i^T q_{j,\tau} &= b_i B_r^T (A_r^T + \lambda_i I_r)^{-1} (A_r^T + \lambda_j I_r)^{-1} \left(I_r - e^{\lambda_j \tau} e^{A_r^T \tau} \right) C_r^T c_j \\ &= \frac{1}{\lambda_i - \lambda_j} b_i B_r^T \left[\left(A_r^T + \lambda_j I_r \right)^{-1} - \left(A_r^T + \lambda_i I_r \right)^{-1} \right] \left(I_r - e^{\lambda_j \tau} e^{A_r^T \tau} \right) C_r^T c_j. \end{aligned} \tag{A.26}$$

Finally, using the same identity and the expressions (A.13) and (A.15), the third term on the right-hand side of (A.24) becomes,

$$\begin{aligned} &\left(\frac{e^{\lambda_i \tau} - e^{\lambda_j \tau}}{\lambda_i - \lambda_j} \right) w_i^T S_\tau v_j \\ &= \left(\frac{e^{\lambda_i \tau} - e^{\lambda_j \tau}}{\lambda_i - \lambda_j} \right) \left(w_i^T X^T e^{A^T \tau} C^T C_r v_j - w_i^T P_r e^{A_r^T \tau} C_r^T C_r v_j \right) \\ &= \left(\frac{e^{\lambda_i \tau} - e^{\lambda_j \tau}}{\lambda_i - \lambda_j} \right) \left(x_i{}^T e^{A^T \tau} C^T C_r v_j - p_i^T e^{A_r^T \tau} C_r^T C_r v_j \right) \\ &= \left(\frac{e^{\lambda_i \tau} - e^{\lambda_j \tau}}{\lambda_i - \lambda_j} \right) \left[\left(-b_i B^T (A^T + \lambda_i I_n)^{-1} e^{A^T \tau} C^T c_j \right) + \left(b_i B_r^T (A_r^T + \lambda_i I_r)^{-1} e^{A_r^T \tau} C_r^T c_j \right) \right]. \end{aligned} \tag{A.27}$$

Adding the expressions (A.25), (A.26) and (A.27), and rearranging the terms gives

$$\begin{aligned} &\frac{1}{\lambda_i - \lambda_j} \left[b_i B_r^T (A_r^T + \lambda_j I_r)^{-1} (I_r - e^{\lambda_j} e^{A_r^T \tau}) C_r^T c_j - b_i B^T (A^T + \lambda_j I_n)^{-1} (I_n - e^{\lambda_j \tau} e^{A^T \tau}) C^T c_j \right] - \\ &\frac{1}{\lambda_i - \lambda_j} \left[b_i B_r^T (A_r^T + \lambda_i I_r)^{-1} (I_r - e^{\lambda_j \tau} I_r + e^{\lambda_j \tau} I_r - e^{\lambda_i \tau} I_r) e^{A_r^T \tau} C_r^T c_j \right] + \\ &\frac{1}{\lambda_i - \lambda_j} \left[b_i B^T (A^T + \lambda_i I_n)^{-1} (I_n - e^{\lambda_j \tau} I_n - e^{\lambda_i \tau} I_n + e^{\lambda_j \tau} I_n) e^{A^T \tau} C^T c_j \right] \\ &= \frac{1}{\lambda_i - \lambda_j} \left[b_i \left((G_{r,\tau}(-\lambda_j^*))^T - (G_\tau(-\lambda_j^*))^T \right) c_j - b_i \left((G_{r,\tau}(-\lambda_i^*))^T - (G_\tau(-\lambda_i^*))^T \right) c_j \right] \\ &= \frac{1}{\lambda_i - \lambda_j} \left[b_i (\nabla_{B_r} J)^T v_j - w_i^T (\nabla_{C_r} J)^T c_j \right]. \end{aligned}$$

□

If the Lyapunov-based $H_2(\tau)$ optimality conditions given by (4.33-4.35) are satisfied, then using (4.17–4.19) results in $\nabla_{A_r} J = 0$, $\nabla_{B_r} J = 0$ and $\nabla_{C_r} J = 0$. This implies that $(\nabla_{A_r} J)^T = 0$, $(\nabla_{B_r} J)^T = 0$ and diag $V^{-1} (\nabla_{C_r} J)^T V = 0$. Imposing these conditions on (A.8–A.10) gives

$$\begin{aligned} \left[(G_{r,\tau}(-\lambda_i^*))^T - (G_\tau(-\lambda_i^*))^T \right] c_i &= 0, \\ b_i \left[(G_{r,\tau}(-\lambda_i^*))^T - (G_\tau(-\lambda_i^*))^T \right] &= 0, \quad \text{and} \\ b_i \frac{d}{ds} \left[(G_\tau(s))^T - (G_{r,\tau}(s))^T \right] \Big|_{s=-\lambda_i^*} c_i &= 0. \end{aligned}$$

The above conditions are the interpolation based $H_2(\tau)$ optimality conditions given by (3.11–3.13). Similarly, assuming that the interpolation-based $H_2(\tau)$ optimality conditions are satisfied, using (A.8-A.10) and (4.17–4.19), it is seen that the Lyapunov-based $H_2(\tau)$ optimality conditions, given by (4.33-4.35), are also satisfied. This shows that Lyapunov-based and interpolation-based $H_2(\tau)$ optimality conditions are equivalent.

Bibliography

[1] Michael S Ackermann and Serkan Gugercin. Frequency-based reduced models from purely time-domain data via data informativity. *arXiv preprint arXiv:2311.05012*, 2023.

[2] A. H. Al-Mohy and N. J. Higham. Computing the Fréchet derivative of the matrix exponential, with an application to condition number estimation. *SIAM J. Matrix Analy. Appl.*, 30(4):1639–1657, 2009.

[3] A. C. Antoulas, C. A. Beattie, and S. Gugercin. *Interpolatory methods for model reduction*. SIAM, 2020.

[4] Athanasios C Antoulas. *Approximation of large-scale dynamical systems*. SIAM, 2005.

[5] C. A. Beattie and S. Gugercin. Inexact solves in Krylov-based model reduction. In *Proceedings of the 45th IEEE Conference on Decision and Control*, pages 3405–3411. IEEE, 2006.

[6] C. A. Beattie and S. Gugercin. Krylov-based minimization for optimal H_2 model reduction. In *2007 46th IEEE Conference on Decision and Control*, pages 4385–4390. IEEE, 2007.

[7] C. A. Beattie and S. Gugercin. A trust region method for optimal H_2 model reduction. In *Proceedings of the 48th IEEE Conference on Decision and Control (CDC) held jointly with 2009 28th Chinese Control Conference*, pages 5370–5375. IEEE, 2009.

[8] C. A. Beattie, S. Gugercin, and S. Wyatt. Inexact solves in interpolatory model reduction. *Linear Algebra and its Applications*, 436(8):2916–2943, 2012.

[9] Christopher A Beattie, Serkan Gugercin, et al. Model reduction by rational interpolation. *Model Reduction and Approximation*, 15:297–334, 2017.

[10] C. M. Bender, S. Orszag, and S. A. Orszag. *Advanced mathematical methods for scientists and engineers I: Asymptotic methods and perturbation theory*, volume 1. Springer Science & Business Media, 1999.

[11] P. Benner, S. Grivet-Talocia, A. Quarteroni, G. Rozza, and L. M. Silveria. *Model Order Reduction: Volume 2: Snapshot-Based Methods and Algorithms*. De Gruyter, Berlin, Boston, 2020.

[12] P. Benner, S. Grivet-Talocia, A. Quarteroni, G. Rozza, and L. M. Silveria. *Model Order Reduction: Volume 3: Applications*. De Gruyter, Berlin, Boston, 2020.

[13] P. Benner, S. Grivet-Talocia, A. Quarteroni, G. Rozza, and L. M. Silveria. *Model Order Reduction: Volume 1: System- and Data-Driven Methods and Algorithms*. De Gruyter, Berlin, Boston, 2021.

[14] P. Benner, M. Köhler, and J. Saak. Sparse-dense Sylvester equations in H_2-model order reduction. Technical Report MPIMD/11-11, Max Planck Institute, Madeburg, Germany, Dec 2011.

[15] T. Breiten and P. Benner. Interpolation-based H_2-model reduction of bilinear control system. *SIAM J. Matrix Anal. Appl*, 33(3):859–885, 2012.

[16] Y. Chahlaoui and P. Van Dooren. Benchmark examples for model reduction of linear time-invariant dynamical systems. In P. Benner, D. C. Sorensen, and V. Mehrmann, editors, *Dimension Reduction of Large-Scale Systems*, volume 45, pages 379–392. Springer, Berlin, Heidelberg, 2005.

[17] Y. Chahlaoui and P. Van Dooren. Model reduction of time-varying systems. In *Dimension reduction of large-scale systems*, pages 131–148. Springer, 2005.

[18] P. Dewilde and A. Van der Veen. *Time-varying systems and computations*. Springer Science & Business Media, 1998.

[19] S.W. Director and R.A. Rohrer. The generalized adjoint network and network sensitivities. *IEEE Transactions on Circuit Theory*, 16(3):318–323, 1969.

[20] V. Druskin and V. Simoncini. Adaptive rational Krylov subspaces for large-scale dynamical systems. *Systems & Control Letters*, 60(8):546–560, 2011.

[21] V. Druskin, V. Simoncini, and M. Zaslavsky. Adaptive tangential interpolation in rational Krylov subspaces for MIMO dynamical systems. *SIAM Journal on Matrix Analysis and Applications*, 35(2):476–498, 2014.

[22] GR Duan and HQ Wang. Multi-model switching control and its application to btt missile design. *Acta Aeronautica et Astronautica Sinica*, 26(2):144–147, 2005.

[23] I. P. Duff and P. Kürschner. Numerical computation and new output bounds for time-limited balanced truncation of discrete-time systems. *Linear Algebra and its Applications*, 623:367–397, 2021.

[24] D. F. Enns. Model reduction with balanced realizations: An error bound and a frequency weighted generalization. In *The 23rd IEEE Conference on Decision and Control*, pages 127–132. IEEE, 1984.

[25] Stanley J Farlow. *Partial differential equations for scientists and engineers*. Courier Corporation, 1993.

[26] G. Flagg, C. A. Beattie, and S. Gugercin. Convergence of the iterative rational Krylov algorithm. *Systems & Control Letters*, 61(6):688–691, 2012.

[27] K. Gallivan, A. Vandendorpe, and P. Van Dooren. Model reduction of MIMO systems via tangential interpolation. *SIAM Journal on Matrix Analysis and Applications*, 26(2):328–349, 2004.

[28] W. Gawronski and J. Juang. Model reduction in limited time and frequency intervals. *International Journal of Systems Science*, 21(2):349–376, 1990.

[29] K. Glover. All optimal Hankel-norm approximations of linear multivariable systems and their L_∞-error bounds. *International Journal of Control*, 39(6):1115–1193, 1984.

[30] P. Goyal and M. Redmann. Time-limited H_2-optimal model order reduction. *Applied Mathematics and Computation*, 355:184–197, 2019.

[31] Michael Green and David JN Limebeer. *Linear robust control*. Courier Corporation, 2012.

[32] Eric Grimme. *Krylov projection methods for model reduction*. PhD thesis, University of Illinois at Urbana Champaign, 1997.

[33] T. Gudmundsson and A. J. Laub. Approximate solution of large sparse Lyapunov equations. *IEEE Transactions on Automatic Control*, 39(5):1110–1114, 1994.

[34] S. Gugercin and A. C. Antoulas. A time-limited balanced reduction method. In *42nd IEEE International Conference on Decision and Control (IEEE Cat. No. 03CH37475)*, volume 5, pages 5250–5253. IEEE, 2003.

[35] S. Gugercin, A. C. Antoulas, and C. Beattie. $\mathcal{H}_2$ model reduction for large-scale linear dynamical systems. *SIAM Journal on Matrix Analysis and Applications*, 30(2):609–638, 2008.

[36] J. Hahn and T. F. Edgar. Balancing approach to minimal realization and model reduction of stable nonlinear systems. *Industrial & engineering chemistry research*, 41(9):2204–2212, 2002.

[37] J. Hahn and T. F. Edgar. An improved method for nonlinear model reduction using balancing of empirical gramians. *Computers & chemical engineering*, 26(10):1379–1397, 2002.

[38] J. Hahn, T. F. Edgar, and W. Marquardt. Controllability and observability covariance matrices for the analysis and order reduction of stable nonlinear systems. *Journal of process control*, 13(2):115–127, 2003.

[39] A. Helmersson. LTV model reduction with upper error bounds. *IEEE transactions on automatic control*, 54(7):1450–1462, 2009.

[40] P. Holmes, J. L. Lumley, G. Berkooz, and C. W. Rowley. *Turbulence, Coherent Structures, Dynamical Systems and Symmetry*. Cambridge Monographs on Mechanics. Cambridge University Press, 2 edition, 2012.

[41] P Howard. Analysis of ode models. *Google Scholar*, 2009.

[42] Kenneth H Huebner, Donald L Dewhirst, Douglas E Smith, and Ted G Byrom. *The finite element method for engineers*. John Wiley & Sons, 2001.

[43] Antonio Ionita. *Lagrange rational interpolation and its applications to approximation of large-scale dynamical systems*. PhD thesis, Rice University, 2013.

[44] I. M. Jaimoukha and E. M. Kasenally. Krylov subspace methods for solving large Lyapunov equations. *SIAM Journal on Numerical Analysis*, 31(1):227–251, 1994.

[45] T. Kailath. *Linear systems*, volume 156. Prentice-Hall Englewood Cliffs, NJ, 1980.

[46] Y. Kawano and J. M. A. Scherpen. Empirical differential balancing for nonlinear systems. *IFAC-PapersOnLine*, 50(1):6326–6331, 2017.

[47] Y. Kawano and J. M. A. Scherpen. Empirical differential Gramians for nonlinear model reduction. *Automatica*, 127:109534, 2021.

[48] O. Kouba and D. S. Bernstein. What is the adjoint of a linear system?[lecture notes]. *IEEE Control Systems Magazine*, 40(3):62–70, 2020.

[49] A. J. Krener and K. Ide. Measures of unobservability. In *Proceedings of the 48h IEEE Conference on Decision and Control (CDC) held jointly with 2009 28th Chinese Control Conference*, pages 6401–6406. IEEE, 2009.

[50] P. Kürschner. Balanced truncation model order reduction in limited time intervals for large systems. *Advances in Computational Mathematics*, 44(6):1821–1844, 2018.

[51] S. Lall and C. Beck. Error-bounds for balanced model-reduction of linear time-varying systems. *IEEE Transactions on Automatic Control*, 48(6):946–956, 2003.

[52] S. Lall, J. E. Marsden, and S. Glavaški. Empirical model reduction of controlled nonlinear systems. *IFAC Proceedings Volumes*, 32(2):2598–2603, 1999.

[53] S. Lall, J. E. Marsden, and S. Glavaški. A subspace approach to balanced truncation for model reduction of nonlinear control systems. *International Journal of Robust and Nonlinear Control: IFAC-Affiliated Journal*, 12(6):519–535, 2002.

[54] P. Lancaster. Explicit solutions of linear matrix equations. *SIAM review*, 12(4):544–566, 1970.

[55] N. Lang, J. Saak, and T. Stykel. Balanced truncation model reduction for linear time-varying systems. *Mathematical and Computer Modelling of Dynamical Systems*, 22(4):267–281, 2016.

[56] J. R. Li and J. White. Low rank solution of Lyapunov equations. *SIAM Journal on Matrix Analysis and Applications*, 24(1):260–280, 2002.

[57] Y. Liu and B. D. O. Anderson. Singular perturbation approximation of balanced systems. *International Journal of Control*, 50(4):1379–1405, 1989.

[58] D. G. Luenberger. *Optimization by vector space methods*. John Wiley & Sons, 1997.

[59] L. Meier and D. Luenberger. Approximation of linear constant systems. *IEEE Transactions on Automatic Control*, 12(5):585–588, 1967.

[60] S. A. Melchior, P. Van Dooren, and K. A. Gallivan. Finite horizon approximation of linear time-varying systems. *IFAC Proceedings Volumes*, 45(16):734–738, 2012.

[61] S. A. Melchior, P. Van Dooren, and K. A. Gallivan. Model reduction of linear time-varying systems over finite horizons. *Applied Numerical Mathematics*, 77:72–81, 2014.

[62] R. R. Mohler. Natural bilinear control processes. *IEEE Transactions on Systems Science and Cybernetics*, 6(3):192–197, 1970.

[63] R. R. Mohler. Nonlinear systems: Applications to bilinear control. Prentice hall. *Automatica*, 1991.

[64] B. Moore. Principal component analysis in linear systems: Controllability, observability, and model reduction. *IEEE Transactions on Automatic Control*, 26(1):17–32, 1981.

[65] C. T. Mullis and R. Roberts. Synthesis of minimum roundoff noise fixed point digital filters. *IEEE Transactions on Circuits and Systems*, 23(9):551–562, 1976.

[66] Niconet e.V., http://www.slicot.org. *SLICOT - Subroutine Library in Systems and Control Theory.*

[67] J. Nocedal and S. Wright. *Numerical optimization.* Springer Science & Business Media, 2006.

[68] R. G. Parr and W. Yang. *Density Functional Theory of Atoms and Molecules.* New York: Oxford Univ Press, 1989.

[69] Benjamin Peherstorfer, Serkan Gugercin, and Karen Willcox. Data-driven reduced model construction with time-domain loewner models. *SIAM Journal on Scientific Computing*, 39(5):A2152–A2178, 2017.

[70] T. Penzl. Algorithms for model reduction of large dynamical systems. *Linear Algebra and its Applications*, 415(2-3):322–343, 2006.

[71] K. Perev. Computation of system gramians for linear time-varying systems. In *AIP Conference Proceedings*, volume 2048. AIP Publishing, 2018.

[72] K. L. Perev. A simple method for orthogonal polynomial approximation of linear time-varying system gramians. *IFAC-PapersOnLine*, 52(17):25–30, 2019.

[73] L. Pernebo and L. Silverman. Model reduction via balanced state space representations. *IEEE Transactions on Automatic Control*, 27(2):382–387, 1982.

[74] D. Petersson and J. Löfberg. Model reduction using a frequency-limited H_2-cost. *Systems & Control Letters*, 67:32–39, 2014.

[75] N. D. Powel and K. A. Morgansen. Empirical observability gramian rank condition for weak observability of nonlinear systems with control. In *2015 54th IEEE Conference on Decision and Control (CDC)*, pages 6342–6348. IEEE, 2015.

[76] R. L. Raffard, K. Amonlirdviman, J. D. Axelrod, and C. J. Tomlin. An adjoint-based parameter identification algorithm applied to planar cell polarity signalling. *IEEE Transactions on Automatic Control*, 53(Special Issue):109–121, 2008.

[77] M. Redmann. An L^2_T-error bound for time-limited balanced truncation. *Systems & Control Letters*, 136:104620, Feb 2020.

[78] M. Redmann and P. Kürschner. An output error bound for time-limited balanced truncation. *Systems & Control Letters*, 121:1–6, Nov 2018.

[79] J. Rommes and N. Martins. Efficient computation of transfer function dominant poles using subspace acceleration. *IEEE Transactions on Power Systems*, 21(3):1218–1226, 2006.

[80] Clarence W Rowley. Model reduction for fluids, using balanced proper orthogonal decomposition. *International Journal of Bifurcation and Chaos*, 15(03):997–1013, 2005.

[81] A. Ruhe. Rational Krylov algorithms for nonsymmetric eigenvalue problems. In *Recent advances in iterative methods*, pages 149–164. Springer, 1994.

[82] Axel Ruhe. Rational krylov sequence methods for eigenvalue computation. *Linear Algebra and its Applications*, 58:391–405, 1984.

[83] Y. Saad. Numerical solution of large Lyapunov equations. Technical report, 1989.

[84] Youcef Saad and Martin H Schultz. Gmres: A generalized minimal residual algorithm for solving nonsymmetric linear systems. *SIAM Journal on scientific and statistical computing*, 7(3):856–869, 1986.

[85] M. G. Safonov and R. Y. Chiang. A Schur method for balanced-truncation model reduction. *IEEE Transactions on Automatic Control*, 34(7):729–733, 1989.

[86] H. Sandberg. A case study in model reduction of linear time-varying systems. *Automatica*, 42(3):467–472, 2006.

[87] H. Sandberg and A. Rantzer. Balanced truncation of linear time-varying systems. *IEEE Transactions on Automatic Control*, 49(2):217–229, 2004.

[88] H. Sato and K. Sato. Riemannian trust-region methods for H_2 optimal model reduction. In *2015 54th IEEE Conference on Decision and Control (CDC)*, pages 4648–4655. IEEE, 2015.

[89] K. Sato. Riemannian optimal model reduction of linear second-order systems. *IEEE Contr. Syst. Lett.*, 1(1):2–7, 2017.

[90] H. R. Shaker and F. Shaker. Generalized time-limited balanced reduction method. In *2013 American Control Conference*, pages 5530–5535. IEEE, 2013.

[91] S. Shokoohi, L. Silverman, and P. Van Dooren. Linear time-variable systems: Balancing and model reduction. *IEEE Transactions on Automatic Control*, 28(8):810–822, 1983.

[92] S. Shokoohi and L. M. Silverman. Identification and model reduction of time-varying discrete-time systems. *Automatica*, 23(4):509–521, 1987.

[93] S. Shokoohi, L. M. Silverman, and P. Van Dooren. Linear time-variable systems: Stability of reduced models. *Automatica*, 20(1):59–67, 1984.

[94] K. Sinani and S. Gugercin. $\mathcal{H}_2(t_f)$ optimality conditions for a finite-time horizon. *Automatica*, 110:108604, 2019.

[95] L Sirovich. Turbulence and the dynamics of coherent structures. part 1: Coherent structures. *Quart Appl Math*, 45:561–571, 1987.

[96] Dimitri Solomatine, Linda M See, and RJ Abrahart. Data-driven modelling: concepts, approaches and experiences. *Practical hydroinformatics: Computational intelligence and technological developments in water applications*, pages 17–30, 2008.

[97] Feng Tan, Bin Zhou, and Guang-Ren Duan. Finite-time stabilization of linear time-varying systems by piecewise constant feedback. *Automatica*, 68:277–285, 2016.

[98] P. Van Dooren, K. A Gallivan, and P. A. Absil. H_2-optimal model reduction of MIMO systems. *Appl. Math. Lett.*, 21(12):1267–1273, 2008.

[99] E. Verriest and T. Kailath. On generalized balanced realizations. *IEEE Transactions on Automatic Control*, 28(8):833–844, 1983.

[100] C. Villemagne and R. E. Skelton. Model reductions using a projection formulation. *International Journal of Control*, 46(6):2141–2169, 1987.

[101] S. W. R. Werner. *Structure-preserving model reduction for mechanical systems*. PhD Dissertation, Department of Mathematics, Otto von Guericke University, Magdeburg, Germany, 2021.

[102] K. Willcox and J. Peraire. Balanced model reduction via the proper orthogonal decomposition. *AIAA journal*, 40(11):2323–2330, 2002.

[103] D. A. Wilson. Optimum solution of model-reduction problem. In *Proceedings of the Institution of Electrical Engineers*, volume 117, pages 1161–1165. IET, 1970.

[104] Y. Xu and T. Zeng. Optimal H_2 model reduction for large-scale MIMO systems via tangential interpolation. *International Journal of Numerical Analysis & Modeling*, 8(1):174–188, 2011.

[105] W. Y. Yan and J. Lam. An approximate approach to H_2 optimal model reduction. *IEEE Transactions on Automatic Control*, 44(7):1341–1358, 1999.

[106] A. Yousuff and R. E. Skelton. Covariance equivalent realizations with application to model reduction of large-scale systems. In *Control and Dynamic Systems*, volume 22, pages 273–348. Elsevier, 1985.

[107] Liqian Zhang and James Lam. On H_2 model reduction of bilinear systems. *Automatica*, 38(2):205–216, 2002.

[108] K. Zhou and J. C. Doyle. *Essentials of robust control*, volume 104. Prentice Hall Upper Saddle River, NJ, 1998.

[109] U. Zulfiqar, V. Sreeram, and X. Du. Time-limited pseudo-optimal H_2-model order reduction. *IET Control Theory & Applications*, 14(14):1995–2007, 2020.